
Wesleyan University

The Development of New Versions of the Organocatalytic,
Asymmetric Feist-Bénary reactions

by

Alexander Korotkov

Faculty Advisor: Michael A. Calter

A dissertation in Chemistry in partial fulfillment of the requirements for the
Degree of Doctor of Philosophy at Wesleyan University

Middletown, Connecticut

February, 2013

Acknowledgements

There are many people I need to thank and acknowledge for their part in helping me through graduate school.

First and foremost, I would like to thank my research advisor, Prof. Michael A. Calter for giving me an opportunity to work in his group. Mike's expertise truly motivated me through my projects from the beginning. His constant guidance and immense support helped me grow as a chemist.

I would like to specially thank my graduate committee, Prof. Albert Fry and Prof. Erika Taylor, for their thoughtful guidance through my entire studies.

The staff of the Chemistry Department, especially Roslyn, Sarah, Doug and Horace, who were always extremely helpful and provided a wonderful environment over these years.

The members of Calter lab, past and present: Olexander Tretyak, Na Li, Henry Liu, Sam Ahles, Max Loewinger, Josh Porter, Jessica Dworak, Patrick Sarver, Rebecca McClellan and Michael Revelas.

I'm also very grateful to my sister and my parents for their encouragement and constant support. And most importantly, I'd like to acknowledge Luda for her companionship, moral support and love.

Abstract

This thesis describes the development of several new methodologies that enable efficient construction of highly functionalized hydroxydihydrofurans by the means of Interrupted Feist-Bénary reaction. In the first reaction, we utilized easily accessible α -tosyloxyacetophenones as electrophiles in the IFB reaction with cyclic 1,3-diones. In analogy to the previously developed asymmetric IFB reaction of α -bromopyruvates, we initiated our search for the appropriate catalyst with bis(pyrimidine)cinchona alkaloid-derived architecture. Optimization of these catalysts involved changing the size of the *front* group between two nitrogens of the catalyst's pyrimidine ring. We found that 1-naphthyl group allows producing desired IFB products in high enantioselectivities starting from para- or meta-substituted acetophenone tosylates.

Further studies of the electrophile scope revealed that α -tosyloxyindanones produce the tetra-cyclic IFB products in excellent yields. The optimization studies were carried out with α -tosyloxy-6,7-dibromoindanone and extensive catalyst screening allowed achieving this IFB product in 84% ee. Also, we proposed a synthetic route to hydroxybrazilin that utilizes this IFB product in a key transformation that furnishes all the required stereochemistry for the synthesis.

Finally, we studied 2-ene-1,4-diketones as electrophiles for the IFB reaction. We discovered a new highly enantio- and diastereoselective variant of the IFB reaction which uses linear 2-ene-1,4-diketones. Catalyst of choice is a catalyst bearing 3,5-(4-tert-butyl)phenyl- group in the *front* position of the catalyst.

List of Abbreviations

aq	aqueous
bn	benzyl
cat	catalyst
dba	dibenzylideneacetone
DIBAL-H	diisobutylaluminium hydride
DHQD	dihydroquinidine
DHQN	dihydroquinine
DMF	N,N-dimethylformamide
DMSO	dimethylsulfoxide
d.r.	diastereomeric ratio
ee	enantiomeric excess
eq.	equivalent
Et	ethyl
Hz	hertz
<i>i</i> -Bi	isobutyl
IFB	Interrupted Feist-Bénary reaction
<i>i</i> -Pr	isopropyl
IR	infra red
J	coupling constant
LDA	lithium diisopropylamide
M	molar

m	meta
Me	methyl
min	minutes
ml	milliliters
mmol	millimoles
NMR	nuclear magnetic resonance
o	ortho
OTf	trifluoromethanesulfonate
p	para
Ph	phenyl
ppm	parts per million
PS	proton sponge
PYR	pyrimidine
QD	quinidine
QN	quinine
rfx	reflux
RT	room temperature
sat.	saturated
TBABr	tetrabutylammonium bromide
<i>t</i> -Bu	tert-butyl
THF	tetrahydrofuran
TMS	trimethylsilyl

Table of Contents

Acknowledgements	i
Abstract	ii.
List of Abbreviations	iii.
1. Introduction	1
1.1 General overview of organocatalysis	1
1.2 Cinchona alkaloids	8
1.3 Interrupted Feist-Bénary reaction	10
References	25
2. The asymmetric, organocatalytic IFB reaction of α -tosyloxy-acetophenones	29
2.1 Initial studies	29
2.2 Substrate scope	43
2.3 The IFB reaction of substituted α -tosyloxyacetophenones	49
2.4 α -Tosyloxyaldehydes as electrophiles	53
References	58
3. Catalytic, asymmetric IFB reaction of α -tosyloxyindanones	59
3.1 Initial optimization studies	59
3.2 Initial catalyst screening	69

3.3 Final state of the catalyst screening	79
3.4 Synthetic plan for hydroxybrazilin	89
3.5 Progress toward the total synthesis of hydroxybrazilin	93
References	102
4. Development of the new asymmetric IFB reaction utilizing 2-ene-1,4-diketones as electrophiles	104
4.1 Initial experiments with cyclic electrophiles	104
4.2 Reaction of linear ene-diketone electrophiles	110
4.3 Initial investigations on the synthesis of rocaglamide via IFB reaction	141
4.4 Conclusions	150
References	151
Experimental	154

1. Introduction

1.1 General overview of organocatalysis

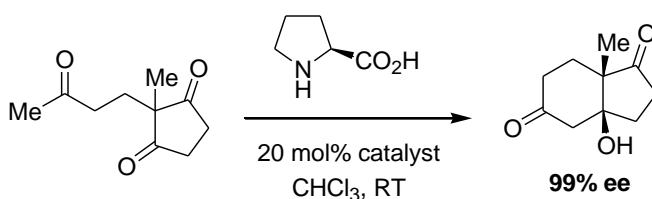
Organocatalysis is defined as a use of small organic molecules to catalyze organic transformations. Examples of organocatalytic reactions have been known for over a century, but enantioselective organocatalysis has emerged as a separate field in organic chemistry only in the last decade.¹ Although this field is in its infancy, organocatalysis has had a significant impact on the latest developments in organic synthesis, providing a wide range of useful transformations, which are often complementary to conventional metal catalysis. Among commonly quoted advantages of using small organic molecules as catalysts are mild reaction conditions, operational simplicity and low toxicity associated with organocatalysis. Organocatalysts are inexpensive and easy to prepare and many of them are now commercially available. Most organocatalytic reactions are tolerant of water and air, what provides a significant advantage over conventional metal catalysis. At the same time those methods give access to complex, functionalized products with high enantiopurity, and, therefore, organocatalytic reactions have great potential in application in organic synthesis, including the construction of natural products.

Most organocatalytic reaction can be classified based on generic modes of activation. A generic activation mode describes a reactive species that can participate in many reaction types with consistently high enantioselectivity.

Such reactive species arise from the interaction of a single chiral catalyst with a basic functional group (such as a ketone, aldehyde, alkene or imine) in a highly organized and predictable manner. Generic activation modes commonly used in organocatalysis are enamine catalysis, iminium catalysis, nucleophilic catalysis and hydrogen-bonding (H-bonding) catalysis.

The first highly enantioselective organocatalytic reaction was reported simultaneously by Hajos and Parrish, and Wiechert, Eder and Sauer in early 1970s.² This intramolecular aldol reaction is catalyzed by proline and produces a chiral bicyclic ketone in 99% ee (Scheme 1.1). Back at the time of discovery, the mechanism of the transformation was not realized and this activation mode was not exploited for other reactions until more than 30 years later.

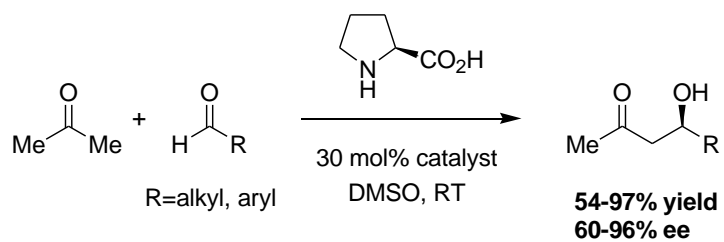
Scheme 1.1 Hajos-Parrish reaction



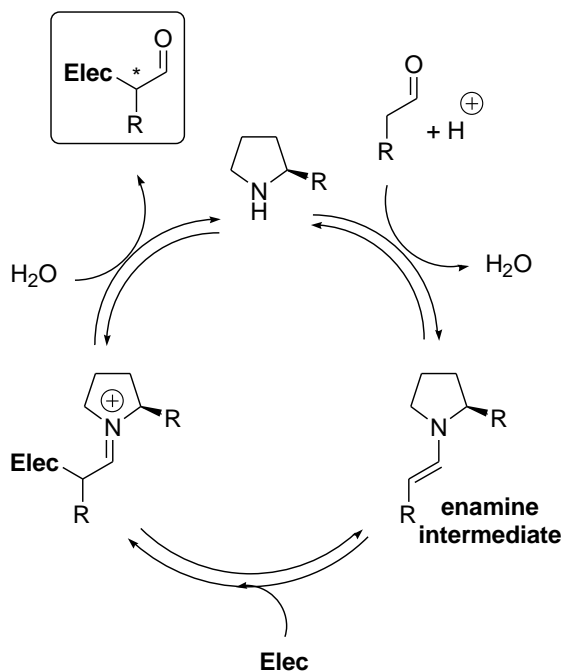
In 2000, Barbas, Lerner and List published a related intermolecular aldol and Mannich reactions which proceed through enamine intermediate (Scheme 1.2).³ In a subsequent decade there have been many publications of organocatalytic reactions via enamine catalysis (Scheme 1.3). Generally

speaking, this activation mode is used to functionalize carbonyl-containing compounds at the α -carbon (Scheme 1.4).⁴

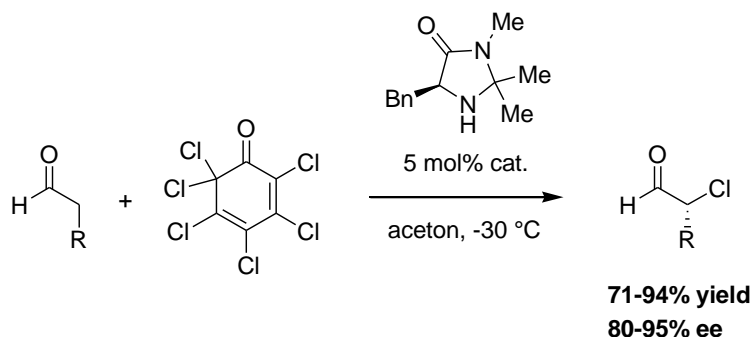
Scheme 1.2 Proline-catalyzed intermolecular aldol reaction



Scheme 1.3 General catalytic cycle for enamine catalysis

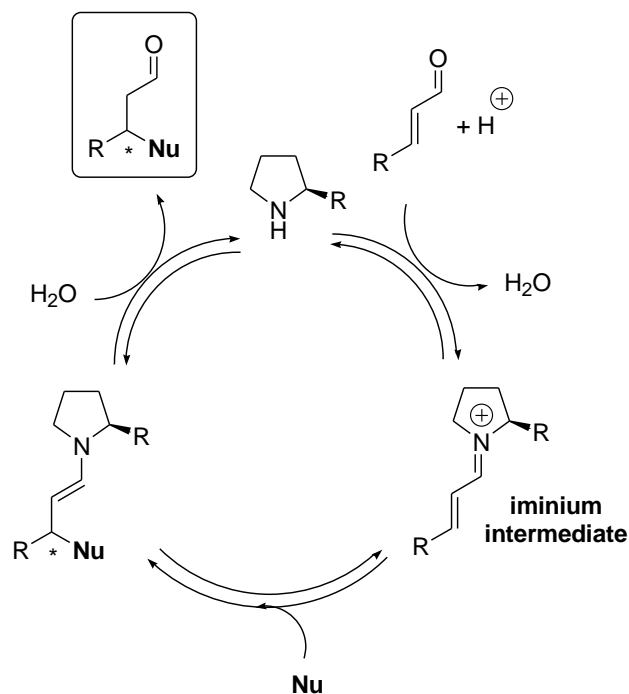


Scheme 1.4 Enantioselective chlorination of aldehydes



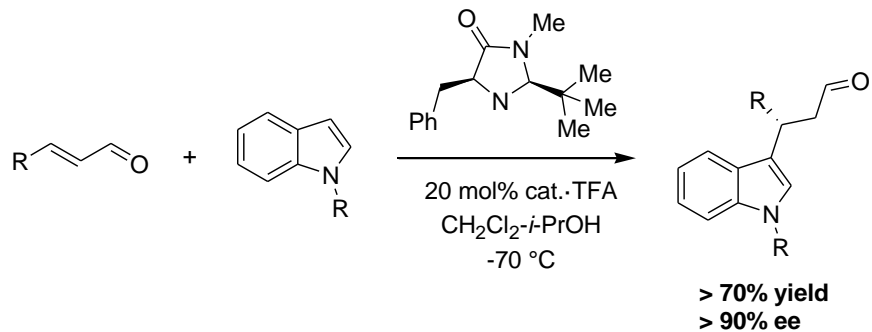
In the late 1990s it was realized that chiral secondary amines can activate enals via the iminium ion and resulting reaction intermediate can participate in a number of useful, asymmetric β -functionalization transformations (Scheme 1.5). The formation of the iminium species lowers LUMO orbital in energy activating enals for ether conjugate addition or pericyclic reaction. In other words, iminium ion catalysis provides an organocatalytic alternative to conventional Lewis acid activation of α,β -unsaturated compounds.

Scheme 1.5 Activation through iminium catalysis



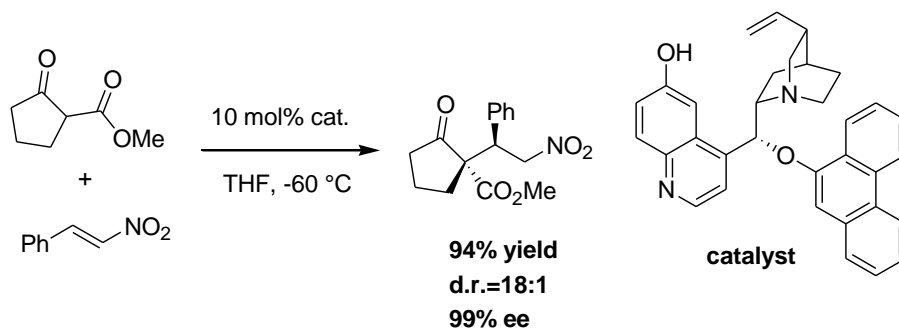
A large number of new asymmetric methods utilizing this general concept were introduced by Macmillan's group, along with the discovery of the new class of imidazolidinone organocatalysts (Scheme 1.6).⁵

Scheme 1.6 Enantioselective conjugate addition of indoles to enals



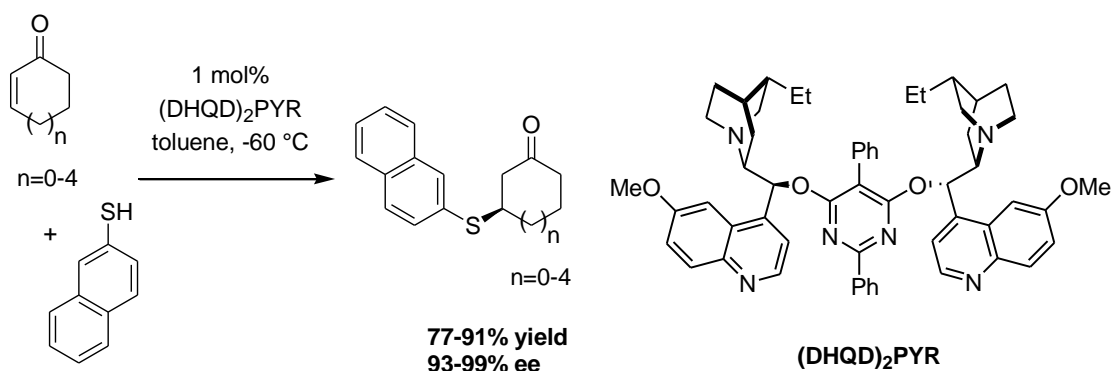
The use of basic catalysts had a major impact on synthesis over the last decades.⁶ In particular, the cinchona alkaloids and their derivatives catalyze many useful transformations with high enantioselectivities. The basic center (quinuclidine tertiary amine) of a cinchona alkaloid acts as a base to deprotonate relatively acidic protons (e.g. 1,3-dicarbonyl compounds or thiols), forming a contact ion pair between the resulting anion and protonated catalyst. This interaction creates a chiral environment around the anion and permits enantioselective reactions with electrophiles. For example, Li Deng's group recently published highly enantioselective C-C bond forming conjugate addition of β -ketoesters to nitroalkenes, that is catalyzed by a cinchona alkaloid derived catalyst (*Scheme 1.7*).⁷ It is worth mentioning that this method represents an ability to control the formation of quaternary stereocenters with high enantiomeric excess.

Scheme 1.7 Cinchona alkaloid-catalyzed conjugate addition to nitroalkenes



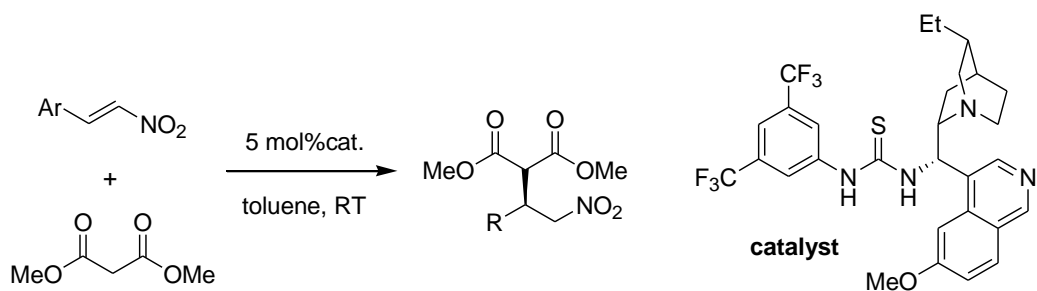
In another example, aromatic thiols undergo 1,4-addition to cyclic enones forming β -mercaptoketones in excellent enantioselectivity in the presence of the catalyst **(DHQD)₂PYR** catalyst (Scheme 1.8).⁸

Scheme 1.8 Cinchona alkaloid-catalyzed thiol conjugate addition to enones



Another mode of activation in organocatalysis that attracted great attention over the last years is H-bonding catalysis. The ability to activate the carbonyl compounds or imines with H-bonding is analogous to Lewis acid activation. A large variety of these catalysts were introduced recently making a big impact on the field. Among these are binol-derived catalysts⁹, thiourea catalysts¹⁰ developed by Jacobsen's group and binol-derived phosphoric acids¹¹. For example, the addition of malonate to nitroalkenes catalyzed by a bifunctional cinchona alkaloid-thiourea catalyst proceeds with high enantiomeric excess. Interestingly, the catalyst used in this transformation is epimeric at C9 from the naturally occurring cinchona alkaloids (Scheme 1.9).¹²

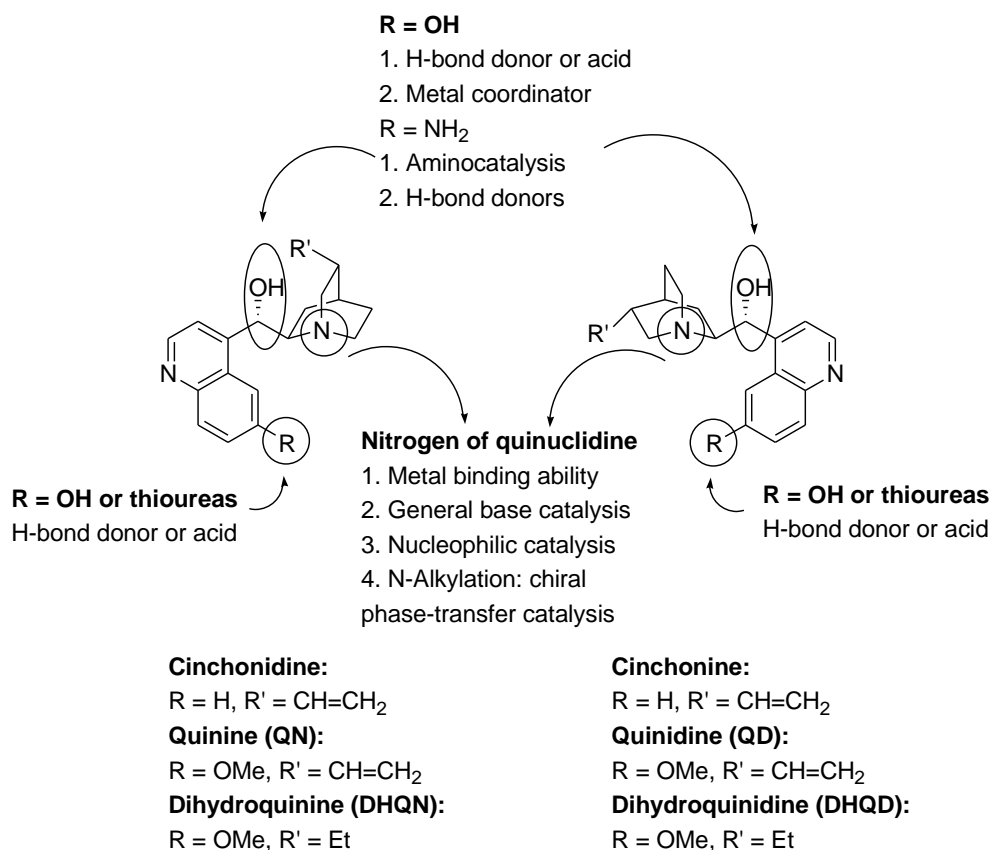
Scheme 1.9 Thiourea-catalyzed malonate addition to nitroalkenes



1.2 Cinchona alkaloids

Cinchona alkaloids are among the most commonly used chirality inducers in the area of asymmetric catalysis.¹³ The key feature responsible for their broad use in catalysis is that they possess diverse functionality responsible for their ability to participate in a large number of the catalytic transformations. Besides that, a number of efficient ways to modify the reacting center of cinchona alkaloids have been developed in order to enhance their catalytic ability (Scheme 1.10).

Scheme 1.10 Common cinchona alkaloids and their active sites



The presence of the tertiary amine base of the quinuclidine part is primarily responsible for their catalytic activity. For example, it makes cinchona alkaloids effective ligands for a variety of metal-catalyzed processes. The most famous example is the osmium-catalyzed asymmetric dihydroxylation of olefins discovered by Sharpless.¹⁴ Additionally, the quinuclidine nitrogen can act as a chiral base or a chiral nucleophilic catalyst promoting many the different types of organocatalytic reaction. Finally, cinchona alkaloids can be alkylated at the

nitrogen center to form quaternary ammonium salts that catalyze numerous reactions under phase-transfer conditions.¹⁵

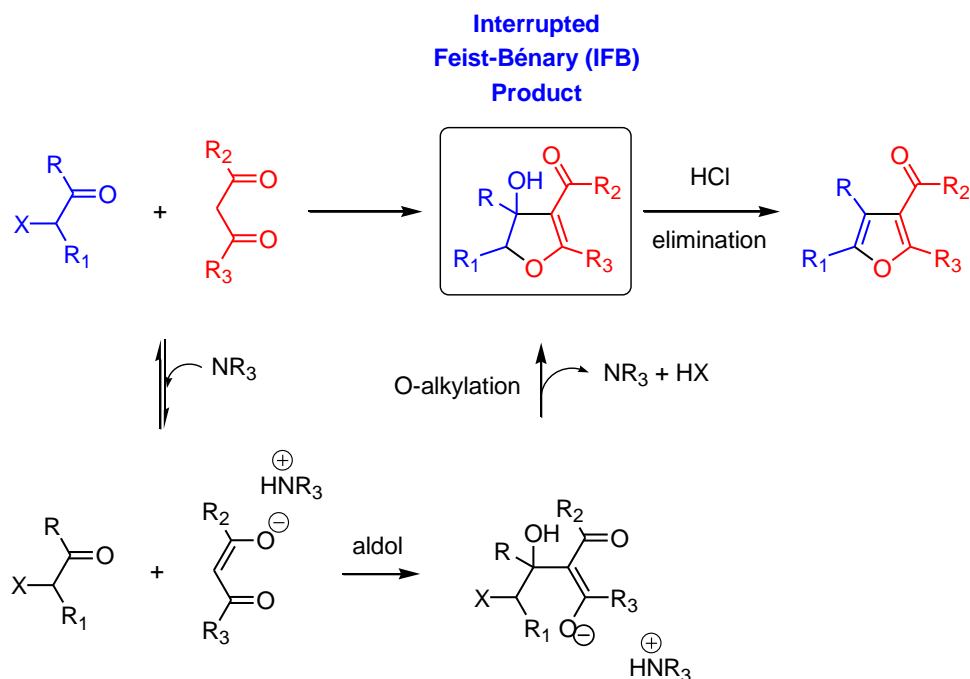
The secondary 9-hydroxy group can serve as an acid or a H-bond donor. Besides that, a number of ways were developed to modify cinchona alkaloids at this position. For example, the introduction of a thiourea or amide functionality allows expanding the utility of cinchona alkaloids to bifunctional catalysis.¹⁶

1.3 Interrupted Feist-Bénary reaction

The Feist-Bénary reaction was initially described over a century ago first by Franz Feist¹⁷, and few years later by Erick Bénary. In the most general way, it involves a condensation of a 1,3-dicarbonyl compound with an α -haloketone to produce, after elimination of water, a highly substituted furan product (Scheme 1.11). The mechanism of Feist-Bénary reaction involves the enolization of 1,3-dicarbonyl compound (usually catalyzed by amines), which then undergoes an aldol reaction with the α -haloketone. Subsequent intramolecular S_N2 O-alkylation furnishes the furan ring. In the classic version of the Feist-Bénary reaction this intermediate is treated with aqueous acid to produce the final product. However, the reaction can be stopped at the “interrupted” stage with the isolatable and perfectly stable hydroxydihydrofuran product, which we will refer to as the IFB product. In this case, the reaction enables the formation of the highly functionalized product containing two adjacent chiral centers, providing

the synthetic community with a challenge of both diastereo- and enantioselectivity control.

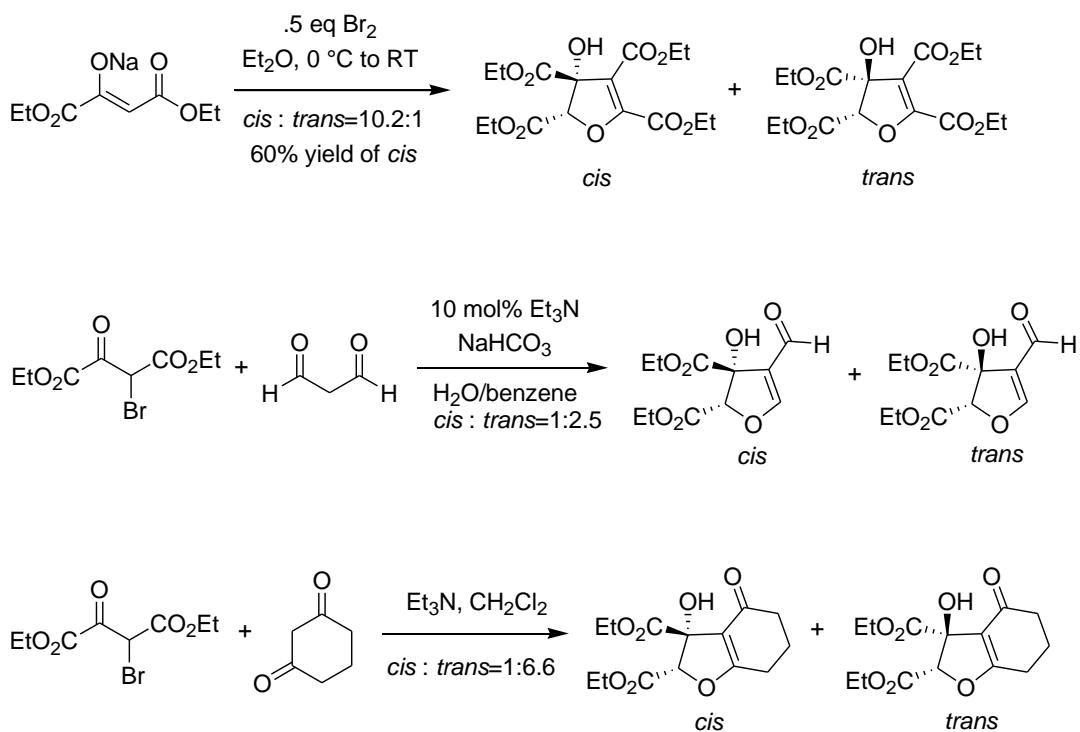
Scheme 1.11 Mechanism of Feist-Bénary reaction



Initially, the investigation of the IFB reaction in Calter's group was focused on the scope and diastereoselectivity of this transformation.¹⁸ The reaction α -bromo oxaloacetates as electrophiles in combination with oxaloacetate nucleophiles produces a mixture of two diastereomers favoring the *cis*-product (Scheme 1.12). However, a switch to more acidic nucleophiles, such as 1,3-cyclohexanedione, resulted in the formation of the *trans*-product as the major one. Making the nucleophile precursor more acidic had two consequences: the retro-aldol reaction became more favorable, and the cyclization became less

favorable. The combination of these factors most likely led to cyclization rather than addition being the product-determining step for the 1,3-cyclohexanedione reaction. Apparently, cyclization favored the *trans* isomer.

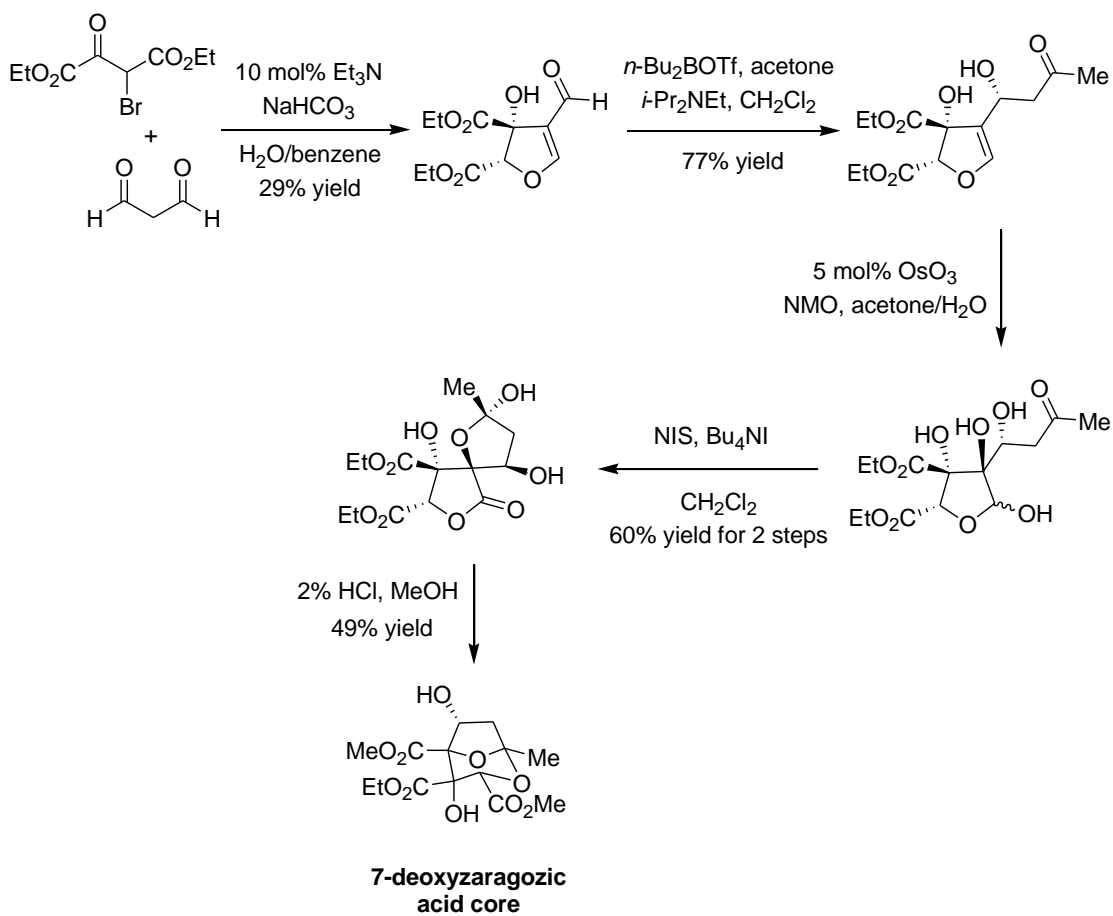
Scheme 1.12



This method for construction of functionalized chiral furans provided a key intermediate for the synthesis of 7-deoxyzaragozic acid core (Scheme 1.13).¹⁹ In the key transformation of the route, α -bromoacrylate reacted with malondialdehyde to give the desired IFB product in 29% yield. A few more steps were required to convert this intermediate into the core of the natural product. Unfortunately, this highly efficient synthesis only provided the racemic product. Therefore, the development of the asymmetric version of the IFB

reaction was chosen to be the main focus for the further research in the Calter group as it would significantly expand the usefulness of this method.

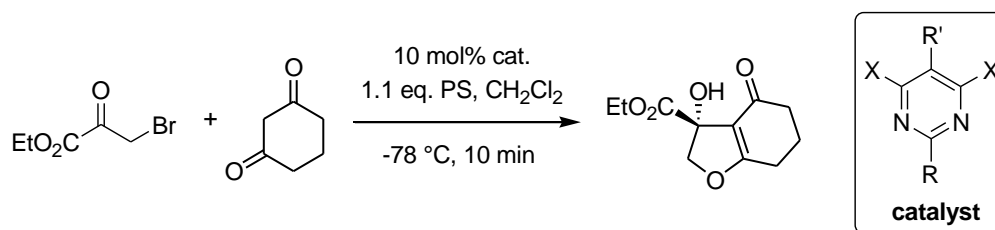
Scheme 1.13 Synthesis of 7-deoxyzaragozic acid core



The first enantioselective IFB reaction was discovered in the Calter group few years later.²⁰ Ryan Phillips found that α -bromopyruvates are excellent electrophiles in a reaction with a cyclic 1,3-dione nucleophile giving an IFB reaction that is rapid and high yielding. He performed an extensive catalyst screen, focusing on cinchona alkaloid-derived structures. He soon found that

high enantiomeric excesses are achieved in the presence of pyrimidine-cinchona alkaloid derived catalysts, such as the Sharpless ligand, **(DHQD)₂PYR**. Additional optimization studies with regard to the effect of the steric nature of the R and R' groups of the pyrimidine core led to the discovery of catalyst **QD-2**, which produced the IFB product in 91% ee (Scheme 1.14). It was expected that applying the diastereomeric quinine-derived catalyst would allow the preparation of the opposite enantiomer of the product with nearly similar results. However, this was not a case, thus the method required further optimization in order to achieve (*R*)-enantiomer in high excess. This problem was solved by introducing a quinine catalyst **QN-3** bearing a t-butyl group at the 2-position of the pyrimidine ring.

Scheme 1.14 The IFB reaction of α -bromopyruvate and 1,3-cyclohexanedione

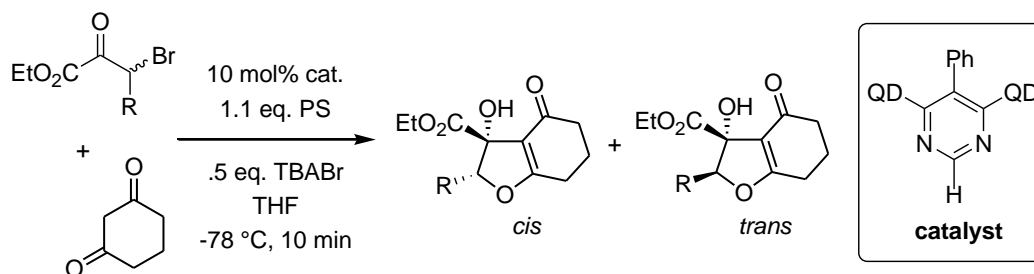


cat.	R	R'	X	yield %	ee %
(DHQD) ₂ PYR	Ph	Ph	DHQD	89	68
QD-1	SMe	Ph	QD	94	88
QD-2	H	Ph	QD	98	91
QD-3	<i>t</i> -Bu	Ph	QD	94	64
QD-4	<i>t</i> -Bu	<i>t</i> -Bu	QD	96	61
QD-5	Ph	<i>t</i> -Bu	QD	99	75
(DHQ) ₂ PYR	Ph	Ph	DHQN	95	-82
QN-1	SMe	Ph	QN	96	-75
QN-2	H	Ph	QN	93	-65
QN-3	<i>t</i>-Bu	Ph	QN	93	-98
QN-4	<i>t</i> -Bu	<i>t</i> -Bu	QN	96	-14
QN-5	Ph	<i>t</i> -Bu	QN	99	-53

First optimized with simple α -bromopyruvate, this method was later extended to the reaction of substituted α -bromopyruvates. Since the reaction

starts with a chiral electrophile, the stereoinduction most likely depends on the conversion of the starting materials. In this case, two enantiomers of the α -bromopyruvate would react with the different rates due to the match/mismatch interaction with the chiral catalyst. If large excess of the optically active electrophile is used in the reaction, 1,3-cyclohexanedione would only react with the enantiomer of the α -bromopyruvate that was “matched” to the catalyst leading to the dynamic resolution. It was reasoned that the addition of the bromide source to the reaction could constantly isomerize α -bromopyruvate by an S_N2 mechanism if the reaction occurred in a polar, aprotic solvent. Consequently, reaction could be run under conditions of a dynamic, kinetic resolution. Indeed, the reaction run in THF in the presence of 0.5 equivalents of tetrabutylammonium bromide and proton sponge resulted in almost complete diastereo- and enantioselectivity favoring the *cis*-isomer of the IFB product (Scheme 1.15).

Scheme 1.15 The asymmetric IFB reaction of substituted α -bromopyruvates

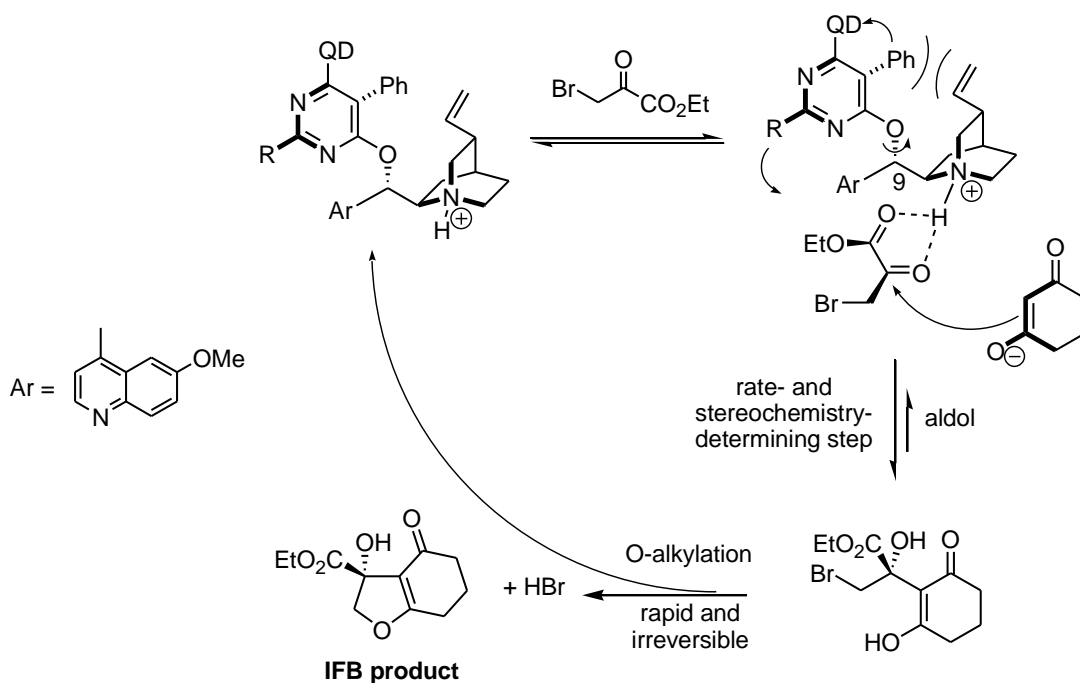


R	<i>cis:trans</i>	yield %	ee %
Me	98:2	96	94
<i>n</i> -Pent	96:4	95	93
<i>i</i> -Bu	97:3	94	96
Ph	96:4	94	93

In his work, Ryan Phillips proposed a mechanism and a transition-state model for the asymmetric IFB reaction of the α -bromopyruvates. In the first step of the proposed mechanism, the quinuclidine nitrogen deprotonates 1,3-cyclohexanedione (Scheme 1.16). It was postulated that the protonated catalyst can form bifurcated H-bonds with the α -ketoester moiety of the α -bromopyruvate, thus activating the carbonyl group for the aldol addition. This interaction creates chiral environment around the electrophile molecule making one side of α -bromopyruvate more accessible for the nucleophile attack. The high enantioselectivity achieved in the reaction arises from the relative

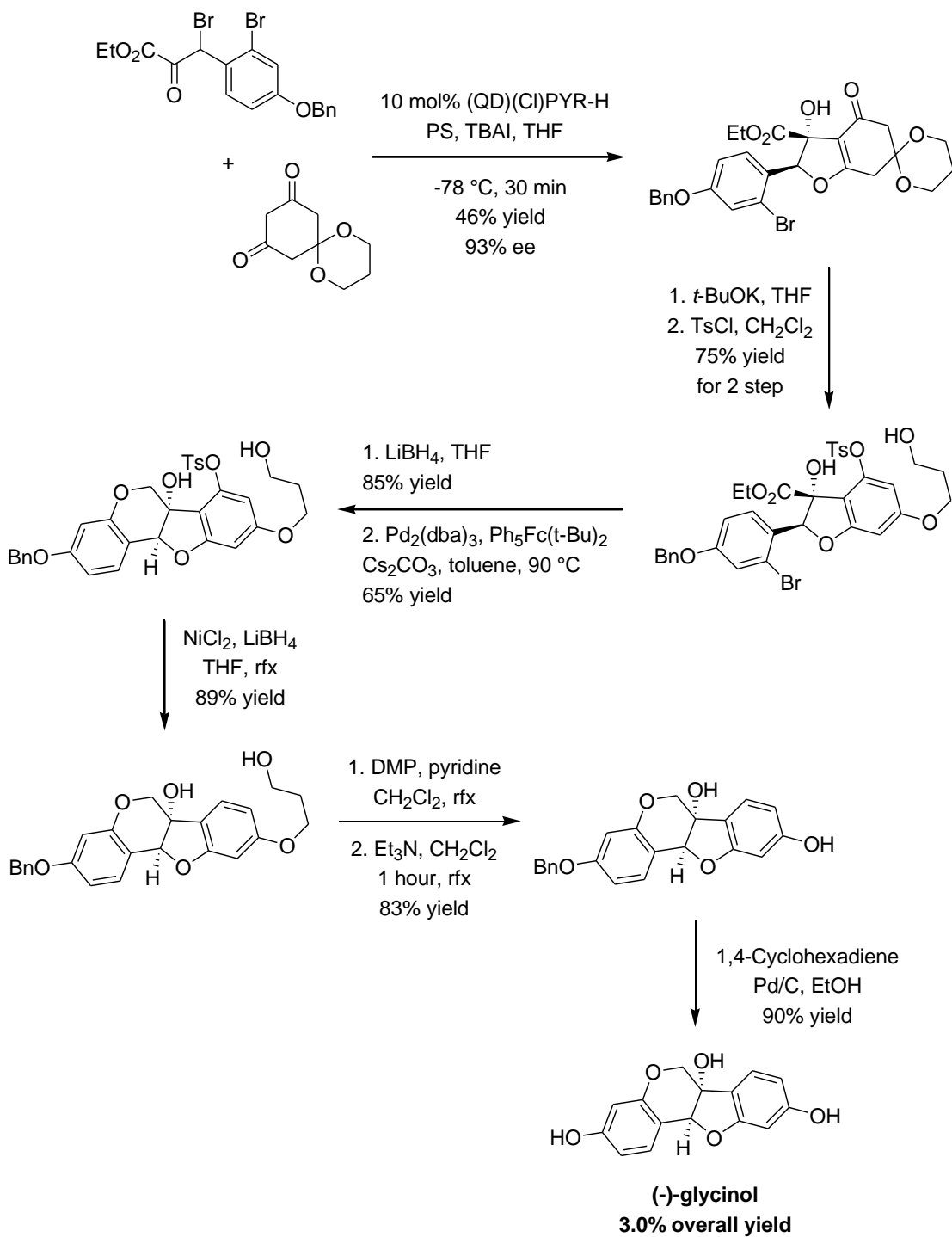
configuration of the electrophile and the most stable conformation of the protonated cinchona alkaloid catalyst. In the case of the quinidine-derived structure, small rotations around the C₉-ether group cause larger movements of both the phenyl and R groups of the pyrimidine ring. In such a case, the alkene attached to the quinuclidine structure runs into the phenyl group (which will be referred to as the back group). This interaction brings the R group (the front group of a catalyst) of the pyrimidine ring closer to the active site of the catalyst. Thus, the nature of this group has a significant effect on the interaction between the catalyst and the electrophile, and, consequently, the enantioselectivity of the reaction.

Scheme 1.16 Proposed mechanism



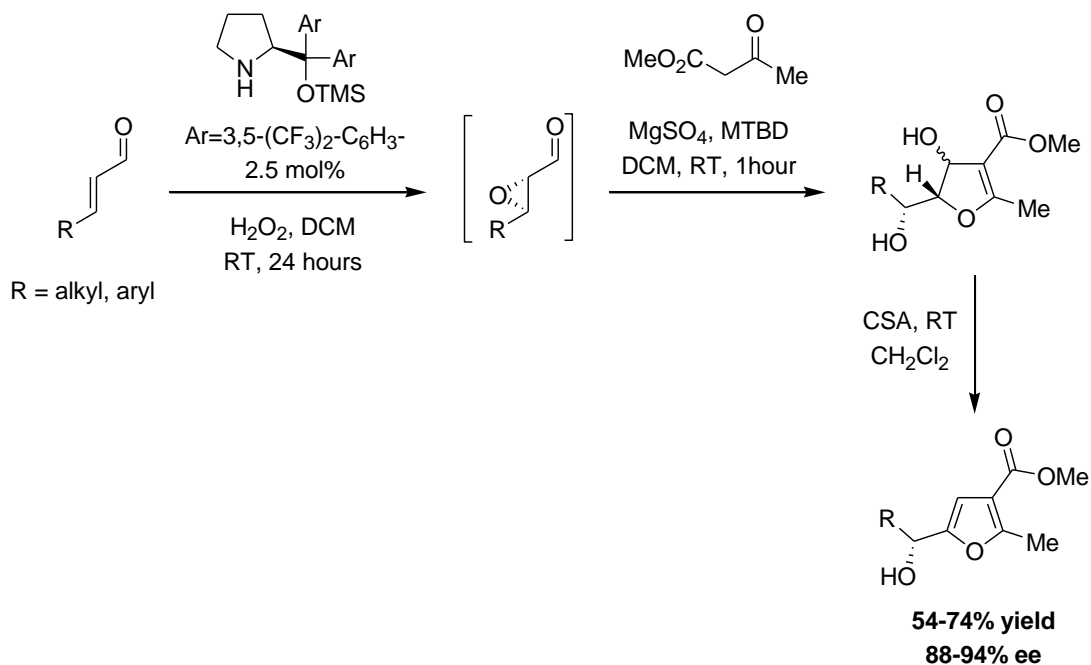
To demonstrate the utility of the newly developed method, the IFB reaction was applied as the key step in the total synthesis of (-)-variabilin and (-)-glycinol, performed by Na Li and published in 2011.²¹ The initial IFB reaction produced the desired product as a *trans*-isomer in moderate yield and high enantioselectivity in the presence of mono-quinidine catalyst **(QD)(Cl)PYR** (Scheme 1.17). Further transformations toward glycinol include aromatization of the dione moiety with potassium tert-butoxide, an intramolecular Buchwald-Hartwig coupling and a nickel-catalyzed aryl tosylate reduction. The final stage elimination of the side chain of the right ring and a deprotection of the phenol gave (-)-glycinol in an overall 3.0% yield.

Scheme 1.17 Asymmetric total synthesis of (-)-glycinol

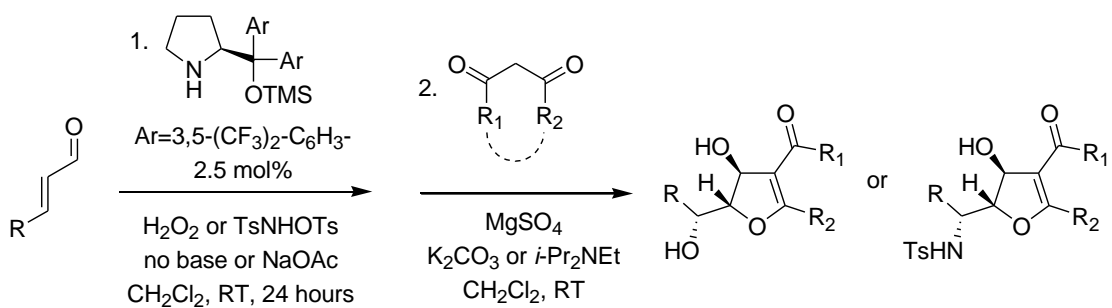


Besides the reaction of α -bromopyruvates developed in our lab, the literature provides only one example of a related organocatalytic process involving the IFB reaction. In a work reported by Jørgensen group in 2010, 2-hydroxyalkyl- and 2-aminoalkyl furans are prepared with high stereoselectivity utilizing an organocatalytic one-pot reaction cascade: epoxidation or aziridination of α,β -unsaturated aldehydes followed by Feist-Bénary reaction of various 1,3-dicarbonyl compounds to give the target furanes (Scheme 1.18).²² The stereochemistry of this multistep process is set up at the initial epoxidation step, utilizing a proline-derived catalyst first discovered by Jørgensen and often used for the similar transformations. The second step of this one-pot reaction is a Feist-Bénary reaction that furnishes 2-hydroxyalkyl furanes in high enantioselectivity. This efficient multibond forming reaction cascade benefits from low catalyst loadings and readily available starting materials.

Scheme 1.18



Furthermore, the possibility to interrupt the reaction sequence at the stage of the corresponding optically active 2-hydroxyalkyl- and 2-aminoalkyl 2,3-dihydrofuranes with three stereogenic centers is also presented (Table 1.1). The products can be isolated in moderate to high yield with the same excellent level of stereoselectivity. Unfortunately, this method suffers from the low diastereoselectivity, as in some cases two diastereomers of the hydroxydihydrofuran product are obtained in equal amounts, although both in high enantioselectivities.

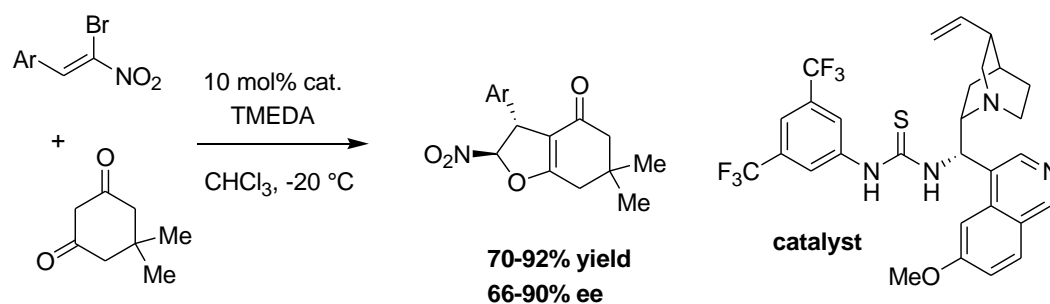
Table 1.1

R	R₁	R₂	X	yield %	d.r.	ee %
Pr	OMe	CH ₃	0	74	3:1	97/98
E-Hex-3-enyl	<i>Ot</i> Bu	CH ₃	0	86	4:1	95/98
CH ₂ OBn	<i>Ot</i> Bu	CH ₃	0	60	2:1	96/nd
CO ₂ Et	<i>Ot</i> Bu	CH ₃	0	46	7:1	97/nd
Pr	CH ₃	CH ₃	0	87	1.6:1	98/98
Pr	dimedone		0	80	2.5:1	98/nd
Pr	OMe	CH ₃	NTs	70	1:2	96/98
Pr	CH ₃	CH ₃	NTs	91	1:2.5	92/98
Pr	dimedone		NTs	80	1:1	97/94

An interesting method for constructing a chiral dihydrofuran product was recently reported by Rueping et al.²³ 1,3-Dicarbonyl derivatives react with bromonitrostyrenes in the presence of a chiral bifunctional thiourea catalyst providing mild and efficient access to diverse polysubstituted dihydrofurans in

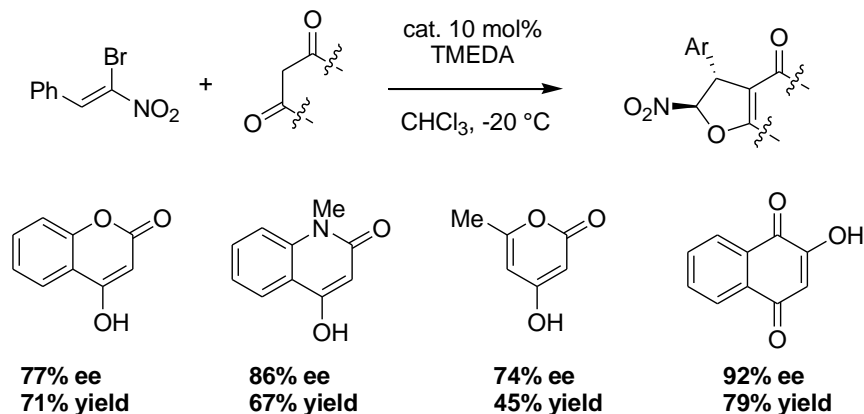
good yields (Scheme 1.19). Both electron-donating and withdrawing groups were well tolerated at the ortho-, meta- or para- position of the aryl ring. Enantiomeric excesses were all in the 80-90% range. Only in the case of the bulky 2-naphthyl substituent was a slight decrease observed (66% ee). In some cases the resulting products were recrystallized from *i*-propanol which resulted in enantiomeric excesses increasing to more than 97% ee.

Scheme 1.19



The reaction also gives reproducible results with a range of different 1,3-dicarbonyl nucleophiles, such as 4-hydroxycoumarin, its lactam analog and 2-hydroxyquinone (Scheme 1.20).

Scheme 1.20



References

1. (a) Dalako, P. I.; Moisan, L., In the golden age of organocatalysis. *Angew Chem Int Edit* **2004**, *43* (39), 5138-5175; (b) List, B., Organocatalysis: A complementary catalysis strategy advances organic synthesis. *Adv Synth Catal* **2004**, *346* (9-10), 1021-1021.
2. (a) Hajos, Z. G.; Parrish, D. R., Asymmetric Synthesis of Bicyclic Intermediates of Natural Product Chemistry. *J Org Chem* **1974**, *39* (12), 1615-1621; (b) Eder, U.; Sauer, G.; Weichert, R., Total Synthesis of Optically Active Steroids .6. New Type of Asymmetric Cyclization to Optically Active Steroid Cd Partial Structures. *Angew Chem Int Edit* **1971**, *10* (7), 496-&.
3. List, B.; Lerner, R. A.; Barbas, C. F., Proline-catalyzed direct asymmetric aldol reactions. *J Am Chem Soc* **2000**, *122* (10), 2395-2396.
4. Ibrahim, H.; Togni, A., Enantioselective halogenation reactions. *Chem Commun* **2004**, (10), 1147-1155.
5. Austin, J. F.; MacMillan, D. W. C., Enantioselective organocatalytic indole alkylations. Design of a new and highly effective chiral amine for iminium catalysis. *J Am Chem Soc* **2002**, *124* (7), 1172-1173.
6. France, S.; Guerin, D. J.; Miller, S. J.; Lectka, T., Nucleophilic chiral amines as catalysts in asymmetric synthesis. *Chem Rev* **2003**, *103* (8), 2985-3012.
7. (a) Li, H. M.; Song, J.; Liu, X. F.; Deng, L., Catalytic enantioselective C-C bond forming conjugate additions with vinyl sulfones. *J Am Chem Soc* **2005**, *127* (25), 8948-8949; (b) Li, H. M.; Wang, Y.; Tang, L.; Deng, L., Highly enantioselective conjugate addition of malonate and beta-ketoester to nitroalkenes: Asymmetric C-C bond formation with new bifunctional organic catalysts based on cinchona alkaloids. *J Am Chem Soc* **2004**, *126* (32), 9906-9907.

8. McDaid, P.; Chen, Y. G.; Deng, L., A highly enantioselective and general conjugate addition of thiols to cyclic enones with an organic catalyst. *Angew Chem Int Edit* **2002**, *41* (2), 338-+.
9. (a) Unni, A. K.; Takenaka, N.; Yamamoto, H.; Rawal, V. H., Axially chiral biaryl diols catalyze highly enantioselective hetero-Diels-Alder reactions through hydrogen bonding. *J Am Chem Soc* **2005**, *127* (5), 1336-1337; (b) McDougal, N. T.; Schaus, S. E., Asymmetric Morita-Baylis-Hillman reactions catalyzed by chiral Bronsted acids. *J Am Chem Soc* **2003**, *125* (40), 12094-12095.
10. (a) Vachal, P.; Jacobsen, E. N., Structure-based analysis and optimization of a highly enantioselective catalyst for the Strecker reaction. *J Am Chem Soc* **2002**, *124* (34), 10012-10014; (b) Joly, G. D.; Jacobsen, E. N., Thiourea-catalyzed enantioselective hydrophosphonylation of imines: Practical access to enantiomerically enriched alpha-amino phosphonic acids. *J Am Chem Soc* **2004**, *126* (13), 4102-4103.
11. (a) Uruguchi, D.; Terada, M., Chiral Bronsted acid-catalyzed direct Mannich reactions via electrophilic activation. *J Am Chem Soc* **2004**, *126* (17), 5356-5357; (b) Akiyama, T.; Itoh, J.; Yokota, K.; Fuchibe, K., Enantioselective Mannich-type reaction catalyzed by a chiral Bronsted acid. *Angew Chem Int Edit* **2004**, *43* (12), 1566-1568.
12. McCooey, S. H.; Connon, S. J., Urea- and thiourea-substituted cinchona alkaloid derivatives as highly efficient bifunctional organocatalysts for the asymmetric addition of malonate to nitroalkenes: Inversion of configuration at C9 dramatically improves catalyst performance. *Angew Chem Int Edit* **2005**, *44* (39), 6367-6370.
13. Song, C. E., *Cinchona alkaloids in synthesis and catalysis : ligands, immobilization and organocatalysis*. Wiley-VCH: Weinheim, 2009; p xx, 525 p.

14. Kolb, H. C.; Vannieuwenhze, M. S.; Sharpless, K. B., Catalytic Asymmetric Dihydroxylation. *Chem Rev* **1994**, *94* (8), 2483-2547.
15. Jew, S. S.; Park, H. G., Cinchona-based phase-transfer catalysts for asymmetric synthesis. *Chem Commun* **2009**, (46), 7090-7103.
16. Siau, W. Y.; Wang, J., Asymmetric organocatalytic reactions by bifunctional amine-thioureas. *Catal Sci Technol* **2011**, *1* (8), 1298-1310.
17. Maercker, G.; Köhne, P.; Feist, R., *Die nachlassbehandlung, das erbrecht, familienrecht und vormundschaftsrecht nebst den auf diese rechtsverhältnisse bezüglichen gesetzlichen bestimmungen und verwaltungsvorschriften für das preussische rechtsgebiet*. 17. Aufl. ed.; R.v. Decker: Berlin,, **1902**; p xii, 2 , 690 p.
18. Calter, M. A.; Zhu, C., Scope and diastereoselectivity of the "interrupted" Feist-Benary reaction. *Org Lett* **2002**, *4* (2), 205-208.
19. Calter, M. A.; Zhu, C.; Lachicotte, R. J., Rapid synthesis of the 7-deoxy zaragozic acid core. *Org Lett* **2002**, *4* (2), 209-212.
20. Calter, M. A.; Phillips, R. M.; Flaschenriem, C., Catalytic, asymmetric, "interrupted" Feist-Benary reactions. *J Am Chem Soc* **2005**, *127* (42), 14566-14567.
21. Calter, M. A.; Li, N., Asymmetric Total Syntheses of (-)-Variabilin and (-)-Glycinol. *Org Lett* **2011**, *13* (14), 3686-3689.
22. Albrecht, L.; Ransborg, L. K.; Gschwend, B.; Jorgensen, K. A., An Organocatalytic Approach to 2-Hydroxyalkyl- and 2-Aminoalkyl Furanes. *J Am Chem Soc* **2010**, *132* (50), 17886-17893.

23. Rueping, M.; Parra, A.; Uria, U.; Besselievre, F.; Merino, E., Catalytic Asymmetric Domino Michael Addition-Alkylation Reaction: Enantioselective Synthesis of Dihydrofurans. *Org Lett* **2010**, *12* (24), 5680-5683.

2. The asymmetric, organocatalytic IFB reaction of α -tosyloxy-acetophenones

2.1 Initial studies

The asymmetric, organocatalytic reaction of α -bromopyruvates and 1,3-cyclohexanedione developed earlier in Calter's group and described in detail in Chapter 1 represented the only example of an enantioselective IFB reaction found in the literature. The hydroxydihydrofuran products produced in the IFB reaction in high enantio- and diastereoselectivity contain a wide variety of complex functionality making them useful tools for stereoselective organic synthesis, including natural product synthesis.

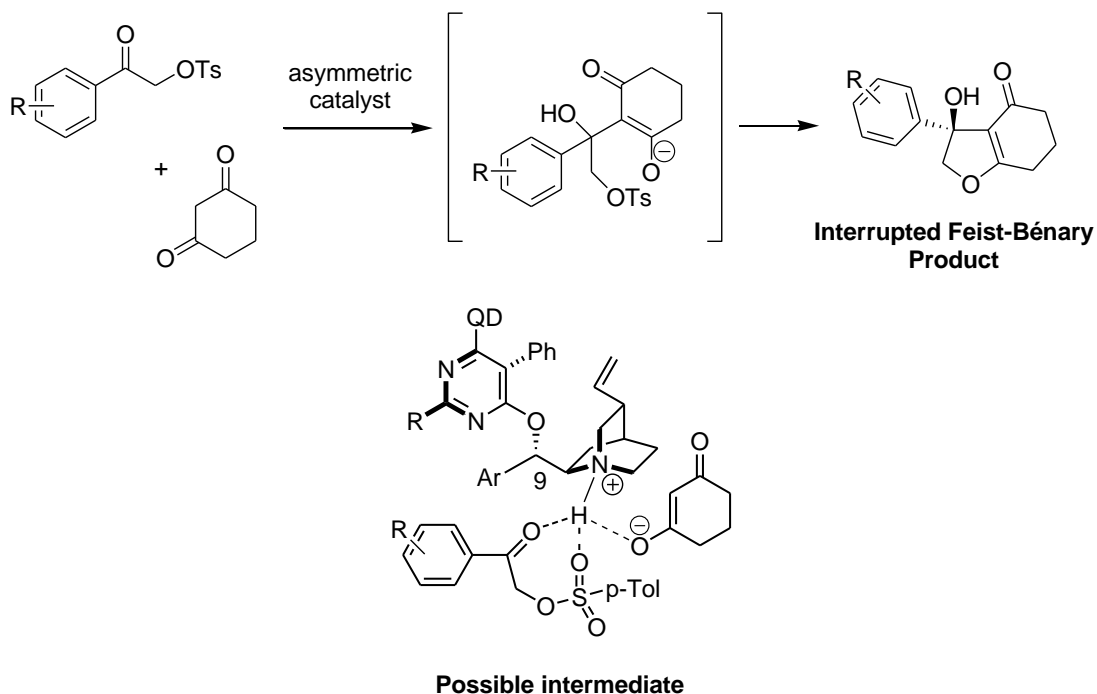
Inspired by these results, we decided to expand the scope of suitable electrophiles in the IFB reaction. This would allow us to access a variety of chiral hydroxydihydrofurans that were unavailable by the IFB reaction of α -bromopyruvates. We also hoped that the bis-cinchona alkaloid substituted pyrimidine catalyst architecture would provide us with enantiomerically pure products after the necessary structural changes in the catalyst were applied.

In the proposed mechanism for the IFB reaction of α -bromopyruvates, the reaction intermediate engages in a bifurcated H-bond between the protonated catalyst and the α -ketoester-group of the electrophile. Since it was postulated that this interaction was crucial and leads to a better organized

transition state, thus, higher enantioselectivity, we were looking for substrates that possess an ability to go through a similar intermediate while the reaction proceeds.

As further consideration, we recognized that α -tosyloxy-acetophenones can be considered promising reactants. The α -tosylate group can provide a second H-bond acceptor (Scheme 2.1). Also, the tosyl group activates the carbonyl towards nucleophilic addition by induction and, at the same time, provides a leaving group to make the initial aldol reaction irreversible. Additionally, the electrophilicity of the carbonyl group of an α -tosyloxy-acetophenone can be enhanced by introducing electron-withdrawing groups on the acetophenone aromatic ring, in case it is required for faster reaction or/and better yield of the desired IFB product.

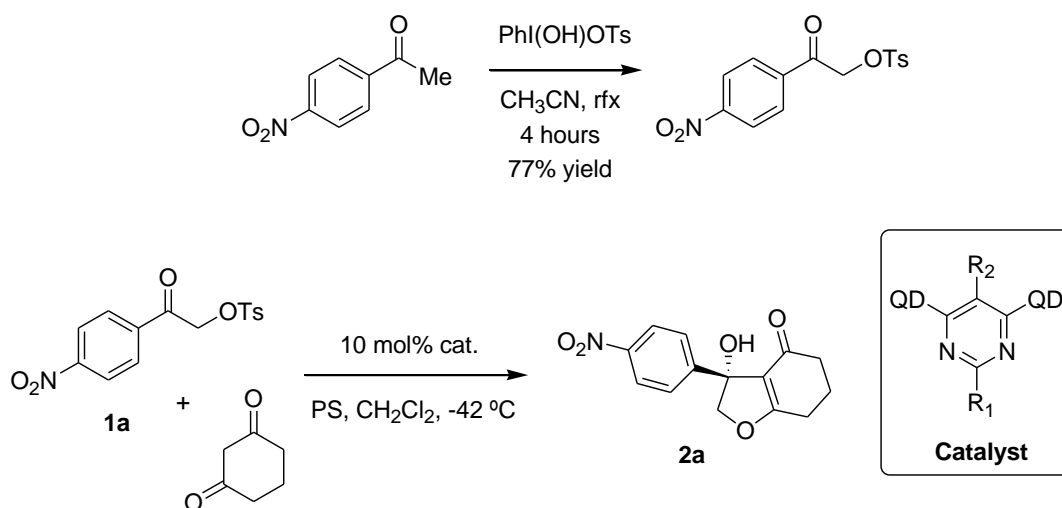
Scheme 2.1 Possible intermediate for the IFB reaction of α -tosyloxy-acetophenones



To test our idea we submitted α -tosyloxy-p-nitroacetophenone, readily available from the corresponding acetophenone¹ (Scheme 2.2), to the reaction with 1,3-cyclohexadione. Under standard conditions using Proton Sponge as a base and quinuclidine as a catalyst the reaction went to the completion in about 10 minutes and the desired product was isolated in moderate yield. As bis(cinchona alkaloid)pyrimidines proved to be effective in the parent reaction, we decided to screen the quinidine catalysts previously synthesized in our group. A quick look at these initial results (Table 2.1) shows that, as expected, the enantioselectivity changes dramatically depending on the size of the front

group. Catalysts containing $R_1 = t\text{-Bu}$ (**QD-3** and **QD-4**) lead to almost racemic IFB product. Catalyst **QD-2**, which gave excellent enantioselectivities with α -bromopyruvates, produced the IFB product in a disappointing 46% ee. Eventually, we saw very noticeable enhancement of stereoinduction with catalyst **(QD)₂PYR** containing a phenyl group at the front position. Dihydroquinine-derived commercially available catalyst **(DHQD)₂PYR** allowed us to improve the ee by few extra percent (77% ee). Also, we synthesized the mono-quinidine catalyst with the same pyrimidine framework, but it resulted in decreased enantioselectivity when compared to the bis-catalyst.

Table 2.1 Initial catalyst screening

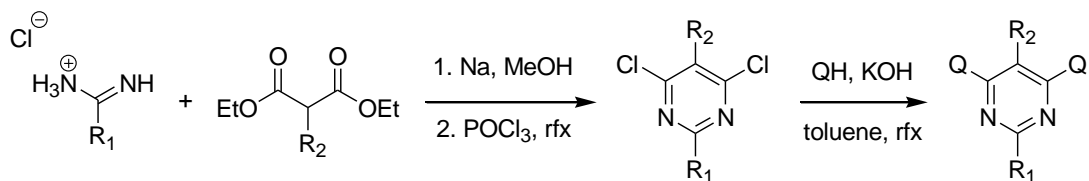


cat.	R_1	R_2	yield %	ee %
QD-2	H	Ph	79	46
QD-3	<i>t</i> -Bu	Ph	72	10
QD-4	<i>t</i> -Bu	<i>t</i> -Bu	69	11
QD-3	Ph	<i>t</i> -Bu	81	60
(QD)₂PYR	Ph	Ph	74	74
(DHQD)₂PYR			73	77
(QD)(Cl)PYR			75	63

Based on these preliminary results, we intended to improve enantioselectivity of the tested IFB reaction by introducing different aryl group at the front position of the catalyst (R_1). Following this idea, we could potentially explore how the electronic nature of the front group effects the enantioselectivity, as well as test the steric effect of the different substituents at ortho-, meta- and para-positions of the aryl group.

The typical reaction sequence for making bis(cinchona alkaloid) pyrimidines is well-documented and occurs in the following steps (Scheme 2.3). First, a condensation of amidine HCl salt and diethyl malonate in refluxing methanol with sodium methoxide produces the dihydroxypyrimidine ring, the hydroxyl groups of which can be converted into chlorines by refluxing with POCl_3 . Displacement of the pyrimidine chlorines then occurs by O-alkylation in refluxing toluene with KOH and the cinchona alkaloid.

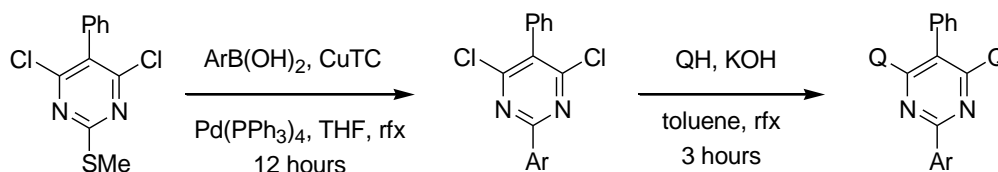
Scheme 2.3



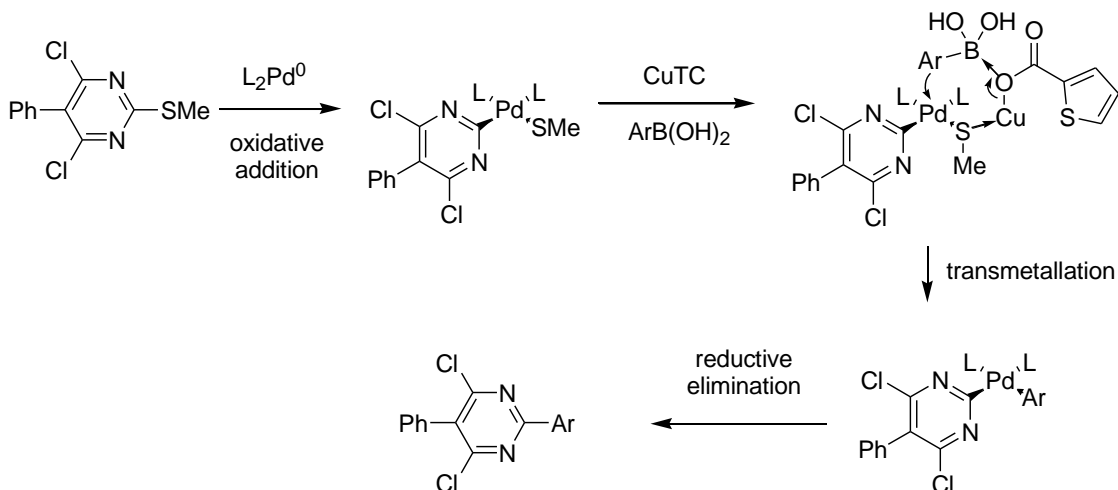
An alternative faster route to dichloropyrimidines is available via the Liebeskind-Srogl reaction (Scheme 2.4).² This reaction is an extension of the Suzuki coupling where the addition of a stoichiometric amount of Cu(I) carboxylate enables oxidative addition at a thiomethyl center. Unlike the Suzuki

reaction, the Liebeskin-Srogl coupling proceeds under non-basic conditions, and the oxidative addition is selective for the thiomethyl group in the presence of arylbromide or arylchloride bonds on the same pyrimidine ring (Scheme 2.5).

Scheme 2.4 Catalyst synthesis



Scheme 2.5 Liebeskind-Srogl reaction

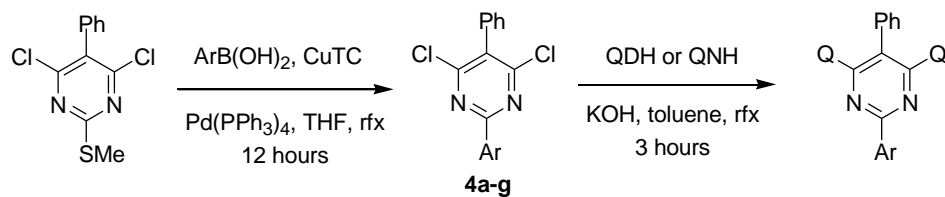


A variety of dichloropyrimidines were prepared using the Liebeskind-Srogl reaction starting from commercially available 2-thiomethyl-4,6-dichloro-5-phenyl pyrimidine. The coupling of both electron-rich and electron-poor aryl boronic acids proceeds smoothly giving the desired product in high yields. As any other Suzuki coupling, Liebesking-Srogl reaction is sensitive to the sterics

around the bond that is being formed in the reaction. As a result, yields suffered when large aryl boronic acids like 9-anthraceneboronic acid and 3-benzothiopheneboronic acid were reacted with 2-thiomethyl-4,6-dichloro-5-phenyl pyrimidine. No product was isolated from the reaction when 9-anthraceneboronic acid was used.

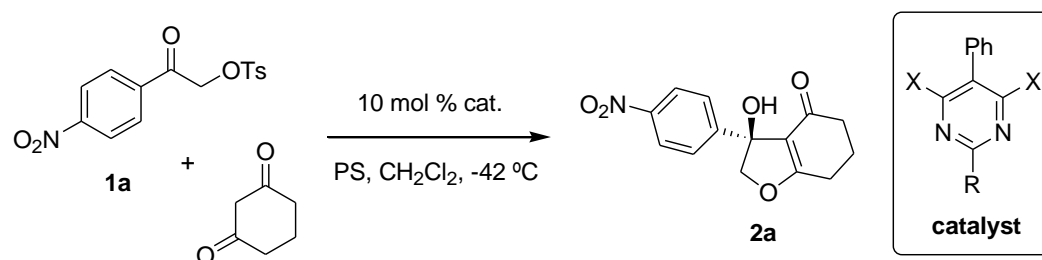
The resulting dichloropyrimidines react with cinchona alkaloids in the presence of KOH in refluxing toluene to afford the bis(cinchona alkaloid)pyrimidine catalysts. This final step appears to be very general giving the catalysts in excellent yields the only exception was the dichloropyrimidine with $R_1=3$ -nitrophenyl, where no product was isolated due to the decomposition of the starting dichloropyrimidine (Table 2.2).

Table 2.2 Synthesis of new catalysts



cat.	Ar	yield of 4	yield of cat.
QD-6		75	94
-		68	NR
QD-7		74	92
QD-8		71	85
QN-8		71	89
QD-9		73	93
QN-10		52	78
QN-11		43	71
-		NR	-

The catalyst screening was next extended to the newly synthesized catalysts (Table 2.3). A catalyst bearing an electron-rich 4-methoxyphenyl group in a front position produced the IFB product in 75% ee, making us conclude that the electronic nature of the R₁ group has a very small effect on enantioselectivity. The introduction of the 2,3-dimethylphenyl group noticeably improves the ee of the product (82%). We believe that a bigger aromatic ring between the nitrogens of pyrimidine could form a larger wall on one side of the quinuclidine active site of a catalyst leading to beneficial results. Gratifyingly, further improvement was realized when the related catalyst **QD-8** containing a 1-naphthyl group was used giving over 90% ee in the test reaction. At this point we wanted to make sure that the opposite enantiomers of the IFB product can be accessed in high ee if a quinidine-derived catalyst is applied. Hence, the quinidine version of the catalyst with 1-naphthyl group at R₁ position was synthesized and it gave the desired IFB product in 92% ee and 81% yield. Other catalysts containing large aryl groups, like 2-naphthyl, 9-phenanthryl or 3-benzothiophene, were found to be less effective for the reaction.

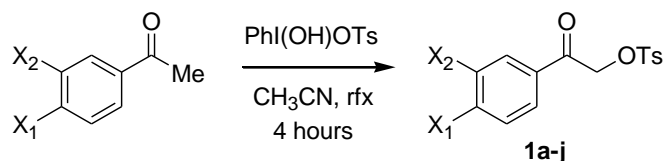
Table 1.3 Screen of new catalysts

cat.	R	yield %	ee %
QD-6	4-methoxyphenyl	81	75
QD-7	2,3-dimethylphenyl	83	82
QD-8	1-naphthyl	80	96
QD-9	2-naphthyl	78	65
QD-10	1-naphthyl	75	86
QN-8	1-naphthyl	81	-92
DHQN-8	1-naphthyl	75	-87
QN-10	9-phenanthryl	73	-84
QN-11	3-benzothiophene	79	-69

After identification of the appropriate catalyst we decided to examine the reaction scope. To test the generality of the reaction we synthesized a series of α -tosyloxyacetophenones that differ in the substitution on the aromatic ring (Table 2.4). Taking into the account the fact that α -tosyloxy-p-nitroacetophenone is probably the most reactive electrophile in series (due to the

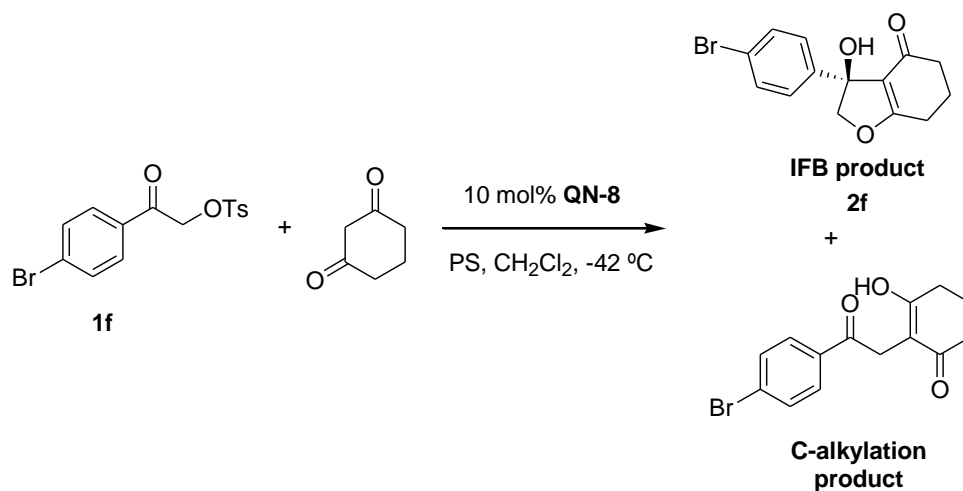
strong induction effect of the nitro group) we expected the IFB reactions of other substrates to require longer reaction times and/or higher reaction temperature in order to get the complete conversion of the starting material and high yields of the desired products. We also hoped that an excellent level of stereoselectivity could be achieved independent of the substitution on the aromatic ring of the electrophile with the same chiral catalyst.

Table 2.4 Synthesis of α -tosyloxyacetophenones



X₁	X₂	product	yield %
NO ₂	H	1a	73
CN	H	1b	77
CF ₃	H	1c	70
F	H	1d	62
Cl	H	1e	81
Br	H	1f	80
I	H	1g	81
H	H	1h	74
H	NO ₂	1i	80
H	Br	1j	77

To our disappointment we found that the less reactive α -tosyloxy-*p*-bromoacetophenone **1f** affords the desired product in an unsatisfying 51% yield under the same conditions. Still, the enantioselectivity of the IFB product was very high (95% ee). It turned out that significant fall of the yield was caused by competitive C-alkylation. The C-alkylation product is formed when the anion of 1,3-cyclohexanedione directly substitutes the tosyl-group. To optimize the reaction conditions we varied solvents, bases and temperatures (Table 2.5). The yield improves if reaction is run at higher temperature (0 °C), but the enantioselectivity drops down significantly in both CH₂Cl₂ and CH₃CN with PS at the same time. Switching from PS to K₂CO₃ allowed us to perform the reaction at higher temperature (0 °C) in acetonitrile without any loss of stereoinduction. Although reaction in CH₂Cl₂ gives better ratios of IFB vs C-alkylation product, and as a result better yield, the ee of the product is too low at 0 °C.

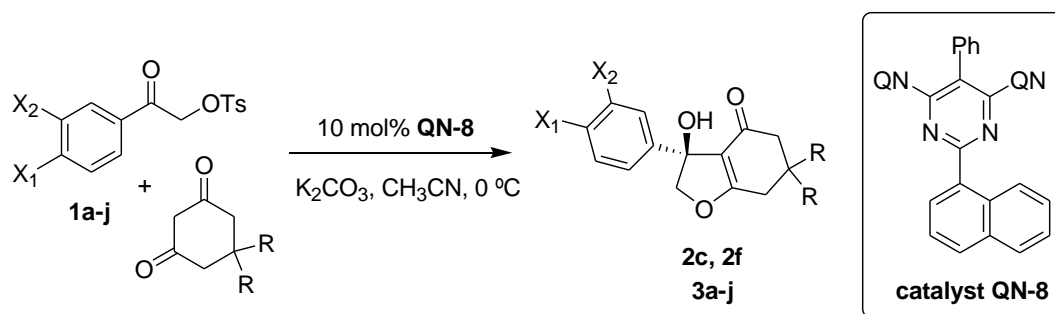
Table 2.5 Optimization for IFB product **2f**

solvent	temp.	base	IFB :		yield %	ee %
			C-alk.			
CH ₂ Cl ₂	-42	PS	1.2 : 1		51	95
CH ₂ Cl ₂	0	PS	9.0 : 1		76	82
CH ₃ CN	-28	PS	1.1 : 1		47	97
CH ₃ CN	0	PS	3.2 : 1		67	88
CH ₂ Cl ₂	-28	K ₂ CO ₃	8.9 : 1		73	86
CH ₂ Cl ₂	0	K ₂ CO ₃	32 : 1		85	80
CH ₃ CN	-28	K ₂ CO ₃	1.2 : 1		50	96
CH ₃ CN	0	K ₂ CO ₃	5.0 : 1		69	94

2.2 Substrate scope

With the optimized reaction conditions in hand, we tested the reaction scope. As was expected, the electron-withdrawing groups (NO₂, CN, CF₃) accelerate the reaction so it is done faster and yields of the IFB products are generally close to quantitative (Table 2.6) while enantioselectivity is at the reproducibly high level. The reaction with α -tosyloxy-*p*-nitroacetophenone **1a** can be carried out at lower temperature, which results in improvement of the ee (91% vs 95%) with no loss of yield in the product.

Table 2.6 Substrate scope

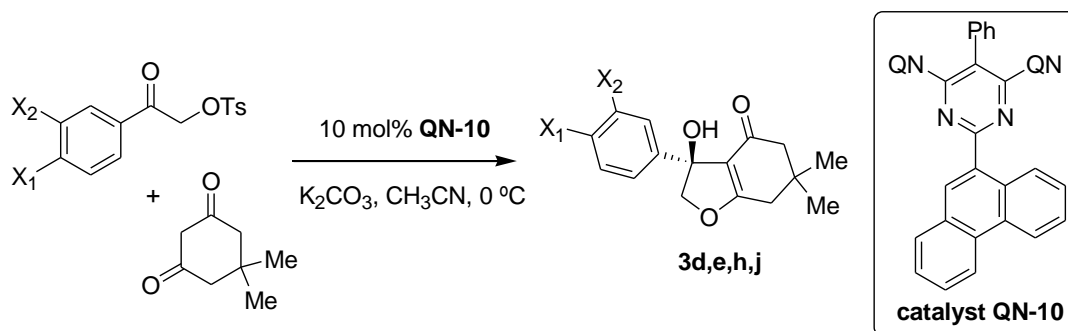


X₁	X₂	R	product	yield %	ee %
NO ₂	H	Me	3a	98	91
NO ₂	H	Me	3a	95	95*
CN	H	Me	3b	82	94
CF ₃	H	Me	3c	87	96
CF ₃	H	H	2c	90	98
F	H	Me	3d	76	90
Cl	H	Me	3e	69	84
Br	H	Me	3f	65	96
Br	H	H	2f	69	94
I	H	Me	3g	70	99
H	H	Me	3h	64	84
H	NO ₂	Me	3i	78	82
H	NO ₂	Me	3i	77	90*
H	Br	Me	3j	61	80

*reaction run at $-42\text{ }^\circ C$

Most of the *p*-halo-substituted α -tosyloxy-acetophenones give IFB products in excellent enantiomeric excesses and good yields with catalyst **QN-8**. To our disappointment, the reaction of *p*-chloro and unsubstituted α -tosyloxy-acetophenone showed reduced enantioselectivity with catalyst **QN-8**. Fortunately, we soon found that it can be significantly improved by switching to the catalyst **QN-10** containing 9-phenanthryl group at C-2 position (Table 2.7). Meta-substituted substrates also react with only slightly reduced ee and yields. Finally, both dimedone and 1,3-cyclohexanedione function as satisfactory nucleophiles for the reaction giving very similar results in terms of yields and enantioselectivities of the IFB products (Table 1.6, products **2c** and **2f**).

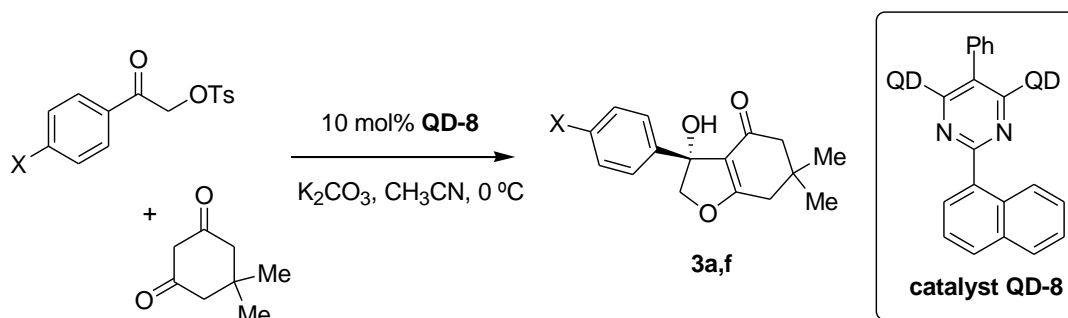
Table 2.7



X₁	X₂	product	yield %	ee %
F	H	3d	73	93
Cl	H	3e	71	96
H	H	3h	66	90
H	Br	3j	61	91

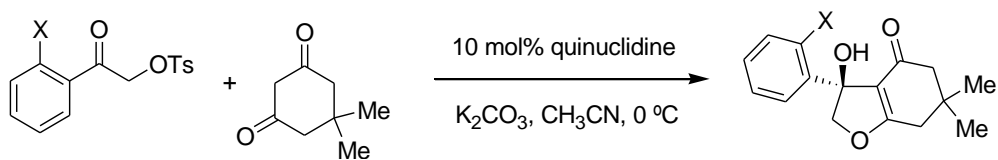
The opposite enantiomer of the IFB product can be achieved when the quinidine catalyst is used. Indeed, both nitro- and bromo- α -tosyloxy-acetophenone reacted with dimedone in the presence of catalyst with the same high level of stereoinduction (Table 2.8).

Table 2.8



X	product	yield %	ee %
NO ₂	3a	97	94
Br	3f	66	96

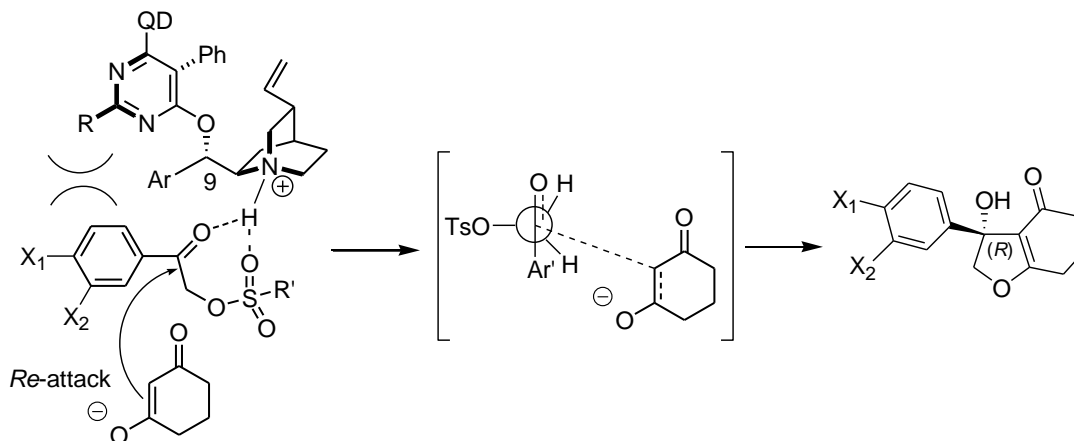
To our dissapointment, ortho-substituted substrates yielded no IFB product under similar reaction conditions. Even α -tosyloxy-acetophenones bearing the strongly activating nitro-group in the ortho-position did not produce any desired product (Table 2.9). This fact can be attributed to the increased angle between aryl ring and a carbonyl group and resulting additional steric hindrance around the carbonyl carbon that can shut down the initial aldol step of the IFB reaction.

Table 2.9

X	result
Br	NR
NO_2	NR

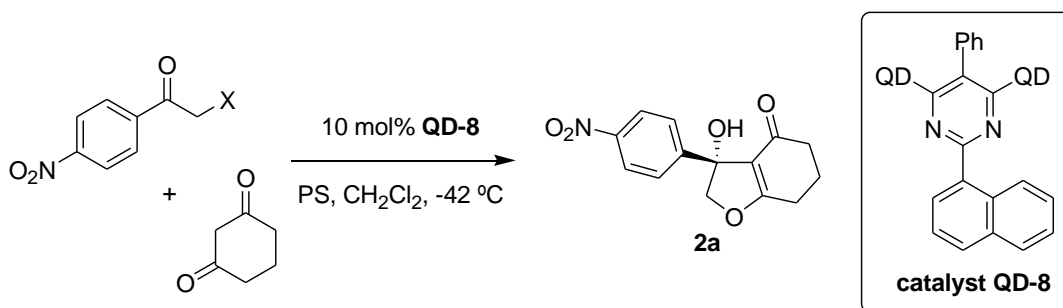
We assigned absolute stereochemistry of IFB product made in the reaction catalyzed by the quinine-catalyst by anomalous dispersion analysis of single crystal X-ray data. By analogy, the remaining IFB products were marked as *S*-isomers if quinine was used and *R* for quinidine-derived catalyst. This data suggests that the molecule of the electrophile arranges around the protonated catalyst in a way shown on Scheme 2.6. Presumably, the activation of the electrophile toward the nucleophilic attack is achieved through the bifurcated H-bond with the protonated catalyst. The aromatic group of the acetophenone points in the direction of the catalyst front group. In this case, the *Re*-face of the α -tosyloxyacetophenone is approachable for the nucleophilic attack resulting in a formation of the (*R*)-isomer of the IFB product.

Scheme 2.6 Transition state model for quinidine catalyst



This transition state model is in agreement with the results obtained for the IFB reaction of electrophiles containing different sulfonyl leaving groups (Table 2.10). In cases of nosylate and mesylate substrates the IFB product was isolated in similar high enantiomeric excesses suggesting that the size of the sulfonyl group does not affect much the arrangement of the electrophile around the protonated catalyst.

Table 2.10

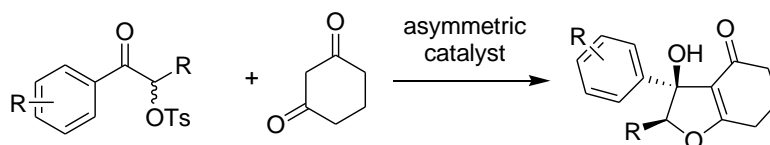


X	yield %	ee %
OTs	81	92
ONs	82	87
OMes	75	86

2.3 The IFB reaction of substituted α -tosyloxyacetophenones

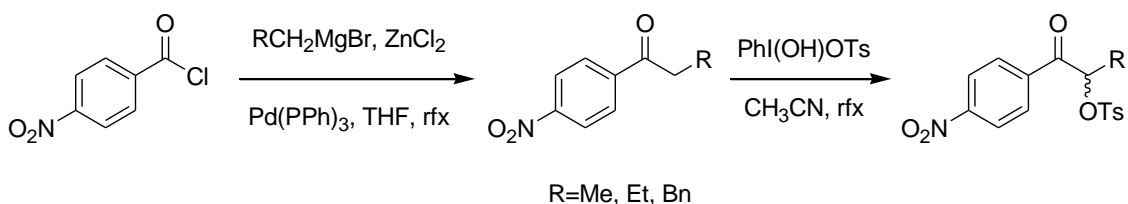
The related IFB reaction of the substituted α -tosyloxyketones can potentially lead to the tetra-substituted hydroxydihydrofurans containing two adjacent stereocenters. This process resembles the IFB reaction of the substituted α -bromopyruvates developed earlier.

Scheme 2.7



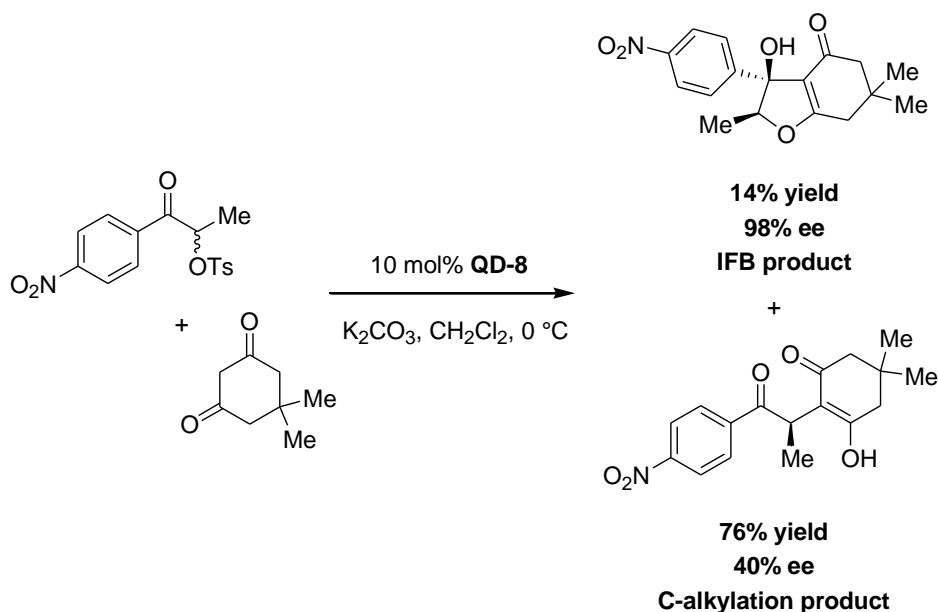
The synthesis of the required substrates is fairly straightforward (Scheme 2.8). The Pd⁰ catalyzed coupling of *p*-nitrobenzoyl chloride and the alkyl zinc reagent generated *in situ* from Grignard reagent delivers the aryl alkyl ketone.³ In the second step, alkyl ketone converted into the corresponding α -tosyloxyketone via the oxidation with Koser's reagent.

Scheme 2.8



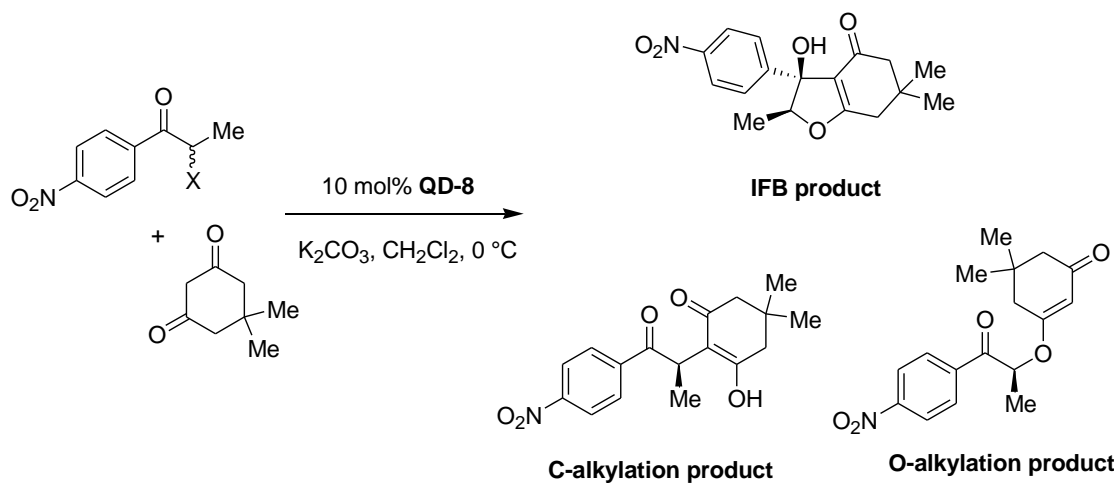
Performing the reaction of α -tosyloxy-*p*-nitropropiofenone under the standard reaction conditions resulted in a formation of the desired IFB product in excellent enantiomeric excess (Scheme 2.9). To our disappointment, this product was isolated in only 14% yield, as later was found due to the formation of the C-alkylation byproduct. Since the reaction of the substituted α -tosyloxyketone still allowed achieving high stereinduction with the same catalyst (98% ee), we intended to investigate this reaction further in order to improve the yield of the IFB product.

Scheme 2.9



We hoped that regioselectivity of this reaction could be turned in favor of the IFB product if other leaving groups are introduced at the place of tosylate. We synthesized a series of the related electrophiles with different sulfonyl groups (Table 2.11). Unfortunately, substrates with better leaving groups (nosylate, 2,4-dinitrobenzenesulfonate, triflate) tend to give the C-alkylation or O-alkylation byproduct. Further screening revealed that changing the leaving group from sulfonyl to bromine or chlorine allowed us to reverse regioselectivity of the reaction in favor of the IFB product. The experiment run with α -chloro-*p*-nitropropiophenone produced a mixture of the IFB and C-alkylation product favoring the IFB product. It was isolated in 65% yield, but unfortunately enantioselectivity dropped significantly (50% ee) compared to the reaction of α -tosyloxy-*p*-nitropropiophenone.

Table 2.11



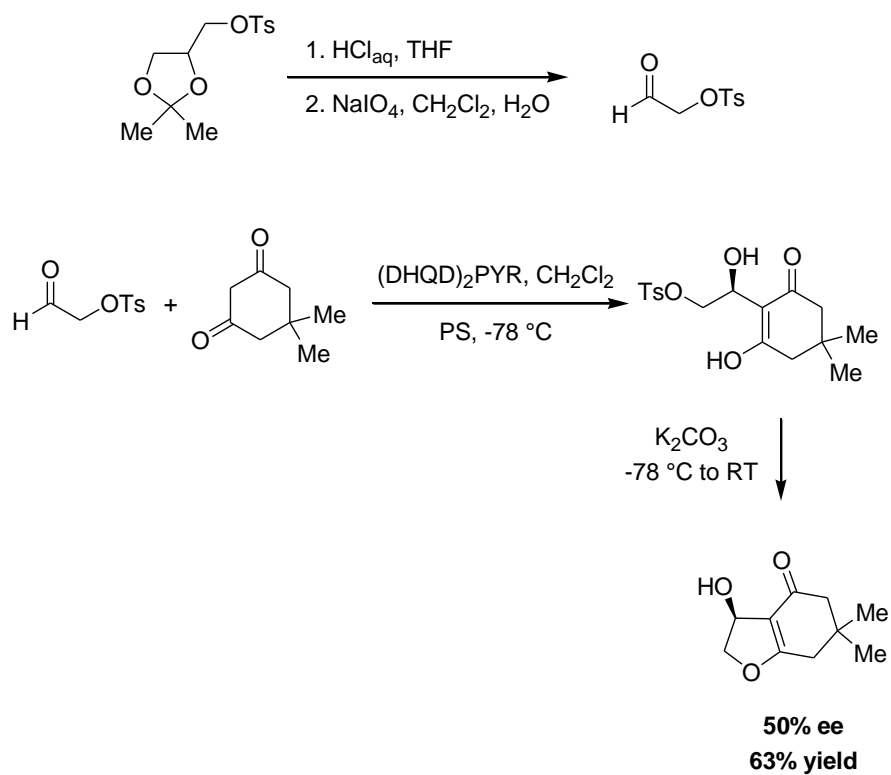
X	IFB/C-alk./O-alk.
ONs	0/100/0
2,4-dinitrobenzenesulfonate	0/0/100
OTf	0/0/100
Br	50/50/0
Cl	70/30/0

2.4 α -Tosyloxyaldehydes as electrophiles

Our attempts to optimize the IFB reaction of the substituted α -tosyloxyacetophenones found to be unsuccessful due to the formation of the C- and O-alkylation byproducts. These results suggest the insufficient electrophilicity of the carbonyl group in substituted α -tosyloxyacetophenones. As a further consideration, we recognized that α -tosyloxyaldehydes should provide us with a reactive carbonyl group and the increased electrophilicity should secure the fast aldol reaction resulting in the formation of the desired IFB product. The feasibility of the presented considerations was also supported by the related method recently published by Jorgensen⁴ and described in details in the first chapter.

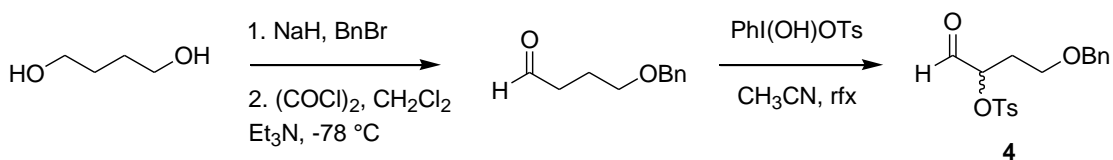
To test this hypothesis, we synthesized tosyloxyacetaldehyde⁵ according the literature procedure. Interestingly, the fast consumption of the starting material resulted in the formation of the aldol intermediate that slowly cyclizes into the desired hydroxydihydrofuran (Scheme 2.10). Thus, this reaction required a separate step in order to get the IFB product in high yield. This was achieved by the addition of the carbonate base to the reaction and warming it up to room temperature. Furthermore, the experiment performed in the presence of the chiral catalyst (DHQD)₂PYR resulted in the formation of the IFB product in moderated enantioselectivity.

Scheme 2.10 The IFB reaction of tosyloxyacetaldehyde



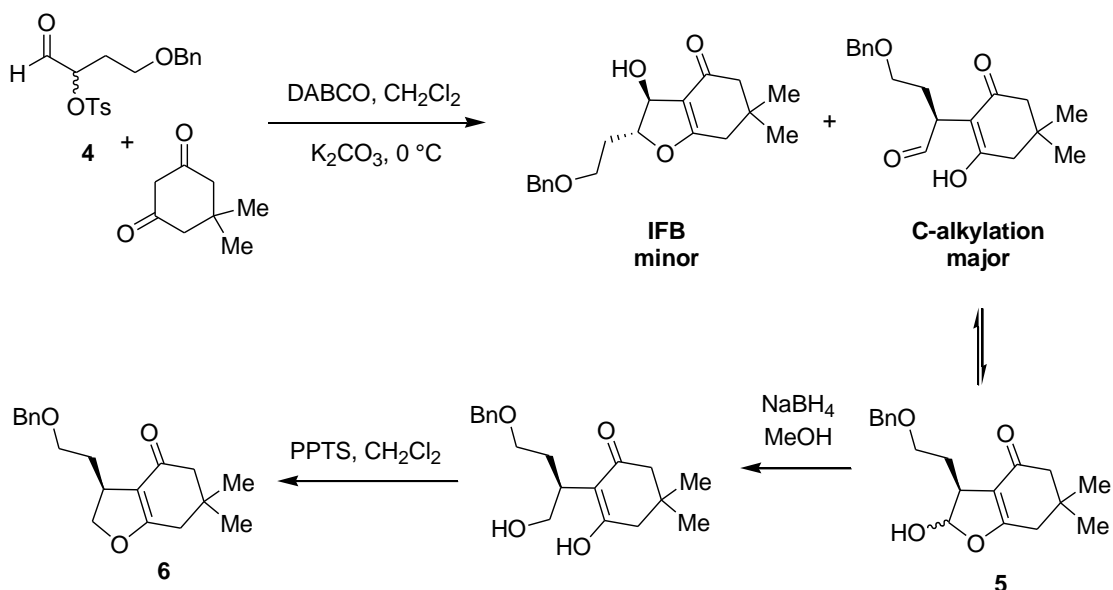
In analogy to the α -tosyloxyacetophenones, we next intended to investigate the reaction of substituted α -tosyloxyaldehydes. An appropriate substrate was successfully synthesized in a few straightforward steps starting from 1,4-butanediol.⁶

Scheme 2.10 Synthesis of **4**



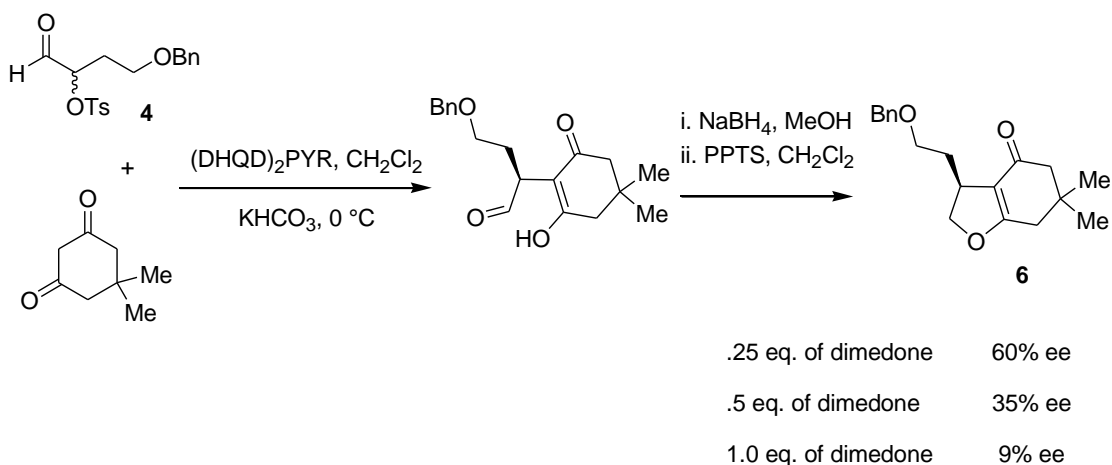
Surprisingly, the reaction of **4** only produced the small amount of the corresponding IFB product and the C-alkylation product was isolated in moderate yield, mostly in a form of hemi-acetal (Scheme 2.11). Further investigation revealed that this product can be easily transformed into the simple chiral dihydrofuran **6** through the reduction of aldehyde with sodium borohydride followed by the cyclization catalyzed by mild acid to deliver **6**.

Scheme 2.11 IFB reaction of **4**



In preliminary attempts to optimize this reaction we performed a series of experiments with quarter, half and full equivalent of dimedone in the presence of commercially available catalyst $(\text{DHQD})_2\text{Pyr}$. We were able to achieve moderate stereoselection with 0.25 mole equivalents of the nucleophile, but the reaction with one equivalent of dimedone resulted in nearly racemic product. These data suggest that the epimerization rate of the starting α -tosyloxyaldehyde is significantly lower than the rate of the reaction. Analogous to the α -bromopyruvate reaction we tried to achieve constant racemization by addition of the tosylate salt, but that did not lead to any improvement of the enantioselectivity in the product.

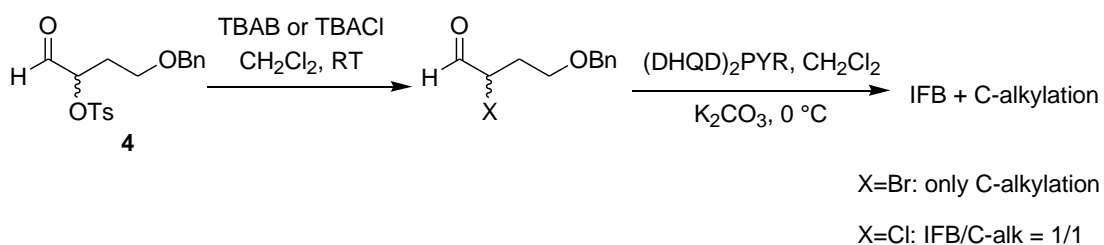
Scheme 2.12



We also tried to optimize this reaction for the IFB product. For that purpose, we made several new aldehyde electrophiles containing different leaving groups in the α -position. α -Bromoaldehyde still produced the C-

alkylation exclusively, while the switch to α -chloroaldehyde led to a mixture of both IFB and C-alkylation products.

Scheme 2.12



In summary, we developed a new variant of the IFB reaction utilizing α -tosyloxyacetophenones as electrophiles. The reaction gives a rise to hydroxydihydrofuran products **3a-j** in high enantioselectivities in the presence of cinchona alkaloid-derived catalysts **QD-8** and **QN-8**.

References

1. Abe, S.; Sakuratani, K.; Togo, H., Synthetic use of poly[4-hydroxy(tosyloxy)iodo]styrenes. *J Org Chem* **2001**, *66* (18), 6174-6177.
2. Liebeskind, L. S.; Srogl, J., Heteroaromatic thioether-boronic acid cross-coupling under neutral reaction conditions. *Org Lett* **2002**, *4* (6), 979-981.
3. Dai, Y. J.; Guo, Y.; Frey, R. R.; Ji, Z. Q.; Curtin, M. L.; Ahmed, A. A.; Albert, D. H.; Arnold, L.; Arries, S. S.; Barlozzari, T.; Bauch, J. L.; Bouska, J. J.; Bousquet, P. F.; Cunha, G. A.; Glaser, K. B.; Guo, J.; Li, J. L.; Marcotte, P. A.; Marsh, K. C.; Moskey, M. D.; Pease, L. J.; Stewart, K. D.; Stoll, V. S.; Tapang, P.; Wishart, N.; Davidsen, S. K.; Michaelides, M. R., Thienopyrimidine ureas as novel and potent multitargeted receptor tyrosine kinase inhibitors. *J Med Chem* **2005**, *48* (19), 6066-6083.
4. Albrecht, L.; Ransborg, L. K.; Gschwend, B.; Jorgensen, K. A., An Organocatalytic Approach to 2-Hydroxyalkyl- and 2-Aminoalkyl Furanes. *J Am Chem Soc* **2010**, *132* (50), 17886-17893.
5. Maguire, R. J.; Thomas, E. J., 1,5-Asymmetric Induction in Reactions between Aldehydes and [(4s)5-(Tert-Butyldimethylsilyloxy)-4-Hydroxypent-2-Enyl](Tributyl)-Stannane Promoted by Tin(IV) Chloride. *J Chem Soc Perk T 1* **1995**, (19), 2477-2485.
6. Perlmutter, P.; Selajerern, W.; Vounatsos, F., Enantioselective synthesis of the dioxabicyclo[3.2.1]octane core of the zaragozic acids via intramolecular Wacker-type cyclisation reactions. *Organic & biomolecular chemistry* **2004**, *2* (15), 2220-2228.

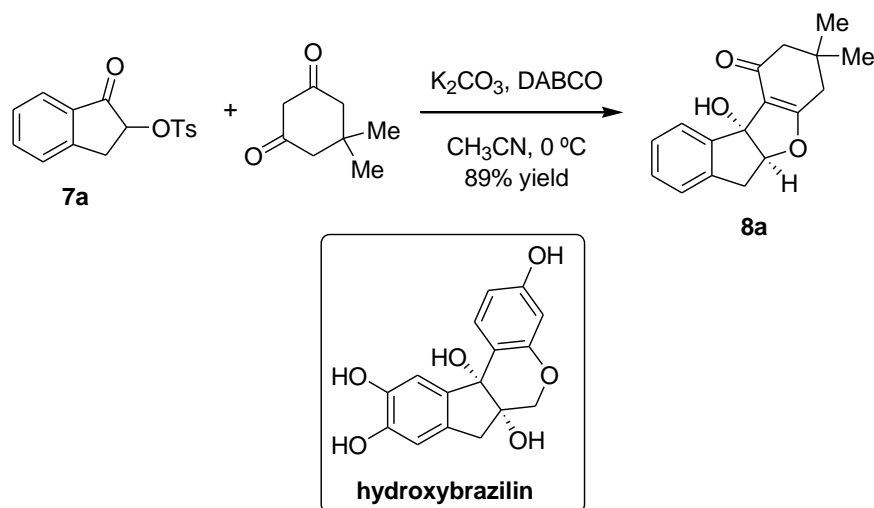
3. Catalytic, asymmetric IFB reaction of α -tosyloxyindanones

3.1 Initial optimization studies

Our attempts to optimize the IFB reaction of substituted α -tosyloxyketones proved to be unsuccessful due to the competitive formation of the C-alkylation product. Looking for new electrophiles, we decided to explore the reaction of cyclic α -tosyloxyketones. Engaging the α -tosyloxyketone moiety in a ring would change the relative orientation of the carbonyl group and tosylate and, therefore, might switch the regioselectivity in favor of the desired IFB product. To test this idea, we prepared α -tosyloxy-1-indanone **7a** and submitted it to the reaction with dimedone under the typical reaction conditions. To our delight, the desired IFB product **8a** was produced exclusively as a single diastereomer in 89% yield (Scheme 3.1). We decided to explore this reaction further, as it provides a one-step synthesis for the relatively complicated and functionalized tetracyclic hydroxydihydrofuran product bearing two adjacent stereocenters (one of which is quaternary), starting from easily accessible precursors. Besides that, the tetra-cyclic IFB product arising from this catalytic process highly resembles with hydroxybrazilin. This natural product is a member of the brazilin family.¹ The parent natural product brazilin has been used for years as a dye and a stain for the nucleus of cells. Few completed syntheses for brazilin have appeared recently², but no synthetic work has been done on hydroxybrazilin. This encouraged us for the development of the

asymmetric IFB reaction of α -tosyloxy-1-indanones that can find a direct application in the synthesis of hydroxybrazilin.

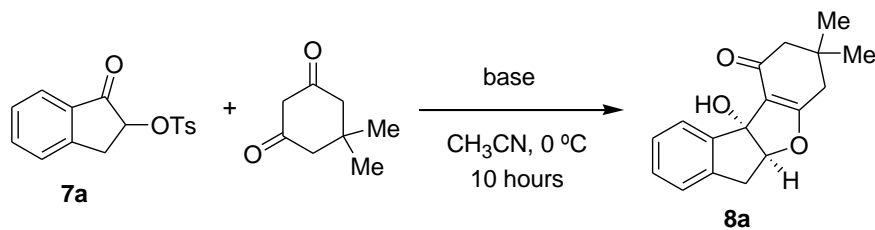
Scheme 3.1 IFB reaction of α -tosyloxyindanone **7a**



We began testing the IFB reaction of α -tosyloxy-1-indanone **7a** by screening the catalyst library available to us at the moment. To our disappointment, the IFB product was isolated in poor enantioselectivity in all the cases independent of the structure of the catalyst. These initial results prompted us to check for the background reaction as it could be responsible for the formation of racemic products. Indeed, we soon established that K_2CO_3 promotes the reaction with the rate comparable to the catalyzed reaction. Therefore, we proceeded to the optimization of the reaction conditions.

Initially, we screened some commonly used stoichiometric bases in order to prevent any background reaction (Table 3.1). Optimally, a base should be

weak enough to not catalyze the IFB reaction, yet still basic enough to pick up any acid that is produced as well as deprotonate any protonated cinchona alkaloid, thereby regenerating the catalyst. Proton Sponge, DBU and DMAP showed significant consumption of the starting α -tosyloxy-1-indanone. The soluble organic bases with lower pK_as (2,6-lutidine and N,N-diethylaniline) did not promote the reaction. Unfortunately, further experiments indicated that 2,6-lutidine and N,N-diethylaniline were not strong enough to regenerate the catalyst as the IFB product was only obtained in a small yield. Finally, we found that KHCO₃ is an optimal base since it is strong enough to recover the catalyst as the reaction proceeds without any noticeable background reaction.

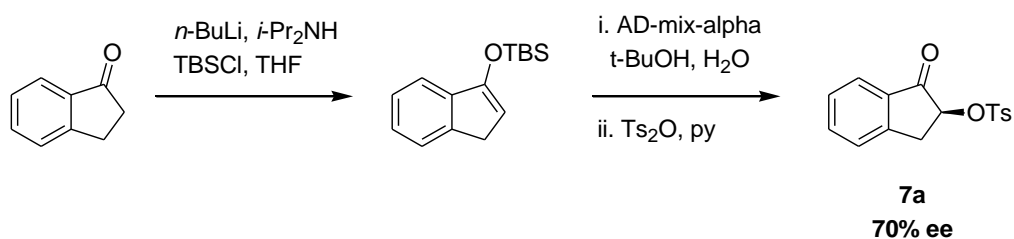
Table 3.1 Screen of bases

base	result
K ₂ CO ₃	100% conversion
PS	35% conversion
DBU	50% conversion
2,6-lutidine	no b/g reaction
N,N-diethylaniline	no b/g reaction
DMAP	50% conversion
N-(<i>n</i> -Bu)-imidazole	traces of IFB product
KHCO ₃	no b/g reaction

Since this reaction involves the kinetic resolution of the chiral α -tosyloxy-1-indanone, the stereoinduction most likely depends on the extent of conversion. In that respect this reaction should resemble the IFB reaction of substituted α -bromopyruvates described earlier. We hoped that the constant racemization of the starting material could be achieved either by the S_N2 reaction or by direct deprotonation at the α -position to the carbonyl group of the α -tosyloxy-1-

indanone. In order to check the rate of epimerization, we synthesized enantioenriched α -tosyloxy-1-indanone (Scheme 3.2). First, 1-indanone was enolized with *n*-butyllithium and the corresponding enolate was trapped with TBSCl. TBS enol ether was submitted to the standard Sharpless dihydroxylation protocol, which afforded the desired chiral hydroxyindanone. At the last step, it was tosylated using Ts₂O in pyridine (the use of TsCl resulted in the formation of α -chloro-1-indanone) providing us with α -tosyloxy-1-indanone **7a**. The enantioselectivity of the final product in this sequence was determined by HPLC to be 70% ee.

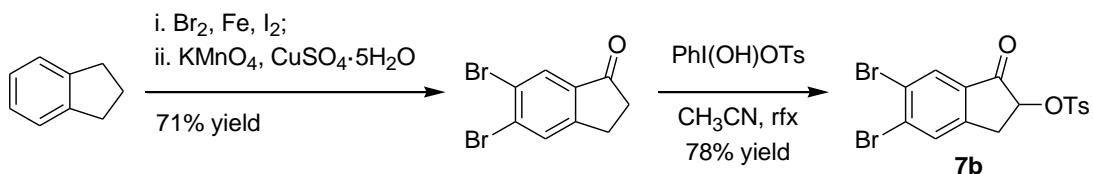
Scheme 3.2



To check the rate of racemization, the non-racemic α -tosyloxy-1-indanone was submitted to the typical reaction conditions (10 mol% DABCO, 1.5 eq K₂CO₃ in acetonitrile). The substrate was recovered after 10 hours and the purified sample was analyzed by HPLC. It turned out that it completely racemized under those conditions. Thus, this experiment has proven that the IFB reaction of α -tosyloxy-1-indanones can be run under the conditions of dynamic, kinetic resolution.

At this point we decided to switch to a more reactive electrophile, as the IFB reaction of α -tosyloxy-1-indanone appeared to be slow and gave complete conversion only after a week. Additionally, we wanted to maximize the similarity between the IFB product and hydroxybrazilin. Thus, we chose α -tosyloxy-6,7-dibromo-1-indanone **7b** for our further studies. Two bromines on the left aromatic ring can be substituted with the oxygens at late stage of the synthesis and at the same time they increase the electrophilicity of the carbonyl group by induction making the IFB reaction faster. This substrate was prepared in a few straightforward steps (Scheme 3.3). First, bromination of indane in the presence of an iron catalyst afforded 6,7-dibromoindane. In the next step, 6,7-dibromoindane was oxidized into the corresponding indanone with potassium permanganate. Finally, the standard procedure using Koser's reagent allowed us to make **7b** in high yield.

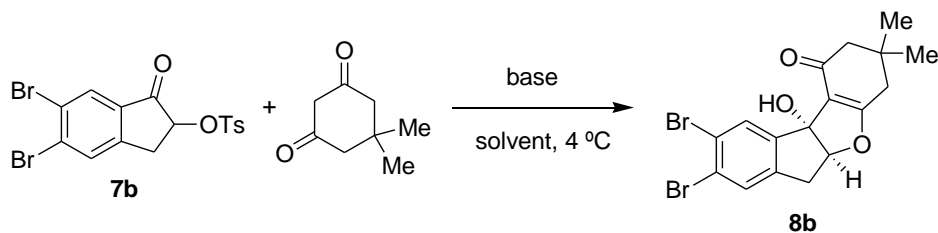
Scheme 3.3



Similar to the reaction of α -tosyloxy-1-indanone, electrophile **7b** provided the desired IFB product **8b** in high yield (Table 3.2). Prior to the catalyst screening we carried out some additional optimization studies. The nature of a base proved to be of importance again as we found that KHCO_3

promotes the reaction in acetonitrile. Several experiments with common bases showed that switching to the less polar solvents allows shutting down the background reaction. The proton sponge background reaction in toluene is very slow. Eventually, we found that potassium bicarbonate is an effective base in chloroform or toluene as it did not catalyze the reaction while turnover of the catalyst was still achieved.

Table 3.2



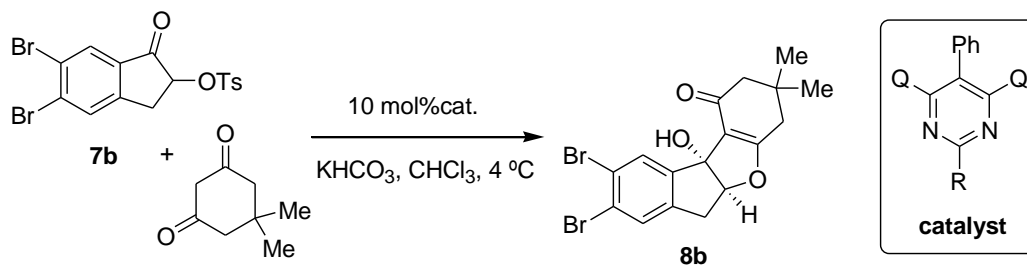
base	solvent	reaction time, hours	conversion %
K ₂ CO ₃	toluene	12	50
K ₂ CO ₃	chloroform	1.5	25
PS	CH ₂ Cl ₂	12	100
PS	toluene	24	<5
KHCO ₃	chloroform	12	0
KHCO ₃	CH ₃ CN	12	100
KHCO ₃	toluene	20	0
KHCO ₃	acetone	20	0

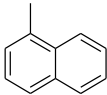
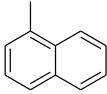
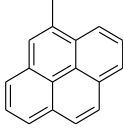
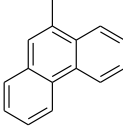
After identification of the optimal reaction conditions we proceeded to screening of the catalyst library that was available to us at the moment. In most cases we stopped the reaction after 12 hours by adding aqueous NaHCO₃. The crude product was purified on a silica gel column and used for the determination of the enantioselectivity. The conversion was calculated based on the ¹H NMR data of the crude reaction mixture.

The first attempt at an asymmetric reaction proved less than promising (Table 3.3). As usual, we started with the **(QD)₂PYR** catalyst. The reaction went to 30% conversion after 12 hours and, unexpectedly, gave racemic product. Further screening was expanded to the catalysts previously used for other IFB reactions developed in the group. The catalysts with small R groups (**QD-1** and **QD-2**) were also found to be ineffective. Further screening revealed that the catalysts with R=1-naphthyl and R=9-phenanthryl show slight improvements (24% ee and 28% ee, respectively). Additionally, the mono-quinidine catalyst **mono-QD-8** was tested and gave a very similar result compared to the bis-catalyst. It should be noted that the rate of the reaction depends on the size of the *front* group. The smallest catalyst **QD-2** gave 80% conversion after 12 hours, while the reaction with 1-naphthyl catalyst **QD-8** went to only 20% conversion after the same time. The enantioselectivity measured at 40% and 80% conversions for the H-catalyst was identical indicating that the rate of the epimerization of α -tosyloxyindanone is much greater than the rate of the

reaction, even in the absence of tosyl salt. A similar result was obtained with catalyst **QD-10**, as the IFB product was isolated in 30% ee after reaction reached 97% conversion after 3 days. Finally, additional solvent screening revealed that the reaction in toluene results in higher enantioselectivity, hence all further experiments were performed in toluene with KHCO_3 as a base.

Table 3.3 Initial catalyst screening



cat.	R	time, hours	conversion %	ee %
(QD)₂PYR	Ph	12	30	racemic
QD-2	H	6	40	16
		12	80	16
QD-1	SMe	12	50	15
QD-8		12	20	25
mono-QD-8		12	23	24
QD-12		12	25	30
QD-10		12	20	28
QN-10	-"	12	28	-35
QN-10	-"	72	97	-30
QN-10	-"	12	35	-42*

* reaction run in toluene

3.2 Initial catalyst screening

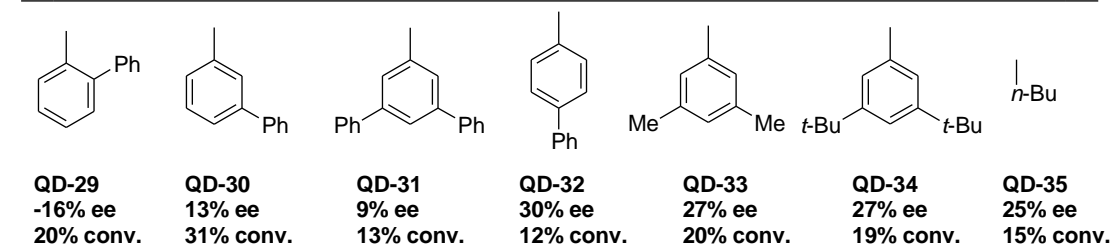
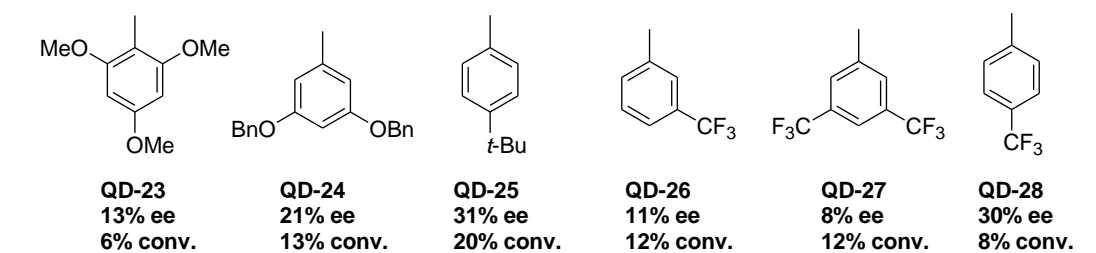
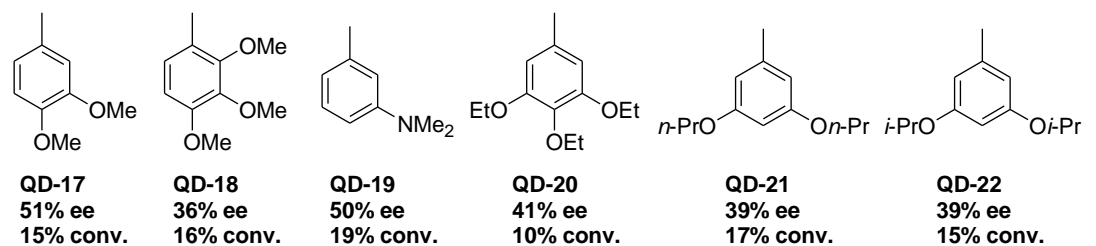
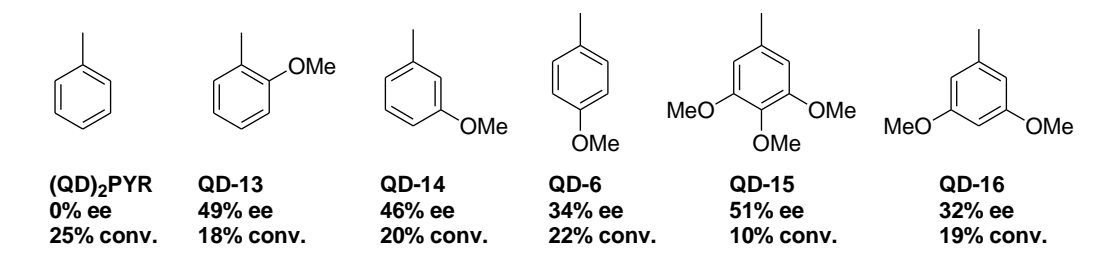
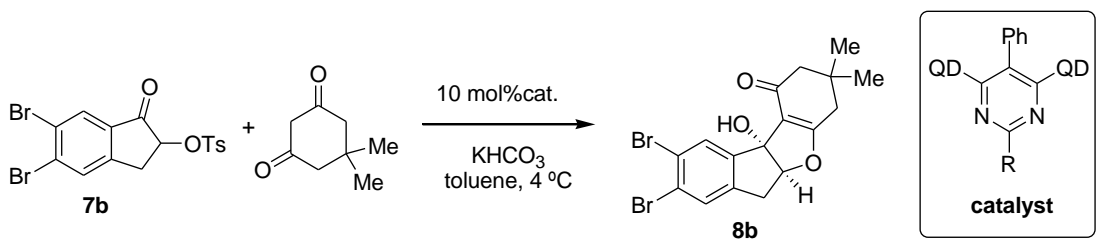
At the outset of these studies we were unable to make significant progress in asymmetric induction using the previously synthesized catalysts. Despite that fact, we decided to continue our search for the optimal catalyst. As postulated earlier, the *front* group is believed to be in close proximity to the active site of the protonated catalyst, and thus modifications of R group could translate into a more ordered transition state, which would lead to the higher enantioselectivity. Therefore, we decided to expand our catalyst library by introducing a broad range of ortho-, meta- and para-substituted aryl rings with diverse steric and electronic properties.

The first few results obtained with the new catalysts looked encouraging (Scheme 3.4). Performing the reaction in the presence of catalyst **QD-13** with a methoxy group in the ortho- position clearly provided significant improvement of the enantioselectivity (49% ee). Since introduction of the methoxy group turned out to be beneficial, we synthesized a set of the catalysts modified with electron-donating substituents. To our disappointment, the meta-OMe and para-OMe catalysts were found to be less effective for the reaction. Further screening revealed that the catalyst with **QD-15** R=3,4,5-trimethoxyphenyl showed slight improvement (51% ee). In the next part of the screening we decided to introduce other alkoxy groups with longer alkyl chains, such as ethyl, propyl, *i*-

propyl and benzyl. Unfortunately, these modifications did not lead to any increase of enantioselectivity in the IFB product.

Since the introduction of substituents on the *front* phenyl group affected the outcome of the tested reaction in a positive way, we continued our search by turning our attention to electron-withdrawing substituents. To our disappointment the use of catalysts **QD-26** and **QD-28** modified with $-(\text{CF}_3)$ groups at meta- or para-positions failed completely. Additionally, the incorporation of biaryl *front* groups into the catalyst architecture also did not provide increased enantiopurity.

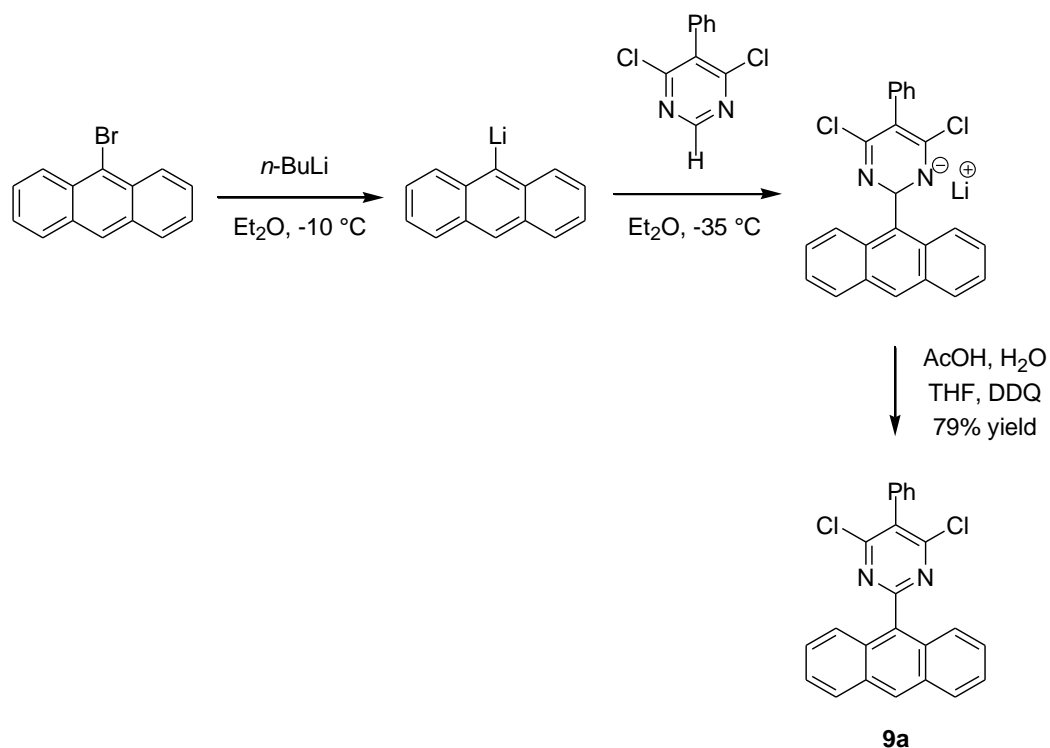
Scheme 3.4 Catalyst screening



Even though we were able to make some progress in the asymmetric induction, it was still far away from the desired synthetically useful level. At this point, it was obvious that catalyst modification with electron-donating or electron-withdrawing groups could not provide further enhancement in the enantioselectivity of the IFB product, thus, our catalyst screening study proceeded further with a focus on big aryl groups in the *front* position of the catalyst. We decided to commence with the catalyst bearing a 9-anthracenyl group in the *front* position. Our attempts to utilize the Liebeskind-Srogl reaction conditions for the coupling of 5-phenyl-4,6-dichloropyrimidine with 9-anthraceneboronic acid proved to be unsuccessful even when large excess of the boronic acid was used along with the prolonged reaction time. This low reactivity is not surprising and it arose from the increased steric hindrance around the biaryl bond which is being formed in the reaction. A literature search provided an alternative method for the construction of this molecule³. It involves the direct addition of the aryl lithium species (generated *in situ* from arylbromide or aryl iodide and butyllithium via metal-halogen exchange) to the most electrophilic carbon of the 4,6-dichloropyrimidine, breaking the aromaticity of the pyrimidine ring (Scheme 3.5). This intermediate is oxidized back with DDQ to afford the desired compound **9a**. This method is substantially more efficient than previously described syntheses of dichloropyrimidines utilizing the condensation of diethylmalonate with an amidine or the Liebeskind-Srogl coupling. Notably, it turned out that this reaction is not sensitive to the size

of the group being coupled, so large di-ortho-substituted arenes can be easily introduced in a *front* position of a catalyst. Generally, any arylbromide or aryl iodide can be coupled using this procedure as long as it withstands the conditions of metal-halogen exchange.

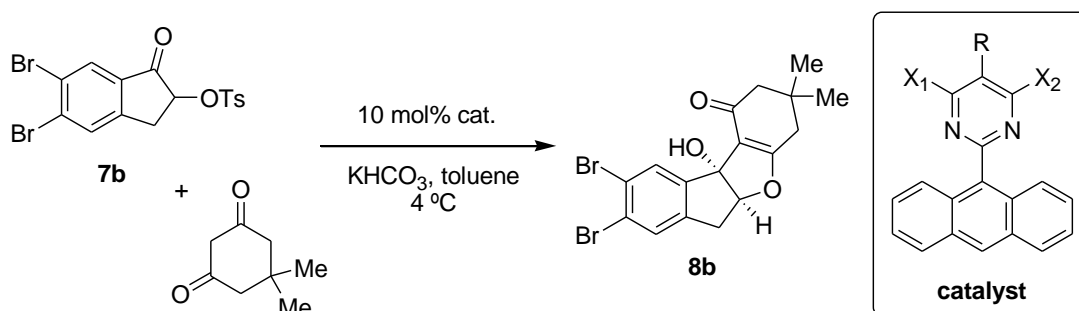
Scheme 3.5 Synthesis of dichloropyrimidine **9a**



The synthesis of dichloropyrimidine **9a** proceeded smoothly and this compound was subsequently used for the preparation of bis-quinidine catalyst (Table 3.4). To our disappointment, this catalyst failed completely giving racemic IFB product.

difference in stereoselectivities between the bis- and mono-quinidine catalysts, it is important to note that the opposite enantiomer of the IFB product was formed in excess. The catalyst screening was next extended to the bis- and mono-quinine catalysts. To our delight, further improvement was realized with the mono-quinine catalyst that gave the IFB product in 55% ee.

Table 3.4



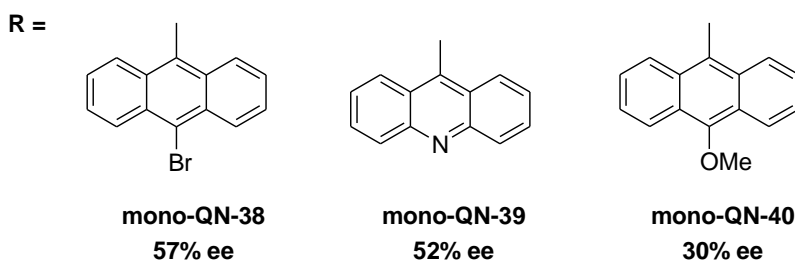
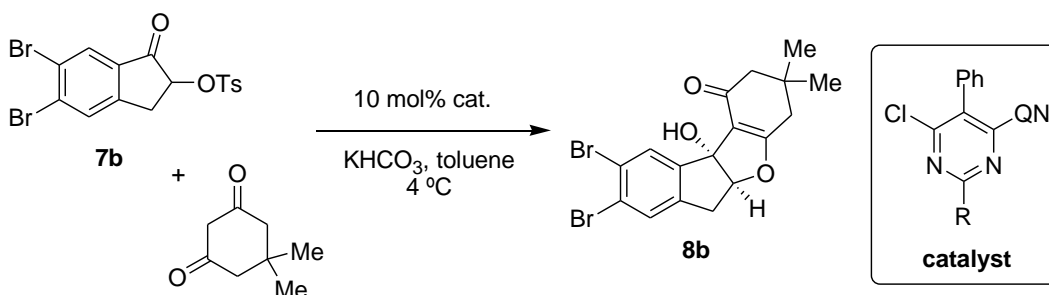
cat.	R	X ₁	X ₂	conv. in 12 hours	ee %
QD-36	Ph	QD	QD	10	-2
mono-QD-36	Ph	QD	Cl	12	-41
QN-36	Ph	QN	QN	9	18
mono-QN-36	Ph	QN	Cl	10	55
mono-QN-37	H	QN	Cl	12	25

The result obtained with the 9-anthracene catalysts **mono-QN-37** suggests that the incorporation of the 9-anthracene group in the catalyst

architecture leads to the conformational changes in the electrophile-protonated catalyst intermediate. We presume that a such drastic difference in behavior of catalyst can be rationalized by the fact that the increased substitution around pyrimidine-Ar biaryl bond presumably increases the biaryl angle, thereby pushing the distal ring of the anthracene group closer to the active site of the catalyst. Consequently, the electrophile faces additional steric strain with the *front* group changing its orientation around the protonated catalyst. As a result, the opposite side of the α -tosyloxyindanone becomes more accessible for the nucleophilic attack and the opposite enantiomer of the IFB product is obtained in excess compared to the previously investigated catalysts.

In our further attempts to improve the enantioselectivity of the IFB reaction we expanded our screening to the catalysts with the modified 9-anthracene group. Readily accessible 9,10-dibromoanthracene was used for the synthesis of the mono-quinine catalyst. It provided slight improvement of the enantioselectivity giving the IFB product in 57% ee (Scheme 3.6). Two other catalysts synthesized for this series were derived from bromoacridine⁴ and 9-bromo-10-methoxyanthracene⁵, but, unfortunately, their use was not beneficial for the tested IFB reaction.

Scheme 3.6

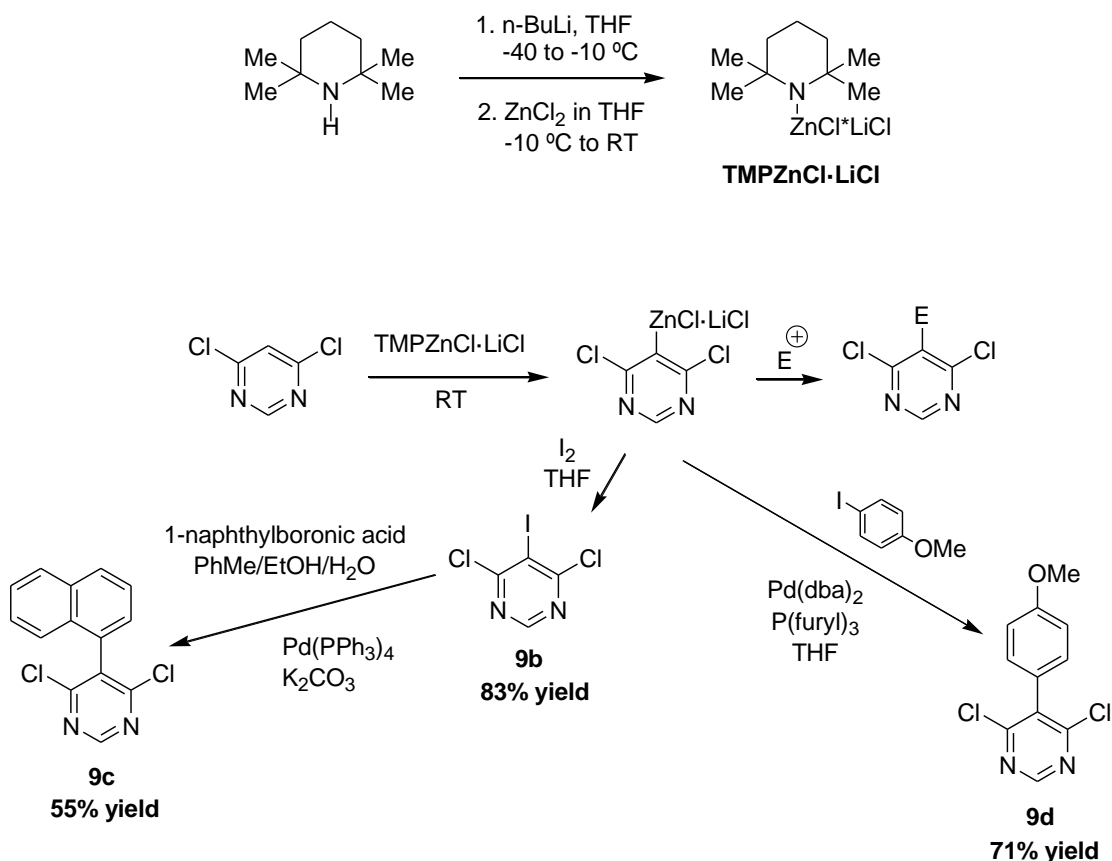


We hypothesized that the nature of the *front* group has an essential role in the determination of the enantioselectivity in the IFB reaction, since, in the most stable conformation of the protonated catalyst the group between two nitrogens of the pyrimidine ring points directly to the active site of the catalyst. At the same time, the steric interaction between the *back* group and the terminal alkene of the cinchona alkaloid moiety leads to a conformational change as well, thus influencing the stereoselection produced in the reaction. Based on these mechanistic considerations we decided to expand our catalyst library via modifications at the 5-position of the pyrimidine ring.

Literature provided a few ways to introduce different aryl groups at the 5-position of the dichloropyrimidine ring. In the report by Paul Knochel⁶

activated arenes and heteroarenes are metalated at room temperature using TMPZnCl·LiCl, an exceptionally mild and efficient base (Scheme 3.7). The resulting zincdichloropyrimidine can be trapped with different electrophiles. Trapping with iodine furnishes 5-iodo-4,6-dichloropyrimidine **9b** in 83% yield. This compound can be further used in Suzuki coupling reactions to deliver dichloropyrimidines modified at 5-position. Additionally, a Negishi coupling of arylzinc with the aryl iodides gives a quick access to the desired dichloropyrimidine in one step.

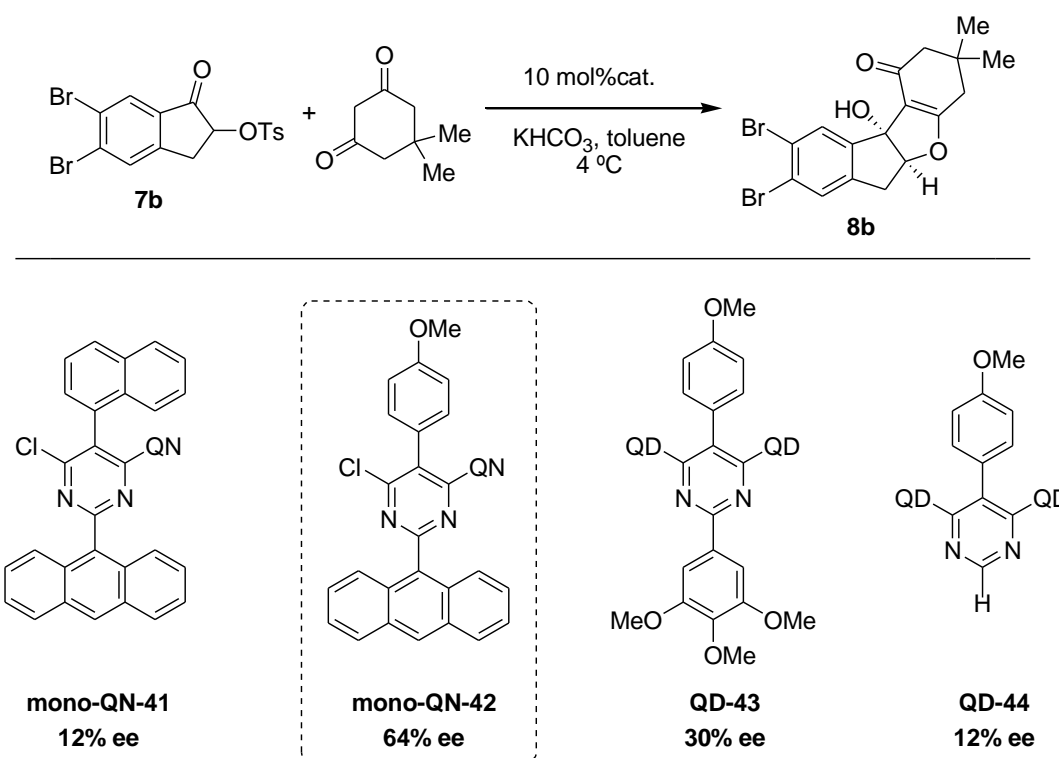
Scheme 3.7 Knochel's synthesis of dichloropyrimidines



Thus, several new dichloropyrimidines were prepared according to the Knochel's method. The last two steps of the catalyst synthesis worked without any complications, so we proceeded to the screening of the newly prepared catalysts (Scheme 3.8). The introduction of a big aryl group (like 1-naphthyl) in the back position of the catalyst led to a significant drop in the enantioselectivity (**mono-QN-41**). The next modification was to a *p*-methoxyphenyl group and, gratifyingly, gave enhanced stereinduction (64% ee). Unfortunately, our

attempts to utilize this strategy further proved to be unsuccessful, so we turned our attention back to the modification of the *front* group of the catalyst.

Scheme 3.8

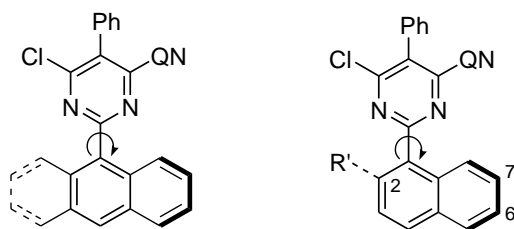


3.3 Final state of the catalyst screening

Taking into account our mechanistic considerations, we assumed that the distal ring of the anthracene group in catalyst comes closer to the active site as a result of the increased pyrimidine-9-anthracene biaryl angle. The second distal ring in this case only creates the additional bulk on the opposite side of the pyrimidine ring that is required for the increased biaryl angle. Consequently, we

proposed that an asymmetric 1-naphthyl group with a substituent at position 2 would substantially behave in a similar fashion, and the size of the group R' would determine the biaryl angle (Scheme 3.9).

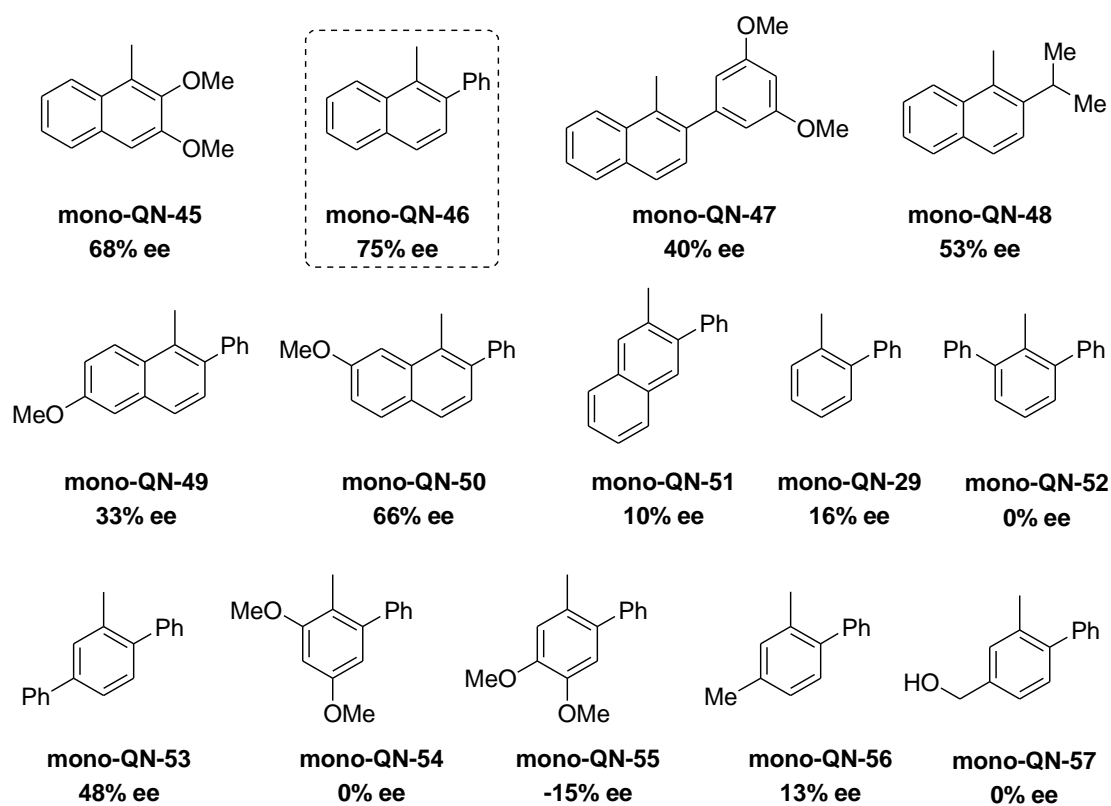
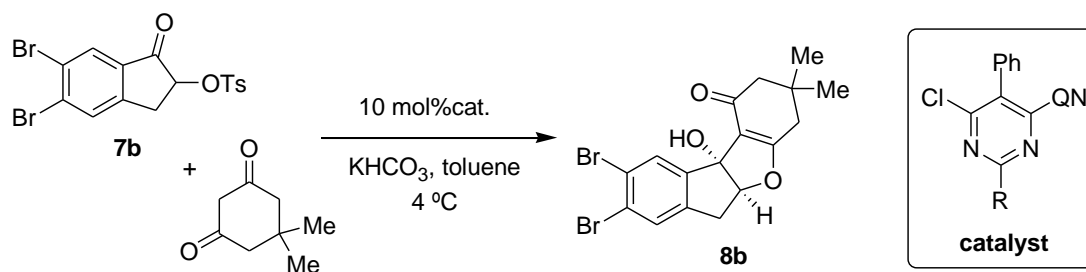
Scheme 3.9



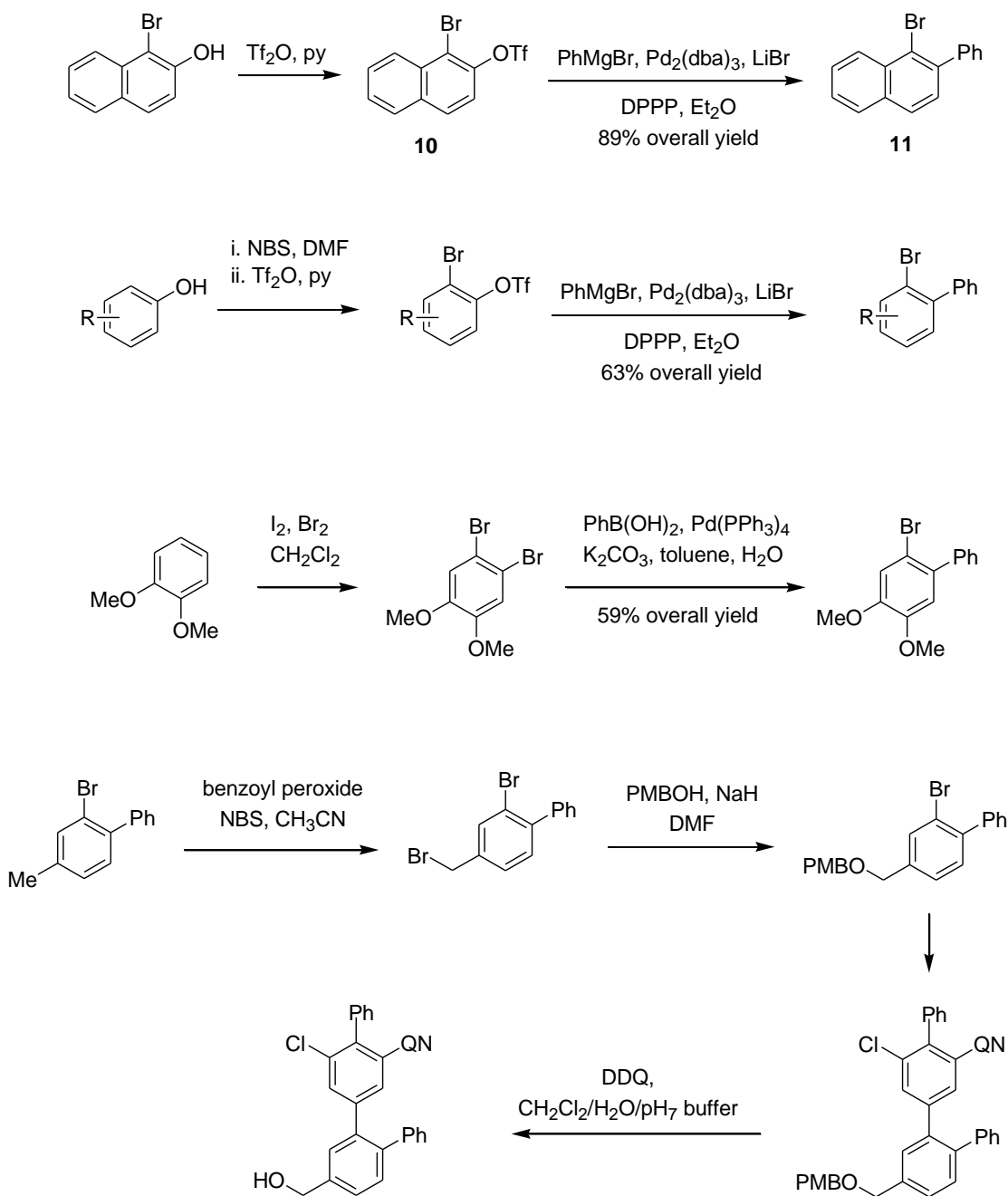
A quick search revealed that 1-bromo-2,3-dimethoxynaphthalene is a commercially available compound, and it was successfully used for the synthesis of catalyst **mono-QN-45**. If our suggestion is correct, this catalyst, unlike 1-naphthalene catalyst **QN-8**, should lead to the formation of the same stereoisomer of the IFB product in excess as in case of 9-anthracene catalyst **mono-QN-36**. Gratifyingly, the IFB product was isolated in 68% ee when **mono-QN-45** was used as a catalyst (Scheme 3.10). This result suggests that the further increasing in the size of the group at 2-position of the naphthyl ring could lead to additional improvement in the enantioselectivity. In order to test this hypothesis we wanted to make several catalysts with R'=aryl or sterically demanding alkyl groups. A literature search revealed the previously synthesized 1-bromo-2-phenylnaphthalene⁷. This compound can be prepared starting from commercially available 1-bromo-2-naphthol (Scheme 3.11). In the first step of

the synthesis aryltriflate **10** was made by reaction of bromonaphthol with Tf₂O. Next, **10** was used for coupling with phenylmagnesium bromide in the presence of a Pd⁰ catalyst to deliver 1-bromo-2-phenylnaphthalene **11**. The last two steps of the catalyst synthesis were not problematic giving catalyst **mono-QN-46** in excellent yield. Much to our delight, it afforded further enhanced enantioselectivity (75% ee) ensuring that we are moving in the right direction. Unfortunately, further modifications at the 2-position (**mono-QN-47**, **mono-QN-48**) only led to diminished enantioselectivities with both aryl and alkyl groups.

Scheme 3.10



Scheme 3.11

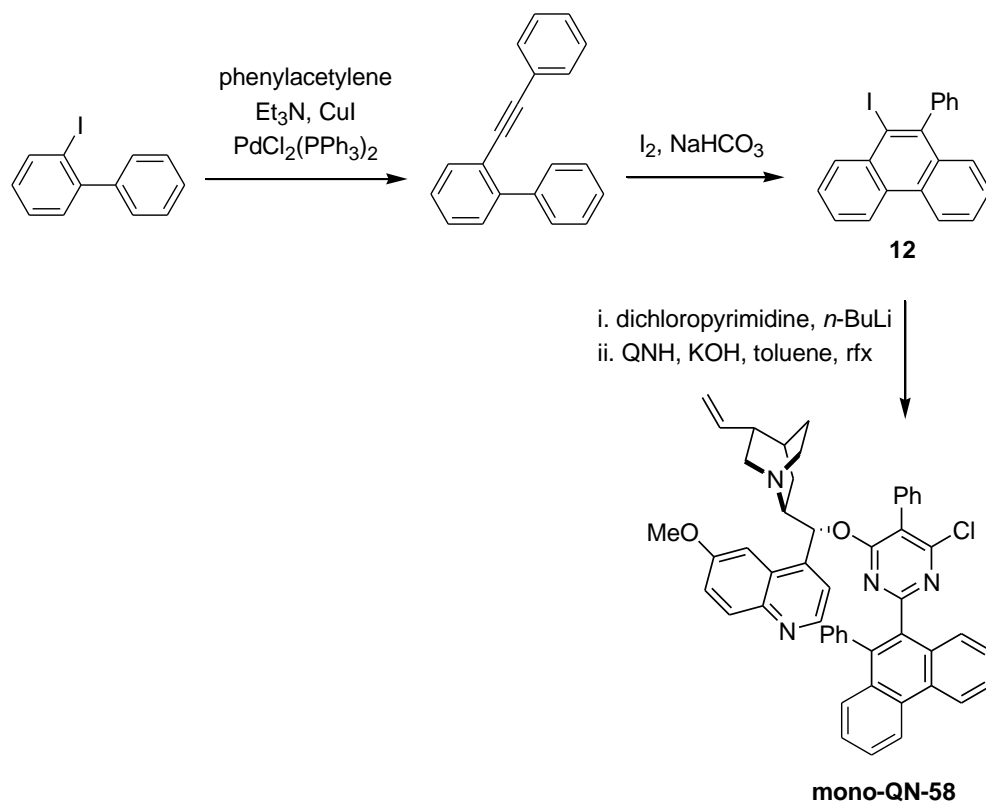


As a further consideration, we recognized that carbons 6 and 7 of the naphthalene ring are in close proximity to the active center of the catalyst, thus

modifications at these positions could potentially lead to beneficial results. The catalyst synthesis was fairly straightforward, starting from the corresponding naphthol (Scheme 3.11). Unfortunately, this suggestion proved to be wrong as methoxy substituted catalysts only led to decreased enantioselectivities (Scheme 3.10, catalysts **mono-QN-49**, **mono-QN-50**). Additionally, the screening was next extended to the catalysts with a 1-(2-phenyl)phenyl group in the *front* position. Unfortunately, our attempts failed completely, as none of these catalysts gave the ee higher than 48%. The data suggest that only big aryl groups allow achieving reasonable level of stereinduction and any bulky substituents would lead to diminished enantioselectivity.

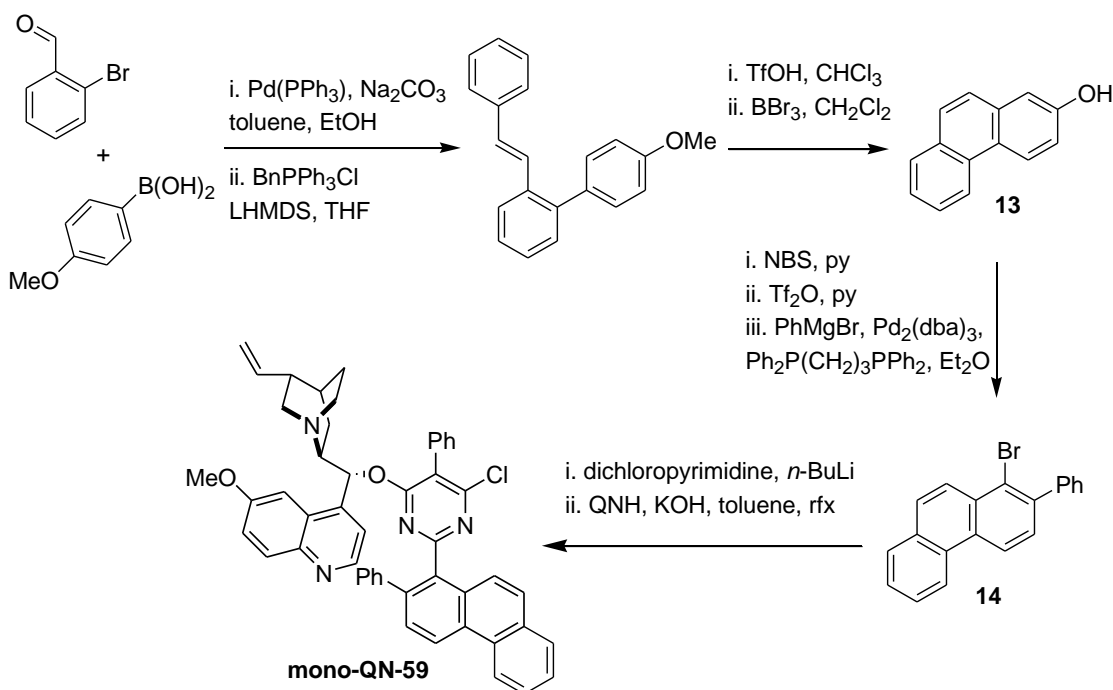
At this point we proceeded further in our attempt to optimize the IFB reaction of tosyloxyindanone **7b**. In our consideration we anticipated that a bigger aryl group in the *front* position of the catalyst could shield one side of the quinuclidine active center more effectively leading to the higher enantiocontrol in the reaction. For this reason, we prepared several catalysts with phenanthrene or anthracene groups. 9-iodo-10-phenylphenanthrene was prepared according to the literature procedure in two straightforward steps⁸ (Scheme 3.12). Compound **12** was successfully coupled with dichloropyrimidine and the desired mono-quinine catalyst **mono-QN-58** was obtained in high yield. To our disappointment, the IFB reaction in the presence of catalyst produced the product in only 58% ee.

Scheme 3.12 Synthesis of catalyst **mono-QN-58**



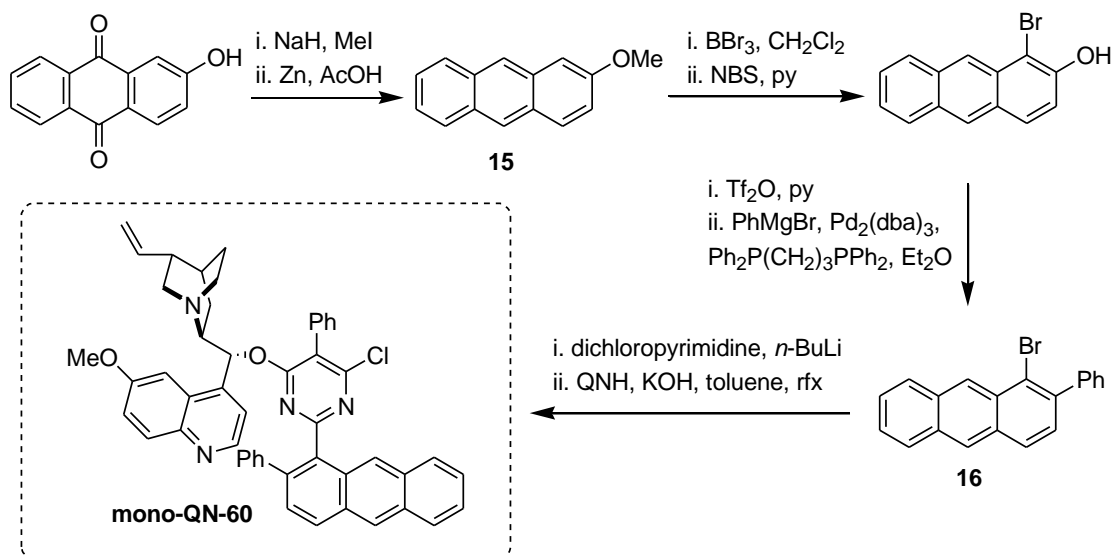
Another catalyst containing a phenylphenanthryl group in the *front* position of the catalyst was synthesized starting from 2-bromobenzaldehyde (Scheme 3.13). 2-Bromobenzaldehyde was converted into 2-methoxyphenanthrene **13** in three steps utilizing the procedure described in the literature⁹. As usual, we did not face any problems at the final stage of the catalyst synthesis, so catalyst **mono-QN-59** was successfully achieved in decent yield. Unfortunately, it did not give any further improvement as the IFB product **8b** was isolated in only 72% ee.

Scheme 3.13



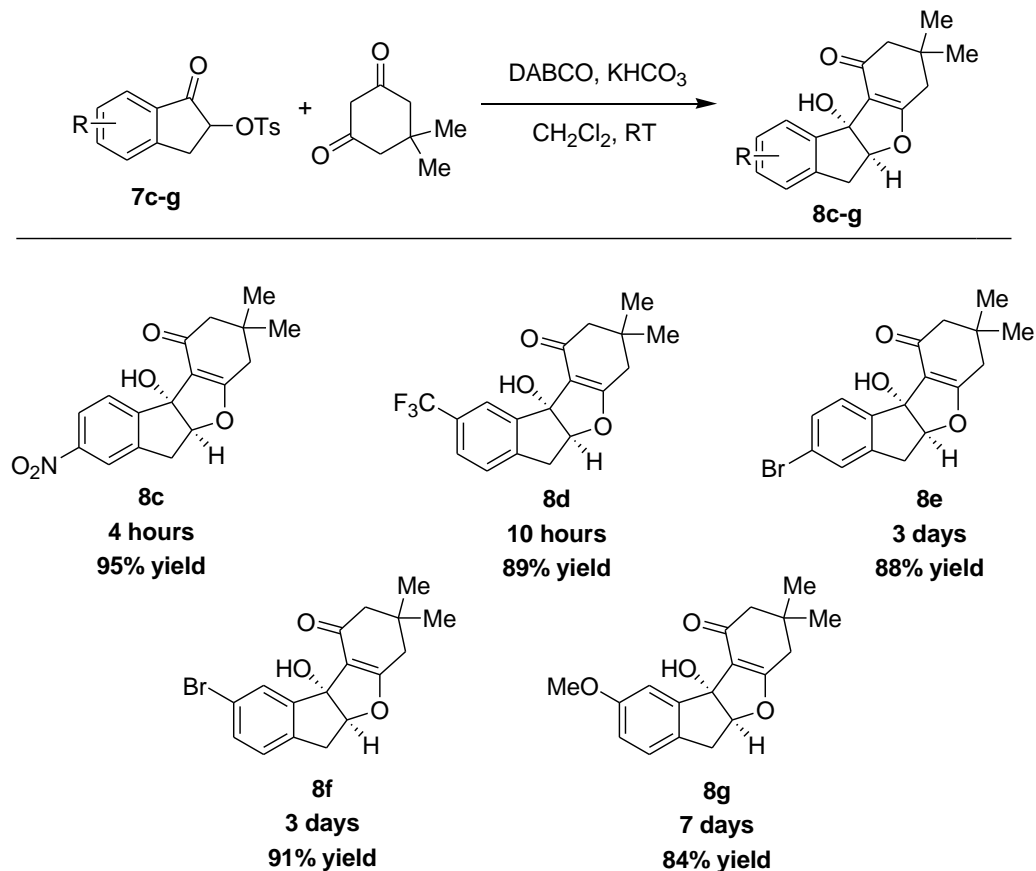
It occurred to us that addition of an extra phenyl ring to the distal end of the naphthalene ring could be beneficial for the enantioselectivity. We started the synthesis of this catalyst with 2-hydroxyanthraquinone (Scheme 3.14). First, the phenol was protected as methyl ether, and the resulting 2-methoxyanthraquinone was reduced with zinc in acetic acid to deliver 2-methoxyanthracene **15**. Then, several straightforward, previously described steps allowed access of the desired 1-bromo-2-phenylanthracene **16** without any complications. Finally, catalyst **mono-QN-60** was made and we were delighted to observe that this catalyst gave a sizable increase affording the IFB product in 84% ee.

Scheme 3.14



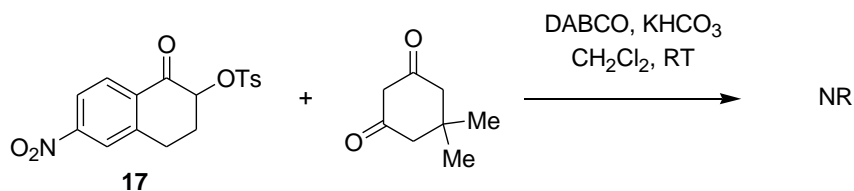
It should be noted that this IFB reaction is not limited to α -toxyloxy-6,7-dibromoindanone. We synthesized several substrates bearing electron-donating or electron-withdrawing substituents on the aromatic ring. In all cases, the IFB products **3.2c-g** were successfully isolated in high yields, although the reaction rate varied significantly (Scheme 3.15). As further consideration, we plan to expand the substrate scope of the IFB products **8c-g** we can achieve in high enantioselectivity and we hope to observe the same high level of stereoselection with catalyst **mono-QN-60**.

Scheme 3.15



We also attempted to run the IFB reaction of tetralone tosylate. In order to assure high reactivity we synthesized α -toxyloxy-6-nitrotetralone **17** and submitted it to the typical reaction conditions. To our disappointment, the reaction did not produce any of the desired product and all the starting material was recovered from the reaction (Scheme 3.16).

Scheme 3.16



3.4 Synthetic plan for hydroxybrazilin

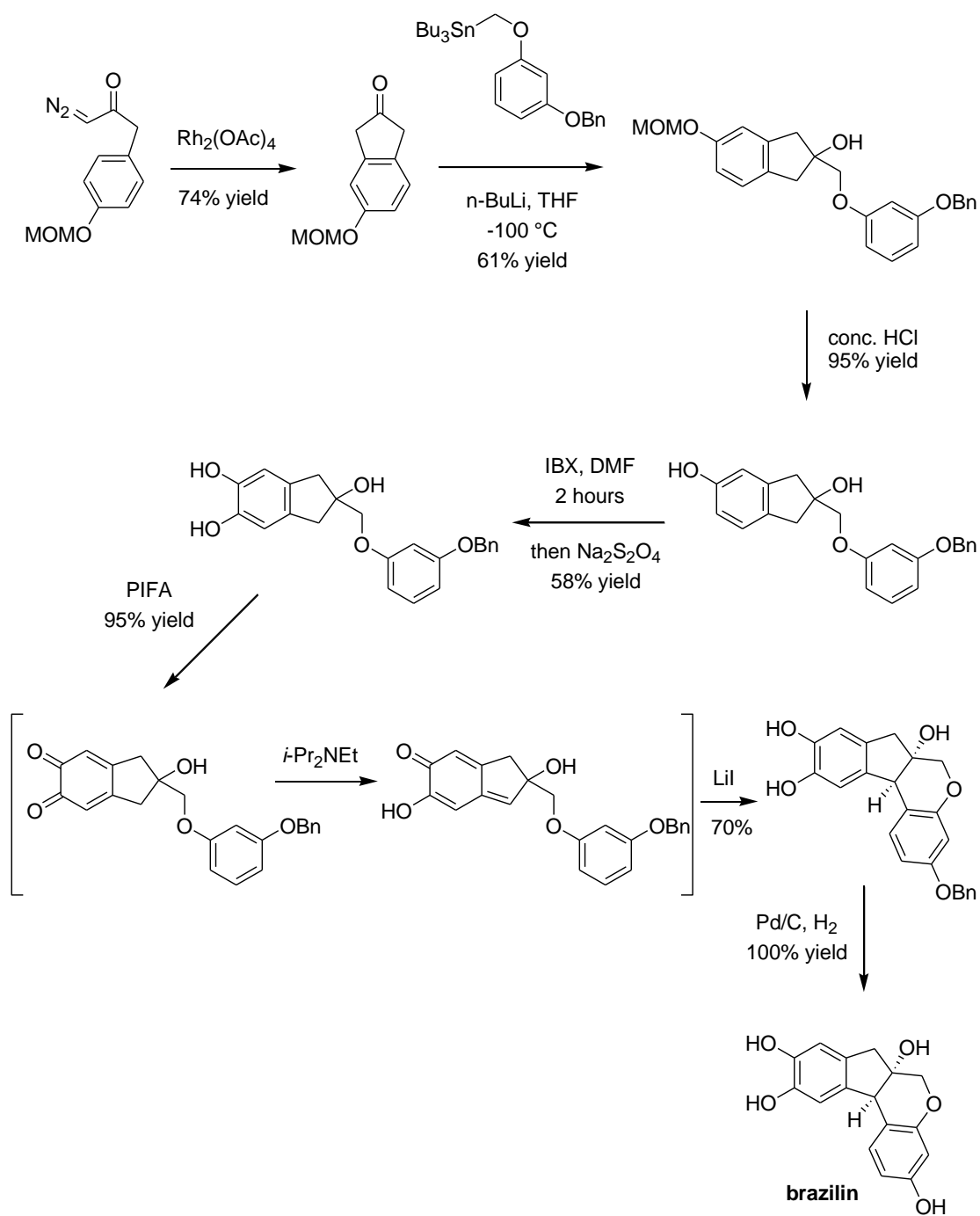
As noted at the beginning of this chapter, we planned to take advantage of the newly developed IFB reaction of α -tosyloxyindanones in order to apply this method as the key step of an asymmetric total synthesis of hydroxybrazilin. The parent compound brazilin has been used since at least the middle ages to dye fabric, and has been used to make paints and inks as well. But only recently it was reported that this natural product shows some interesting biological effects, including immunosuppressive and cardiotoxic activities.¹⁰ These activities most likely come not from brazilin, but rather from brazilein, a quinone methide formed by *in situ* oxidation. Recently, Nagai and Nagumo isolated hydroxybrazilin and related compounds. It was proposed that it can also form brazilein *in situ*, but by elimination rather than oxidation.¹¹ In the same paper authors have shown that hydroxybrazilin can be converted into brazilin by treatment with sodium borohydride. This transformation presumably includes brazilein as an intermediate (Scheme 3.17).

Scheme 3.17



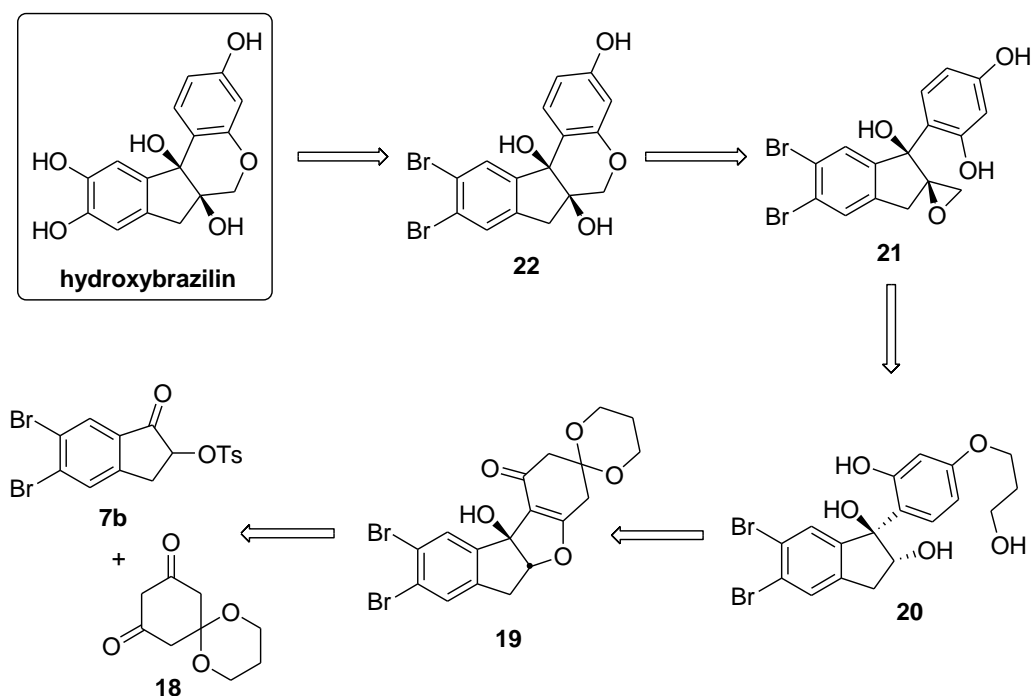
Several reports on the total synthesis of brazilin and related compounds are found in the literature.^{2b} Among these, Pettus and co-workers afforded the fastest and most elegant construction of tetracyclic brazilin skeleton^{2a}. This synthesis uses several interesting and underutilized transformations, including a regioselective dirhodium-catalyzed aryl C–H insertion, a regioselective IBX phenol oxidation into an *o*-quinone and a tautomerization of an *o*-quinone to a *p*-quinone methide (Scheme 3.18). The key step of this synthesis includes an intramolecular aryl cyclization with a *p*-quinone methide that furnishes the central pyran ring of brazilin. It is worth mentioning that no asymmetric synthesis of brazilin or related compounds was reported by this date.

Scheme 3.18 Pettus's synthesis of brazilin



Retrosynthetically, our route begins with the IFB reaction of 6,7-dibromo-1-indanone **7b** and protected 1,3-cyclohexanedione **18** (Scheme 3.19). This step sets up the required stereochemistry and tetra-cyclic framework of hydroxybrazilin early in the synthesis. The IFB product **19** will then be submitted to a conjugate reduction followed by an opening of the furan ring to deliver compound **20**. Oxidation and methylenation of aromatized product **20** will prepare the substrate for a directed epoxidation which produces compound **21**. Opening of the epoxide will furnish benzopyran **22**. Finally, two hydroxyl groups can be introduced via Hartwig-Buckwald chemistry to finish the synthesis of hydroxybrazilin.

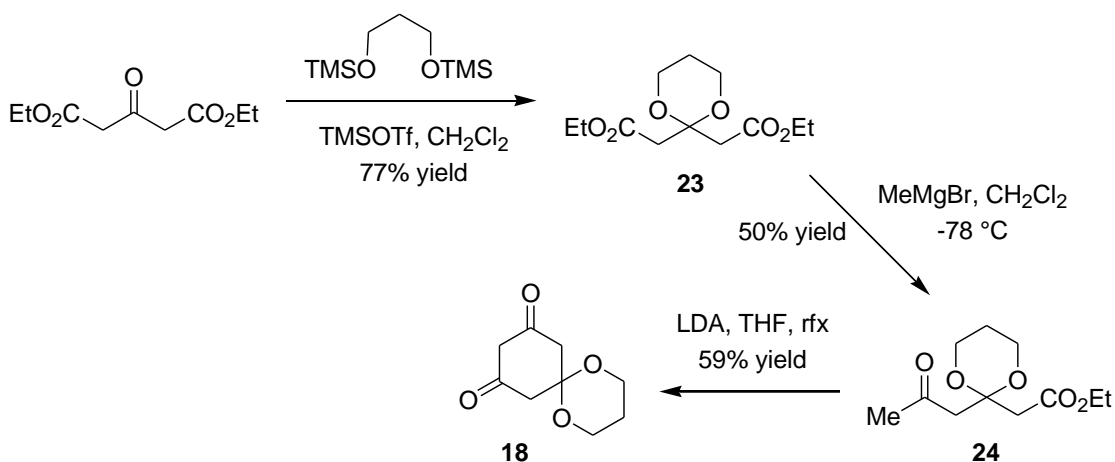
Scheme 3.19 Retrosynthetic route to hydroxybrazilin



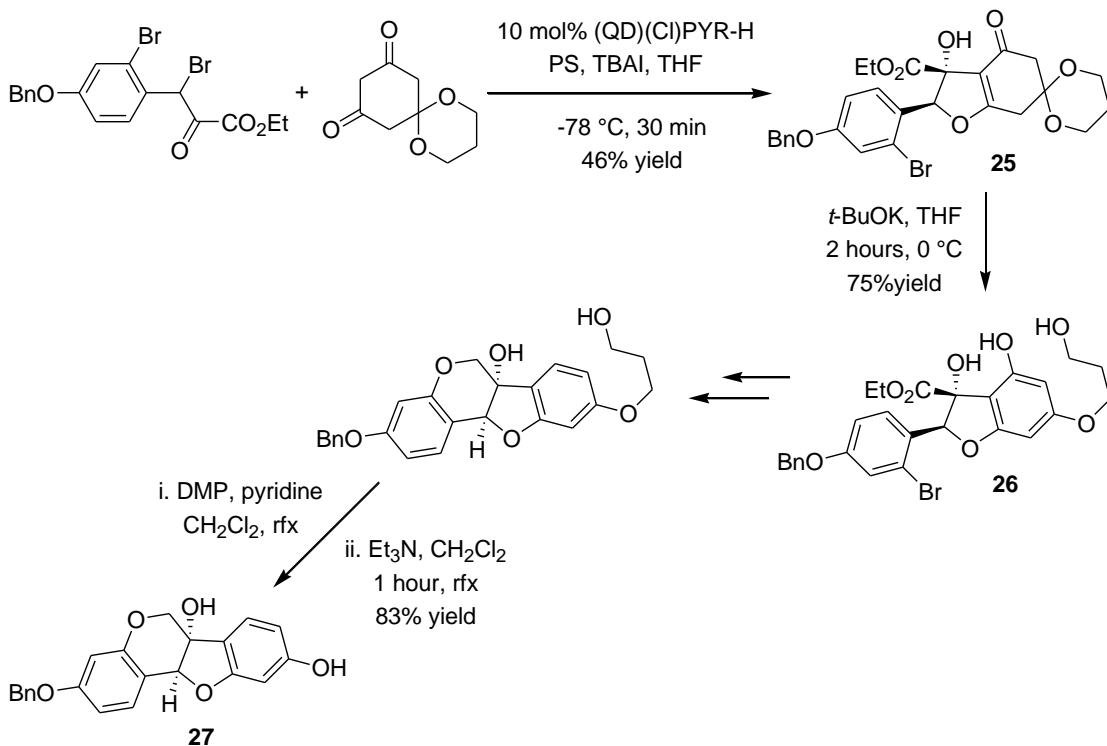
3.5 Progress toward the total synthesis of hydroxybrazilin

The first step of the synthesis involves the IFB reaction of electrophile **7b** and 1,3-cyclohexanedione **18**. This protected dione was previously synthesized in our group and successfully used for the total synthesis of glycinol.¹² The synthesis of **18** begins with the acetal protection of the commercially available acetone-1,3-dicarboxylate (Scheme 3.20). One of the ester groups of **23** is converted into the methyl ketone to deliver compound **24**, which then undergoes a Dieckmann condensation promoted by LDA in refluxing THF solution. Additionally, Na Li discovered a convenient procedure for the aromatization of the cyclohexenone moiety of the IFB product under basic conditions (Scheme 3.21). In this reaction sequence, the IFB product **25** was treated with *t*-BuOK in THF resulting in a formation of the aromatized product **26** in good yield. The hydroxypropyl side chain was successfully eliminated at the later stage of the synthesis yielding product **27**.

Scheme 3.20 Na Li's synthesis of dione **18**

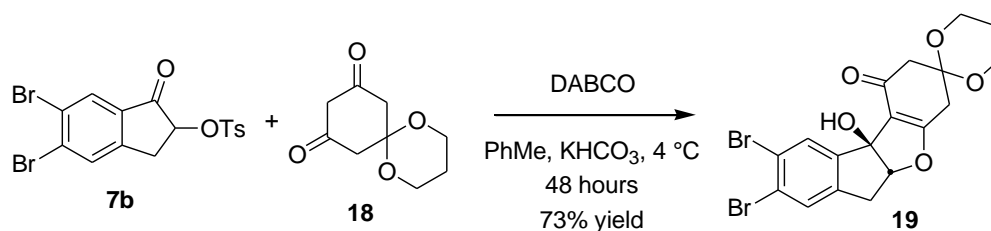


Scheme 3.21



As expected, the IFB reaction between substrate **7b** and 1,3-cyclohexanedione **18** in the presence of DABCO proceeded smoothly giving the desired product **19** in good yield (Scheme 3.22). Additionally, the same IFB product was isolated in high enantioselectivity (88% ee) when **mono-QN-60** was used as a catalyst.

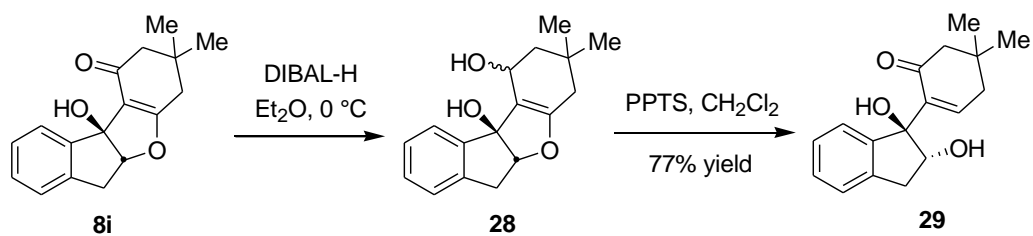
Scheme 3.22



We commenced our investigation of the reductive elimination sequence on the model substrate **8i** made from α -tosyloxyindanone **7a** and dimedone. Initially, we submitted **8i** to the reaction with DIBAL-H hoping that it would lead to the desired hydride-1,4-reduction and subsequent furan ring opening (Scheme 3.23). Instead of giving compound **29** directly, this reaction produced a mixture of two diastereomers of **28** resulting from reduction of the ketone of dimedone moiety. To our delight, this intermediate slowly converts into desired compound **29** if left on a silica gel for few hours. Alternately, the same transformation was done much faster in the presence of catalytic PPTS in CH₂Cl₂ at room temperature. The overall yield was satisfying (77%), so we proceeded

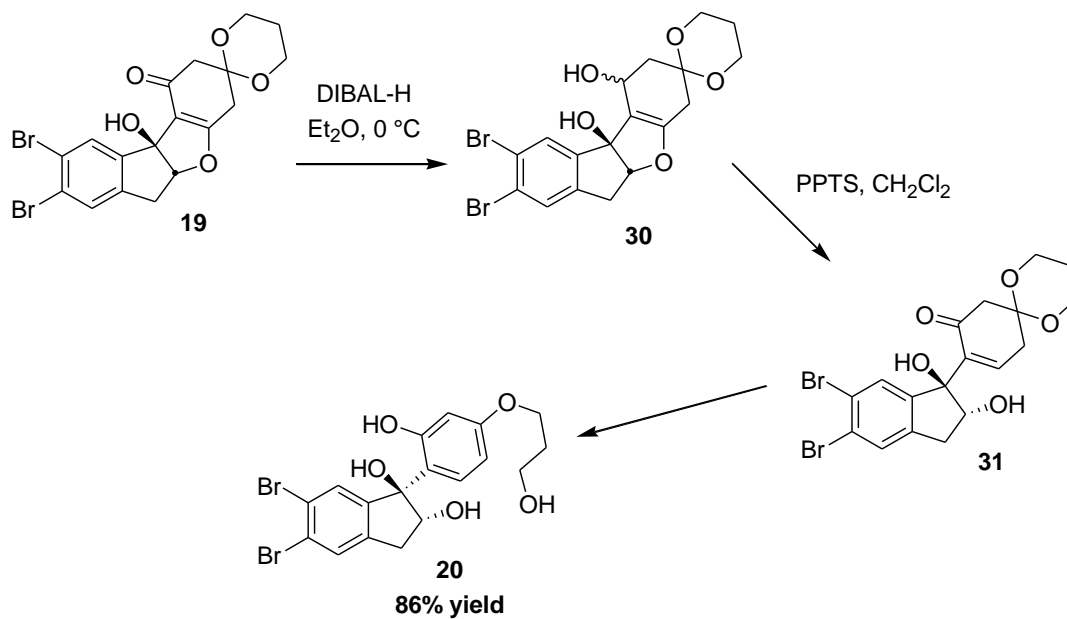
further in our attempt to use the same conditions for the reductive opening of IFB product **19**.

Scheme 3.23



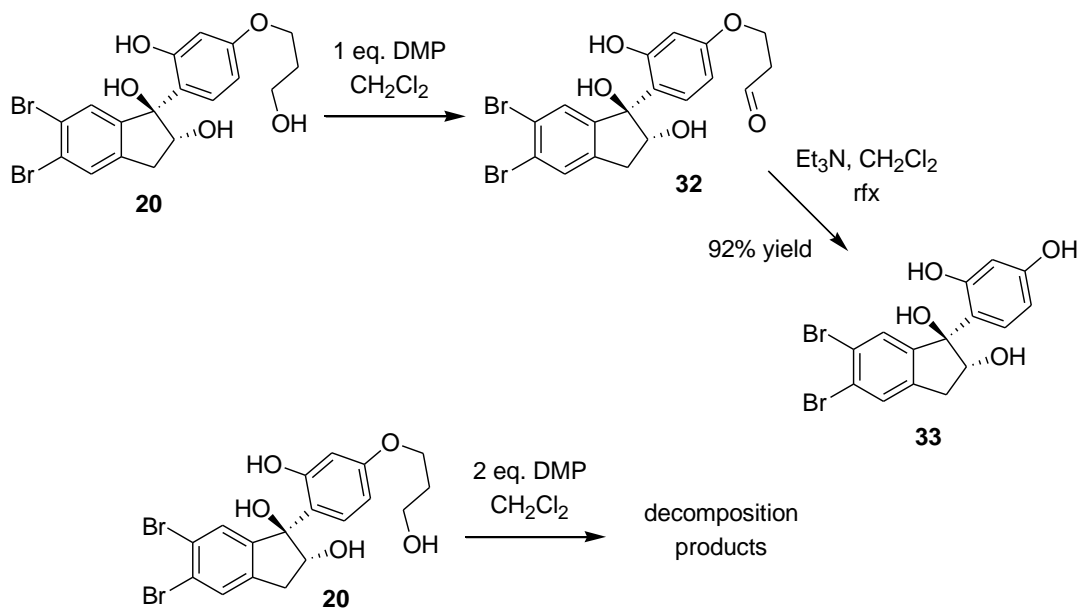
Reduction of **19** with DIBAL-H gave the desired secondary alcohol **30** as a mixture of two diastereomers (Scheme 3.24). Gratifyingly, when **30** was treated with PPTS the reaction produced the aromatized product **20**. The small amount of enone **31** was isolated as well, but no separate step was required for the aromatization of **30** as it happened immediately under the same conditions.

Scheme 3.24



Following our synthesis plan, we need to eliminate the side chain of **20** and then to oxidize the secondary alcohol to furnish a ketone required for further methylenation and epoxidation. First, treatment of **20** with one equivalent of DMP resulted in selective oxidation of the primary alcohol in the presence of the secondary (Scheme 3.25). Then, the aldehyde was treated with triethylamine in refluxing CH₂Cl₂ and the desired diphenol **33** was isolated in excellent yield, proving the generality of the procedure developed earlier in the group.

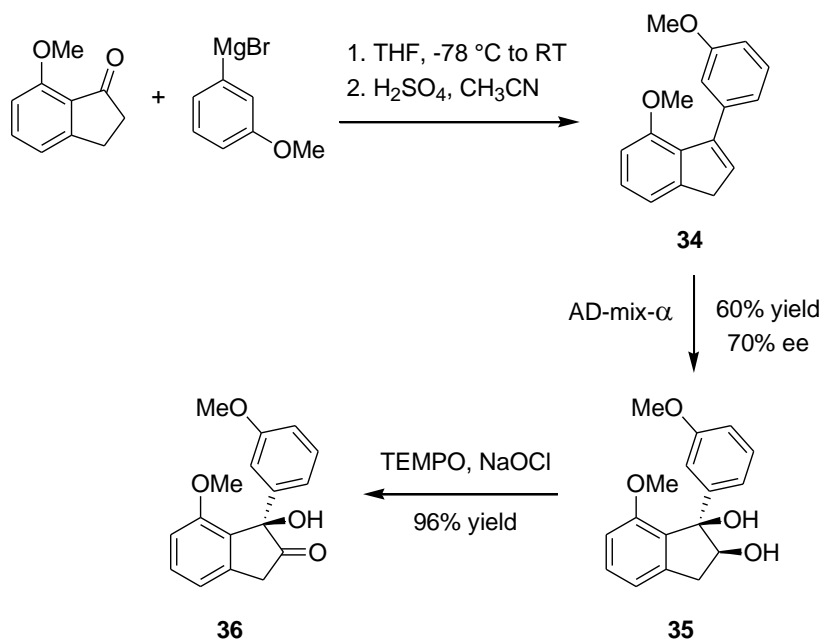
Scheme 3.25



Having established the principal feasibility to use the typical procedure for the elimination of the side chain, we submitted compound **20** to the reaction with two equivalents of DMP intending to achieve the oxidation of both alcohols in one step. Unfortunately, this oxidation procedure has proven to be more troublesome than we expected. The reaction gave a complete conversion, but it resulted only in a decomposition product. We could not detect even a trace amount of the desired ketone, so we decided to test several common protocols used for the oxidation of secondary alcohols into ketones. Besides Dess-Martin conditions, we screened such common methods such as Swern, PCC and TPAP oxidation, but in all the cases no desired product was isolated.

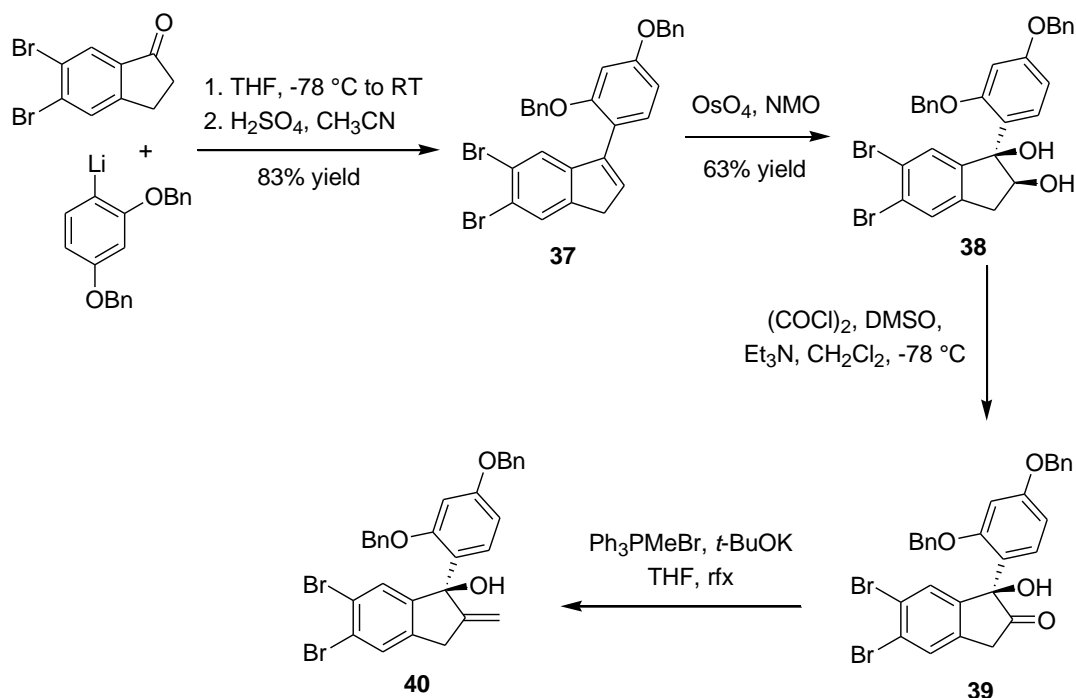
In the course of our studies we found that a structurally similar dihydroxyindanone product **35** was synthesized in Baran's group as an intermediate for the total synthesis of haouamine alkaloids¹³ (Scheme 3.26). In their work diol **35** was made in two straightforward steps. The addition of arylmagnesium bromide to 1-indanone and subsequent water elimination in acidic media afforded aryl indene **34**. Sharpless asymmetric dihydroxylation on indene **34** achieved moderate levels of enantioselectivity yielding optically active diol in 70% ee. Notably, they were able to significantly improve enantioselectivity of diol after recrystallization (racemic diol forms crystals leaving the enantiopure diol in solution). Subsequent oxidation with TEMPO/NaOCl afforded hydroxyketone **36** in excellent yield. Interestingly, they mention that other oxidants lead to diol cleavage proving the high sensitivity of this type of dihydroxyindanone molecule.

Scheme 3.26 Baran's route as part of total synthesis of haouamine alkaloids



By adapting Baran's work, we synthesized diol **38** using the same reaction sequence. Addition of the aryllithium (generated from the corresponding bromoarene by metal-halogen exchange) to 6,7-dibromoindanone and subsequent treatment with sulfuric acid yielded indene **37** in high yield. Indene **37** was dihydroxylated with catalytic osmium tetroxide and NMO to give **38**. Following Baran's synthesis, we submitted diol to the TEMPO/NaOCl conditions, but it only yielded diol cleavage product. Similar results were obtained when we used DMP or PCC as oxidants. Eventually, we were able to isolate desired ketone **39** in moderate yield utilizing a Swern oxidation protocol. Additionally, **39** was successfully olefinated via a Wittig reaction to produce **40**.

Scheme 3.27



In conclusion, we made a progress in optimization of the asymmetric IFB reaction of α -tosyloxy-6,7-dibromoinanone **7b**. This reaction produces tetra-cyclic IFB product **8b** that we intend to use as a key intermediate in the total synthesis of hydroxybrazilin. Our synthetic route requires further exploration as we faced difficulties in oxidation of diol **20** that tend to form decomposition products under various oxidation conditions.

References

1. Namikoshi, M.; Nakata, H.; Yamada, H.; Nagai, M.; Saitoh, T., Homoisoflavonoids and Related-Compounds .2. Isolation and Absolute-Configurations of 3,4-Dihydroxylated Homoisoflavans and Brazilins from *Caesalpinia Sappan* L. *Chem Pharm Bull* **1987**, *35* (7), 2761-2773.
2. (a) Huang, Y. D.; Zhang, J. S.; Pettus, T. R. R., Synthesis of (+/-)-Brazilin using IBX. *Org Lett* **2005**, *7* (26), 5841-5844; (b) Yen, C. T.; Nakagawa-Goto, K.; Hwang, T. L.; Wu, P. C.; Morris-Natschke, S. L.; Lai, W. C.; Bastow, K. F.; Chang, F. R.; Wu, Y. C.; Lee, K. H., Antitumor agents. 271: Total synthesis and evaluation of brazilein and analogs as anti-inflammatory and cytotoxic agents. *Bioorg Med Chem Lett* **2010**, *20* (3), 1037-1039.
3. Hanan, G. S.; Schubert, U. S.; Volkmer, D.; Riviere, E.; Lehn, J. M.; Kyritsakas, N.; Fischer, J., Synthesis, structure, and properties of oligo-tridentate ligands; Covalently assembled precursors of coordination arrays. *Can J Chem* **1997**, *75* (2), 169-182.
4. Kawai, H.; Takeda, T.; Fujiwara, K.; Suzuki, T., Isolation and low-temperature X-ray analysis of intramolecular triarylmethane-triarylmethylum complex: Preference for a C-H-bridged unsymmetric structure exhibiting a facile 1,5-hydride shift and charge-transfer interaction. *J Am Chem Soc* **2005**, *127* (35), 12172-12173.
5. Dash, P.; Janni, M.; Peruncheralathan, S., Trideuteriomethoxylation of Aryl and Heteroaryl Halides. *Eur J Org Chem* **2012**, (26), 4914-4917.

6. Mosrin, M.; Knochel, P., TMPZnCl center dot LiCl: A New Active Selective Base for the Directed Zincation of Sensitive Aromatics and Heteroaromatics. *Org Lett* **2009**, *11* (8), 1837-1840.
7. Spivey, A. C.; Zhu, F. J.; Mitchell, M. B.; Davey, S. G.; Jarvest, R. L., Concise synthesis, preparative resolution, absolute configuration determination, and applications of an atropisomeric biaryl catalyst for asymmetric acylation. *J Org Chem* **2003**, *68* (19), 7379-7385.
8. Yao, T. L.; Campo, M. A.; Larock, R. C., Synthesis of polycyclic aromatics and heteroaromatics via electrophilic cyclization. *J Org Chem* **2005**, *70* (9), 3511-3517.
9. Li, A.; DeSchepper, D. J.; Klumpp, D. A., Triflic acid promoted synthesis of polycyclic aromatic compounds. *Tetrahedron Lett* **2009**, *50* (17), 1924-1927.
10. Oh, S. R.; Kim, D. S.; Lee, I. S.; Jung, K. Y.; Lee, J. J.; Lee, H. K., Anticomplementary activity of constituents from the heartwood of *Caesalpinia sappan*. *Planta Med* **1998**, *64* (5), 456-458.
11. Nagai, M.; Nagumo, S., Protosappanin-E-1 and Protosappanin-E-2, Stereoisomeric Dibenzoxocins Combined with Brazilin from Sappan Lignum. *Chem Pharm Bull* **1990**, *38* (6), 1490-1494.
12. Calter, M. A.; Li, N., Asymmetric Total Syntheses of (-)-Variabilin and (-)-Glycinol. *Org Lett* **2011**, *13* (14), 3686-3689.
13. Burns, N. Z.; Baran, P. S., On the origin of the haouamine alkaloids. *Angew Chem Int Edit* **2008**, *47* (1), 205-208.

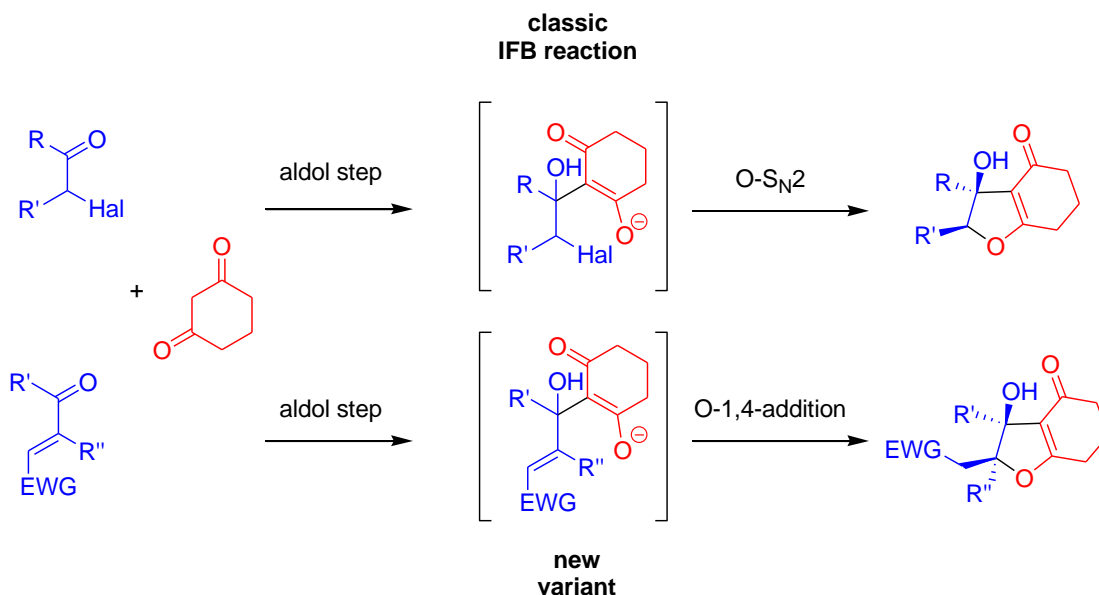
4. Development of the new asymmetric IFB reaction utilizing 2-ene-1,4-diketones as electrophiles

4.1 Initial experiments with cyclic electrophiles

In the classic version of the IFB reaction, the initial and reversible aldol reaction is followed by an intramolecular O-alkylation. While the stereochemistry is set at the aldol step, the following S_N2 process traps the aldol adduct prior to equilibration. In our search for the new electrophiles we envisioned the possibility of using a different mechanistic step to close the furan ring, such as an O-1,4-addition to an activated alkene (Scheme 4.1). This approach opens the possibility of accessing optically active hydroxydihydrofuran products containing two adjacent stereocenters starting from achiral building blocks. Additionally, this process represents the simple addition of a 1,3-dicarbonyl compound to an enone electrophile that only requires a catalytic amount of tertiary amine and avoids the use of a stoichiometric base since no acid is generated in the reaction. Therefore, we expect this atom-economical protocol to be very practical and efficient with minimal purification procedures required. But the most intriguing consequence of this strategy is the possibility to access the IFB products bearing two adjacent quaternary stereocenters, if one starts with a tri-substituted alkene (with $R'' \neq H$) electrophile, an outcome that would be impossible using the old methods. This will significantly expand the variety of optically active furans available and will

provide us with the highly-functionalized intermediates that could be applied to the total synthesis of natural products.

Scheme 4.1

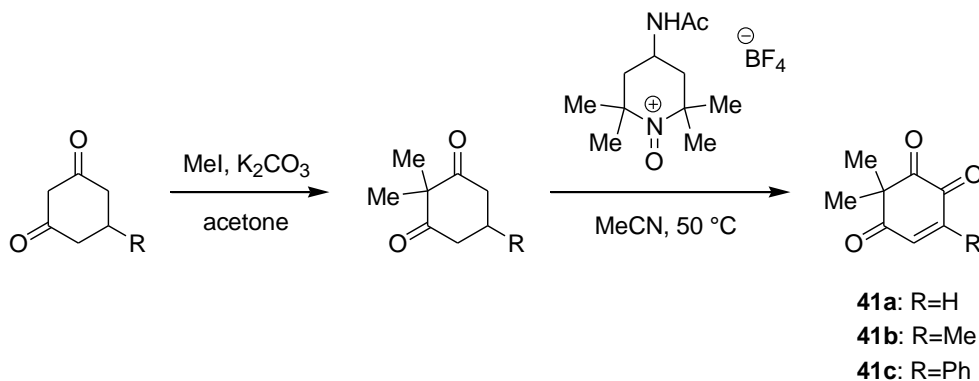


With this new general concept in mind, we started searching for potential substrates that comply with the general scheme. As pointed out earlier, a formation of H-bond between protonated catalyst and the α -ketoester group of α -bromopyruvate was crucial for the highly-organized transition state and high stereoselectivity of the IFB reaction. Taking into the account the mechanistic considerations presented above, we intended to limit the substrate search for the electrophiles that can engage in a similar H-bond interaction with a catalyst.

A quick literature search provided us with a few potential substrates bearing the α -ketoester or the 1,2-diketone functionality. Recently, G. Fenteany

and et al. reported a convenient procedure for the oxidation of 1,3-cyclohexanediones with 4-acetamido-2,2,6,6-tetramethylpiperidine-1-oxoammonium tetrafluoroborate (Bobbitt's salt) to generate 5-ene-1,2,4-triones in moderate to good yields¹ (Scheme 4.2). Bobbitt's salt is a commercially available reagent, so this method allows us to quickly access several cyclic ene-1,4-diketone electrophiles that we intended to use for the new IFB reaction, including those containing tri-substituted alkene.

Scheme 4.2 Fenteany's synthesis of cyclic 5-ene-1,2,4-triones

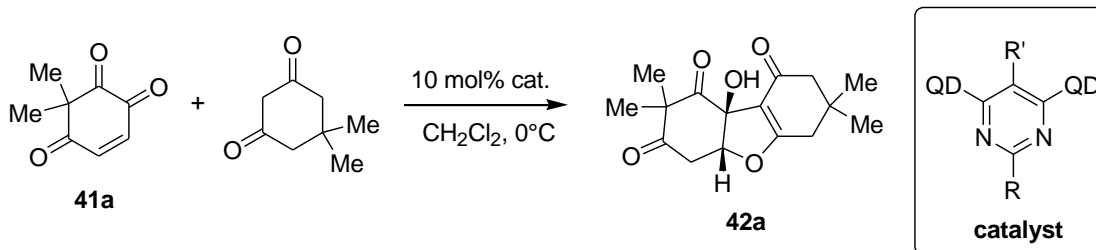


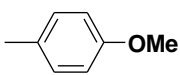
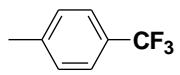
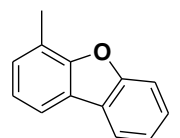
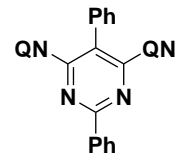
It occurred to us that the 1,2-diketone functionality provides us with a very reactive carbonyl group, but unlike the α -ketoester it also raises a question of regioselectivity. We expected that for the simplest substrate **41a**, with a disubstituted double bond (R=H), the two methyl groups create steric hindrance around the adjacent carbonyl group, directing nucleophilic attack toward the desired electrophilic center. With R \neq H (**41b** and **41c**), an extra substituent on

the double bond could be an additional factor that might affect the regioselectivity of the reaction.

To start testing our idea, ene-triketone **41a** was synthesized according to the literature procedure. To our delight it gave a rapid and high yielding reaction with dimedone in the presence of DABCO as a catalyst producing the desired product **42a** in 73% yield as a single diastereomer. Since the reaction was fast, giving a good yield in dichloromethane at 0 °C, we decided to skip the optimization studies and proceeded directly to the catalyst screening. With the help of Michael Revelas we screened several previously synthesized catalysts. The tricyclic product was isolated in reproducibly moderate yields independently on a catalyst structure, but the enantioselectivities varied significantly depending on a *front* group of a catalyst (Table 4.1). We initiated our screening with the **(QD)₂PYR** catalyst. The resulting IFB product was isolated in a 65% yield and an unsatisfying 24% ee. In our attempt to improve this result we screened catalysts with a tert-butyl group at both the *front* and *back* positions, but this did not lead to any beneficial results. Modification of the *front* group with electron-donating and electron-withdrawing groups did not affect the ee. Unexpectedly, we achieved very a noticeable improvement with catalyst **QD-61** bearing a 4-dibenzofuran moiety in the *front* position (71% ee).

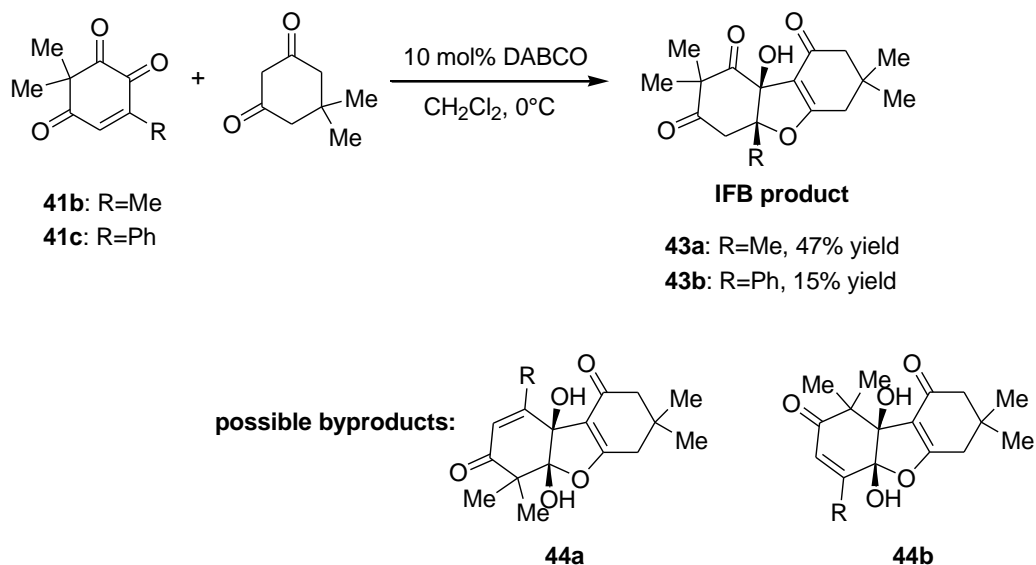
Table 4.1 Catalyst screening for electrophile **41a**



cat.	R	R'	yield %	ee %
(QD) ₂ PYR	Ph	Ph	65	24
QD-2	H	Ph	69	35
QD-3	<i>t</i> -Bu	Ph	68	13
QD-5	Ph	<i>t</i> -Bu	68	2
QD-8	1-naphthyl	Ph	72	20
QD-6		Ph	66	16
QD-28		Ph	75	20
QD-61		Ph	70	71
(QN) ₂ PYR			70	48

Related cyclic ene-triketones with a tri-substituted double bond were also synthesized using the same procedure. Their reactivity was examined in the reaction with dimedone in the presence of the achiral catalyst (Scheme 4.3). For electrophile **41b**, a complete conversion was achieved after 20 hours, and, to our delight, we were able to isolate the desired IFB product in 47% yield. The IFB reaction of substrate **41c** also produced the tricyclic product, but it was isolated in significantly a diminished yield (15%). It should be noted that such a significant drop of the yield is attributed to the formation of byproducts, which were assigned as structures **44a** and **44b**. Nevertheless, this initial result encouraged us to explore this reaction further as it represents the first example of the reaction which led to the IFB product containing two adjacent quaternary stereocenters.

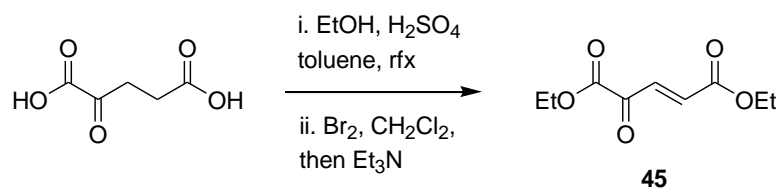
Scheme 4.3



4.2 Reaction of linear ene-diketone electrophiles

Since the novel concept of combining an aldol reaction with an O-1,4-addition proved to be feasible, we turned our attention to related linear substrates bearing the same functionality as cyclic ene-triketones **41a-c**. A literature search revealed one known substrate of this type². It is easily prepared from commercially available α -ketoglutaric acid (Scheme 4.4). In a first step two carboxylic acid groups are converted into ethyl esters under standard esterification conditions. The resulting keto-diester is brominated in the α -position to produce α -bromopyruvate, which is treated with triethylamine to yield desired compound **45**.

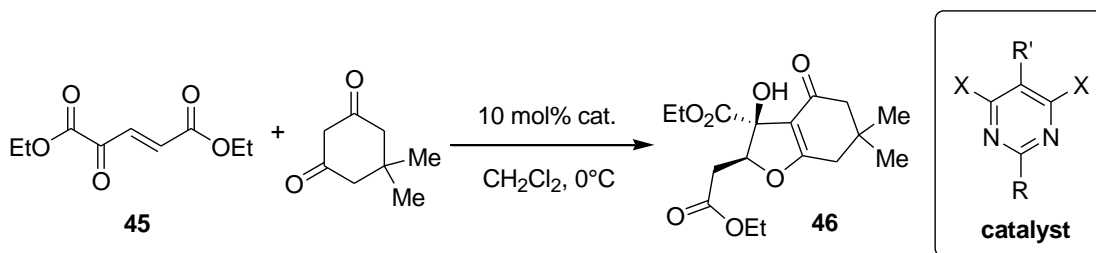
Scheme 4.4



Substrate **45** provided us with another proof of the general concept, as its reaction with dimedone in the presence of DABCO resulted in a formation of the IFB product **46** in good yield (Scheme 4.5). We attempted to optimize this reaction and with the help of Patrick Sarver we performed a catalyst screening. Product **46** was generally isolated in reasonable yields and the best result was

achieved with the quinine-derived catalyst **QN-4** containing tert-butyl group in both *front* and *back* positions (71% ee).

Table 4.2 Catalyst screening for electrophile **45**

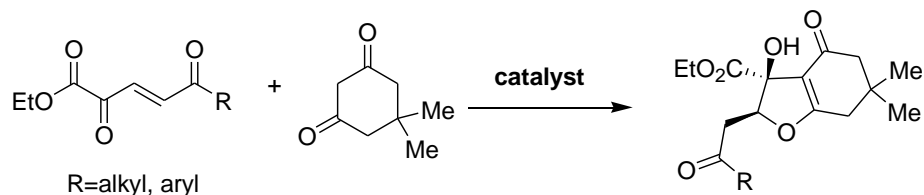


cat.	R	R'	X	yield %	ee %
QD-2	H	Ph	QD	65	64
QD-62	Me	Ph	QD	73	48
QN-4	<i>t</i> -Bu	<i>t</i> -Bu	QN	70	71
QN-3	<i>t</i> -Bu	Ph	QN	71	65
QD-4	<i>t</i> -Bu	<i>t</i> -Bu	QD	70	47
QD-3	<i>t</i> -Bu	Ph	QD	69	57

Motivated by the initial positive results obtained with cyclic and acyclic ene-diketones, we decided to further expand the range of suitable reactants. There are two functionalities in the electrophile molecule that determine its reactivity: an activated carbonyl group on the left end of the substrate which is attacked in an initial aldol step and the electron-withdrawing group on the

opposite side of the molecule (Scheme 4.6). Since we postulated the importance of the bifurcated H-bond interaction between the protonated catalyst and the substrate we intended to stick with the α -ketoester group for further studies. Thus, we decided to introduce new substrates that differ in electron-withdrawing groups. The obvious choice here is EWG=alkyl or aryl ketone. Enones are significantly more reactive toward conjugate addition than the corresponding unsaturated esters, hence we expected the O-1,4-addition that furnishes the furan ring in a second step of the mechanism to proceed faster. Thus, the overall reaction was expected to proceed faster producing the product in higher yield. Unfortunately, literature did not provide us with any examples for synthesizing such compounds, so we had to come up with a general way to access them.

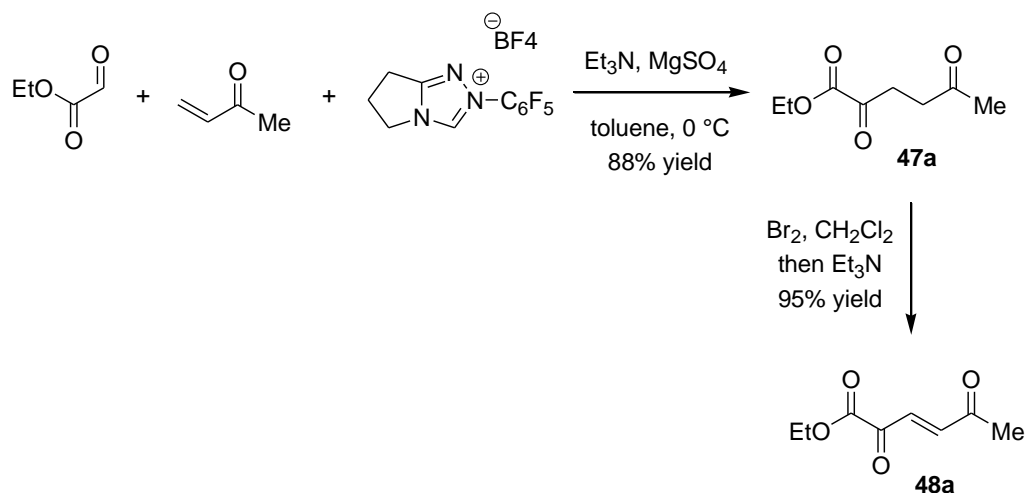
Scheme 4.5



Retrosynthetically, we anticipated preparing the required ene-diketone from the corresponding 1,4-dicarbonyl compound, analogously to the diethyl ketoglutarate oxidation described earlier. Among the few common ways to access 1,4-diketones we chose the Stetter reaction as the most general and well-documented. Looking for relevant methods described in the literature, we found

that Rovis and co-workers developed an asymmetric Stetter reaction of glyoxamides with alkylidenemalonates catalyzed by a chiral triazolium salt.³ The related reaction between ethyl glyoxalate and methylvinyl ketone in a presence of the achiral triazolium catalyst proceeded smoothly affording the desired product **47a** in high yield (Scheme 4.6). The resulting 1,4-diketone is easily brominated with bromine in CH₂Cl₂. Addition of two equivalents of triethylamine allowed the formation of the double bond via elimination of HBr and the required ene-1,4-diketone **48a** was isolated in excellent yield.

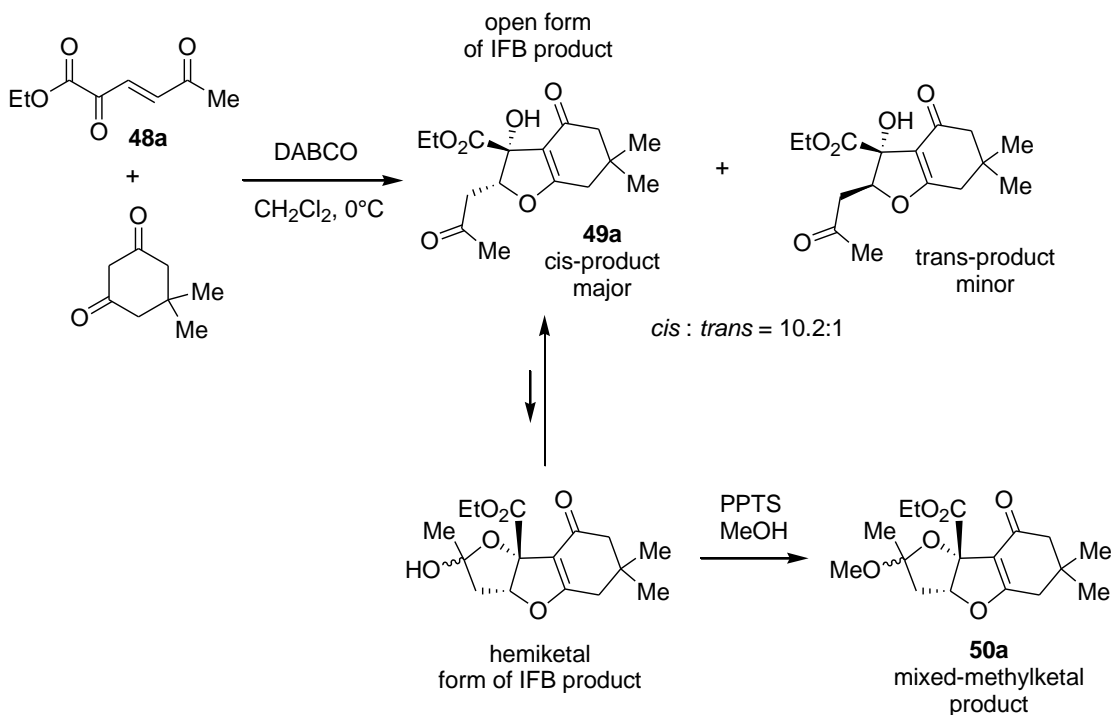
Scheme 4.6 Synthesis of **48a**



We were delighted to observe that under the standard reaction conditions the corresponding hydroxydihydrofuran **49a** was formed as the only product in excellent yield (Scheme 4.7). As we expected, reaction proceeded rapidly giving complete conversion in 10 min at 0 °C. Additionally, this IFB product was obtained in high diastereoselectivity (d.r.=10.2:1) favoring the cis-

isomer. The ^1H NMR spectrum of purified product **49a** shows that it exists as a mixture of the open form (the major component in the mixture) and two diastereomers of the cyclic hemiketal product formed by the attack of the tertiary hydroxyl onto the methylketone. These products turned out to be inseparable on a silica gel column. Our effort to use this mixture for HPLC analysis was fruitless, which probably can be explained by the fact that the IFB product constantly interconverts between the two forms. Thus, in order to determine the enantiopurity of the IFB product it was necessary to transform this mixture into a single stable compound. This was achieved by treating the mixture with PPTS in methanol, which resulted in the formation of a 2:1 mixture of two diastereomers of the mixed methyl ketal **50a**. The two diastereomers were successfully separated via silica gel chromatography and used for determination of the enantioselectivity by HPLC.

Scheme 4.7



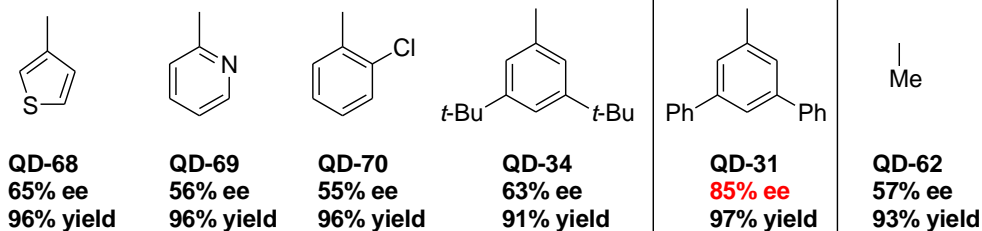
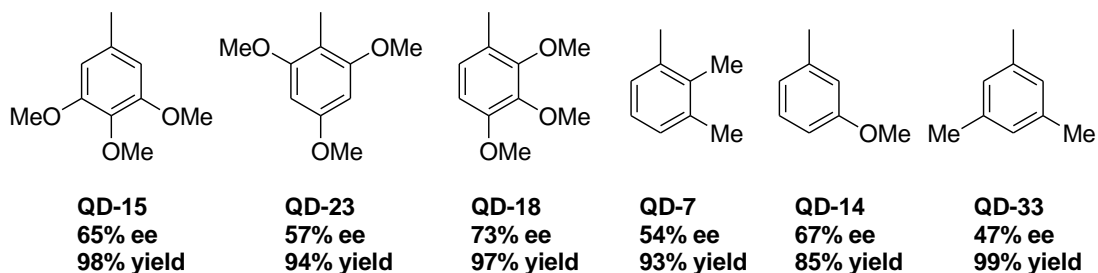
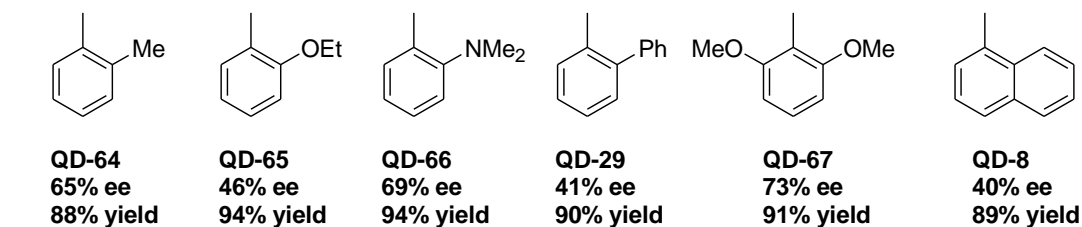
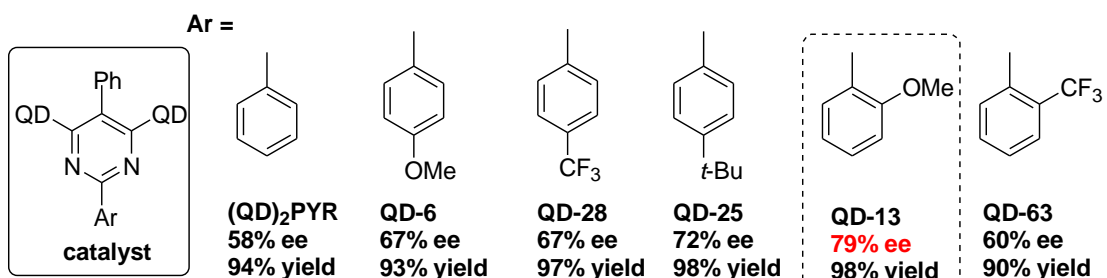
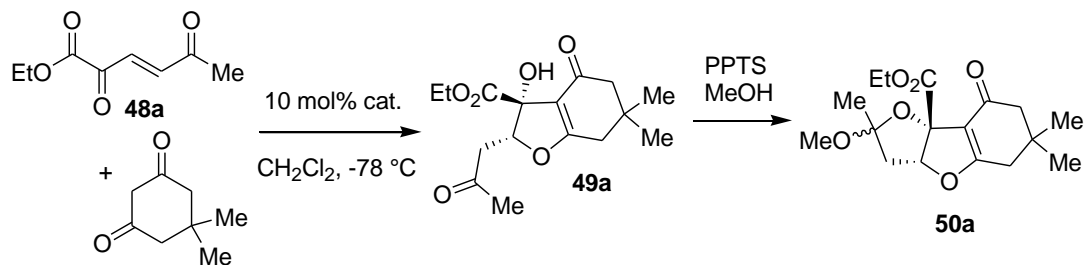
Prior to the beginning of the catalyst screening, we did some preliminary optimization studies. Since the reaction was completed almost instantaneously at 0°C we ran an experiment at lower temperature. It turned out that complete conversion can be achieved after 1 hour at -78°C in dichloromethane in the presence of 10 mol% of the catalyst. We set these as the standard reaction conditions and proceeded to the screening in order to find the optimal catalyst.

We initiated our screening with **(QD)₂PYR** catalyst. As expected, the reaction proceeded smoothly giving the IFB product in high yield. The initial product was converted into the mixed methyl ketal as described above and this reaction sequence afforded the product in a respectable 58% ee. This result

encouraged us to explore this reaction further since an extended library of the structurally similar catalysts was available to us.

Initially tested catalysts with substituents in the para-position of the *front* phenyl group led to the higher enantioselectivity with both electron-withdrawing and electron-donating groups (Scheme 4.8). Presumably, the electronic nature of the *front* group did not play any significant role in the determination of the enantioselectivity, thus we continued on the investigation of the steric effects. Further screening revealed that catalyst **QD-13** with Ar=*o*-methoxyphenyl gave the product in 79% ee. At this point we hoped that the introduction of structurally different groups at the ortho-position of the *front* aryl group would lead to further improvement. Those hopes proved to be unfounded as in all cases (R=CF₃, Me, OEt) the enantioselectivity was diminished significantly. Further disappointments arose when we looked at di- and trimethoxysubstituted ring systems (**QD-15**, **QD-23** and **QD-18**), all of which performed more poorly than the original catalyst **QD-13**. Thus, we were left with only the possibility of modifying the *front* aryl group at the meta-positions. Introduction of the methyl and tert-butyl groups at the meta-position worked out very poorly (**QD-33**, **QD-34**), but unexpectedly the big break came when we applied catalyst **QD-31** with Ar=3,5-diphenylphenyl group. The IFB product was isolated in 85%, ee leaving us just a few percent away from the synthetically useful level of stereoinduction.

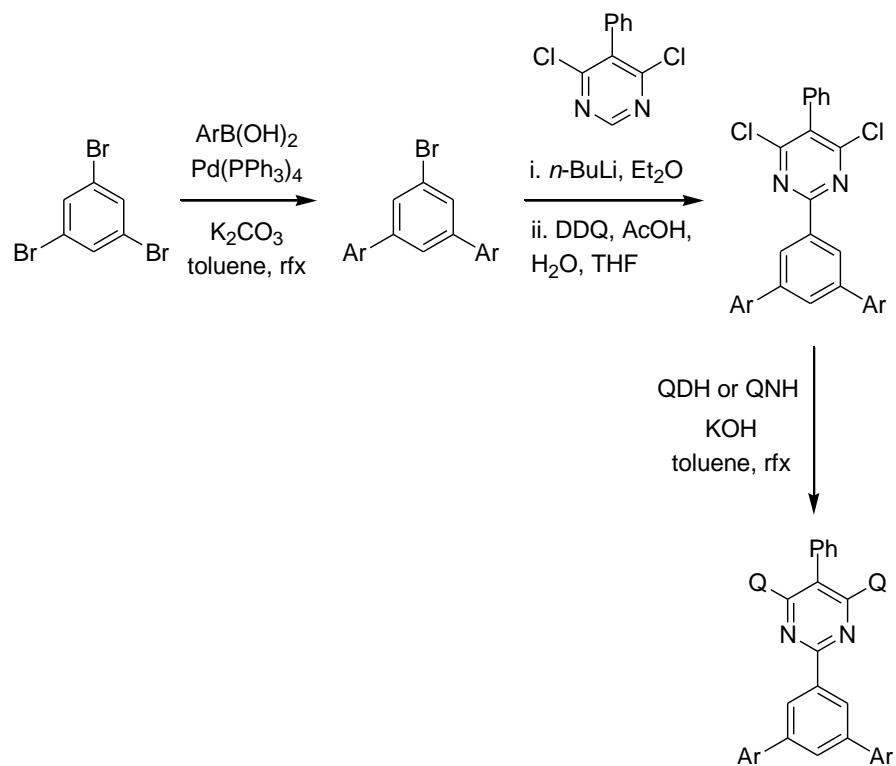
Scheme 4.8 Catalyst screening for the IFB reaction of **48a**



The result with catalyst **QD-31** was the highlight of our research at this point. The high level of asymmetric induction produced by catalyst made us look at the di-meta aryl substituted catalysts. The meta-phenyl groups could be modified by the introduction of the substituents at ortho-, meta- and para-positions. Additionally, we could modify the central ring of the *front* group at ortho- and para-positions. Besides that, we kept in mind that we have not performed a complete optimization of the reaction conditions yet, so screening of solvents and the substrate or catalyst concentration might allow us to get enantioselectivity over 90% ee.

The synthesis of the new catalysts started with 1,3,5-tribromobenzene (Scheme 4.9). Two bromines can be substituted with aryl groups if two equivalents of aryl boronic acid are used under the standard Suzuki coupling conditions. The resulting arylbromide is coupled with 5-phenyl-4,6-dichloropyrimidine following the procedure described earlier allowing us to get the dichloropyrimidine catalyst precursor. Displacement of the two chlorides with a cinchona alkaloid completed the synthesis of the novel catalysts.

Scheme 4.9

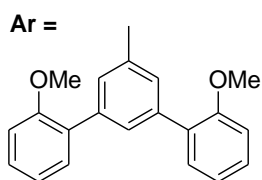
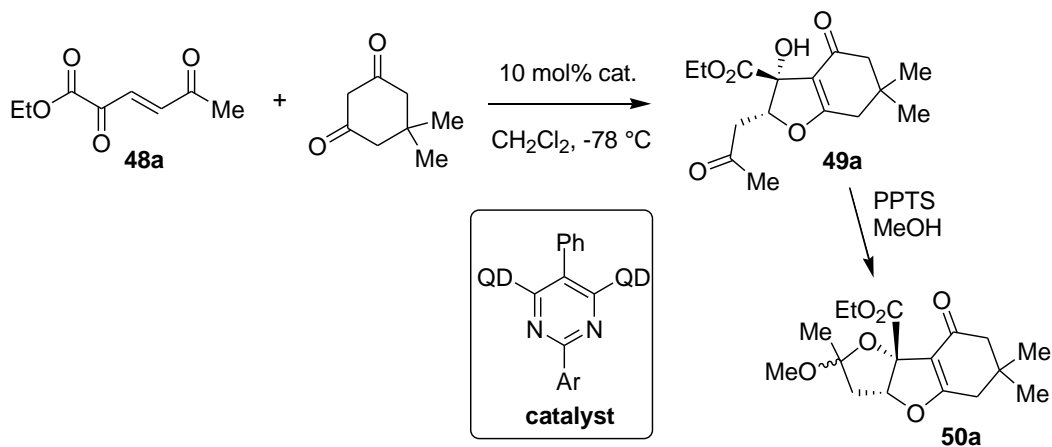


We next focused our attention toward the optimization of enantioselectivity by screening the new library (Scheme 4.10). To our disappointment the introduction of methoxy groups in ortho-positions had only a negative effect on the stereochemical outcome of the reaction (catalyst **QD-71**). Further screening revealed that meta-substitution with both methoxy and methyl groups led to an even more drastic decrease in the stereoselectivity, leaving us with only the possibility of modification at the para-position. The catalyst screening was next extended to the introduction of methoxy group in a para-position (**QD-74**) which gave a positive influence on the enantioselectivity. This result prompted us to try other catalysts bearing substituents at the para-

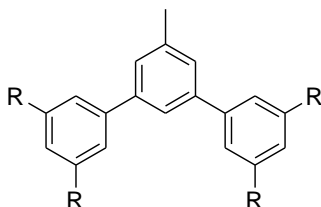
position. One of them (**QD-75**), containing a tert-butyl group, demonstrated further improvement giving the IFB product in 88% ee.

We also considered the possibility that electronic or steric modification of the central ring of the catalyst *front* group could lead to the better enantioselectivity from the reaction (catalysts **QD-81** and **QD-84**). Unfortunately, this gave only a negative effect on the stereoselectivity with product formed in 81% ee.

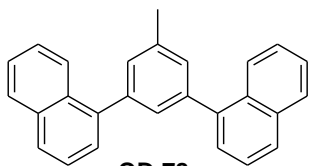
Scheme 4.10



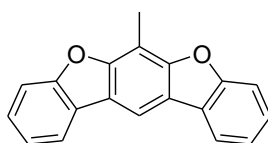
QD-71
76% ee
91% yield



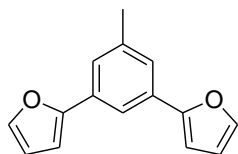
QD-72:
R=OMe: 57% ee, 97% yield
QD-73:
R=Me: 56% ee, 94% yield



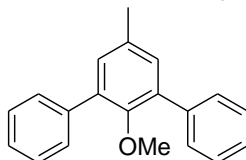
QD-78
74% ee
90% yield



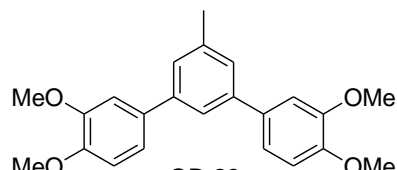
QD-79
66% ee
91% yield



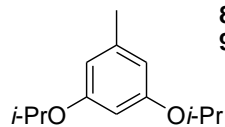
QD-80
80% ee
97% yield



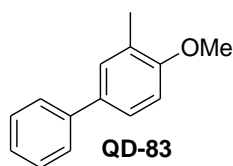
QD-81
81% ee
94% yield



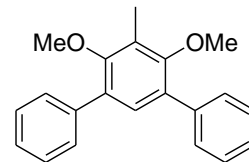
QD-82
87% ee
98% yield



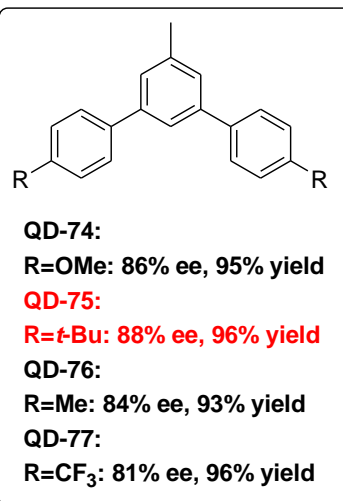
QD-22
68% ee
95% yield



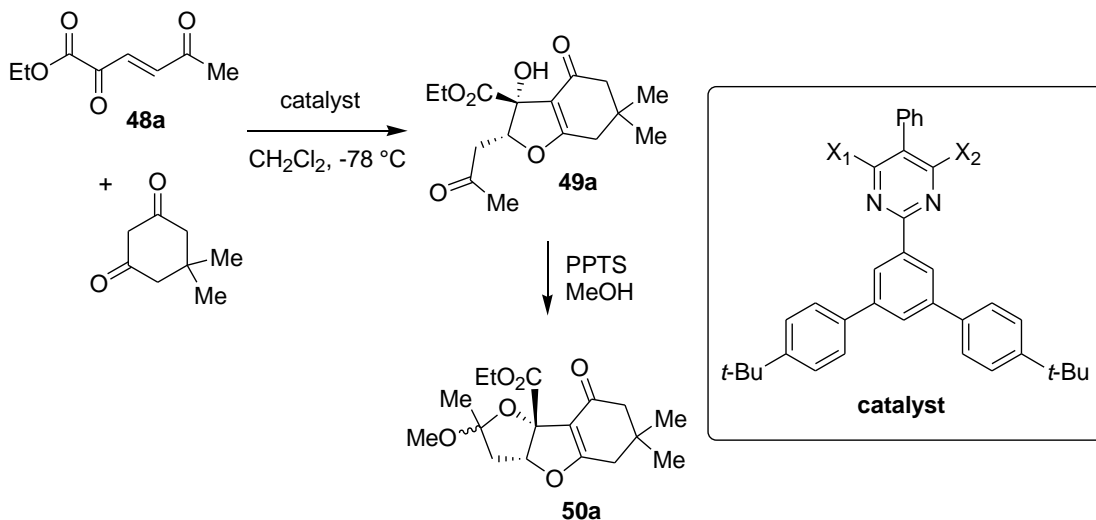
QD-83
81% ee
97% yield



QD-84
34% ee
90% yield



At the final stage of our search, we again decided to look at the reaction conditions. Initially, we synthesized several catalysts with the same dichloropyrimidine architecture that differ in the identity of the cinchona alkaloids. As we found, mono-quinidine and bis-cinchonine-derived catalyst gave significantly diminished results, while the bis-DHQD-version of the same catalyst gave the IFB product in slightly lower enantioselectivity compared to the bis-QD catalyst (Table 4.3). As we could not achieve the required improvement, we examined how the concentration of the ene-1,4-diketone and catalyst loading affected the stereoselectivity. To our delight we found that lowering the catalyst loading from 10 to 5 mol% allowed us to achieve synthetically useful levels of enantioselectivity.

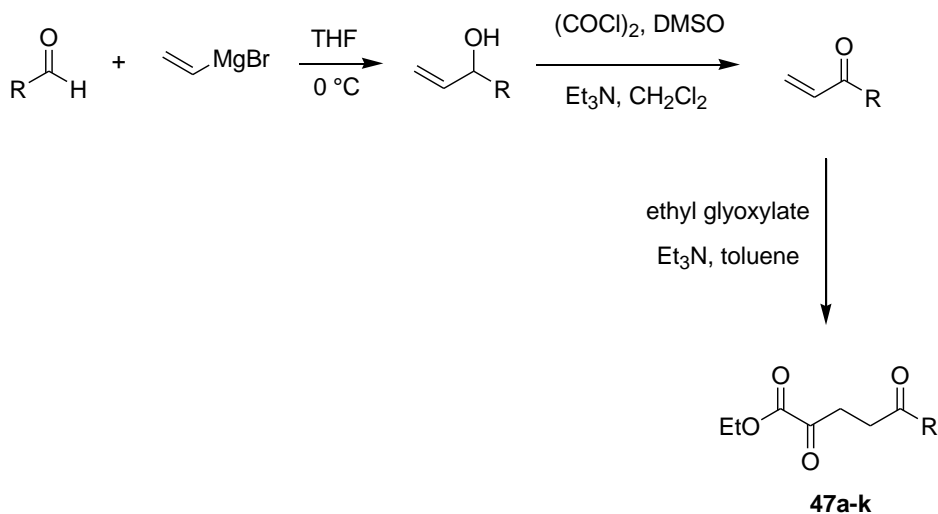
Table 4.3 Optimization of the reaction conditions with **QD-75**

cat.	X ₁ , X ₂	cat. mol%	conc. of 48a, mmol/ml	yield %	ee %
QD-75	X ₁ =X ₂ =QD	10	0.1	92	88
mono-QD-75	X ₁ =Cl, X ₂ =QD	10	0.1	96	60
DHQD-75	X ₁ =X ₂ =DHQD	10	0.1	95	85
CN-75	X ₁ =X ₂ =cinchonine	10	0.1	92	55
QD-75	X ₁ =X ₂ =QD	10	0.2	98	89
QD-75	X ₁ =X ₂ =QD	20	0.1	90	88
QD-75	X₁=X₂=QD	5	0.1	97	92
QD-75	X ₁ =X ₂ =QD	5	0.2	94	89

With the optimized conditions in hand, we turned our attention to the reaction scope. To demonstrate the generality of this method we intended to

expand it to other alkylketones. Analogous to the synthesis of methylketone substrate, we started with the Stetter reaction of ethyl glyoxalate and alkyl vinyl ketone. Ethylvinyl and propylvinyl ketones are commercially available. Other alkylvinyl ketones are easily accessible in a few straightforward steps. In the first step vinylmagnesium bromide reacts with the corresponding alkyl aldehyde to produce secondary alcohol that can be converted into the corresponding alkylvinyl ketone using the Swern protocol (Scheme 4.11).

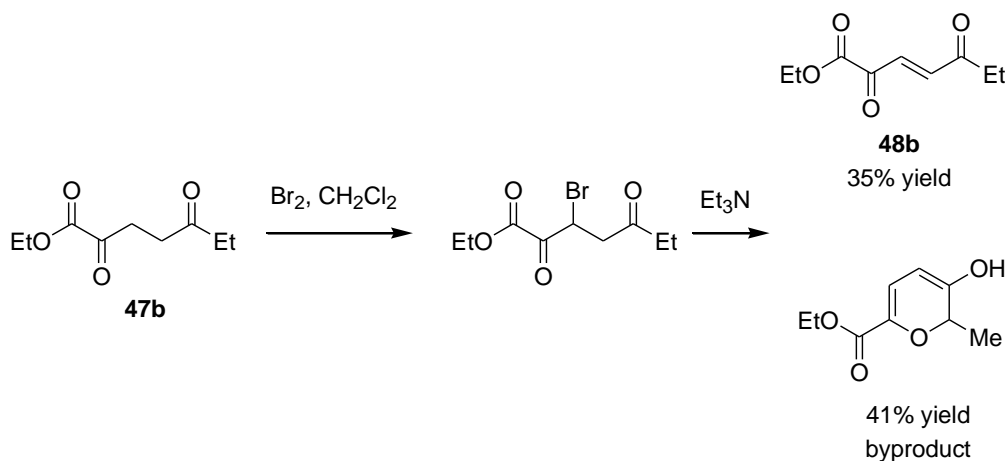
Scheme 4.11



The Stetter reaction proceeds without any complications, allowing us to access a series of 1,4-diketones that differ in the alkyl group on the right side of the molecule. Unexpectedly, the final bromination-elimination sequence resulted in only a small amount of the desired product isolated after the purification. Significant loss of yield was attributed to the formation of the byproduct that

was assigned as pyrone (Scheme 4.12). Besides the low yield, these two products are inseparable on a silica gel column, thus we were in need for a new reproducible procedure for the oxidation of 1,4-diketones into ene-1,4-diketones.

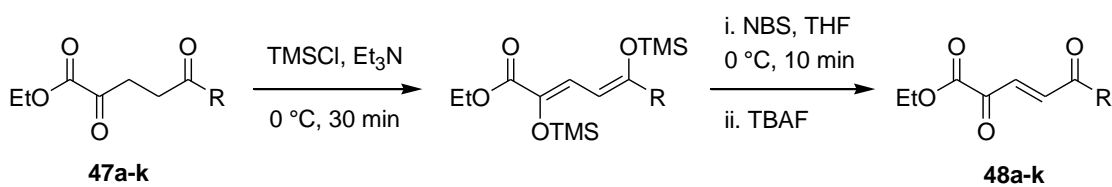
Scheme 4.12

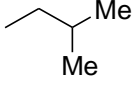
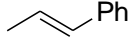


To overcome this problem we developed a new approach to ene-1,4-diketones starting from the same 1,4-diketone. It begins with the addition of TMSCl and triethylamine to the Stetter product to give a perfectly stable bis-TMS ether (Scheme 4.13). This compound, which was used for the next step without purification, was treated with NBS in THF resulting in the bromination of one of the TMS-ethers. At the last step TBAF solution was added to the reaction mixture and the desired product was obtained in good yield. The crude NMR of all reactions show complete consumption of the 1,4-diketone and no significant amount of any side products. To test the generality of the new method, we

synthesized a variety of the alkylketone substrates: ketones with short alkyl chains as ethyl, propyl; substrates with sterically more demanding groups such as benzyl, CH₂Bn, CH₂OBn ketones; and alkyl chains branched at the α- or β-position. Thus, this synthesis turned out to be substantially more efficient and general than previously described method.

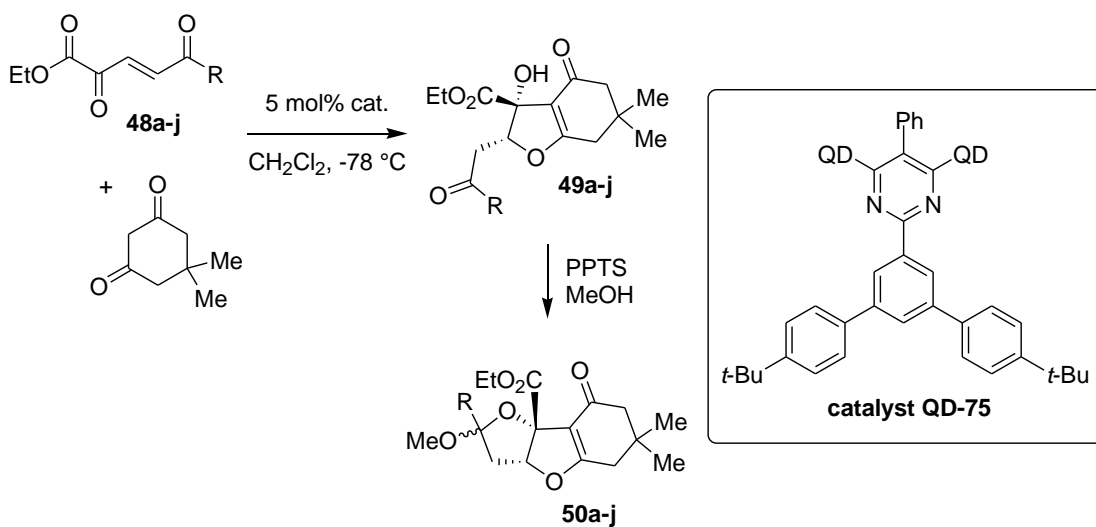
Table 4.4



product	R	yield %
48b	Et	78
48c	<i>n</i> -Pr	75
48d	<i>i</i> -Pr	95
48e	<i>t</i> -Bu	62
48f		89
48g	CH ₂ Bn	83
48h	CH ₂ OBn	64
48i	CH ₂ Ph	36
48j	cyclohexyl	85
48k		57

With a series of substrates in hand, we studied the scope of the reaction. Substrates with short alkyl chains behaved in a similar fashion to methyl ketone in terms of enantioselectivities and yields of the IFB products (**50b,c**). More sterically demanding chains as 3-methylpropyl, CH₂Bn and CH₂OBn could be incorporated without losing enantiocontrol, with these substrates giving the corresponding products in high yields and enantioselectivities in range 90-94% ee (Scheme 4.15). To our disappointment, substrates branched at the α -position of the ketone (**48f,i,j**) showed significant decrease in the ees. This is especially noticeable with isopropyl ketone which gave the IFB product in only 62% ee. In spite of the varying enantioselectivities, we observed excellent yields and diastereoselectivities in all of the cases, confirming the generality of the developed approach.

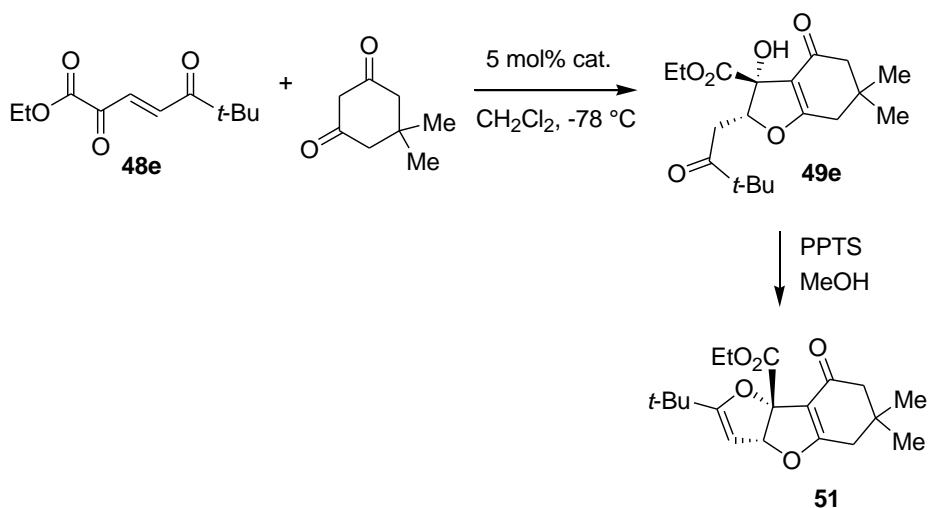
Table 4.15 Substrate scope



electrophile	R	yield % of 49a-j	d.r.	ee %
48a	Me	97	11.2:1	92
48b	Et	98	9.9:1	92
48c	<i>n</i> -Pr	93	10.3:1	94
48d	<i>i</i> -Pr	99	12.1:1	62
48e	<i>t</i> -Bu	89	9.9:1	-
48f		92	11.6:1	95
48g	CH ₂ Bn	98	10.6:1	93
48h	CH ₂ OBn	90	8.5:1	89
48i	CH ₂ Ph	89	9.3:1	78
48j	cyclohexyl	97	10.9:1	74

It is worth mentioning that instead of yielding the mixed methyl ketal product, the cyclization reaction of the tert-butyl IFB product results in formation of the eliminated product **51**. This compound was successfully used for the determination of the %ee of the reaction (Scheme 4.16).

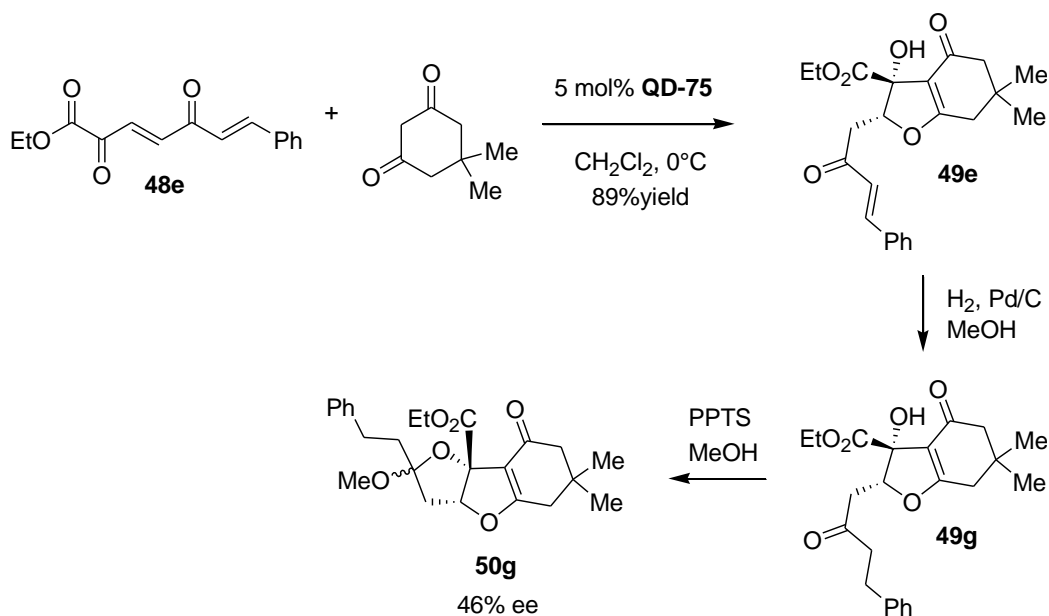
Scheme 4.16



Additionally, unlike other IFB products compound **49a** tends to exist in the open form exclusively (Scheme 4.17). When it was submitted to the standard cyclization conditions (PPTS, MeOH) the reaction did not yield any desired mixed methyl ketal. All our attempts to separate the enantiomers of the major diastereomer by HPLC were unsuccessful, so we decided to convert this IFB product into the previously made hydroxyfuran by reduction with H_2 on Pd/C in methanol. This reaction proceeded without any complications, leaving the double bond of the vinylogous ester functionality untouched. Compound was

then transformed into the mixed methyl ketal. Unfortunately, the enantiopurity of this product was significantly lower than expected.

Scheme 4.17

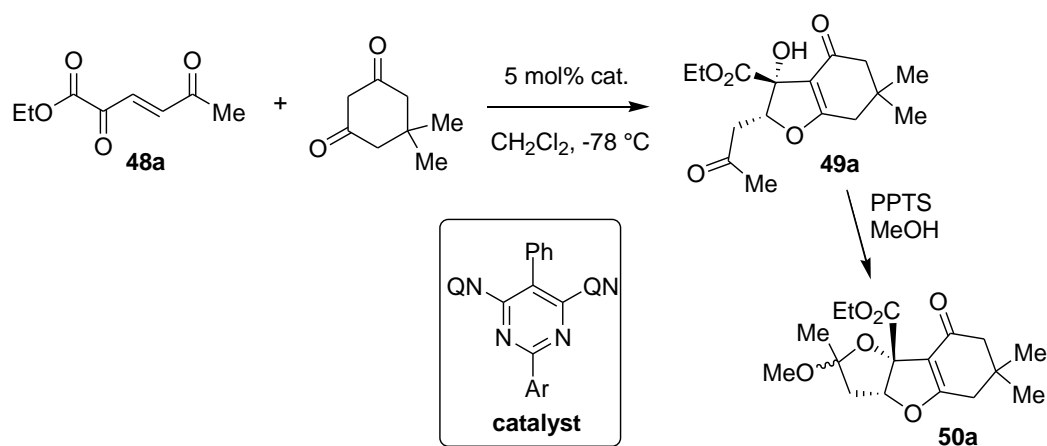


We hoped that the use of the quinine-derived catalyst would provide us with the opposite enantiomer of the IFB product in high stereoselectivity. To our disappointment, the reaction performed under the same conditions using as a catalyst produced the IFB product in diminished enantioselectivity (84% ee). This result prompted us to do an additional screen in for the quinine catalyst series.

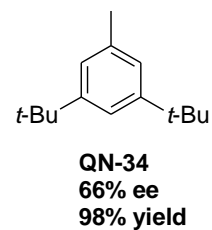
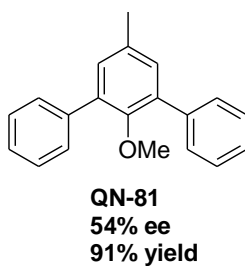
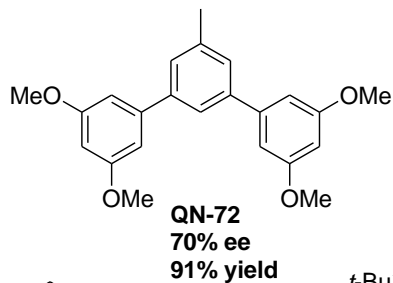
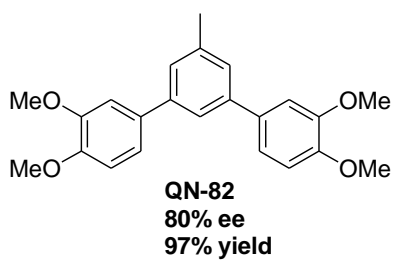
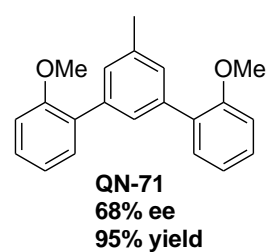
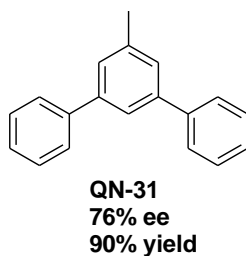
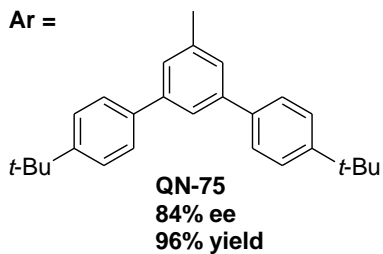
We commenced with the quinine-derived (3,5-diphenyl)phenyl catalyst **QN-31**, but unfortunately the result was still unsatisfactory (Scheme 4.18). Further screening of catalysts bearing substituents at the ortho- and/or meta-

positions also found to be less effective than catalyst. These data suggested that the introduction of a substituent at the para-position has the biggest positive influence on enantioselectivity.

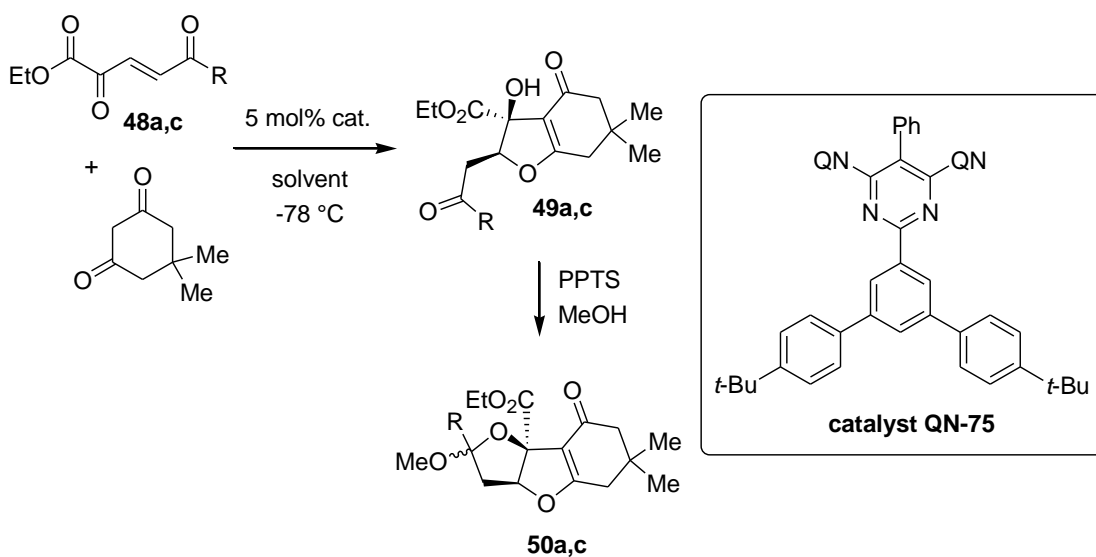
Scheme 4.18



Ar =



At this point, we decided to perform additional optimization studies with regard to the effect of solvents and concentration on enantioselectivity. To our delight the solvent screening quickly gave the required improvement: the reaction in THF resulted in 90% ee, while switching to toluene allowed us to get the IFB product in 96% ee (Table 4.6). Additionally, this result was proved to be general when we applied the same conditions to the reaction *n*-propylketone electrophile **48c**, which gave the corresponding product in 96% ee. Thus, ready access to both enantiomers was possible by choosing the appropriate catalyst.

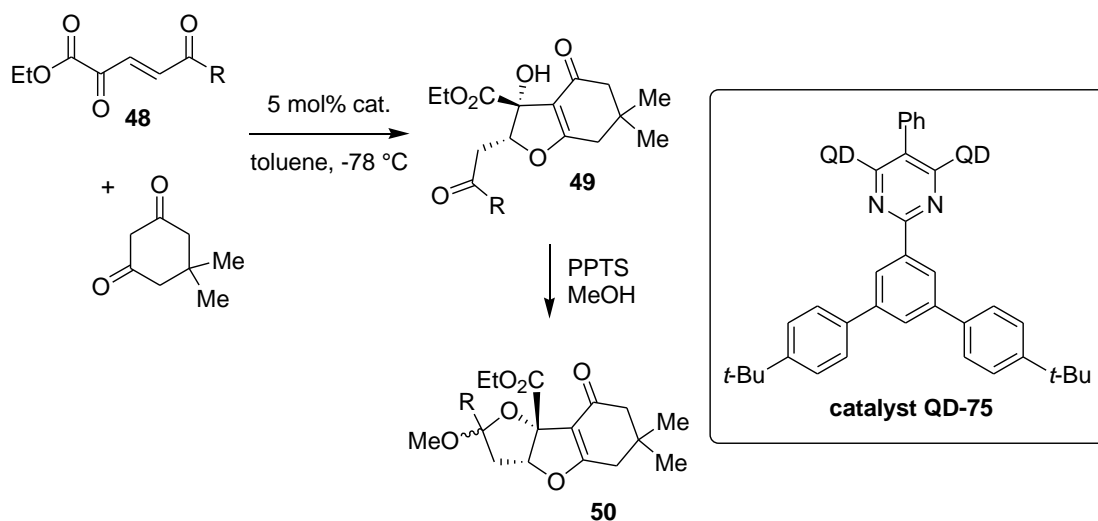
Table 4.6 Final optimizations of reaction conditions

electrophile	R	solvent	yield % of 49a,c	ee %
48a	Me	CH_2Cl_2	95	84
48a	Me	THF	95	90
48a	Me	toluene	97	96
48c	<i>n</i> -Pr	toluene	98	96

Finally, with the optimized conditions in hand we again studied the reaction scope hoping that switching to toluene as a solvent would give a general improvement for the structurally different electrophiles (Table 4.7). We first showed that the new conditions were beneficial for substrates with simple linear groups, like ethyl **48b** and *n*-propyl **48c**. Other electrophiles with more sterically

demanding alkyl groups reacted in toluene affording the corresponding products **49f-h** with the enhanced enantioselectivities compared to the reaction in dichloromethane. This improvement was especially noticeable with benzyloxy substrate **48h**, where the enantioselectivity was increased from 90 to 96% ee. Moreover, we were pleasantly surprised to find that more sterically hindered electrophiles **48f**, **48i** and **48j** now produce the IFB products in synthetically useful level of stereinduction.

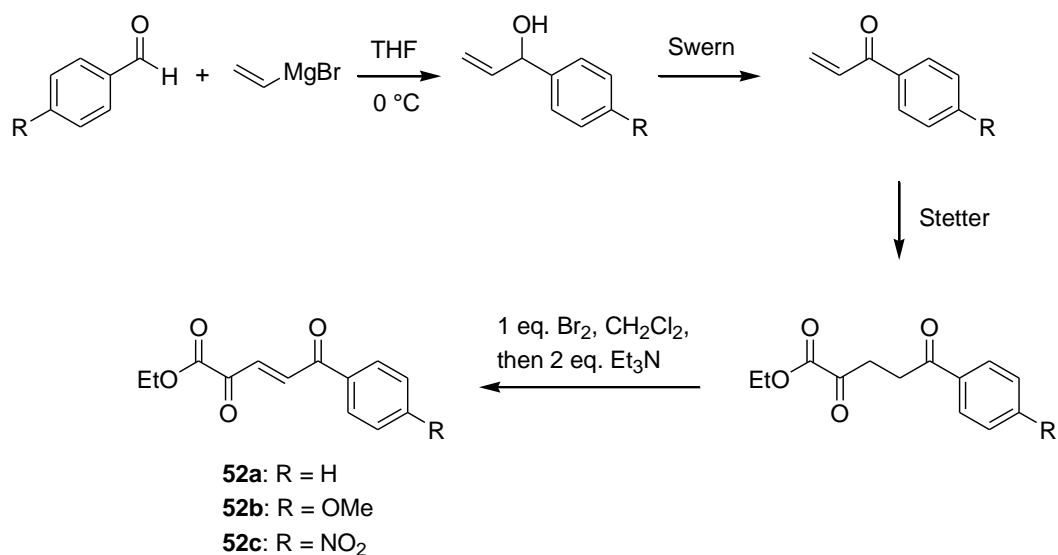
Table 4.7 Substrate scope



electrophile	R	yield % of 49	d.r.	ee %
48a	Me	99	10.3:1	96
48b	Et	95	9.8:1	94
48c	<i>n</i> -Pr	98	10.1:1	96
48d	<i>i</i> -Pr	98	11.3:1	90
48f		97	12.8:1	95
48g	CH ₂ Bn	99	11.8:1	95
48h	CH ₂ OBn	98	8.2:1	95
48i	CH ₂ Ph	93	8.9:1	89
48j	cyclohexyl	98	10.1:1	85

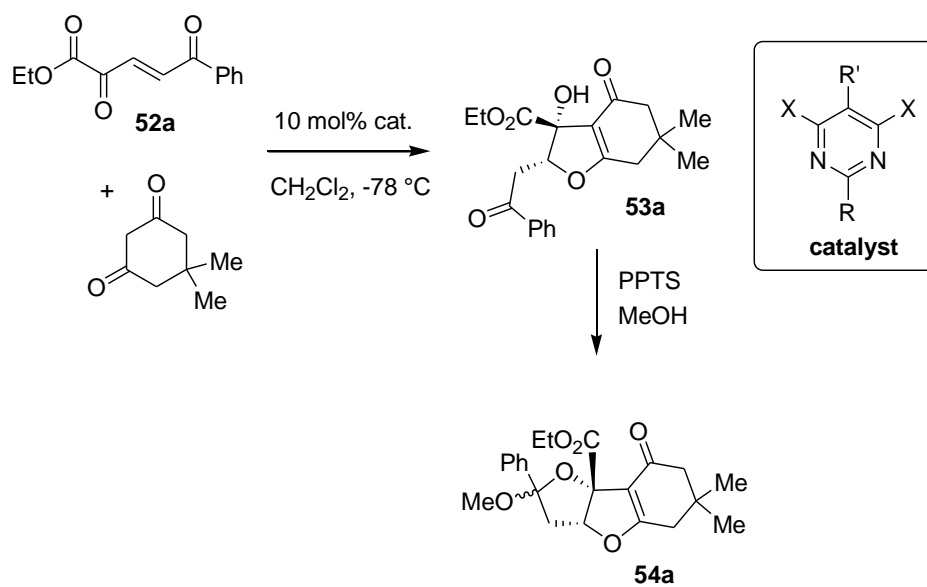
As the newly developed method provided us with enantioselective and high-yielding access for the new class IFB products, we intended to expand the variety of suitable substrates to aryl ketones. The synthesis of these new electrophiles was achieved in a straightforward reaction sequence, analogous to the one previously described. It commenced with vinyl Grignard addition to benzaldehyde followed by a Swern oxidation to afford aryl vinyl ketone (Scheme 4.19). Then, a Stetter reaction provided the 1,4-diketone in a satisfying yield, and the subsequent bromination-elimination one-pot process afforded the desired ene-diketone. This typical procedure for the substrate synthesis gave reproducible results for a series of ene-diketones independently on the electronic properties of the aryl group.

Scheme 4.19



With a set of new substrates in hand, we explored their reactivity under the standard IFB reaction conditions. Gratifyingly, the new substrates gave the corresponding IFB products in excellent yields at -78 °C in dichloromethane. Patrick Sarver should be granted credit for performing a series of experiments with chiral catalysts in order to optimize this reaction (Table 4.8). The first attempt at an asymmetric reaction proved to be less than promising: the **(QD)₂PYR** catalyst produced a racemic IFB product (Table 4.8). Further screening of the catalyst library revealed that the introduction of *t*-Bu group in the *front* position of the catalyst (**QN-3**) leads to the significant enhancement of the enantioselectivity.

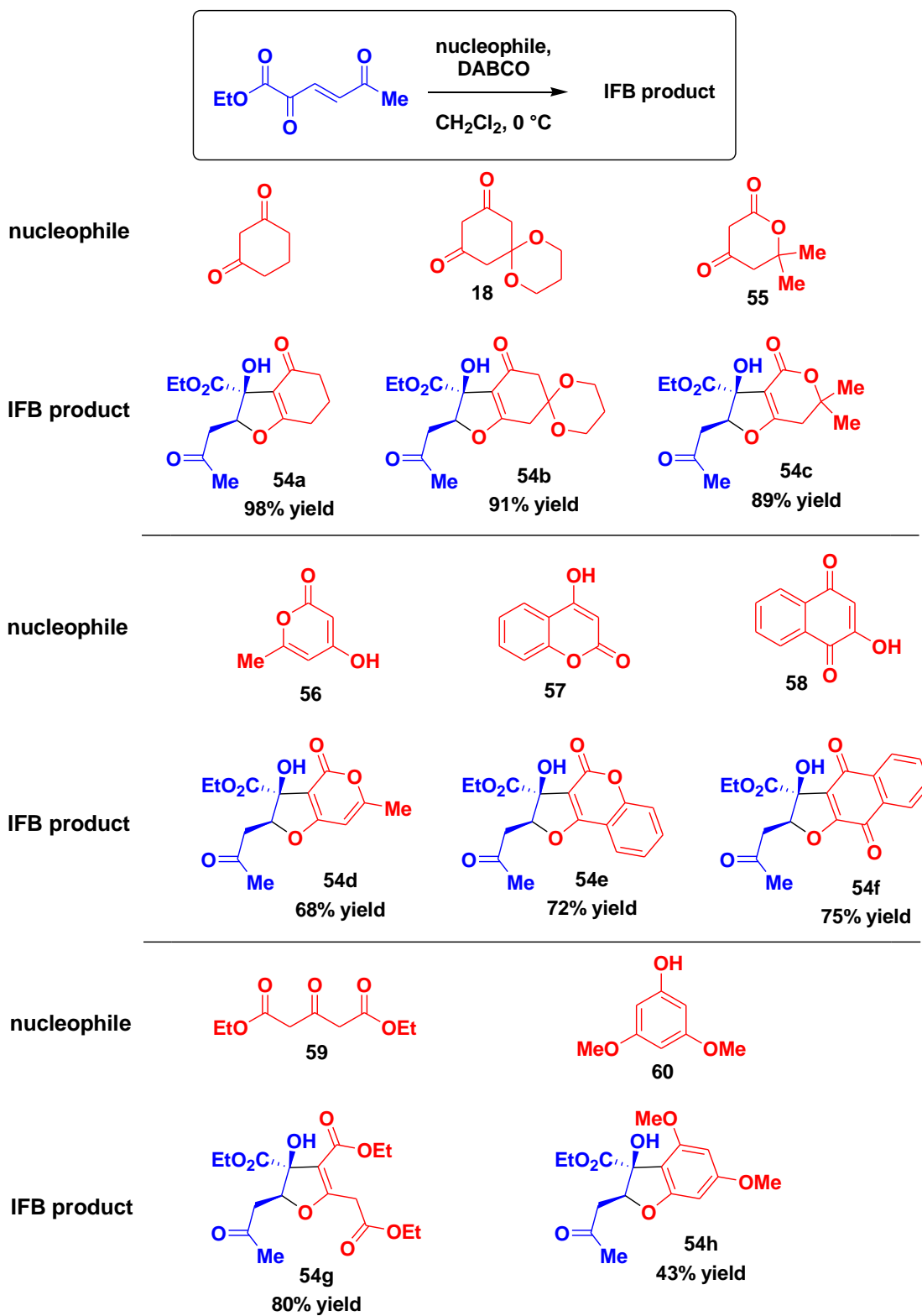
Table 4.8



cat.	R	R'	X	yield % of 53a	ee %
(QD)₂PYR	Ph	Ph	QD	87	0
QD-3	<i>t</i> -Bu	Ph	QD	78	23
QN-3	<i>t</i> -Bu	Ph	QN	82	56
QN-4	<i>t</i> -Bu	<i>t</i> -Bu	QN	80	28
QN-85	<i>t</i> -Bu	Me	QN	90	50
mono-QN-3	<i>t</i> -Bu	Ph	mono-QN	91	41
QN-86	<i>t</i> -Bu	9-anthracenyl	QN	85	14

All studies on the asymmetric IFB reaction conducted in our lab so far were concentrated on the evaluation of the electrophile scope. However, the synthetic utility of the asymmetric IFB reaction could be significantly expanded further if a range of suitable nucleophiles was broadened retaining the high level of stereoselection. We tested a variety of commonly used nucleophiles in the reaction with electrophile **48a** in the presence of DABCO (Scheme 4.20). 1,3-Cyclohexanedione produced the corresponding IFB product **54a** in high yield, as well as dione **18** and structurally similar lactone **55**. Other tested nucleophiles such as pyrone **56**, 4-hydroxycoumarin **57** and 2-hydroxy-1,4-naphthoquinone **58** allowed to expand a range of IFB products further. Interestingly, linear nucleophile **59** also delivered hydroxydihydrofuran product **54g**. Finally, aromatic nucleophile **60** reacted with **48a** giving benzofuran product **54h** in moderate yield. This example is of the most importance as the benzofuran structural motif is common in natural products. Thus, a large variety of nucleophiles are tolerated in the IFB reaction. Further studies should reveal if catalyst **QD-75** can sustain high level of stereoselection independent on the nucleophile structure.

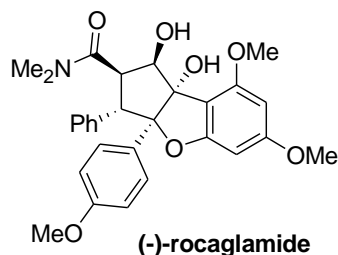
Scheme 4.20 A range of suitable nucleophiles



4.3 Initial investigations on the synthesis of rocaglamide via IFB reaction

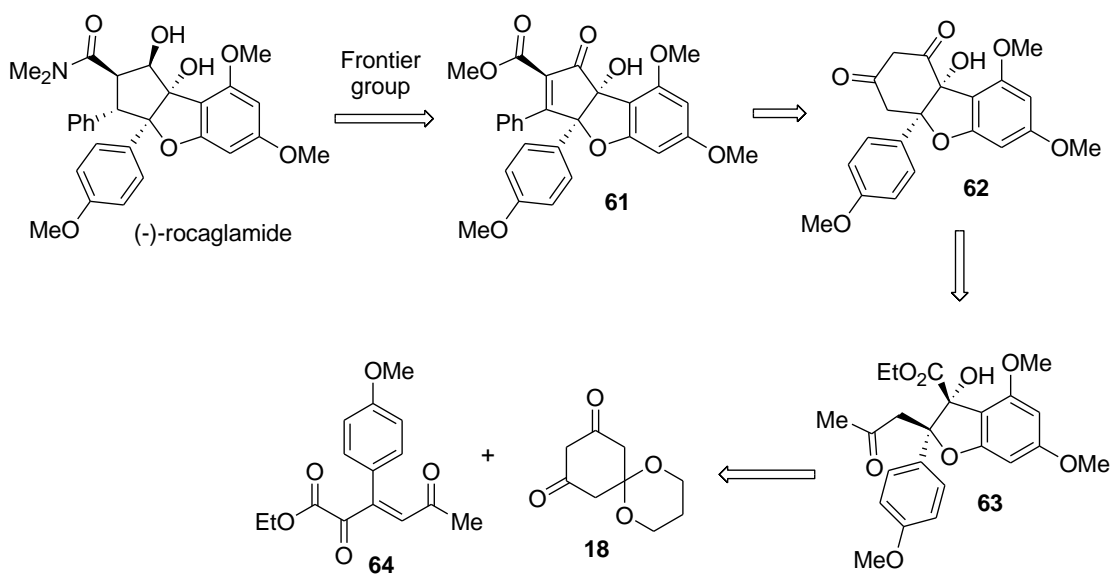
The usefulness of the new methodology is demonstrated through the application for the total synthesis of natural products. For example, the syntheses of variabilin and (-)-glycinol were completed in our group recently utilizing the asymmetric IFB reaction of α -bromopyruvates. Another natural product which attracted our attention due to its hydroxydihydrofuran architecture is rocaglamide. Rocaglamide was initially isolated from the roots and stems of *Aglaia elliptifolia* found primarily in the tropical forests of Southeast Asia and on the Pacific Islands by King et al.⁴ in 1982. King's initial report indicated that rocaglamide showed significant *in vivo* activity in P388 lymphocytic leukemia infected mice. In the later reports, it has been shown by several groups that rocaglamide and related compounds possess cytostatic and cytotoxic activity against a variety of human cancer cell lines, with IC₅₀ values in the range 1.0–6.0 ng/mL⁵. As a result of its complex and unusual structure, as well as an impressive biological profile, rocaglamide has attracted significant attention from the synthetic community. The first total synthesis was reported in 1990 by Trost et al.⁶, and since then numerous approaches⁷ were realized making rocaglamide one of the most attractive targets. However, only two asymmetric syntheses of rocaglamide were accomplished so far by Trost and Porco⁸.

Scheme 4.18



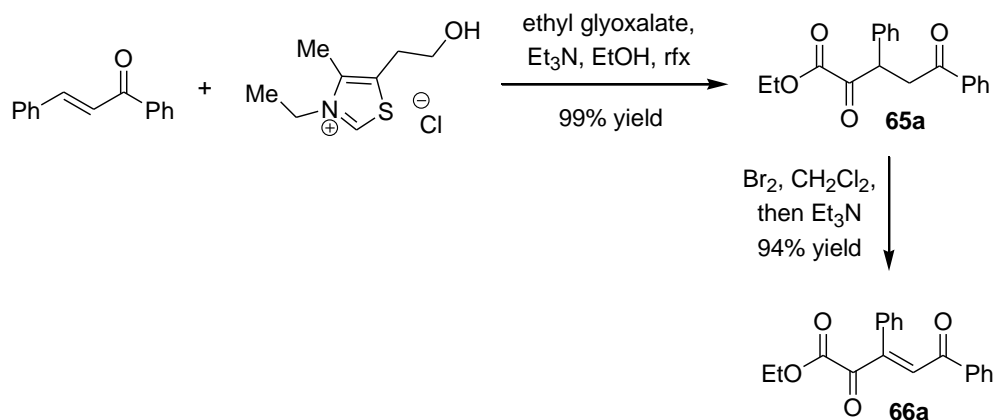
The main synthetic challenge of rocaglamide is a densely functionalized cyclopentane ring bearing five contiguous stereocenters, which include two adjacent quaternary carbons fused with the benzofuran moiety. Giving credit to the extensive synthetic work done on this natural product, the molecule of rocaglamide can be simplified to the advanced intermediate **61** described in the literature by several groups⁹, thus leaving the installment of the three stereogenic center for the later stage of the synthesis (Scheme 4.19). We proposed that **61** can be made from compound **62** by a ring contraction reaction, such as a Wolff rearrangement. 1,3-Cyclohexanedione moiety of **62** could be achieved by Dieckmann condensation performed on compound **63**, that breaks down to the tri-substituted alkene **64** and 1,3-cyclohexanedione **18**. In this proposed sequence, all required stereochemistry is installed in the initial IFB reaction.

Scheme 4.21 Proposed retrosynthesis of (-)-rocaglamide



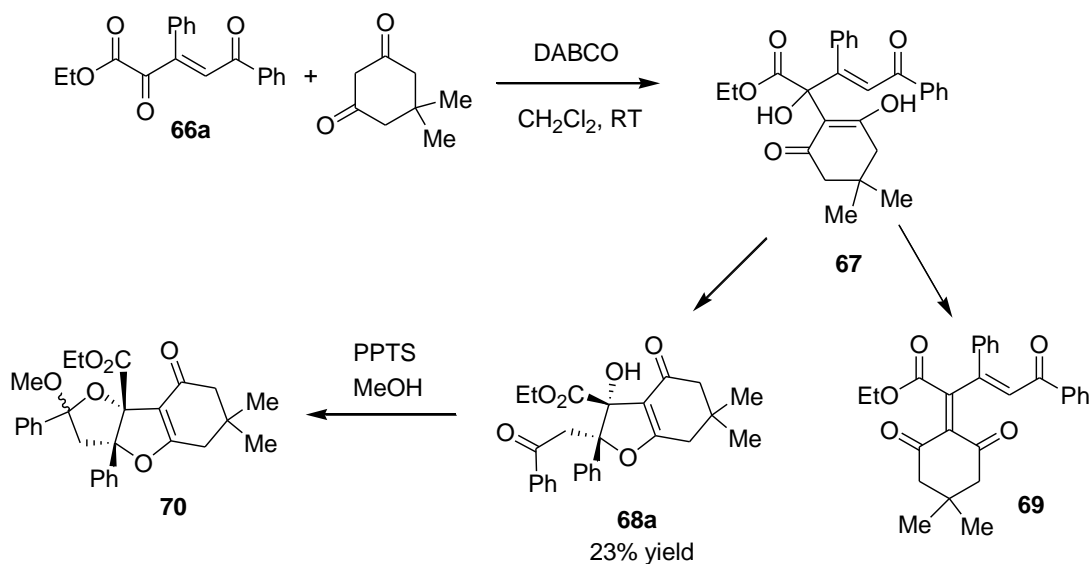
This proposed synthetic plan is based on the hypothesis that the IFB reaction of tri-substituted ene-diketone is feasible and it delivers the required *cis*-isomer of the IFB product. In order to test this idea we synthesized a related substrate **66a** in two steps starting from chalcone (Scheme 4.22). The Stetter reaction gave a rise to 1,4-diketone **65a**¹⁰, which was converted into the desired ene-diketone using bromination-elimination sequence.

Scheme 4.22



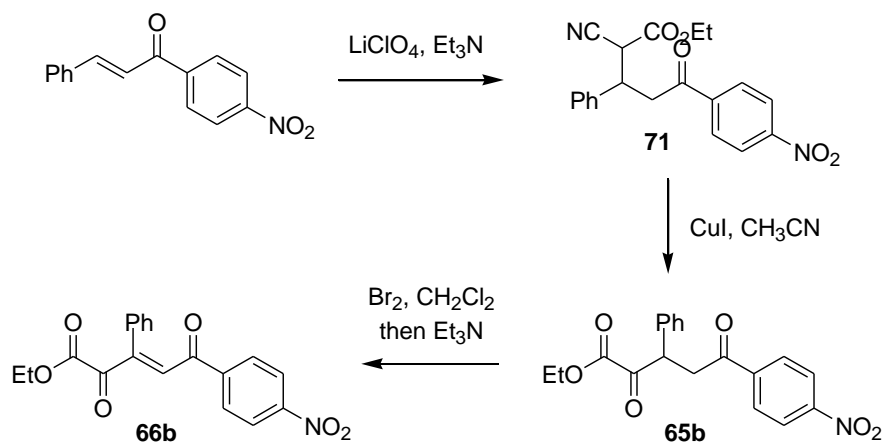
This newly prepared electrophile **66a** was submitted to the standard reaction conditions (Scheme 4.23). To our delight, all starting material was consumed after 4 hours at room temperature and the IFB product **68a** was isolated after the purification by column chromatography. Interestingly, we detected a significant amount of the aldol product **67** in the crude reaction mixture that failed to undergo the desired cyclization to compound **68a**. Purification on a silica gel column resulted in the elimination of water and formation of achiral product **69**, that turned out to be the major product of this reaction. Additionally, the ^1H NMR data suggest the formation of *cis*-isomer, the opposite to the required for the total synthesis of rocaglamide.

Scheme 4.23



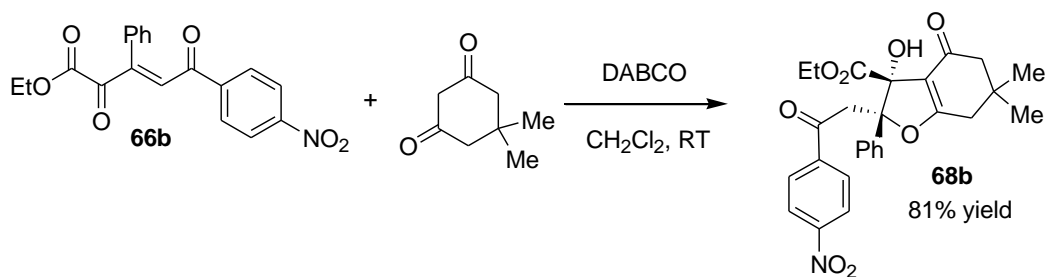
Initial results with electrophile **66a** suggest that the O-1,4-cyclization is a rate-determining step in this reaction. In order to improve the efficiency of this process, we wanted to make the cyclization faster by the introduction of an activating group on the phenyl ring. We applied the previously used Stetter reaction procedure, but unexpectedly it failed to form any of the desired product. An alternative two-step synthesis¹⁰ gave the desired compound **65b** in high yield and then **65b** was successfully converted into ene-diketone **66b** (Scheme 4.24).

Scheme 4.24



Gratifyingly, this modification led to the faster reaction and the corresponding IFB product **68b** was isolated in 81% yield (Scheme 4.25). Only small amount of the aldol product was detected on the crude ^1H NMR of the reaction mixture.

Scheme 4.25

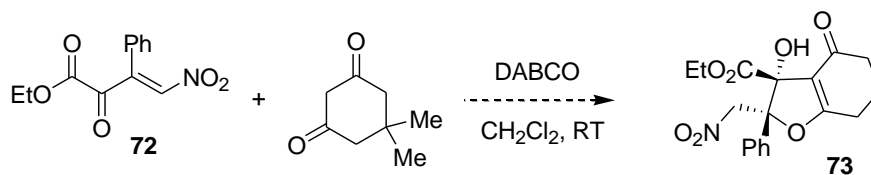


Although initial results show inability of application for the total synthesis of rocaglamide, itself this reaction enables an efficient construction of the highly functionalized dihydrofuran product bearing two adjacent quaternary

stereocenters. Therefore, it is definitely worth pursuing the optimization studies in order to achieve synthetically useful enantioselectivities.

Further enhancement of the reactivity can be achieved with the nitro-alkene substrate **72** (Scheme 4.26). We intend to synthesize this compound utilizing the same reaction sequence that we used for electrophile **66b** starting from nitro-styrene. The nitro group should ensure the sufficient reactivity in order to achieve rapid cyclization to yield the corresponding IFB product **73**. Switching to the compound **72** might also affect the diastereoselectivity of the reaction resulting in the formation of the desired *trans*-isomer of the IFB product.

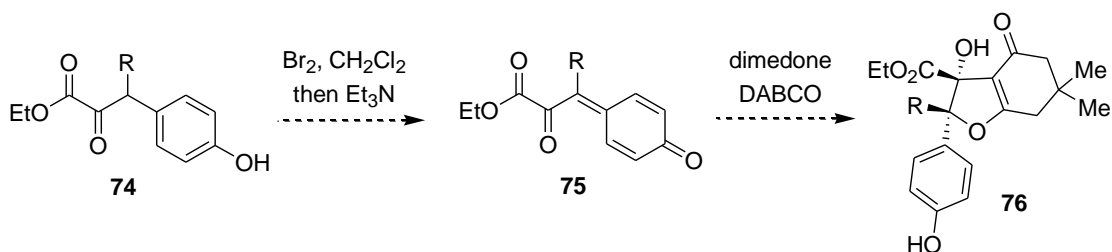
Scheme 4.26



Finally, another approach to access highly functionalized hydroxydihydrofuran intermediates (that potentially can be used in rocaglamide synthesis) did not escape our attention. This strategy utilizes para-quinone methide¹¹ **75** as an electrophile for the IFB reaction (Scheme 4.27). Para- and ortho-quinone methides are extremely reactive species that attracted significant attention from the synthetic community recently, including the numerous examples of the application in the synthesis of natural products.¹² We suggest

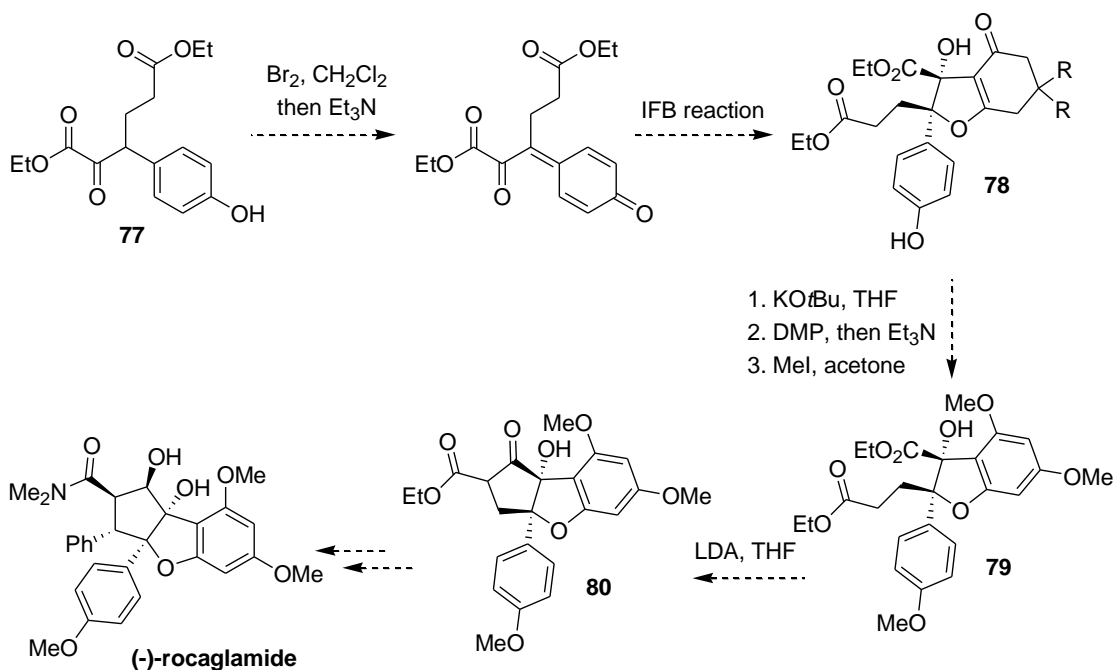
that para-quinone methide can be generated from phenol **74**, and the reaction with dimedone should result in a formation of the IFB product **76**.

Scheme 4.27



If this reaction produces the *trans*-isomer of the IFB product, then a very quick synthesis of rocaglamide could be achieved starting from compound **77**. The aromatization of the right ring of the IFB product **78** and consequent elimination of the side chain and methylation will deliver compound **79**. The Dieckmann condensation will deliver cyclopentane ring of the advanced intermediate **79**. Finally, several straightforward steps would be required to convert **79** into rocaglamide.

Scheme 4.28



4.4 Conclusions

In conclusion, we have developed several new asymmetric IFB reactions. We've shown that α -tosyloxyketones can function as satisfactory electrophiles in the IFB reaction. α -Tosyloxyacetophenones produce the corresponding IFB products in moderate to high yields and high enantioselectivities with newly synthesized bis(pyrimidine)cinchona alkaloid-derived catalysts **QN-8** and **QD-8** bearing a 1-naphthyl group in the *front* position. The IFB reaction of α -tosyloxyindanones gives a rise to the tetra-cyclic IFB products containing two adjacent stereocenters. An extensive catalyst search revealed **mono-QN-60** as

an optimal catalyst giving the IFB product in 84% ee. This methodology provides a key intermediate for the total synthesis of hydroxybrazilin which we are pursuing now. Finally, an ene-1,4-diketones represent a new class of highly reactive electrophiles for the IFB reaction. We optimized the IFB reaction of linear alkyl ketones **48a-j**. The best enantioselective catalyst for this reaction was found to be **QD-75** and **QN-75** bearing a 3,5-di(4-tert-butylphenyl)phenyl group in the *front* position of the catalyst.

References

1. Eddy, N. A.; Kelly, C. B.; Mercadante, M. A.; Leadbeater, N. E.; Fenteany, G., Access to Dienophilic Ene-Triketone Synthons by Oxidation of Diketones with an Oxoammonium Salt. *Org Lett* **2012**, *14* (2), 498-501.
2. Laras, Y.; Hugues, V.; Chandrasekaran, Y.; Blanchard-Desce, M.; Acher, F. C.; Pietrancosta, N., Synthesis of Quinoline Dicarboxylic Esters as Biocompatible Fluorescent Tags. *J Org Chem* **2012**, *77* (18), 8294-8302.
3. Liu, Q.; Perreault, S.; Rovis, T., Catalytic Asymmetric Intermolecular Stetter Reaction of Glyoxamides with Alkylidenemalonates. *J Am Chem Soc* **2008**, *130* (43), 14066-+.
4. King, M. L.; Chiang, C. C.; Ling, H. C.; Fujita, E.; Ochiai, M.; Mcphail, A. T., X-Ray Crystal-Structure of Rocaglamide, a Novel Antileukemic 1h-Cyclopenta[B]Benzofuran from *Aglaia-Elliptifolia*. *J Chem Soc Chem Comm* **1982**, (20), 1150-1151.
5. (a) Proksch, P.; Giaisi, M.; Treiber, M. K.; Palfi, K.; Merling, A.; Spring, H.; Krammer, P. H.; Min, L. W., Rocaglamide derivatives are immunosuppressive phytochemicals that target NF-AT activity in T cells. *J Immunol* **2005**, *174* (11), 7075-7084; (b) Wu, T. S.; Liou, M. J.; Kuoh, C. H.; Teng, C. M.; Nagao, T.; Lee, K. H., Cytotoxic and antiplatelet aggregation principles from *Aglaia elliptifolia*. *J Nat Prod* **1997**, *60* (6), 606-608; (c) Zhu, J. Y.; Lavrik, I. N.; Mahlkecht, U.; Giaisi, M.; Proksch, P.; Krammer, P. H.; Li-Weber, M., The traditional Chinese herbal

compound rocaglamide preferentially induces apoptosis in leukemia cells by modulation of mitogen-activated protein kinase activities. *Int J Cancer* **2007**, *121* (8), 1839-1846.

6. Trost, B. M.; Greenspan, P. D.; Yang, B. V.; Saulnier, M. G., An Unusual Oxidative Cyclization - a Synthesis and Absolute Stereochemical Assignment of (-)-Rocaglamide. *J Am Chem Soc* **1990**, *112* (24), 9022-9024.

7. (a) Feldman, K. S.; Burns, C. J., Radical Mediated Intramolecular [3-Atom + 2-Atom] Addition and the Synthesis of (+/-)-Rocaglamide - Model Studies. *J Org Chem* **1991**, *56* (15), 4601-4602; (b) Watanabe, T.; Shiraga, Y.; Takeuchi, T.; Otsuka, M.; Umezawa, K., Formal total synthesis of aglaiastatin: Pd(0)-mediated construction of benzofurocyclopentane system. *Heterocycles* **2000**, *53* (5), 1051-+; (c) Schoop, A.; Greiving, H.; Gohrt, A., A new analogue of rocaglamide by an oxidative dihydrofuran synthesis. *Tetrahedron Lett* **2000**, *41* (12), 1913-1916; (d) Thede, K.; Diedrichs, N.; Ragot, J. P., Stereoselective synthesis of (+/-)-rocaglaol analogues. *Org Lett* **2004**, *6* (24), 4595-4597; (e) Giese, M. W.; Moser, W. H., Stereoselective synthesis of the rocaglamide skeleton via a silyl vinylketene formation/[4+1] annulation sequence. *Org Lett* **2008**, *10* (19), 4215-4218.

8. Gerard, B.; Jones, G.; Porco, J. A., A biomimetic approach to the rocaglamides employing photogeneration of oxidopyryliums derived from 3-hydroxyflavones. *J Am Chem Soc* **2004**, *126* (42), 13620-13621.

9. Malona, J. A.; Cariou, K.; Spencer, W. T.; Frontier, A. J., Total Synthesis of (+/-)-Rocaglamide via Oxidation-Initiated Nazarov Cyclization. *J Org Chem* **2012**, *77* (4), 1891-1908.
10. Kim, S. H.; Kim, K. H.; Kim, J. N., Construction of 1,2,5-Tricarbonyl Compounds using Methyl Cyanoacetate as a Glyoxylate Anion Synthons Combined with Copper(I) Iodide-Catalyzed Aerobic Oxidation. *Adv Synth Catal* **2011**, *353* (18), 3335-3339.
11. (a) Angle, S. R.; Arnaiz, D. O.; Boyce, J. P.; Frutos, R. P.; Louie, M. S.; Mattsonarnaiz, H. L.; Rainier, J. D.; Turnbull, K. D.; Yang, W. J., Formation of Carbon-Carbon Bonds Via Quinone Methide-Initiated Cyclization Reactions. *J Org Chem* **1994**, *59* (21), 6322-6337; (b) Landucci, L. L.; Ralph, J., Adducts of Anthrahydroquinone and Anthranol with Lignin Model Quinone Methides .1. Synthesis and Characterization. *J Org Chem* **1982**, *47* (18), 3486-3495.
12. (a) Willis, N. J.; Bray, C. D., ortho-Quinone Methides in Natural Product Synthesis. *Chem-Eur J* **2012**, *18* (30), 9160-9173; (b) Pathak, T. P.; Sigman, M. S., Applications of ortho-Quinone Methide Intermediates in Catalysis and Asymmetric Synthesis. *J Org Chem* **2011**, *76* (22), 9210-9215.

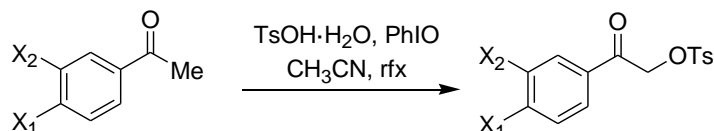
Experimental

General Methods

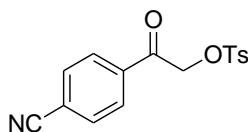
Commercial reagents were used directly as received. Purification of products by chromatography was performed by forced-flow chromatography on Dynamic Adsorbents 60 Å, 32-63 µm silica gel. Thin-layer chromatography (TLC) was accomplished using SiliCycle 0.25 mm thickness, 60 Å pore size silica gel plates. Visualization of the developed TLC was accomplished using fluorescence quenching. ¹H and ¹³C NMR spectra were recorded on Varian Mercury-300BB (300 MHz) and Varian-400 (400 MHz) spectrometer. IR spectra were recorded on a Perkin Elmer 1605 FTIR. Optical rotations were obtained using a Perkin Elmer 241 polarimeter. Mass spectra were obtained from the UC Riverside Mass Spec Facility. Elemental analyses were performed by Atlantic Microlab. The crystal structure of **5f** was determined by Dr. Christopher Incarvito at the Yale University X-ray Crystallographic Facility.

Experimental Procedures and Compound Characterization Data

Representative procedure for synthesis of α -tosyloxyacetophenones:¹

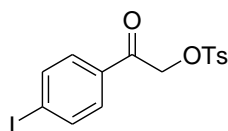


To a solution of iodosobenzene (660 mg, 3.0 mmol) and *p*-toluenesulfonic acid monohydrate (567 mg, 3.0 mmol) in acetonitrile (15 ml), was added the acetophenone (2.0 mmol) and the reaction mixture was refluxed for 5 h. After the solution had cooled to ambient temperature, the solvent was removed under vacuum, the unpurified product was dissolved in CH₂Cl₂ (50 ml) and washed with NaHCO₃ (50 ml), water (50 ml), and then brine (50 ml). The product was purified by recrystallization from a toluene-hexane mixture. Compounds **1a**, **1c-1f**, and **1h-1j** have been prepared before.¹⁻²

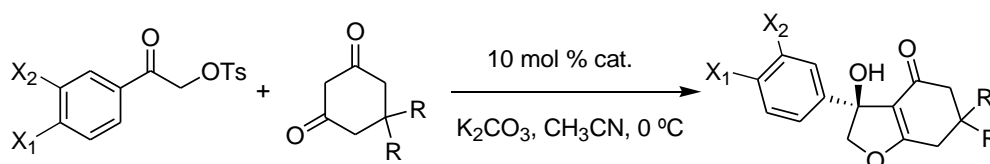


4-(tosyloxyacetyl)benzonitrile (1b). This compound was prepared according to the representative procedure described above (white solid, mp=119 °C, 83% yield). IR (thin film) ν_{max} 2226, 1713, 1347, 1174, 1054, 965 cm⁻¹; ¹H NMR (CDCl₃, 300 MHz) 7.95 (d, J=8.4, 2H), 7.82 (d, J=8.1, 2H), 7.78 (d, J=8.4, 2H), 7.36

(d, J=7.8, 2H), 5.21 (s, 2H), 2.46 (s, 3H); ^{13}C NMR (CDCl_3 , 300 MHz). Elemental Analysis calculated for $\text{C}_{16}\text{H}_{13}\text{N}_1\text{O}_4\text{S}_1$: C 60.94, H 4.16, N 4.44. Found: C 61.13, H 4.18, 4.47.



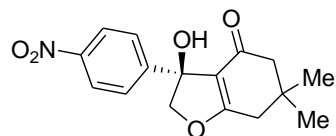
α -tosyloxy-4-iodoacetophenone (1g). This compound was prepared according to the representative procedure described above (white solid, mp=123 °C, 71% yield). IR (thin film) ν_{max} 2925, 1708, 1582, 1363, 1176, 1057, 964 cm^{-1} ; ^1H NMR (CDCl_3 , 300 MHz) 7.83 (d, J=8.4, 4H), 7.54 (d, J=7.8, 2H), 7.35 (d, J=8.4, 2H), 5.19 (s, 2H), 2.45 (s, 3H); ^{13}C NMR (CDCl_3 , 300 MHz) 190.26, 145.68, 138.49, 133.21, 132.69, 130.20, 129.55, 128.38, 102.69, 69.98, 21.96. Elemental Analysis calculated for $\text{C}_{15}\text{H}_{13}\text{I}_1\text{O}_4\text{S}_1$: C 47.27, H 3.15. Found: C 43.42, H 3.05.



Representative procedure for IFB reaction of α -tosyloxyacetophenones:

To a solution of α -tosyloxyacetophenone (0.20 mmol) and catalyst (0.020 mmol) in CH_3CN (4 ml) at 0 °C were added 5,5-dimethyl-1,3-cyclohexanedione (42 mg, 0.30 mmol) or 1,3-cyclohexanedione (34 mg, 0.30 mmol) and K_2CO_3 (55 mg, 0.40 mmol). After 1 h the reaction mixture was concentrated, dissolved in CH_2Cl_2 (5 ml), washed

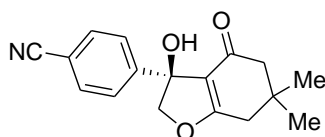
with 1 M aqueous sodium bisulfate (5 ml) and concentrated *in vacuo*. The resulting mixture was purified by flash chromatography (silica, EtOAc:Hexanes = 50:50).



(S)-3-hydroxy-6,6-dimethyl-3-(4-nitrophenyl)-octahydro-1-benzofuran-4-one

(3a). This compound was prepared according to the representative procedure described above (white solid, mp=141 °C, 98% yield) using catalyst **QN-8**; reaction time is 1 h.

The enantioselectivity was determined by HPLC analysis (Daicel Chiralpak AD, 80:20 hexane : *i*-PrOH, 1.2 ml/min, 257 nm) $R_{t(R)}=9.1$ min, $R_{t(S)}=16.9$ min, ee=91%. $[\alpha]^{25}_D=+93.7$ (c 1.0, CH₂Cl₂); IR (thin film) ν_{max} 3308, 2963, 1620, 1512, 1344, 1072 cm⁻¹; ¹H NMR (CDCl₃, 300 MHz) 8.20 (d, J=9.3, 2H), 7.57 (d, J=8.7, 2H), 4.74 (d, J=10.8, 1H), 4.39 (d, J=10.8, 1H), 3.42 (s, 1H), 2.50, 2.27, 1.20 (s, 3H), 1.16 (s, 3H); ¹³C NMR (CDCl₃, 300 MHz) 194.69, 180.33, 151.19, 147.54, 126.50, 124.02, 117.02, 87.30, 81.97, 51.29, 38.27, 34.88, 29.11, 28.77. Elemental Analysis calculated for C₁₆H₁₇N₁O₅: C 63.34; H 5.65; N 4.62. Found: C 63.42; H 5.61; N 4.46.

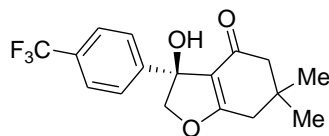


(S)-3-hydroxy-6,6-dimethyl-4-oxo-octahydro-1-benzofuran-3-yl)benzonitrile

(3b). This compound was prepared according to the representative procedure

described above (white solid, mp=132 °C, 82% yield) using catalyst **QN-8**; reaction time is 1 h.

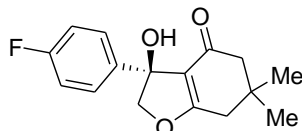
The enantioselectivity was determined by HPLC analysis (Daicel Chiralpak AD, 85:15 hexane : *i*-PrOH, 1.2 ml/min, 257 nm) $R_{t(R)}$ =10.6 min, $R_{t(S)}$ =19.6 min, ee=94%. $[\alpha]^{25}_D$ =+76.4 (c 1.0, CH₂Cl₂); IR (thin film) ν_{\max} 3426, 2959, 2227, 1399, 1221, 1058cm⁻¹; ¹H NMR (CDCl₃, 300 MHz) 7.64 (d, J=8.4, 2H), 7.51 (d, J=8.4, 2H), 4.72 (d, J=10.8, 1H), 4.37 (d, J=10.8, 1H), 3.47 (s, 1H), 2.48, 2.26, 1.19 (s, 3H), 1.16 (s, 3H); ¹³C NMR (CDCl₃, 300 MHz) 194.68, 180.25, 149.28, 123.61, 126.29, 118.93, 116.92, 111.69, 87.30, 82.00, 51.30, 38.27, 34.86, 29.10, 28.79. Elemental Analysis calculated for C₁₇H₁₇N₁O₃: C 72.05; H 6.05; N 4.95. Found: C 71.81; H 6.02; N 4.88.



(S)-3-hydroxy-6,6-dimethyl-3-(4-trifluoromethylphenyl)-octahydro-1-benzofuran-4-one (3c). This compound was prepared according to the representative procedure described above (white solid, mp=87 °C, 87% yield) using catalyst **QN-8**; reaction time is 1 h.

The enantioselectivity was determined by HPLC analysis (Daicel Chiralpak AD, 90:10=hexane : *i*-PrOH, 1.0 ml/min, 257 nm) $R_{t(R)}$ =7.3 min, $R_{t(S)}$ =8.8 min, ee=96%. $[\alpha]^{25}_D$ =+82.2 (c 1.0, CH₂Cl₂); IR (thin film) ν_{\max} 3331, 2960, 1628, 1400, 1124, 1070 cm⁻¹; ¹H NMR (CDCl₃, 300 MHz) 7.59 (d, J=8.4, 2H), 7.51 (d, J=8.4, 2H), 4.73 (d, J=10.8, 1H),

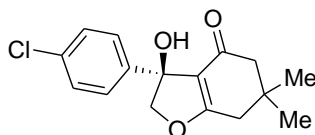
4.37 (d, $J=10.8$, 1H), 3.47 (s, 1H), 2.47, 2.26, 1.19 (s, 3H), 1.15 (s, 3H); ^{13}C NMR (CDCl_3 , 300 MHz) 194.77, 180.08, 148.00, 130.17, 129.74, 125.82, 117.11, 99.18, 87.45, 82.02, 51.35, 38.28, 34.81, 29.06, 28.81. Elemental Analysis calculated for $\text{C}_{17}\text{H}_{17}\text{F}_3\text{O}_3$: C 62.56; H 5.25. Found: C 62.66; H 5.25.



(S)-(4-fluorophenyl)-3-hydroxy-6,6-dimethyl-octahydro-1-benzofuran-4-one

(3d). This compound was prepared according to the representative procedure described above (white solid, 73% yield) using catalyst **QN-8**; reaction time is 5 h.

The enantioselectivity was determined by HPLC analysis (Daicel Chiralpak AD, 90:10=hexane : *i*-PrOH, 1.0 ml/min, 257 nm) $R_{t(R)}=8.2$ min, $R_{t(S)}=11.2$ min, ee=93%. $[\alpha]_{\text{D}}^{25}=+95.3$ (c 1.0, CH_2Cl_2); IR (thin film) ν_{max} 3334, 2959, 1628, 1426, 1221, 1056 cm^{-1} ; ^1H NMR (CDCl_3 , 300 MHz) 7.31 (m, 4H), 4.69 (d, $J=10.5$, 2H), 4.36 (d, $J=10.5$, 2H), 3.31 (s, 1H), 2.46, 2.26, 1.18 (s, 3H), 1.15 (s, 3H); ^{13}C NMR (CDCl_3 , 300 MHz) 194.74, 179.77, 142.64, 133.61, 128.85, 126.83, 117.122, 87.43, 81.95, 51.42, 38.30, 34.77, 29.07, 28.84. Elemental Analysis calculated for $\text{C}_{16}\text{H}_{17}\text{F}_1\text{O}_3$: C 69.54, H 6.20. Found: C 69.41, H 6.10.

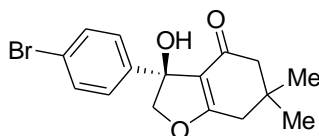


(S)-(4-chlorophenyl)-3-hydroxy-6,6-dimethyl-octahydro-1-benzofuran-4-one

(3e). This compound was prepared according to the representative procedure

described above (white solid, mp=109 °C, 71% yield) using catalyst **QN-10**; reaction time is 5 h.

The enantioselectivity was determined by HPLC analysis (Daicel Chiralpak AD, 90:10=hexane : *i*-PrOH, 1.0 ml/min, 257 nm) $R_{t(R)}$ =9.3 min, $R_{t(S)}$ =12.3 min, ee=96%. $[\alpha]^{25}_D$ =+93.6 (c 1.0, CH₂Cl₂); IR (thin film) ν_{\max} 3334, 2958, 1627, 1405, 1223, 1074 cm⁻¹; ¹H NMR (CDCl₃, 300 MHz) 7.31 (m, 4H), 4.69 (d, J=10.5, 1H), 4.35 (d, J=10.8, 1H), 3.26 (s, 1H), 2.46, 2.26, 1.19 (s, 3H), 1.15 (s, 3H); ¹³C NMR (CDCl₃, 300 MHz) 194.80, 179.81, 142.61, 133.64, 128.87, 126.82, 117.12, 87.41, 81.97, 51.40, 38.30, 34.80, 29.09, 28.84. Elemental Analysis calculated for C₁₆H₁₇ClO₃: C 65.63; H 5.86. Found: C 65.58, 5.73.

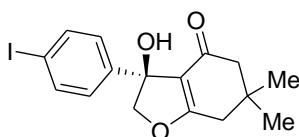


(S)-3-(4-bromophenyl)-3-hydroxy-6,6-dimethyl-octahydro-1-benzofuran-4-one

(3f). This compound was prepared according to the representative procedure described above (white solid, mp=125 °C, 65% yield) using catalyst **QN-8**; reaction time is 5 h.

The enantioselectivity was determined by HPLC analysis (Daicel Chiralpak AD, 85:15 hexane:*i*-PrOH, 1.2 ml/min, 257 nm) $R_{t(R)}$ =6.4 min, $R_{t(S)}$ =7.9 min, ee=96%. $[\alpha]^{25}_D$ =+30.1 (c 1.0, CH₂Cl₂); IR (thin film) ν_{\max} 3405, 2958, 1676, 1627, 1074, 1010 cm⁻¹; ¹H NMR (CDCl₃, 300 MHz) 7.45 (d, J=9.0, 2H), 7.25 (J=8.4, 2H), 4.67 (d, J=10.5, 1H), 4.34 (d, J=10.5, 1H), 3.43 (1H, 1H), 2.45, 2.24, 1.18 (s, 3H), 1.14 (s, 3H); ¹³C NMR (CDCl₃,

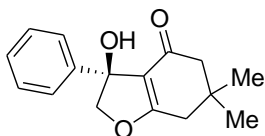
300 MHz) 194.77, 179.88, 143.14, 131.79, 127.22, 121.77, 117.08, 87.42, 81.95, 51.40, 38.30, 34.77, 29.08, 28.84. Elemental Analysis calculated for C₁₆H₁₇BrO₃: C 56.97, H 5.08. Found C 57.36, H4.97.



(S)-3-hydroxy-3-(4-iodophenyl)-6,6-dimethyl-octahydro-1-benzofuran-4-one

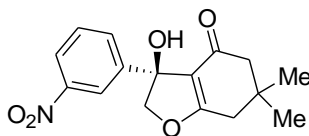
(3g). This compound was prepared according to the representative procedure described above (white solid, mp=131 °C, 70% yield) using catalyst **QN-8**; reaction time is 5 h.

The enantioselectivity was determined by HPLC analysis (Daicel Chiralpak AD, 90:10 hexane:*i*-PrOH, 1.2 ml/min, 257 nm) R_{t(R)}=8.5 min, R_{t(S)}=10.6 min, ee=99%. [α]_D²⁵=+108.3 (c 1.0, CH₂Cl₂); IR (thin film) ν_{max} 3314, 2956, 1632, 1223, 1079, 1004, 966 cm⁻¹; ¹H NMR (CDCl₃, 300 MHz) 7.65 (d, J=8.4, 2H), 7.12 (d, J=8.4, 2H), 4.67 (d, J=10.8, 1H), 4.34 (d, J=10.8, 1H), 3.42 (s, 1H), 2.45, 2.26, 1.18 (s, 3H), 1.14 (s, 3H); ¹³C NMR (CDCl₃, 300 MHz) 194.76, 179.88, 143.86, 137.76, 127.46, 117.07, 93.50, 87.42, 82.00, 51.39, 38.30, 34.77, 29.08, 28.85. Elemental Analysis calculated for C₁₆H₁₇I₁O₃: C 50.00; H 4.46. Found: C 50.29; H 4.51.



(S)-3-hydroxy-6,6-dimethyl-3-phenyl-octahydro-1-benzofuran-4-one (3h). This compound was prepared according to the representative procedure described above (white solid, mp=95 °C, 66% yield) using catalyst **QN-10**; reaction time is 5 h.

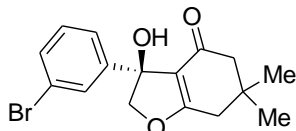
The enantioselectivity was determined by HPLC analysis (Daicel Chiralpak AD, 90:10=hexane : *i*-PrOH, 1.0 ml/min, 257 nm) $R_{t(R)}=8.7$ min, $R_{t(S)}=11.1$ min, ee=90%. $[\alpha]_{D}^{25}=+106.6$ (c 1.0, CH₂Cl₂); IR (thin film) ν_{max} 3357, 2958, 1677, 1451, 1167, 1039 cm⁻¹; ¹H NMR (CDCl₃, 300 MHz) 7.31 (m, 5H), 4.70 (d, J=10.8, 1H), 4.40 (d, J=10.8, 1H), 3.29 (s, 1H), 2.46, 2.26, 1.20 (s, 3H), 1.16 (s, 3H); ¹³C NMR (CDCl₃, 300 MHz) 194.80, 179.48, 144.06, 128.73, 127.76, 125.29, 117.38, 87.55, 82.36, 51.45, 38.32, 34.75, 29.05, 28.94. Elemental Analysis calculated for C₁₆H₁₈O₃: C 74.38; H 7.03. Found: C 74.19; H 7.08.



(S)-3-hydroxy-6,6-dimethyl-3-(3-nitrophenyl)-octahydro-1-benzofuran-4-one (3i). This compound was prepared according to the representative procedure described above (white solid, mp=90 °C, 77% yield) using catalyst **QN-10**; reaction temperature is -42 °C, reaction time is 3 h.

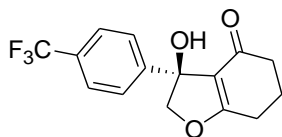
The enantioselectivity was determined by HPLC analysis (Daicel Chiralpak AD, 93:7=hexane : *i*-PrOH, 1.0 ml/min, 257 nm) $R_{t(R)}=26.3$ min, $R_{t(S)}=29.3$ min, ee=90%. $[\alpha]_{D}^{25}=+75.6$; IR (thin film) ν_{max} 3310, 2959, 1620, 1505, 1332, 1082 cm⁻¹; ¹H NMR (CDCl₃, 300 MHz) 8.26 (s, 1H), 8.14 (d, J=8.1, 1H), 7.76 (d, J=8.1, 1H), 7.53 (t, J=7.8,

1H), 4.75 (d, J=10.8, 1H), 4.39 (d, J=11.1, 1H), 2.51, 2.28, 1.22 (s, 1H), 1.17 (s, 1H); ¹³C NMR (CDCl₃, 300 MHz) 194.70, 180.37, 148.67, 146.41, 131.53, 129.76, 122.86, 120.72, 116.85, 87.33, 81.85, 51.31, 38.28, 34.93, 29.12, 28.76. Elemental Analysis calculated for C₁₆H₁₇N₁O₅: C 63.34; H 5.65; N 4.62. Found: C 63.62; H 5.73; N 4.53.



(S)-3-(3-bromophenyl)-3-hydroxy-6,6-dimethyl-octahydro-1-benzofuran-4-one (3j). This compound was prepared according to the representative procedure described above (white solid, mp=113 °C, 61% yield) using catalyst **QN-10**; reaction time is 5 h.

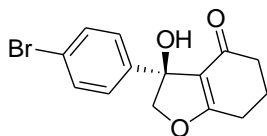
The enantioselectivity was determined by HPLC analysis (Daicel Chiralpak AD, 93:7=hexane : *i*-PrOH, 1.0 ml/min, 257 nm) R_{t(R)}=14.5 min, R_{t(S)}=18.3 min, ee=91%. [α]_D²⁵=+103.2; IR (thin film) ν_{max} 3406, 2967, 1672, 1421, 1054, 1009 cm⁻¹; ¹H NMR (CDCl₃, 300 MHz) 7.39 (s, 1H), 7.25 (m, 3H), 4.67 (d, J=10.5, 1H), 4.36 (d, J=10.8, 1H), 3.35 (br s, 1H), 2.46 (2H), 2.25 (2H), 1.19 (s, 3H), 1.15 (s, 3H); ¹³C NMR (CDCl₃, 300 MHz) 194.67, 179.80, 146.25, 134.73, 130.00, 127.92, 125.75, 123.56, 87.44, 81.94, 51.93, 38.29, 34.81, 29.12, 28.77. Elemental Analysis calculated for C₁₆H₁₇Cl₁O₃: C 65.63, H 5.86. Found: C 65.77, H 5.84.



(S)-3-hydroxy-3-[4-(trifluoromethyl)phenyl]-octahydro-1-benzofuran-4-one

(3k). This compound was prepared according to the representative procedure described above (white solid, mp=95 °C, 90% yield) using catalyst **QN-8**; reaction time is 1 h.

The enantioselectivity was determined by HPLC analysis (Daicel Chiralpak AD, 85:15=hexane : *i*-PrOH, 1.0 ml/min, 257 nm) $R_{t(R)}$ =6.4 min, $R_{t(S)}$ =9.0 min, ee=98%. $[\alpha]^{25}_D$ =+99.6; IR (thin film) ν_{\max} 3339, 2948, 1636, 1409, 1125, 1064 cm^{-1} ; ^1H NMR (CDCl_3 , 300 MHz) 7.59 (d, J =8.4, 2H), 7.51 (d, J =8.4, 2H), 4.70 (d, J =11.1, 1H), 4.36 (d, J =10.8, 1H), 3.54 (s, 1H), 2.61(m, 2H), 2.38 (m, 2H), 2.15 (m, 2H); ^{13}C NMR (CDCl_3 , 300 MHz) 195.44, 181.10, 147.98, 130.15, 129.73, 125.80, 122.51, 118.42, 87.21, 82.07, 36.95, 24.54, 21.84. Elemental Analysis calculated for $\text{C}_{15}\text{H}_{13}\text{F}_3\text{O}_3$: C 60.39; H 4.40. Found: 60.55, H 4.36.

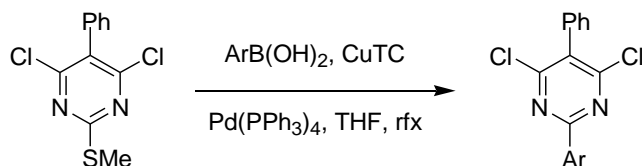


(S)-3-(4-bromophenyl)-3-hydroxy-octahydro-1-benzofuran-4-one (3l). This compound was prepared according to the representative procedure described above (colorless oil, 69% yield) using catalyst **QN-10**; reaction time is 5 h.

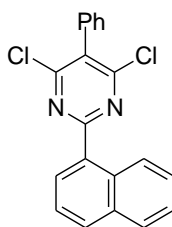
The enantioselectivity was determined by HPLC analysis (Daicel Chiralpak AD, 85:15=hexane : *i*-PrOH, 1.0 ml/min, 257 nm) $R_{t(R)}$ =8.6 min, $R_{t(S)}$ =13.1 min, ee=93%. $[\alpha]^{25}_D$ =+117.6 (c 1.0, CH_2Cl_2); IR (thin film) ν_{\max} 3341, 2949, 1619, 1401, 1074, 1009 cm^{-1} .

1; ^1H NMR (CDCl_3 , 300 MHz) 7.44 (d, $J=8.4$, 2H), 7.25 (d, $J=8.4$, 2H), 4.66 (d, $J=10.8$, 1H), 4.33 (d, $J=10.8$, 1H), 2.58 (m, 2H), 2.35 (m, 2H), 2.10 (m, 2H); ^{13}C NMR (CDCl_3 , 300 MHz) 195.43, 180.91, 143.15, 131.76, 127.20, 121.76, 118.39, 87.317, 82.00, 37.00, 26.56, 21.87. Elemental Analysis calculated for $\text{C}_{14}\text{H}_{13}\text{Br}_1\text{O}_3$: C 54.37; H 4.24. Found: C 54.73, H 4.28.

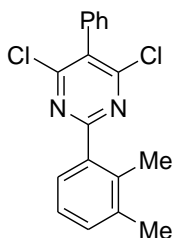
Representative procedure for synthesis of Ph-aryl-dichloropyrimidines:³



4,6-Dichloro-2-methylthio-5-phenylpyrimidine (271 mg, 1mmol), arylboronic acid (1.5 mmol), CuTC (191 mg, 2 mmol) and Pd(PPh₃)₄ (1156 mg, 0.05 mmol) were placed in a flame-dried flask under argon and THF (15 ml) was added. The reaction was stirred for 12 h at 55 °C. The mixture was then cooled to rt, EtOAc (30 ml) was added, and the mixture was filtered. The filtrate was washed sequentially with 1N NaHSO₄ (30 ml), sat. aq. NaHCO₃ (30 ml), and brine(30 ml). The organic layer was dried over MgSO₄, filtered, and concentrated under vacuum. The residue was purified by flash chromatography.

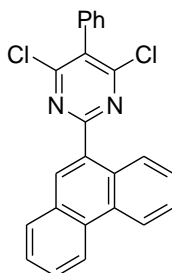


4,6-dichloro-2-(naphthalen-1-yl)-5-phenylpyrimidine. This compound was prepared according to the representative procedure described above (white solid, mp=117 °C, 71% yield). IR (thin film) ν_{\max} 1553, 1481, 1414, 1380, 1274, 1180 cm^{-1} ; ^1H NMR (CDCl_3 , 300 MHz) 8.91 (d, $J=8.4$, 1H), 8.29 (d, $J=6.9$, 1H), 8.03, (d, $J=8.4$, 1H), 7.94 (d, $J=7.8$, 1H), 7.64-7.26 (m, 6H), 7.52-7.26 (m, 2H); ^{13}C NMR (CDCl_3 , 300 MHz) 165.79, 161.31, 134.36, 133.28, 132.75, 132.39, 131.07, 130.93, 129.71, 129.70, 129.513, 128.96, 127.80, 126.43, 125.64, 125.32, 76.82. Elemental Analysis calculated for $\text{C}_{20}\text{H}_{12}\text{Cl}_2\text{N}_2$: C 68.37; H 3.45; N 7.98. Found: C 68.19; H 3.30; N 7.93.

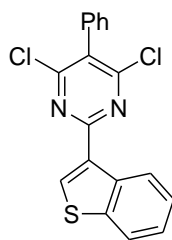


4,6-dichloro-2-(2,3-dimethylphenyl)-5-phenylpyrimidine. This compound was prepared according to the representative procedure described above (white solid, mp=108 °C, 74% yield). ^1H NMR (CDCl_3 , 300 MHz) 7.67 (d, $J=7.2$, 1H), 7.51 (m, 3H), 7.39 (m, 2H), 7.30-7.20 (m, 2H), 2.48 (s, 3H), 2.37 (s, 2H); ^{13}C NMR

(CDCl₃, 300 MHz) 167.18, 161.02, 138.24, 136.32, 136.27, 133.32, 132.30, 130.56, 129.69, 129.45, 128.96, 128.92, 125.81, 20.90, 17.11.

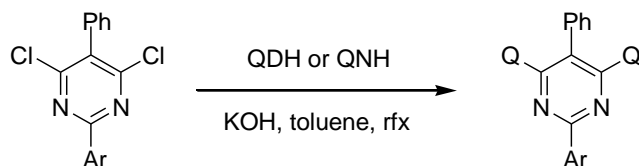


4,6-dichloro-2-(phenanthren-9-yl)-5-phenylpyrimidine. This compound was prepared according to the representative procedure described above (white solid, mp=121 °C, 52% yield). IR (thin film) ν_{max} 3059, 2927, 1552, 1478, 1357, 1273, 1181 cm⁻¹; ¹H NMR (CDCl₃, 300 MHz) 8.87 (d, J=8.4, 1H), 8.83 (d, J=10.5, 1H), 8.73 (d, J=8.1, 1H), 8.55 (s, 1H), 8.04 (d, J=7.5, 1H), 7.74 (m, 4H), 7.75 (m, 3H), 7.50 (m, 2H); ¹³C NMR (CDCl₃, 300 MHz) 165.88, 161.39, 133.27, 132.89, 131.91, 131.80, 131.24, 131.13, 130.96, 130.18, 129.71, 129.55, 129.27, 129.00, 128.67, 127.49, 127.25, 127.17, 126.52, 123.29, 122.88. Elemental Analysis calculated for C₂₄H₁₄Cl₂N₂: C 70.02, H 3.74, N 7.43. Found: C 70.08, H 3.45, N 7.26.



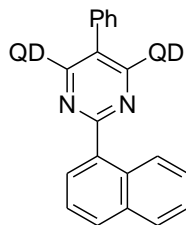
2-(1-benzothiophen-3-yl)-4,6-dichloro-5-phenylpyrimidine. This compound was prepared according to the representative procedure described above (white solid, mp=101 °C, 43% yield). ¹H NMR (CDCl₃, 300 MHz) 9.09 (d, J=8.4, 1H), 8.77 (s, 1H), 7.82 (d, J=7.8, 1H), 7.55-7.36 (m, 7H); ¹³C NMR (CDCl₃, 300 MHz) 161.08, 141.18, 136.59, 135.20, 133.48, 132.07, 129.77, 129.39, 128.90, 125.75, 125.61, 125.25, 122.92.

Representative procedure for synthesis of bis-cinchona alkaloid-pyrimidine catalysts:



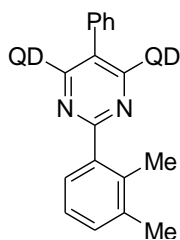
A round-bottom flask equipped with a Dean-Stark condenser was charged with potassium hydroxide (336 mg, 6.0 mmol) and toluene (20 ml). The mixture was refluxed for 1 h and then 2-aryl- 4,6-dichloro-5-phenylpyrimidine (1.0 mmol) along with quinine or quinidine (648 mg, 2.0 mmol) were added in one portion. The mixture was refluxed for 3 h, after which the toluene was

removed in vacuo. The residue was subjected to alumina flash chromatography (activity III basic alumina, EtOAc:Hex=1:1).

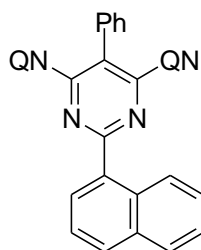


2-(naphthalen-1-yl)-5-phenylpyrimidine-bis-(9-O-quinidine)ether (QD-8).

This compound was prepared according to the representative procedure described above (white foam, 85% yield). $[\alpha]_D^{25} = -95.20$ (c 1.0, CH_2Cl_2); IR (thin film) ν_{max} 2936, 1620, 1539, 1507, 1368, 1228, 1113 cm^{-1} ; ^1H NMR (CDCl_3 , 300 MHz) 8.79 (d, $J=4.5$, 2H), 8.07 (d, $J=9.0$, 2H), 7.75-7.55 (m, 9H), 7.41-7.36 (m, 4H), 7.26-7.20 (m, 3H), 7.04 (t, 1H), 6.93-6.86 (m, 3H), 6.36 (br s, 1H), 5.40-5.32 (m, 2H), 4.89-4.76 (m, 4H), 3.48 (s, 6H), 3.17-3.14 (m, 2H), 2.75-2.54 (m, 7H), 2.09-2.04 (m, 3H), 1.87-1.79 (m, 2H), 1.64 (s, 2H), 1.42-1.23 (m, 7H), 0.93-0.86 (m, 2H); ^{13}C NMR (CDCl_3 , 300 MHz) 166.45, 163.68, 157.98, 147.76, 145.37, 144.97, 140.53, 134.89, 133.72, 132.00, 131.29, 130.84, 130.65, 130.46, 129.63, 128.75, 128.16, 127.25, 126.25, 125.60, 125.54, 124.69, 122.33, 119.11, 114.81, 104.47, 102.03, 59.98, 55.53, 52.40, 50.05, 49.86, 40.63, 37.60, 28.51, 26.54, 23.41, 12.36. HRMS (ESI/APCI) m/z , 927.4592 ($\text{M} + \text{H}^+$), calcd for $\text{C}_{60}\text{H}_{58}\text{N}_6\text{O}_4\text{H}^+$ 927.4553.

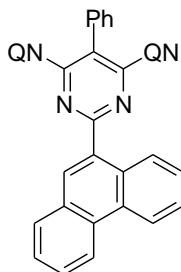


2-(2,3-dimethylphenyl)-5-phenylpyrimidine-bis-(9-O-quinine)ether (QD-7). This compound was prepared according to the representative procedure described above (white foam, 92% yield). ¹H NMR (CDCl₃, 300 MHz) 8.71 (d, J=4.5, 2H), 8.01 (J=9.0, 2H), 7.58-7.57 (m, 4H), 7.51-7.47 (m, 1H), 7.37-7.25 (m, 6H), 7.03 (d, J=7.5, 1H), 6.74 (bs, 3H), 6.57 (d, J=7.5, 1H), 5.74-5.64 (m, 2H), 4.94-4.88 (m, 4H), 3.61 (s, 3H), 3.22 (m, 2H), 2.97-2.92 (m, 4H), 2.53-2.49 (m, 4H), 2.17 (m, 2H), 2.04 (s, 3H), 1.67-1.51 (m, 6H), 1.40 (s, 3H); ¹³C NMR (CDCl₃, 300 MHz) 166.07, 164.97, 157.97, 147.58, 144.92, 142.09, 137.82, 137.38, 135.68, 131.90, 131.29, 130.87, 130.79, 128.56, 128.48, 128.06, 127.07, 124.85, 122.27, 119.08, 114.53, 104.28, 101.77, 59.87, 57.16, 55.65, 43.07, 40.06, 27.86, 27.50, 23.65, 20.65, 15.89. HRMS (ESI/APCI) m/z, 905.4749 (M + H⁺), calcd for C₅₈H₆₀N₆O₄H⁺ 905.4710.



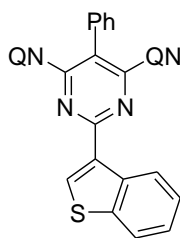
2-(naphthalen-1-yl)-5-phenylpyrimidine-bis-(9-O-quinine)ether (QN-8).

This compound was prepared according to the representative procedure described above (white foam, 89% yield). $[\alpha]^{25}_D = +102.36$ (c 1.0, CH_2Cl_2); IR (thin film) ν_{max} 2942, 1620, 1537, 1508, 1369, 1242, 1230, 1117, 1027, 912 cm^{-1} ; ^1H NMR (CDCl_3 , 300 MHz) 8.77 (d, $J=3.4$, 2H), 8.07 (d, $J=9.3$, 2H), 7.77-7.51 (m, 8H), 7.39-7.36 (m, 4H), 7.26-7.16 (m, 3H), 7.05-7.02 (m, 1H), 6.96-6.93 (m, 1H), 6.83 (d, 2H), 6.34 (bs, 1H), 5.76-5.64 (m, 2H), 4.94-4.88 (m, 4H), 3.50 (s, 6H), 3.22 (m, 2H), 2.04-2.95 (m, 4H), 2.52-2.49 (m, 4H), 2.16 (m, 2H), 1.88 (m, 2H), 1.68-1.60 (m, 4H), 1.26 (m, 4H); ^{13}C NMR (CDCl_3 , 300 MHz) 187.83, 185.00, 177.98, 167.29, 167.00, 166.31, 163.83, 158.03, 148.80, 147.70, 147.03, 145.00, 142.12, 134.65, 133.76, 131.99, 131.23, 130.77, 130.64, 129.72, 128.53, 128.20, 128.14, 127.06, 126.21, 125.57, 124.73, 122.37, 119.08, 114.49, 104.66, 101.90, 59.95, 57.22, 55.59, 43.08, 40.10, 27.88, 27.57, 23.67. HRMS (ESI/APCI) m/z , 927.4592 ($\text{M} + \text{H}^+$), calcd for $\text{C}_{60}\text{H}_{58}\text{N}_6\text{O}_4\text{H}^+$ 927.4553.

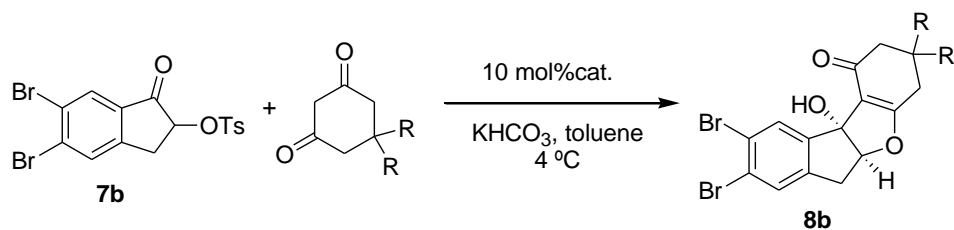


2-(phenanthren-1-yl)-5-phenylpyrimidine-bis-(9-O-quinine)ether (QN-10).

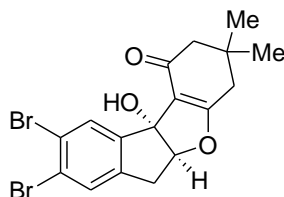
This compound was prepared according to the representative procedure described above (white foam, 78% yield). $[\alpha]^{25}_D = +104.98$ (c 1.0, CH_2Cl_2); IR (thin film) ν_{max} 2940, 1620, 1577, 1538, 1421, 1346, 1117, 1028 cm^{-1} ; ^1H NMR (CDCl_3 , 300 MHz) 8.81 (d, $J=4.2$, 2H), 8.56 (d, $J=8.1$, 2H), 8.12 (d, $J=9.3$, 2H), 7.74 (d, $J=8.1$, 1H), 7.69-7.59 (m, 6H), 7.54-7.47 (m, 2H), 7.41-7.36 (m, 5H), 7.59 (s, 2H), 7.20 (s, 1H), 6.84 (bs, 2H), 6.39 (bs, 1H), 5.76-5.64 (m, 2H), 4.94-4.88 (m, 4H), 3.44 (s, 3H), 3.22 (m, 2H), 3.05-2.91 (m, 4H), 2.53-2.48 (m, 4H), 2.16 (m, 2H), 1.90 (m, 2H), 1.68-1.59 (m, 6H), 1.28-1.20 (m, 4H); ^{13}C NMR (CDCl_3 , 300 MHz) 166.34, 163.91, 158.08, 147.73, 145.05, 142.12, 133.52, 132.01, 131.35, 131.35, 131.25, 131.06, 130.77, 130.50, 129.64, 129.16, 128.59, 128.19, 127.86, 127.03, 126.73, 126.39, 126.29, 122.57, 122.43, 119.25, 114.49, 110.00, 104.83, 101.91, 77.67, 77.45, 77.25, 76.82. HRMS (ESI/APCI) m/z , 977.4749 ($\text{M} + \text{H}^+$), calcd for $\text{C}_{64}\text{H}_{58}\text{N}_6\text{O}_4\text{H}^+$ 977.4710.



2-(1-benzothiophen-3-yl)-5-phenylpyrimidine-bis-(9-O-quinine)ether (QN-11). This compound was prepared according to the representative procedure described above (white foam, 71% yield). ^1H NMR (CDCl_3 , 300 MHz) 8.76 (d, $J=4.8$, 2H), 8.09 (d, $J=9.2$, 2H), 7.89 (d, $J=8.6$, 1H), 7.66-7.57 (m, 5H), 7.52-7.39 (m, 8H), 7.08 (t, $J=7.5$, 1H), 6.93 (d, $J=2.7$, 2H), 6.32 (t, $J=7.2$, 1H), 7.71-5.59 (m, 2H), 4.92-4.84 (m, 4H), 3.81 (s, 3H), 3.22 (m, 2H), 3.05-2.97 (m, 4H), 2.61-2.48 (m, 6H), 2.15 (m, 2H), 1.67-1.62 (m, 2H), 1.52-1.49 (m, 2H), 1.25-1.20 (m, 2H), 0.96 (m, 2H); ^{13}C NMR (CDCl_3 , 300 MHz) 166.71, 159.36, 158.36, 147.79, 144.90, 144.68, 142.08, 140.58, 136.35, 133.81, 132.48, 132.33, 131.39, 130.79, 128.65, 128.16, 126.75, 125.09, 124.46, 124.02, 122.45, 122.29, 118.31, 114.53, 104.77, 101.53, 59.67, 57.54, 55.99, 43.52, 40.06, 27.93, 27.21, 22.25. HRMS (ESI/APCI) m/z , 933.4117 ($\text{M} + \text{H}^+$), calcd for $\text{C}_{58}\text{H}_{56}\text{N}_6\text{O}_4\text{S}_1\text{H}^+$ 933.4157.

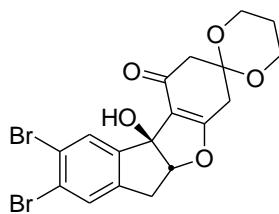


To a solution of α -tosyloxyindanone **7b** (0.20 mmol) and catalyst (0.020 mmol) in toluene (4 ml) at 0 °C were added 5,5-dimethyl-1,3-cyclohexanedione or compound **18** (0.30 mmol) and KHCO_3 (55 mg, 0.40 mmol). After 3 days the reaction mixture was washed with 1 M aqueous sodium bicarbonate (5 ml) and concentrated *in vacuo*. The resulting mixture was purified by flash chromatography (silica, EtOAc:Hexanes = 50:50).



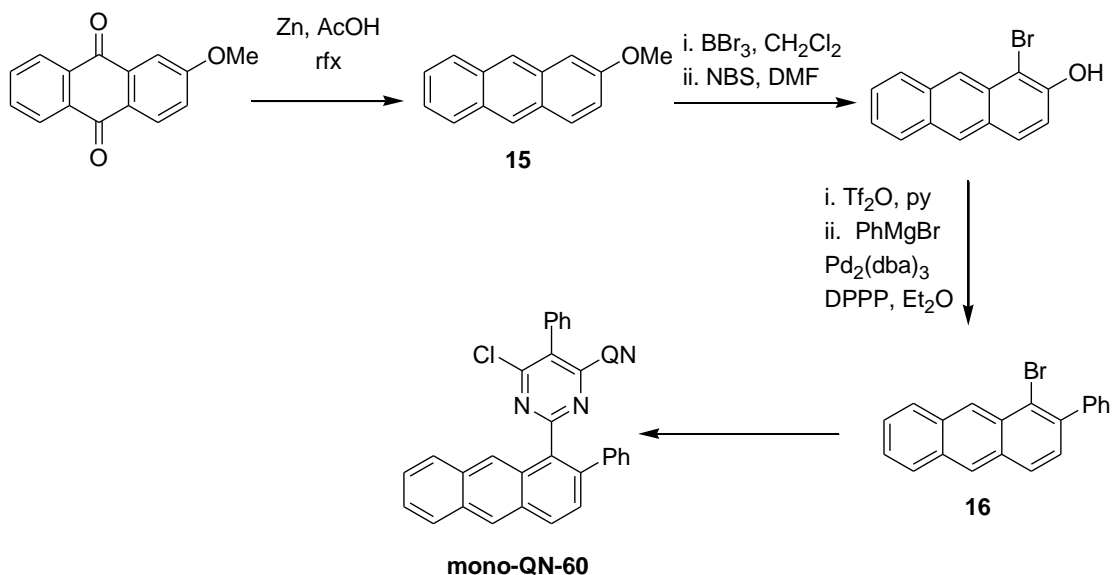
13,14-dibromo-1-hydroxy-5,5-dimethyl-8-oxatetracyclo[7.7.0.0^{2,7}.0^{11,16}]hexadeca- 11(16),12,14-trien-3-one (8b).

This compound was prepared according to the representative procedure described above (white solid, 81% yield). ^1H NMR (CDCl_3 , 300 MHz) 8.03 (s, 1H), 7.47 (s, 1H), 5.34 (dd, 1H), 3.57 (dd, 1H), 3.01 (dd, 1H), 2.36 (d, $J=19.6$ Hz, 1H), 2.28 (d, $J=19.6$ Hz, 1H), 2.24 (app. s, 2H), 1.14 (s, 3H), 1.04 (s, 3H).



19

This compound was prepared according to the representative procedure described above (white foam, 73% yield). ¹H NMR (CDCl₃, 300 MHz) 8.03 (s, 1H), 7.42 (s, 1H), 5.37 (dd, J₁=7.6 Hz, J₂=3.0 Hz, 1H), 3.97-3.375 (m, 4H), 3.58 (dd, J₁=18.0 Hz, J₂=7.6 Hz, 1H), 3.04-2.92 (m, 3H), 2.75 (dd, 2H), 1.81-1.61 (m, 2H).



1-bromo-2-phenylanthracene (16).

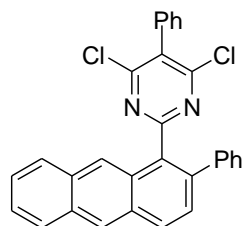
To a suspension of 2-methoxyanthraquinone⁴ (1.0 mmol) in glacial AcOH (30 mL) was added zinc dust (1.7 g, 26 mmol) in one portion. The reaction

mixture was refluxed for 20 hours. After the reaction was complete (monitored by TLC), the mixture was poured into ice water and extracted with CH_2Cl_2 . The combined organic phase was washed with water and sat. solution of NaHCO_3 , respectively, and then dried. After removal of the solvent *in vacuo*, the residue was recrystallized from benzene to afford 2-methoxyanthracene in 71% yield.

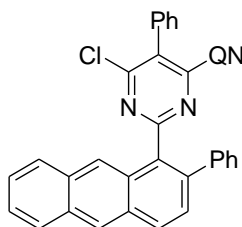
To a solution of 1-bromo-2-methoxyanthracene (10 mmol) in pyridine at 0 °C was added trifluoromethanesulfonic anhydride (12 mmol). The mixture was stirred at 0 °C for 1 h and then allowed to warm to room temperature and stirred for a further 3 h. The resulting mixture was partitioned between 2 M HCl and Et_2O , the organic layer was washed with two further portions of acid and then filtered through a thin pad of silica gel. The solvent was removed *in vacuo* to give 1-bromo-2-trifluoromethoxyanthracene in 95% yield as a yellow oil which was used without further purification.

To a solution of 1-bromo-2-trifluoromethoxyanthracene (12.3 mmol) in Et_2O (12 mL) was added $\text{Pd}_2(\text{dba})_3$ (180 mg, 0.195 mmol), 1,3-bis(diphenylphosphino)propane (161 mg, 0.39 mmol), and LiBr (1.13 g, 13.0 mmol). The resulting mixture was stirred at room temperature for 5 min, then a solution of PhMgBr in Et_2O (3.0 M, 5.2 mL, 15.5 mmol) was added using a water bath to cool the mildly exothermic reaction. The mixture was then stirred at room temperature for 7 h, before quenching with methanol (1.5 mL) and filtering through a plug of silica gel with Et_2O and the solvent removed *in vacuo*.

Product was recrystallized from toluene-hexanes mixture to give 1-bromo-2-phenylanthracene **16** as a white solid (95% yield). ^1H NMR (CDCl_3 , 300 MHz) 8.98 (s, 1H), 8.42 (s, 1H), 8.15-7.95 (m, 3H), 7.58-7.30 (m, 8H).



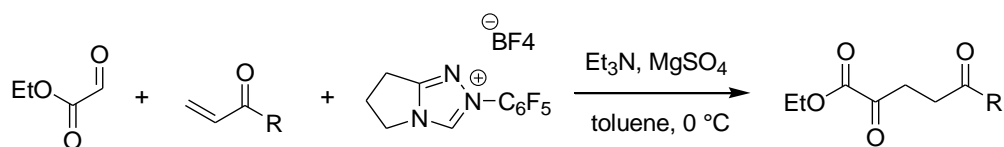
^1H NMR (CDCl_3 , 300 MHz) 8.58 (s, 1H), 8.37 (s, 1H), 8.19 (d, $J=7.0$ Hz, 1H), 8.07-7.95 (m, 2H), 7.61-7.14 (m, 13H).



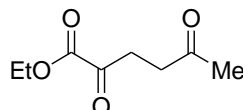
Catalyst mono-QN-60.

^1H NMR (CDCl_3 , 300 MHz) 8.63 (d, $J=4.6$ Hz, 1H), 8.42 (s, 1H), 8.07 (d, $J=7.0$ Hz, 1H), 7.96 (d, $J=6.6$ Hz, 1H), 7.80 (br. s, 1H), 7.61-7.38 (m, 7H), 7.20-6.80 (m, 5H), 6.70 (br. s, 1H), 5.61 (m, 1H), 4.89 (m, 2H), 3.10 (s, 3H), 2.82 (m, 2H), 2.41 (m, 2H), 2.18 (m, 2H), 1.62 (m, 2H).

Representative procedure for the Stetter reaction:⁵

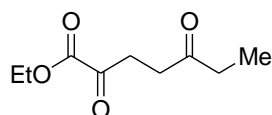


A dry flask was charged with triazolium salt² (.36 g, 1 mmol), vinylketone³ (10 mmol), ethyl glyoxalate (2.4 g of 50 wt.% in toluene, 12 mmol), MgSO₄ (.6 g, 5 mmol) and 50 ml toluene. The flask was placed in an ice bath and triethylamine (1.4 ml, 10 mmol) was added in one portion. The mixture was allowed to stir at 0 °C for 15 min and then filtered through silica gel to afford a crude product. The product was purified via flash chromatography to provide desired 1,4-diketone.



ethyl 2,5-dioxohexanoate (47a). This compound was prepared according to the representative procedure described above (colorless oil, 92% yield). Flash chromatography: 35% EtOAc/Hexanes.

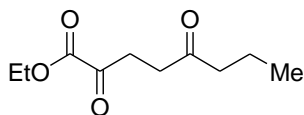
¹H NMR (CDCl₃, 400 MHz) 4.23 (q, J=6.0 Hz, 2H), 2.99 (t, J=6.0 Hz, 2H), 2.75 (t, J=6.4 Hz, 2H), 2.12 (s, 3H), 1.28 (t, J=6.8 Hz, 3H); ¹³C NMR (CDCl₃, 400 MHz) 206.31, 193.23, 160.75, 62.64, 37.03, 33.12, 29.81, 14.13; HRMS (ESI/APCI) m/z, 173.0812 (M + H⁺), calcd for C₈H₁₂O₄H⁺ 173.0808.



ethyl 2,5-dioxoheptanoate (47b). This compound was prepared according to the representative procedure described above (colorless oil, 95% yield). Flash chromatography: 30% EtOAc/Hexanes.

^1H NMR (CDCl_3 , 400 MHz) 4.28 (q, $J=7.2$ Hz, 2H), 3.05 (t, $J=6.4$ Hz, 2H), 2.76 (t, $J=6.4$ Hz, 2H), 2.45 (q, $J=7.6$ Hz, 2H), 1.33 (t, $J=7.2$ Hz, 3H), 1.02 (t, $J=7.6$ Hz, 3H);

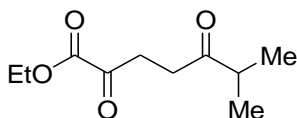
^{13}C NMR (CDCl_3 , 400 MHz) 209.19, 193.42, 160.83, 62.70, 35.92, 35.83, 33.16, 14.17, 7.95; HRMS (ESI/APCI) m/z , 187.0961 ($\text{M} + \text{H}^+$), calcd for $\text{C}_9\text{H}_{14}\text{O}_4\text{H}^+$ 187.0965.



ethyl 2,5-dioxooctanoate (47c). This compound was prepared according to the representative procedure described above (colorless oil, 91% yield). Flash chromatography: 30% EtOAc/Hexanes.

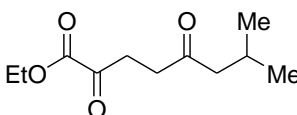
^1H NMR (CDCl_3 , 400 MHz) 4.28 (q, $J=6.8$ Hz, 2H), 3.5 (t, $J=5.6$ Hz, 2H), 2.75 (t, $J=6.4$ Hz, 2H), 2.41 (t, $J=7.2$ Hz, 2H), 1.57 (m, 2H), 1.33 (t, $J=7.2$ Hz, 3H), .87 (t, $J=7.2$ Hz, 3H); ^{13}C NMR (CDCl_3 , 400 MHz) 208.76, 193.39, 160.82, 62.71, 44.65,

36.24, 33.10, 17.49, 14.17, 13.86; HRMS (ESI/APCI) m/z , 201.1119 ($M + H^+$),
calcd for $C_{10}H_{16}O_4H^+$ 201.1121.



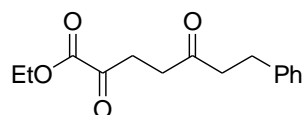
ethyl 6-methyl-2,5-dioxoheptanoate (47d). This compound was prepared according to the representative procedure described above (colorless oil, 97% yield). Flash chromatography: 30% EtOAc/Hexanes.

1H NMR ($CDCl_3$, 400 MHz) 4.28 (q, $J=7.2$ Hz, 2H), 3.04 (t, $J=6.8$ Hz, 2H), 2.80 (t, $J=6.8$ Hz, 2H), 2.62 (m, 1H), 1.32 (t, $J=7.6$ Hz, 3H), 1.09 (s, 3H); 1.07 (s, 3H); ^{13}C NMR ($CDCl_3$, 400 MHz) 212.46, 193.43, 160.83, 62.67, 40.85, 34.04, 33.12, 18.44, 14.17.



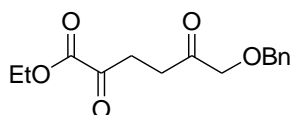
ethyl 7-methyl-2,5-dioxooctanoate (47f). This compound was prepared according to the representative procedure described above (colorless oil, 89% yield). Flash chromatography: 30% EtOAc/Hexanes.

^1H NMR (CDCl_3 , 400 MHz) 4.25 (q, $J=7.2$ Hz, 2H), 3.01 (t, $J=6.0$ Hz, 2H), 2.71 (t, $J=6.0$ Hz, 2H), 2.27 (d, $J=6.8$ Hz, 2H), 2.07 (m, 1H), 1.30 (t, $J=6.8$ Hz, 3H), 0.85 (d, $J=6.4$ Hz, 6H); ^{13}C NMR (CDCl_3 , 400 MHz) 208.40, 193.31, 160.79, 62.64, 51.66, 36.76, 33.02, 24.92, 22.68, 14.14; HRMS (ESI/APCI) m/z , 215.1275 ($\text{M} + \text{H}^+$), calcd for $\text{C}_{11}\text{H}_{18}\text{O}_4\text{H}^+$ 215.1278.



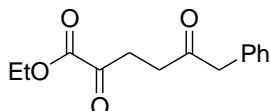
ethyl 2,5-dioxo-7-phenylheptanoate (48g). This compound was prepared according to the representative procedure described above (colorless oil, 90% yield). Flash chromatography: 25% EtOAc/Hexanes.

^1H NMR (CDCl_3 , 400 MHz) 7.35-7.25 (m, 2H), 7.21-7.15 (m, 3H), 4.31 (q, $J=6.8$ Hz, 2H), 3.08 (t, $J=6.0$ Hz, 2H), 2.88 (t, $J=6.0$ Hz, 2H), 2.79 (m, 4H), 1.36 (t, $J=6.8$ Hz, 3H); ^{13}C NMR (CDCl_3 , 400 MHz) 207.70, 193.33, 160.82, 141.06, 128.75, 128.51, 126.38, 62.76, 44.29, 36.38, 33.19, 29.91, 14.21; HRMS (ESI/APCI) m/z , 263.1276 ($\text{M} + \text{H}^+$), calcd for $\text{C}_{15}\text{H}_{18}\text{O}_4\text{H}^+$ 263.1278.

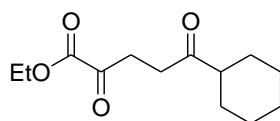


ethyl 6-(benzyloxy)-2,5-dioxohexanoate (48h). This compound was prepared according to the representative procedure described above (colorless oil, 85% yield). Flash chromatography: 35% EtOAc/Hexanes.

^1H NMR (CDCl_3 , 400 MHz) 7.36-7.24 (m, 5H), 4.59 (s, 2H), 4.31 (q, $J=6.8$ Hz, 2H), 4.12 (s, 2H), 3.13 (t, $J=6.8$ Hz, 2H), 2.84 (t, $J=6.8$ Hz, 2H), 1.35 (t, $J=6.8$ Hz, 3H); ^{13}C NMR (CDCl_3 , 400 MHz) 207.06, 191.16, 160.73, 137.34, 128.77, 128.28, 128.15, 75.13, 75.10, 73.68, 73.65, 32.86, 14.21; HRMS (ESI/APCI) m/z , 301.1036 ($\text{M} + \text{Na}^+$), calcd for $\text{C}_{15}\text{H}_{18}\text{O}_5\text{Na}^+$ 301.1046.

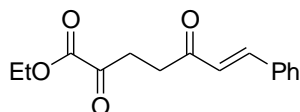


ethyl 2,5-dioxo-6-phenylhexanoate (48i). This compound was prepared according to the representative procedure described above (colorless oil, 83% yield). Flash chromatography: 25% EtOAc/Hexanes. ^1H NMR (CDCl_3 , 400 MHz) 7.35-7.18 (m, 5H), 4.30 (q, $J=7.2$ Hz, 2H), 3.74 (s, 2H), 3.05 (t, $J=6.4$ Hz, 2H), 2.81 (t, $J=6.4$ Hz, 2H), 1.33 (q, $J=7.2$ Hz, 3H).



ethyl 5-cyclohexyl-2,5-dioxopentanoate (48j). This compound was prepared according to the representative procedure described above (colorless oil, 88% yield). Flash chromatography: 25% EtOAc/Hexanes.

^1H NMR (CDCl_3 , 400 MHz) 4.30 (q, $J=6.8$ Hz, 2H), 3.05 (t, $J=5.6$ Hz, 2H), 2.80 (t, $J=6.0$ Hz, 2H), 2.47-2.27 (m, 1H), 1.85 (m, 2H), 1.75 (m, 2H), 1.64 (m, 1H), 1.38-1.08 (m, 8H); ^{13}C (CDCl_3 , 400 MHz) 211.80, 193.48, 160.87, 62.70, 50.73, 34.35, 33.09, 28.69, 26.00, 25.79, 14.20.

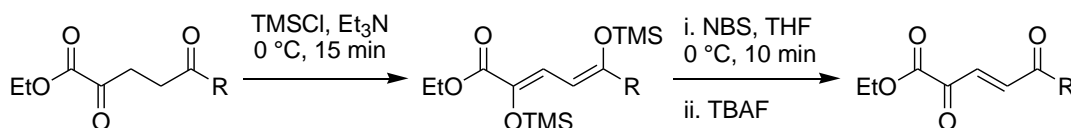


ethyl (6E)-2,5-dioxo-7-phenylhept-6-enoate (48k). This compound was prepared according to the representative procedure described above (colorless oil, 88% yield). Flash chromatography: 25% EtOAc/Hexanes.

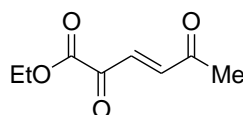
^1H NMR (CDCl_3 , 400 MHz) 7.59-7.50 (m, 3H), 7.37 (m, 3H), 6.73 (d, $J=16.4$ Hz, 1H), 4.32 (q, $J=7.2$ Hz, 2H), 3.16 (t, $J=6.8$ Hz, 2H), 3.07 (t, $J=6.8$ Hz, 2H), 1.35 (t,

J=7.2 Hz, 3H); ^{13}C (CDCl_3 , 400 MHz) 197.65, 193.45, 160.94, 143.49, 134.49, 130.88, 129.20, 128.57, 125.69, 62.74, 34.57, 33.26, 14.22.

Representative procedure for the oxidation of 1,4-diketone into 2-ene-1,4-diketone:

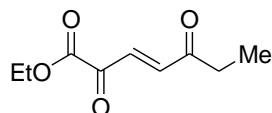


1,4-diketone (2 mmol) was dissolved in 20 ml CH_2Cl_2 and cooled down to 0 °C. To this solution in one portion was added TMSCl (.64 ml, 2.2 mmol) followed by dropwise addition of triethylamine (.7 ml, 2.2 mmol) and the resulting solution was stirred for 20 min at room temperature. After that, the reaction mixture was washed with water, brine and then concentrated *in vacuo*. The resulting bis-TMS-ether was dissolved in 20 ml THF and the solution was cooled down to 0 °C. NBS (356 mg, 2 mmol) was added in one portion, reaction stirred for 5 min at 0 °C and TBAF (2 ml of 1M solution in THF) was added slowly. The reaction was immediately quenched with water (40 ml), 50 ml of CH_2Cl_2 added, layers were separated and organic layer was washed with brine and then concentrated. The crude product was purified by flash silica gel chromatography to afford the desired product as yellow oil.



ethyl (3E)-2,5-dioxohex-3-enoate (48a). This compound was prepared according to the representative procedure described above (yellow oil, 90% yield). Flash chromatography: 20% EtOAc/Hexanes.

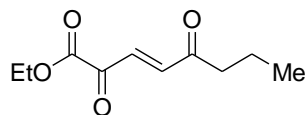
^1H NMR (CDCl_3 , 400 MHz) 7.42 (d, $J=16.0$ Hz, 1H), 7.09 (d, $J=16.0$ Hz, 1H), 4.38 (q, $J=7.2$ Hz, 2H), 2.41 (s, 3H), 1.39 (t, $J=7.2$ Hz, 3H); ^{13}C NMR (CDCl_3 , 400 MHz) 197.69, 183.59, 160.97, 141.32, 131.78, 63.25, 28.66, 14.16; HRMS (ESI/APCI) m/z , 171.0652 ($\text{M} + \text{H}^+$), calcd for $\text{C}_8\text{H}_{10}\text{O}_4\text{H}^+$ 171.0652.



ethyl (3E)-2,5-dioxohept-3-enoate (48b). This compound was prepared according to the representative procedure described above (yellow oil, 78% yield). Flash chromatography: 20% EtOAc/Hexanes.

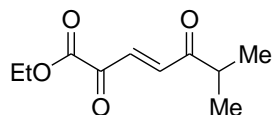
^1H NMR (CDCl_3 , 400 MHz) 7.43 (d, $J=16.4$ Hz, 1H), 7.13 (d, $J=16.4$ Hz, 1H), 4.37 (q, $J=7.2$ Hz, 2H), 2.72 (q, $J=6.8$ Hz, 2H), 1.37 (t, $J=7.2$ Hz, 3H), 1.15 (t, $J=7.2$ Hz, 3H); ^{13}C NMR (CDCl_3 , 400 MHz) 200.23, 183.65, 160.97, 140.71, 130.98, 63.20,

35.44, 14.17, 7.69; HRMS (ESI/APCI) m/z , 185.0812 ($M + H^+$), calcd for $C_9H_{12}O_4H^+$ 185.0808.



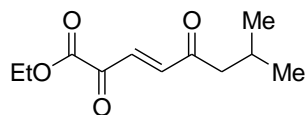
ethyl (3E)-2,5-dioxooct-3-enoate (48c). This compound was prepared according to the representative procedure described above (yellow oil, 75% yield). Flash chromatography: 20% EtOAc/Hexanes.

1H NMR ($CDCl_3$, 400 MHz) 7.41 (d, $J=16$, 1H), 7.11 (d, $J=16$, 1H), 4.36 (q, $J=6.8$, 2H), 2.65 (t, $J=7.2$, 2H), 1.66 (m, 2H), 1.37 (t, $J=7.2$, 3H), .93 (t, $J=7.2$, 3H); ^{13}C NMR ($CDCl_3$, 400 MHz) 199.86, 183.68, 161.02, 140.93, 131.03, 63.23, 43.97, 17.27, 14.19, 13.81; HRMS (ESI/APCI) m/z , 199.0966 ($M + H^+$), calcd for $C_{10}H_{14}O_4H^+$ 199.0965.



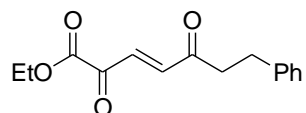
ethyl (3E)-6-methyl-2,5-dioxohept-3-enoate (48d). This compound was prepared according to the representative procedure described above (yellow oil, 95% yield). Flash chromatography: 20% EtOAc/Hexanes.

¹H NMR (CDCl₃, 400 MHz) 7.46 (d, J=16 Hz, 1H), 7.23 (d, J=16 Hz, 1H), 4.36 (q, J=6.8 Hz, 2H), 2.87 (m, 1H), 1.37 (t, J=7.2 Hz, 3H), 1.15 (s, 1H); 1.13 (s, 1H); ¹³C NMR (CDCl₃, 400 MHz) 202.99, 183.53, 160.99, 139.74, 131.37, 63.19, 40.52, 17.94, 14.19.



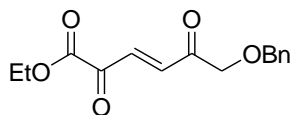
ethyl (3E)-7-methyl-2,5-dioxooct-3-enoate (48f). This compound was prepared according to the representative procedure described above (yellow oil, 89% yield). Flash chromatography: 20% EtOAc/Hexanes.

¹H NMR (CDCl₃, 400 MHz) 7.35 (d, J=16.0 Hz, 1H), 7.04 (d, J=16.0 Hz, 1H), 4.31 (q, J=7.2 Hz, 2H), 2.50 (d, J=6.8 Hz, 2H), 2.13 (m, 1H), 1.32 (t, J=7.2 Hz, 3H), .88 (d, J=6.8 Hz, 6H); ¹³C NMR (CDCl₃, 400 MHz) 199.58, 183.63, 160.98, 141.05, 131.02, 36.13, 50.87, 24.81, 22.65, 14.13; HRMS (ESI/APCI) m/z, 213.1122 (M + H⁺), calcd for C₁₁H₁₆O₄H⁺ 213.1121.



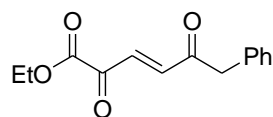
ethyl (3E)-2,5-dioxo-7-phenylhept-3-enoate (48g). This compound was prepared according to the representative procedure described above (yellow oil, 83% yield). Flash chromatography: 15% EtOAc/Hexanes.

^1H NMR (CDCl_3 , 400 MHz) 7.42 (d, $J=16.0$ Hz, 1H, 7.33-7.29 (m, 2H), 7.21-7.18 (m, 3H), 7.12 (d, $J=16.0$ Hz, 1H), 4.37 (q, $J=7.2$ Hz, 2H), 3.05-2.95 (m, 4H), 1.39 (t, $J=7.2$ Hz, 3H); ^{13}C NMR (CDCl_3 , 400 MHz) 198.84, 183.53, 160.96, 140.67, 140.57, 131.27, 128.84, 128.58, 126.60, 63.26, 43.65, 29.68, 14.22; HRMS (ESI/APCI) m/z , 261.1122 ($\text{M} + \text{H}^+$), calcd for $\text{C}_{15}\text{H}_{16}\text{O}_4\text{H}^+$ 261.1121.



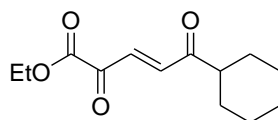
ethyl (3E)-6-(benzyloxy)-2,5-dioxohex-3-enoate (48h). This compound was prepared according to the representative procedure described above (yellow oil, 64% yield). Flash chromatography: 30% EtOAc/Hexanes.

^1H NMR (CDCl_3 , 400 MHz) 7.51 (d, $J=16.0$ Hz, 1H), 7.40-7.19 (m, 6H), 4.61 (s, 2H), 4.36 (q, $J=6.8$ Hz, 2H), 4.29 (s, 2H), 1.37 (t, $J=6.8$ Hz, 3H); ^{13}C NMR (CDCl_3 , 400 MHz) 197.09, 183.35, 160.84, 136.95, 132.02, 128.86, 128.51, 128.37, 75.00, 74.96, 73.83, 63.26, 14.21; HRMS (ESI/APCI) m/z , 277.1067 ($\text{M} + \text{H}^+$), calcd for $\text{C}_{15}\text{H}_{16}\text{O}_5\text{H}^+$ 277.1071.



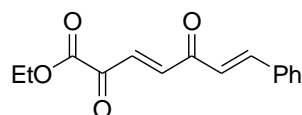
ethyl (3E)-2,5-dioxo-6-phenylhex-3-enoate (48i). This compound was prepared according to the representative procedure described above (yellow oil, 36% yield). Flash chromatography: 20% EtOAc/Hexanes.

^1H NMR (CDCl_3 , 400 MHz) 7.50 (d, $J=16.0$ Hz, 1H), 7.35-7.16 (m, 6H), 4.36 (q, $J=6.8$ Hz, 2H), 3.95 (s, 2H), 1.37 (t, $J=6.8$ Hz, 3H);



ethyl (3E)-5-cyclohexyl-2,5-dioxopent-3-enoate (48j). This compound was prepared according to the representative procedure described above (yellow oil, 85% yield). Flash chromatography: 20% EtOAc/Hexanes.

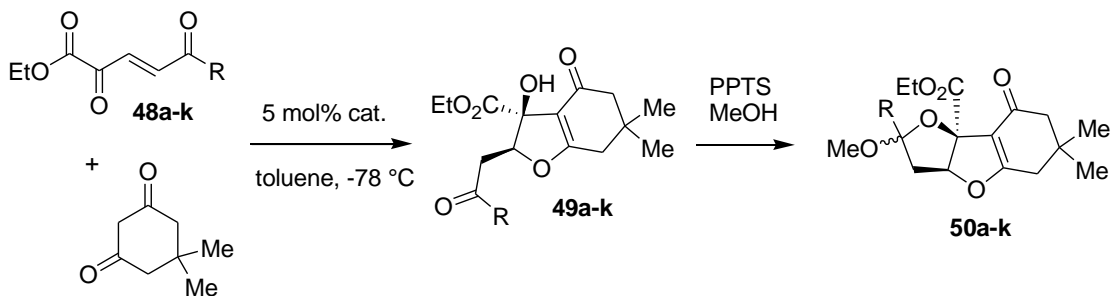
^1H NMR (CDCl_3 , 400 MHz) 7.42 (d, $J=16.0$ Hz, 1H), 7.22 (d, $J=16.0$ Hz, 1H), 4.35 (q, $J=7.2$ Hz, 2H), 2.59 (m, 1H), 1.91-1.76 (m, 4H), 1.67-1.60 (m, 1H), 1.38-1.15 (m, 8H); ^{13}C NMR (CDCl_3 , 400 MHz) 202.35, 183.59, 161.02, 140.03, 131.18, 63.15, 50.21, 28.19, 25.88, 25.62, 14.18.



ethyl (3E,6E)-2,5-dioxo-7-phenylhepta-3,6-dienoate (48k). This compound was prepared according to the representative procedure described above (yellow solid, 57% yield). Flash chromatography: 20% EtOAc/Hexanes

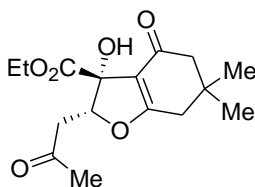
^1H NMR (CDCl_3 , 400 MHz) 7.74 (d, $J=16.0$ Hz, 1H), 7.60 (m, 4H), 7.44 (m, 3H), 7.01 (d, $J=16.0$ Hz, 1H), 4.40 (q, $J=7.2$ Hz, 2H), 1.41 (t, $J=7.2$ Hz, 3H); ^{13}C NMR (CDCl_3 , 400 MHz) 188.32, 183.48, 161.05, 146.45, 140.26, 134.24, 131.76, 131.63, 129.38, 128.98, 125.29, 63.28, 14.25.

Representative procedure for the IFB reaction:



Dimedone (70 mg, .5 mmol) and catalyst (23 mg, .02 mmol) were placed in a round-bottom flask followed by 2 ml of CH_2Cl_2 . Solution was cooled to $-78\text{ }^\circ\text{C}$ and 2-ene-1,4-diketone (.4 mmol) was added in one portion. Reaction stirred for

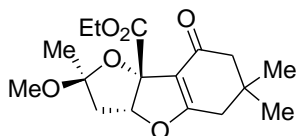
1 hour at -78 °C and then was allowed to warm up slowly to room temp. After that, reaction mixture was washed with NaHCO₃, concentrated, filtered through silica gel and concentrated again to provide pure IFB product. This initial IFB product was treated with PPTS (50 mg, .2 mmol) in methanol (1ml), solution stirred for 5hours, after which it was concentrated. Two diastereomers of mixed-methyl-ketal were separated on a flash column with 50% EtOAc/Hexanes. The minor (less polar) diastereomer of the final product was used for determination of the enantioselectivity.



ethyl (2R,3R)-3-hydroxy-6,6-dimethyl-4-oxo-2-(2-oxopropyl)-2,3,4,5,6,7-hexahydro-1-benzofuran-3-carboxylate (49a). This compound was prepared according to the representative procedure described above. Isolated yield is 99%. d.r.=10.3:1. ¹HNMR indicates that product exists in a mixture of open keto- (major component of the mixture) and closed hemiketal forms (minor). Here we report the NMR data for the major component of the mixture.

¹H NMR (CDCl₃, 400 MHz) 5.21 (dd, J₁=12.8 Hz, J₂=6.0 Hz, 1H), 4.29 (q, J=7.2 Hz, 2H), 3.93 (s, 1H), 3.08 (dd, J₁=16.8 Hz, J₂=8.4 Hz, 2H), 2.94 (dd, J₁=16.8 Hz, J₂=7.2 Hz, 1H), 2.34 (d, J=17.2 Hz, 1H), 2.27 (d, J=17.2 Hz, 1H), 2.18-2.12 (m, 5H), 1.23

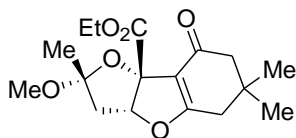
(t, J=6.8 Hz, 3H), 1.09 (s, 3H), 1.04 (s, 3H); ¹³C NMR (CDCl₃, 400 MHz) 205.55, 193.34, 178.54, 172.97, 116.05, 87.76, 79.12, 63.28, 51.12, 42.04, 37.97, 34.57, 30.25, 28.89, 28.38, 14.30; HRMS (ESI/APCI) m/z, 311.1492 (M + H⁺), calcd for C₁₆H₂₂O₆H⁺ 311.1489.



ethyl(2R,4R,6R)-4-methoxy-4,10,10-trimethyl-12-oxo-3,7-

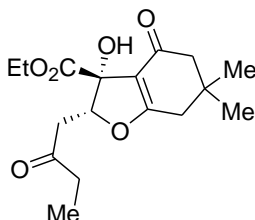
dioxatricyclo[6.4.0.0^{2,6}]dodec-1(8)-ene-2-carboxylate (50a_{minor}). The enantioselectivity was determined by HPLC analysis (Daicel Chiralpak AD-column, 90:10=hexane:ethanol, 1.0 ml/min, 260 nm). Major: 14.1 min, minor: 7.8 min. ee=96%. [α]_D²⁵=+76.4 (c=1.0, CH₂Cl₂);

¹H NMR (CDCl₃, 400 MHz) 5.54 (dd, J₁=8.0 Hz, J₂=6.8 Hz, 1H), 4.20 (q, J=6.8 Hz, 2H), 3.29 (s, 3H), 2.65 (dd, J₁=14.0 Hz, J₂=7.6 Hz, 1H), 2.38 (d, J=17.2 Hz, 1H), 2.28 (d, J=17.2 Hz, 1H), 2.21 (d, J=16.4 Hz, 1H), 2.15 (d, J=16.4 Hz, 1H), 1.85 (dd, J₁=14.0 Hz, J₂=6.8 Hz, 1H), 1.48 (s, 3H), 1.09 (s, 3H), 1.02 (s, 3H); ¹³C NMR (CDCl₃, 400 MHz) 192.87, 178.40, 170.98, 114.93, 109.36, 93.32, 91.11, 61.96, 51.32, 50.09, 47.13, 38.32, 34.60, 29.36, 27.73, 20.72, 14.35; HRMS (ESI/APCI) m/z, 347.1473 (M + Na⁺), calcd for C₁₇H₂₀O₆Na⁺ 347.1465.



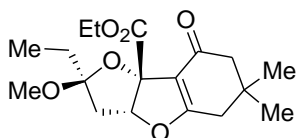
ethyl(2R,4S,6R)-4-methoxy-4,10,10-trimethyl-12-oxo-3,7-dioxatricyclo[6.4.0.0^{2,6}]dodec-1(8)-ene-2-carboxylate (50a_{major}).

¹H NMR (CDCl₃, 400 MHz) 5.23 (app.d, J=7.2 Hz, 1H), 4.26-4.18 (m, 2H), 3.10 (s, 3H), 2.47 (app.d, J=14.8 Hz, 1H), 2.32 (app.s, 2H), 2.21 (app.s, 2H), 2.10 (dd, J₁=14.8 Hz, J₂=7.2 Hz, 1H), 1.52 (s, 3H), 1.25 (t, J=6.8 Hz, 3H), 1.11 (s, 2H), 1.08 (s, 3H); ¹³C NMR (CDCl₃, 400 MHz) 192.76, 179.50, 169.92, 115.34, 11.67, 93.40, 92.06, 62.29, 51.21, 49.57, 44.64, 38.23, 34.28, 29.13, 28.27, 21.31, 14.29; HRMS (ESI/APCI) m/z, 347.1457 (M + Na⁺), calcd for C₁₇H₂₄O₆Na⁺ 347.1465.



ethyl(2R,3R)-3-hydroxy-6,6-dimethyl-4-oxo-2-(2-oxobutyl)-2,3,4,5,6,7-hexahydro-1-benzofuran-3-carboxylate (49b). This compound was prepared according to the representative procedure described above. Isolated yield is 95%. d.r.=9.8:1.

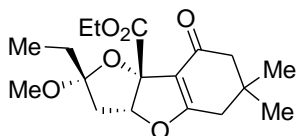
¹H NMR (CDCl₃, 400 MHz) 5.21 (dd, J₁=7.6 Hz, J₂=6.8 Hz, 1H), 4.30-4.24 (m, 2H), 3.92 (s, 1H), 3.04 (dd, J₁=18.0 Hz, J₂=8.8 Hz, 1H), 2.91 (dd, J₁=17.6 Hz, J₂=6.0 Hz, 1H), 2.44 (q, J=6.8 Hz, 2H), 2.37 (d, J=11.2 Hz, 1H), 2.21 (d, J=11.2 Hz, 1H), 2.16 (d, J=12.0 Hz, 1H), 2.34 (d, J=12.0 Hz, 1H), 1.22 (t, J=6.8 Hz, 3H), 1.09-1.00 (m, 9H); ¹³C NMR (CDCl₃, 400 MHz) 208.27, 193.34, 178.57, 172.97, 116.04, 87.93, 79.12, 63.26, 51.12, 70.78, 37.96, 36.27, 34.57, 28.91, 28.34, 14.30, 7.83; HRMS (ESI/APCI) m/z, 325.1641 (M + H⁺), calcd for C₁₇H₂₄O₆H⁺ 325.1646.



ethyl(2R,4R,6R)-4-ethyl-4-methoxy-10,10-dimethyl-12-oxo-3,7-dioxatricyclo[6.4.0.0^{2,6}]dodec-1(8)-ene-2-carboxylate (50b_{minor}). The enantioselectivity was determined by HPLC analysis (Daicel Chiralpak AD-column, 90:10=hexane:ethanol, 1.0 ml/min, 260 nm). Major: 14.2 min, minor: 8.3 min. ee=94%. [α]_D²⁵=+83.7 (c=1.0, CH₂Cl₂);

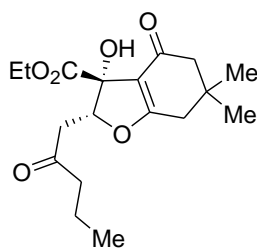
¹H NMR (CDCl₃, 400 MHz) 5.56 (dd, J₁=7.6 Hz, J₂=1.6 Hz, 1H), 4.24 (q, J=7.2 Hz, 2H), 3.29 (s, 3H), 2.61 (dd, J₁=12.8 Hz, J₂=8.0 Hz, 1H), 2.38 (d, J=17.6 Hz, 1H), 2.32 (d, J=17.6 Hz, 1H), 2.26 (d, J=16.8 Hz, 1H), 2.16 (d, J=16.8 Hz, 1H), 2.05-1.98 (m, 1H), 1.87 (dd, J₁=12.8 Hz, J₂=6.8 Hz, 1H), 1.69-1.64 (m, 1H), 1.30 (t, J=6.8 Hz,

3H), 1.08 (s, 3H), 1.02 (s, 3H), .85 (m, 3H); ^{13}C NMR (CDCl_3 , 400 MHz) 192.89, 178.33, 171.08, 114.95, 112.28, 93.07, 91.25, 62.04, 51.31, 49.59, 44.26, 38.33, 34.56, 29.65, 29.06, 28.05, 26.32, 14.38, 8.94; HRMS (ESI/APCI) m/z , 361.1632 ($\text{M} + \text{Na}^+$), calcd for $\text{C}_{18}\text{H}_{26}\text{O}_6\text{Na}^+$ 361.1622.



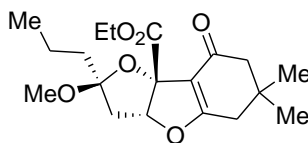
ethyl(2R,4S,6R)-4-ethyl-4-methoxy-10,10-dimethyl-12-oxo-3,7-dioxatricyclo[6.4.0.0^{2,6}]dodec-1(8)-ene-2-carboxylate (50b_{major}).

^1H NMR (CDCl_3 , 400 MHz) 2.23 (app.d, $J=7.2$ Hz, 1H), 4.27-4.16 (m, 2H), 3.06 (s, 3H), 2.38 (app.d, $J=14.8$ Hz, 1H), 2.32 (app.s, 2H), 2.21 (app.s, 2H), 2.11-2.02 (m, 2H), 1.71-1.64 (m, 1H), 1.24 (t, $J=7.2$ Hz, 3H), 1.12 (s, 3H), 1.08 (s, 3H), .90 (t, $J=6.9$ Hz, 3H); ^{13}C NMR (CDCl_3 , 400 MHz) 192.80, 179.47, 169.97, 115.44, 113.36, 93.12, 91.99, 62.29, 51.19, 49.07, 41.75, 38.23, 34.26, 29.13, 28.32, 26.62, 14.29, 8.85; HRMS (ESI/APCI) m/z , 339.1801 ($\text{M} + \text{H}^+$), calcd for $\text{C}_{18}\text{H}_{26}\text{O}_6\text{H}^+$ 339.1802.



ethyl(2R,3R)-3-hydroxy-6,6-dimethyl-4-oxo-2-(2-oxopentyl)-2,3,4,5,6,7-hexahydro-1-benzofuran-3-carboxylate (49c). This compound was prepared according to the representative procedure described above. Isolated yield is 98%. d.r.=10.1:1.

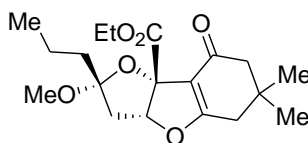
^1H NMR (CDCl_3 , 400 MHz) 5.25 (dd, $J_1=7.6$ Hz, $J_2=6.4$ Hz, 1H), 4.34-4.26 (m, 2H), 3.90 (s, 1H), 3.06 (dd, $J_1=17.6$ Hz, $J_2=8.8$ Hz, 1H), 2.34 (m, 4H), 2.22 (d, $J=12.6$ Hz, 1H), 2.16 (d, $J=12.6$ Hz, 1H), 1.62-1.56 (m, 2H), 1.26 (t, $J=7.2$ Hz, 3H), 1.12 (s, 3H), 1.06 (s, 3H), .88 (t, $J=6.8$ Hz, 3H); ^{13}C NMR (CDCl_3 , 400 MHz) 207.79, 193.23, 178.50, 172.91, 116.00, 87.92, 79.06, 63.16, 51.08, 44.93, 41.11, 37.92, 34.51, 28.86, 28.30, 17.25, 14.26, 13.77; HRMS (ESI/APCI) m/z , 361.1642 ($\text{M} + \text{Na}^+$), calcd for $\text{C}_{18}\text{H}_{26}\text{O}_6\text{Na}^+$ 361.1646.



ethyl(2R,4R,6R)-4-methoxy-10,10-dimethyl-12-oxo-4-propyl-3,7-dioxatricyclo[6.4.0.0^{2,6}]dodec-1(8)-ene-2-carboxylate (50c_{minor}). The

enantioselectivity was determined by HPLC analysis (Daicel Chiralpak AD-column, 90:10=hexane:ethanol, 1.0 ml/min, 260 nm). Major: 14.8 min, minor: 8.3 min. ee=95%. $[\alpha]^{25}_D=+82.5$ (c=1.0, CH₂Cl₂);

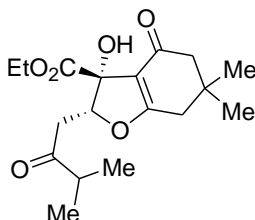
¹H NMR (CDCl₃, 400 MHz) 5.57 (dd, J₁=8 Hz, J₂=6.0 Hz, 1H), 4.24 (q, J=6.8 Hz, 2H), 3.29 (s, 3H), 2.61 (dd, J₁=13.6 Hz, J₂=7.6 Hz, 1H), 2.38 (d, J₁=16.8 Hz, J₂=7.6 Hz, 1H), 2.32 (d, J=16.8 Hz, 1H), 2.25 (d, J=20.0 Hz, 1H), 2.19 (d, J=20.0 Hz, 1H), 1.97 (m, 1H), 1.89 (dd, J₁=13.6 Hz, J₂=7.6 Hz, 1H), 1.62 (m, 2H), 1.29 (m, 4H), 1.11 (s, 3H), 1.06 (s, 3H), 0.92 (t, J=6.8 Hz, 3H); ¹³C NMR (CDCl₃, 400 MHz) 192.93, 178.33, 171.10, 144.25, 114.94, 111.67, 93.16, 91.02, 62.05, 51.32, 49.67, 44.71, 38.34, 35.51, 34.60, 29.11, 28.02, 18.09, 14.40; HRMS (ESI/APCI) m/z, 375.1789 (M + Na⁺), calcd for C₁₉H₂₈O₆Na⁺ 375.1778.



ethyl(2R,4S,6R)-4-methoxy-10,10-dimethyl-12-oxo-4-propyl-3,7-dioxatricyclo[6.4.0.0^{2,6}]dodec-1(8)-ene-2-carboxylate (50c_{major}).

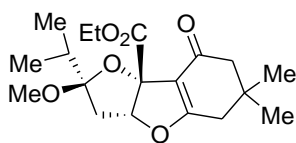
¹H NMR (CDCl₃, 400 MHz) 5.24 (app.d, J=6.8 Hz, 1H), 4.30-4.17 (m, 2H), 3.08 (s, 3H), 2.42 (app.d, J=15.2 Hz, 1H), 2.34 (app.s, 2H), 2.23 (app.s, 2H), 2.14-1.99 (m, 2H), 1.62 (m, 1H), 1.34 (m, 2H), 1.26 (t, J=6.8 Hz, 3H), 1.13 (s, 3H), 1.10 (s,

3H), .93 (t, J=7.6 Hz, 3H); ^{13}C NMR (CDCl_3 , 400 MHz) 192.84, 179.49, 170.00, 115.46, 112.82, 93.23, 91.79, 62.32, 51.21, 49.16, 42.23, 38.24, 35.92, 34.28, 29.16, 28.32, 17.99, 14.40, 14.31; HRMS (ESI/APCI) m/z , 353.1971 ($\text{M} + \text{H}^+$), calcd for $\text{C}_{19}\text{H}_{28}\text{O}_6\text{H}^+$ 353.1959.



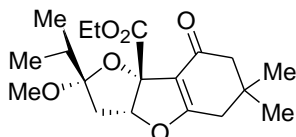
ethyl(2R,3R)-3-hydroxy-6,6-dimethyl-2-(3-methyl-2-oxobutyl)-4-oxo-2,3,4,5,6,7-hexahydro-1-benzofuran-3-carboxylate (49d). This compound was prepared according to the representative procedure described above. Isolated yield is 98%. d.r.=11.3:1.

^1H NMR (CDCl_3 , 400 MHz) 5.22 (dd, $J_1=12.8$ Hz, $J_2=6.0$ Hz, 1H), 4.31 (q, $J=7.2$ Hz, 2H), 3.91 (s, 1H), 3.09 (dd, $J_1=16.8$ Hz, $J_2=8.4$ Hz, 2H), 2.96 (dd, $J_1=16.8$ Hz, $J_2=7.2$ Hz, 1H), 2.58 (m, 1H), 2.34-2.08 (m, 4H), 1.17 (t, $J=6.8$ Hz, 3H), 1.04-1.00 (m, 12H); ^{13}C NMR (CDCl_3 , 400 MHz) 211.60, 193.32, 178.57, 178.40, 173.03, 116.02, 112.83, 111.58, 93.34, 88.13, 88.09, 79.03, 77.67, 77.35, 77.03, 63.28, 62.43, 51.13, 51.05, 41.78, 41.23, 38.89, 38.16, 38.12, 37.99, 37.79, 36.37, 34.76, 34.56, 28.94, 28.86, 28.35, 28.13, 18.40, 18.22, 17.81, 17.42, 14.32;



ethyl(2R,4R,6R)-4-methoxy-10,10-dimethyl-12-oxo-4-(propan-2-yl)-3,7-dioxatricyclo[6.4.0.0^{2,6}]dodec-1(8)-ene-2-carboxylate (50d_{minor}).

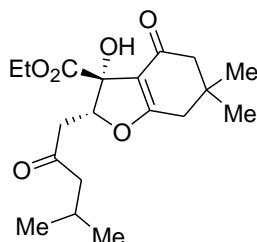
¹H NMR (CDCl₃, 400 MHz) 5.58 (dd, J₁=7.6 Hz, J₂=6.8 Hz, 1H), 4.25 (q, J=6.8 Hz, 2H), 3.28 (s, 3H), 2.43-2.37 (m, 4H), 1.95 (dd, J₁=14.0 Hz, J₂=6.8 Hz, 1H), 1.37 (t, J=7.2 Hz, 3H), 1.12 (app.s, 6H), .82 (s, 3H), .80 (s, 3H); ¹³C NMR (CDCl₃, 400 MHz) 217.37, 192.86, 178.32, 171.13, 114.99, 114.73, 93.05, 93.00, 91.53, 62.11, 51.26, 49.02, 49.04, 39.73, 38.28, 34.48, 28.80, 28.68, 28.36, 17.78, 17.64, 14.40;



ethyl(2R,4S,6R)-4-methoxy-10,10-dimethyl-12-oxo-4-(propan-2-yl)-3,7-dioxatricyclo[6.4.0.0^{2,6}]dodec-1(8)-ene-2-carboxylate (50d_{major}).

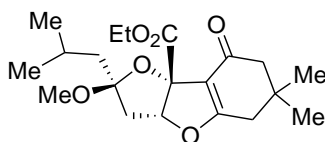
¹H NMR (CDCl₃, 400 MHz) 5.58 (app.d, J=5.2 Hz, 1H), 4.37-4.17 (m, 2H), 3.07 (s, 3H), 2.43 (m, 1H), 2.38 (app.s, 2H), 2.12 (app.s, 2H), 2.09 (app.s, 2H), 1.26 (t, J=7.2 Hz, 3H), 1.13 (s, 3H), 1.10 (s, 3H), 1.01 (d, J=6.0 Hz, 3H), .95 (d, J=6.0 Hz, 3H); ¹³C NMR (CDCl₃, 400 MHz) 217.38, 192.92, 179.53, 170.10, 115.89, 115.46,

93.07, 93.03, 92.04, 62.32, 51.18, 48.48, 38.24, 36.76, 34.26, 29.26, 29.22, 28.34,
17.74, 17.65, 14.31;



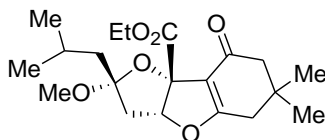
ethyl(2R,3R)-3-hydroxy-6,6-dimethyl-2-(4-methyl-2-oxopentyl)-4-oxo-2,3,4,5,6,7-hexahydro-1-benzofuran-3-carboxylate (49f). This compound was prepared according to the representative procedure described above. Isolated yield is 97%. d.r.=12.8:1.

^1H NMR (CDCl_3 , 400 MHz) 5.21 (dd, $J_1=9.2$ Hz, $J_2=5.6$ Hz, 1H), 4.30-4.22 (m, 2H), 3.01 (dd, $J_1=17.6$ Hz, $J_2=8.8$ Hz, 1H), 2.86 (dd, $J_1=17.6$ Hz, $J_2=5.6$ Hz, 1H), 2.35-2.15 (m, 4H), 2.13-2.06 (m, 2H), 1.21 (t, $J=6.4$ Hz, 3H), 1.07 (d, $J=11.2$ Hz, 6H), 0.86 (s, 3H), 0.84 (s, 3H); ^{13}C NMR (CDCl_3 , 400 MHz) 207.56, 193.28, 178.50, 172.96, 116.02, 87.92, 87.88, 79.09, 63.25, 52.08, 51.12, 41.66, 37.96, 34.55, 28.90, 28.35, 24.69, 22.66, 14.29; HRMS (ESI/APCI) m/z , 375.1766 ($\text{M} + \text{Na}^+$), calcd for $\text{C}_{19}\text{H}_{28}\text{O}_6\text{Na}^+$ 375.1778.



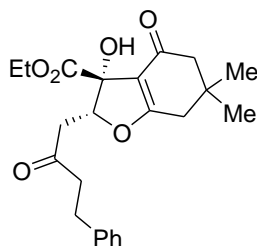
ethyl(2R,4R,6R)-4-methoxy-10,10-dimethyl-4-(2-methylpropyl)-12-oxo-3,7-dioxatricyclo[6.4.0.0^{2,6}]dodec-1(8)-ene-2-carboxylate (50f_{minor}). The enantioselectivity was determined by HPLC analysis (Daicel Chiralcel OD-H-column, 90:10=hexane:ethanol, 1.0 ml/min, 260 nm). Major: 11.5 min, minor: 10.0 min. ee=95%. $[\alpha]^{25}_D=+68.3$ (c=1.0, CH₂Cl₂);

¹H NMR (CDCl₃, 400 MHz) 5.57 (dd, J₁=7.6 Hz, J₂=6.0 Hz, 1H), 4.23 (q, J=6.0 Hz, 2H), 2.29 (s, 3H), 2.66 (dd, J₁=9.6 Hz, J₂=8.4 Hz, 1H), 2.35 (d, J=17.6 Hz, 1H), 2.31 (d, J=17.6 Hz, 1H), 2.25 (d, J=16.0 Hz, 1H), 2.20 (d, J=16.0 Hz, 1H), 2.00 (dd, J₁=14.8 Hz, J₂=4.8 Hz, 1H), 1.91 (dd, J₁=14.8 Hz, J₂=6.0 Hz, 1H), 1.66 (m, 1H), 1.50 (dd, J₁=15.2 Hz, J₂=8.0 Hz, 1H), 1.28 (t, J=7.2 Hz, 3H), 1.12 (s, 3H), 1.06 (s, 3H), 0.94 (d, J=6.8 Hz, 3H), .91 (d, J=6.8 Hz, 3H); ¹³C NMR (CDCl₃, 400 MHz) 192.86, 178.22, 170.98, 114.94, 111.58, 93.32, 90.45, 62.02, 51.35, 49.76, 45.26, 41.70, 38.34, 34.57, 29.23, 27.92, 24.90, 23.88, 23.56, 14.39; HRMS (ESI/APCI) m/z, 389.1928 (M + Na⁺), calcd for C₂₀H₃₀O₆Na⁺ 389.1935.



ethyl(2R,4S,6R)-4-methoxy-10,10-dimethyl-4-(2-methylpropyl)-12-oxo-3,7-dioxatricyclo[6.4.0.0^{2,6}]dodec-1(8)-ene-2-carboxylate (50f_{major}).

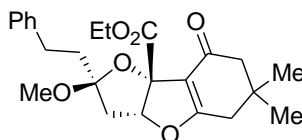
¹H NMR (CDCl₃, 400 MHz) 5.25 (app.d, J=7.2 Hz, 1H), 4.27-4.15 (m, 2H), 3.06 (s, 3H), 2.48 (app.d, J=14.8 Hz, 1H), 2.38 (d, J=16.0 Hz, 1H), 2.34 (d, J=16.0 Hz, 1H), 2.22 (app.s, 2H), 2.13-2.08 (m, 2H), 1.68 (m, 1H), 1.49 (dd, J₁=16 Hz, J₂=7.6 Hz, 1H), 1.23 (t, J=7.6 Hz, 3H), 1.13 (s, 3H), 1.09 (s, 3H), .89 (d, J=6.8 Hz, 6H); ¹³C NMR (CDCl₃, 400 MHz) 192.84, 179.49, 169.99, 115.42, 112.72, 93.45, 93.41, 91.19, 62.30, 51.23, 49.31, 43.12, 42.29, 38.27, 34.28, 29.37, 28.12, 24.75, 23.72, 14.30; HRMS (ESI/APCI) m/z, 367.2110 (M + H⁺), calcd for C₂₀H₃₀O₆H⁺ 367.2115.



ethyl(2R,3R)-3-hydroxy-6,6-dimethyl-4-oxo-2-(2-oxo-4-phenylbutyl)-2,3,4,5,6,7-hexahydro-1-benzofuran-3-carboxylate (49g). This compound was prepared according to the representative procedure described above. Isolated yield is 99%. d.r.=11.8:1.

¹H NMR (CDCl₃, 400 MHz) 7.29-7.14 (m, 5H), 5.25 (dd, J₁=8.8 Hz, J₂=5.6 Hz, 1H), 4.34-4.26 (m, 2H), 3.08 (dd, J₁=17.2 Hz, J₂=8.8 Hz, 1H), 2.95-2.82 (m, 3H), 7.82-2.74 (m, 2H), 2.39 (d, J=12.4 Hz, 1H), 2.33 (d, J=12.4 Hz, 1H), 2.28 (d, J=12.0 Hz, 1H), 2.19 (d, J=12.0 Hz, 1H) 1.27 (t, J=6.4 Hz, 3H), 1.11 (s, 3H), 1.07 (s, 3H); ¹³C

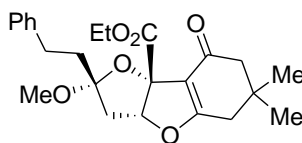
NMR (CDCl₃, 400 MHz) 206.76, 193.96, 178.54, 172.97, 140.85, 128.75, 128.66, 128.52, 126.45, 116.05, 87.82, 79.14, 63.36, 51.15, 44.53, 41.48, 38.00, 36.61, 29.69, 28.97, 28.37, 14.35; HRMS (ESI/APCI) m/z, 423.1778 (M + Na⁺), calcd for C₂₃H₂₈O₆Na⁺ 423.1778.



ethyl(2R,4R,6R)-4-methoxy-10,10-dimethyl-12-oxo-4-(2-phenylethyl)-3,7-dioxatricyclo[6.4.0.0^{2,6}]dodec-1(8)-ene-2-carboxylate (50g_{minor}). The enantioselectivity was determined by HPLC analysis (Daicel Chiralcel OD-H-column, 90:10=hexane:ethanol, 1.0 ml/min, 260 nm). Major: 12.7 min, minor: 10.7 min. ee=94%. [α]_D²⁵=+57.6 (c=1.0, CH₂Cl₂);

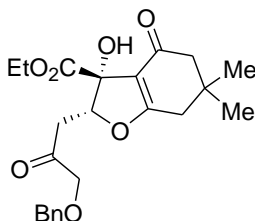
¹H NMR (CDCl₃, 400 MHz) 7.30-7.26 (m, 2H), 7.19-7.15 (m, 3H), 5.58 (dd, J₁=8.4 Hz, J₂=5.6 Hz, 1H), 4.25 (q, J=7.2 Hz, 2H), 3.35 (s, 3H), 2.67-2.58 (m, 3H), 2.41-2.18 (m, 5H), 2.06-1.90 (m, 2H), 1.31 (t, J=6.8 Hz, 3H), 1.11 (s, 3H), 1.07 (s, 3H);

¹³C NMR (CDCl₃, 400 MHz) 192.91, 178.40, 170.92, 141.34, 128.72, 128.57, 128.47, 126.32, 114.96, 111.31, 93.08, 91.16, 62.13, 51.31, 49.77, 44.68, 38.33, 35.09, 34.62, 30.96, 29.14, 27.99, 14.38; HRMS (ESI/APCI) m/z, 437.1927 (M + Na⁺), calcd for C₂₄H₃₀O₆Na⁺ 437.1935.



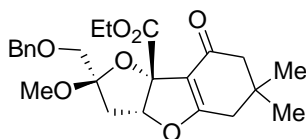
ethyl(2R,4S,6R)-4-methoxy-10,10-dimethyl-12-oxo-4-(2-phenylethyl)-3,7-dioxatricyclo[6.4.0.0^{2,6}]dodec-1(8)-ene-2-carboxylate (50g_{major}).

¹H NMR (CDCl₃, 400 MHz) 7.30-7.22 (m, 2H), 7.20-7.15 (m, 3H), 5.24 (app.d, J=6.8 Hz, 1H), 4.29-4.19 (m, 2H), 3.14 (s, 3H), 2.66 (app.t, J=6.8 Hz, 2H), 2.43-2.36 (m, 4H), 2.25 (app.s, 2H), 2.15-2.03 (m, 2H), 1.27 (t, J=6.8 Hz, 3H), 1.14 (s, 3H), 1.11 (s, 3H); ¹³C NMR (CDCl₃, 400 MHz) 192.87, 179.57, 169.90, 141.45, 128.70, 128.51, 126.28, 115.39, 112.41, 93.18, 91.87, 62.38, 51.22, 49.25, 42.33, 38.26, 35.26, 34.30, 30.84, 29.17, 28.33, 14.33; HRMS (ESI/APCI) m/z, 437.1937 (M + Na⁺), calcd for C₂₄H₃₀O₆Na⁺ 437.1935.



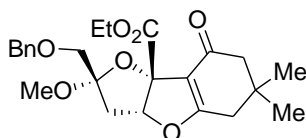
ethyl(2R,6R)-4-[(benzyloxy)methyl]-4-hydroxy-10,10-dimethyl-12-oxo-3,7-dioxatricyclo[6.4.0.0^{2,6}]dodec-1(8)-ene-2-carboxylate (49h). This compound was prepared according to the representative procedure described above. Isolated yield is 98%. d.r.=8.2:1.

^1H NMR (CDCl_3 , 400 MHz) 7.35-7.25 (m, 5H), 5.50 (dd, $J_1=8.0$ Hz, $J_2=5.6$ Hz, 1H), 5.30 (app.d, $J=7.2$ Hz, 1H), 4.69 (d, $J=8.8$ Hz, 1H), 4.59 (d, $J=8.8$ Hz, 1H), 4.58 (m, 2H), 4.35-4.26 (m, 2H), 4.24-4.16 (m, 2H), 3.63 (d, $J=10.8$ Hz, 1H), 3.56 (d, $J=10.8$ Hz, 1H), 2.61 (dd, $J_1=12.0$ Hz, $J_2=9.6$ Hz, 1H), 2.42-2.18(m, 6H), 1.32-1.22 (m, 3H), 1.14 (m, 6H); ^{13}C NMR (CDCl_3 , 400 MHz) 192.86, 192.78, 179.63, 178.81, 171.89, 169.80, 138.40, 138.14, 128.78, 128.68, 128.60, 128.42, 128.31, 128.06, 127.70, 116.21, 114.84, 108.26, 108.06, 93.16, 93.12, 92.96, 92.52, 92.03, 73.88, 73.80, 73.69, 73.66, 62.70, 62.27, 51.20, 51.15, 51.01, 42.58, 40.36, 38.16, 38.08, 37.99, 34.69, 34.62, 9.13, 28.94, 27.90, 14.31; HRMS (ESI/APCI) m/z , 417.1909 ($\text{M} + \text{H}^+$), calcd for $\text{C}_{23}\text{H}_{28}\text{O}_7\text{H}^+$ 417.1908.



ethyl(2R,4S,6R)-4-[(benzyloxy)methyl]-4-methoxy-10,10-dimethyl-12-oxo-3,7-dioxatricyclo[6.4.0.0^{2,6}]dodec-1(8)-ene-2-carboxylate (50h_{minor}). The enantioselectivity was determined by HPLC analysis (Daicel Chiralpak AD-column, 90:10=hexane:ethanol, 1.0 ml/min, 260 nm). Major: 17.3 min, minor: 12.4 min. ee=95%. $[\alpha]^{25}_{\text{D}}=+72.5$ ($c=1.0$, CH_2Cl_2);

¹H NMR (CDCl₃, 400 MHz) 7.35-7.25 (m, 5H), 5.52 (dd, J₁=8.0 Hz, J₂=5.6 Hz, 1H), 4.56 (s, 2H), 4.25 (m, 2H), 3.77 (d, J=10.4 Hz, 1H), 3.45 (d, J=10.4 Hz, 1H), 3.35 (s, 3H), 2.69 (dd, J₁=13.6 Hz, J₂=8.4 Hz, 1H), 2.27-2.21 (m, 3H), 2.16 (dd, J₁=12.0 Hz, J₂=9.6 Hz, 2H), 1.28 (t, J=7.6 Hz, 3H), 1.04 (s, 6H); ¹³C NMR (CDCl₃, 400 MHz) 192.87, 178.59, 170.70, 138.09, 128.63, 127.96, 114.95, 110.20, 92.90, 91.68, 73.66, 69.22, 62.18, 51.19, 50.21, 43.22, 38.17, 34.56, 29.13, 27.90, 14.36; HRMS (ESI/APCI) m/z, 417.1909 (M + H⁺), calcd for C₂₃H₂₈O₇H⁺ 417.1908.



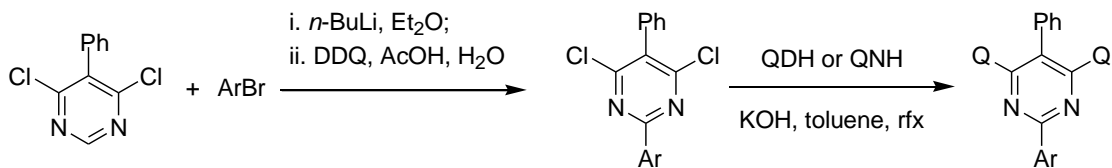
ethyl(2R,4R,6R)-4-[(benzyloxy)methyl]-4-methoxy-10,10-dimethyl-12-oxo-3,7-dioxatricyclo[6.4.0.0^{2,6}]dodec-1(8)-ene-2-carboxylate (50h_{major}).

¹H NMR (CDCl₃, 400 MHz) 7.33-7.25 (m, 5H), 5.28 (app.d, J=6.4 Hz, 1H), 4.66 (d, J=12.0 Hz, 1H), 4.55 (d, J=12.0 Hz, 1H), 4.24-4.14 (m, 2H), 3.81 (d, J=11.6 Hz, 1H), 3.51 (d, J=11.6 Hz, 1H), 3.12 (s, 3H), 2.49 (d, J=12.4 Hz, 1H), 2.40 (d, J=12.4 Hz, 1H), 2.35 (app.s, 2H), 2.27 (app.s, 2H), 1.29 (t, J=6.8 Hz, 3H), 1.12 (s, 3H), 1.10 (s, 3H); ¹³C NMR (CDCl₃, 400 MHz) 192.79, 179.62, 196.71, 138.14, 128.61, 128.00, 127.97, 127.90, 115.34, 110.99, 93.06, 93.03, 92.40, 73.71, 69.14, 62.37, 51.21,

49.80, 41.45, 38.22, 34.32, 28.95, 28.45, 14.29; **HRMS (ESI/APCI) m/z**, 453.1879

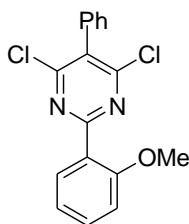
(M + Na⁺), calcd for C₂₃H₂₈O₇Na⁺ 453.1884.

Representative procedure for the synthesis of 4,6-dichloro-2-aryl-5-phenylpyrimidines:



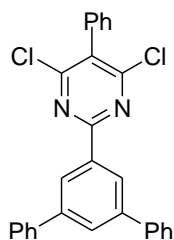
To arylbromide (1 mmol) in a flame-dry round-bottom flask under argon was added 6 ml of diethyl ether. This solution was cooled to -10 °C and *n*-butyllithium (.63 ml 1.6 M solution in hexane, 1 mmol) was added while maintaining the temperature below 0 °C. The reaction mixture was stirred at 0 °C for 20 min and then was cooled to -35 °C. To this mixture was added 4,6-dichloro-5-phenylpyrimidine (180 mg, .8 mmol) in 3 ml of diethyl ether over 15 min. After stirring at -30 °C for 20 min, the temperature was left to rise to 0 °C. To this mixture were added acetic acid (6 drops), water (6 drops) and THF (.5 ml) followed by DDQ (200 mg, .9 mmol). The resulting solution was stirred at room temperature for 10 min, and 10 ml of 1M NaOH was added. Phases were separated and the aqueous phase was extracted with dichloromethane (10 ml) twice. The combined organic phases were dried, concentrated and purified on

silica gel column to afford pure 4,6-dichloro-2-aryl-5-phenylpyrimidine. If the column did not provide pure product, it can be recrystallized from toluene-hexanes mixture.



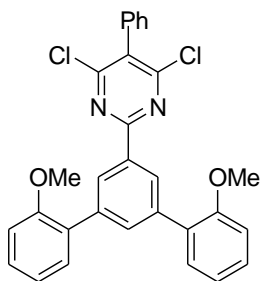
4,6-dichloro-2-(2-methoxyphenyl)-5-phenylpyrimidine: This compound was prepared according to the representative procedure described above (white solid, 90% yield). Flash chromatography: 50% CH₂Cl₂/Hexanes.

¹H NMR (CDCl₃, 400 MHz) 7.83 (d, J=7.2 Hz, 1H), 7.52-7.45 (m, 4H), 3.37 (m, 2H), 7.09-7.03 (m, 2H); ¹³C NMR (CDCl₃, 400 MHz) 164.65, 161.08, 158.38, 133.41, 132.53, 132.24, 130.77, 129.67, 129.40, 128.89, 125.92, 120.97, 112.49, 56.40; GCMS 330.0313 calcd for C₁₇H₁₂N₂OCl₂ 330.0321.



4,6-dichloro-2-(3,5-diphenylphenyl)-5-phenylpyrimidine. This compound was prepared according to the representative procedure described above (white solid, 81% yield). Flash chromatography: 25% CH₂Cl₂/Hexanes.

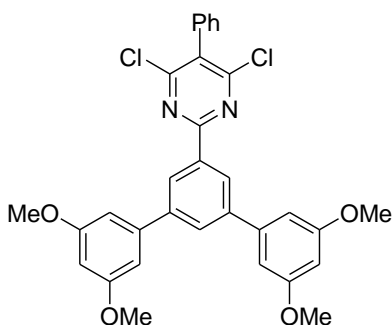
¹H NMR (CDCl₃, 400 MHz) 8.71 (s, 2H), 8.00 (s, 1H), 7.76 (d, J=7.6 Hz, 4H), 7.54-7.49 (m, 7H), 7.45-7.37 (m, 4H); ¹³C NMR (CDCl₃, 400 MHz) 163.69, 161.65, 142.65, 140.75, 136.16, 133.47, 131.27, 129.92, 129.74, 129.44, 129.13, 128.92, 128.02, 127.64, 126.61; HRMS (ESI/APCI) m/z, 453.0929 (M + H⁺), calcd for C₂₈H₁₈N₂Cl₂H⁺ 453.0920.



2-[3,5-bis(2-methoxyphenyl)phenyl]-4,6-dichloro-5-phenylpyrimidine.

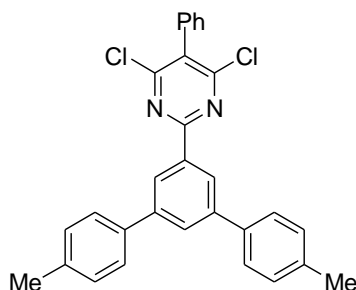
¹H NMR (CDCl₃, 400 MHz) 8.64 (s, 2H), 7.97 (s, 1H), 7.54-7.49 (m, 5H), 7.41-7.36 (m, 4H), 7.12-7.03 (m, 4H), 7.87 (s, 6H); ¹³C NMR (CDCl₃, 400 MHz) 164.19,

161.51, 156.88, 139.07, 135.02, 134.88, 133.64, 131.35, 130.86, 130.46, 129.79,
129.36, 129.20, 128.89, 128.80, 121.13, 111.52, 55.93; HRMS (ESI/APCI) m/z,
513.1143 (M + H⁺), calcd for C₃₀H₂₂N₂O₂Cl₂H⁺ 513.1131.



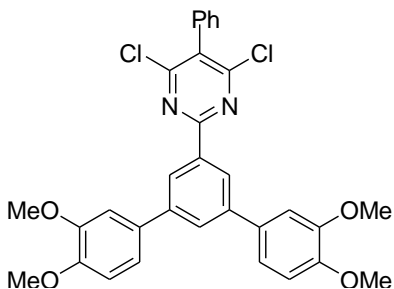
2-[3,5-bis(3,5-dimethoxyphenyl)phenyl]-4,6-dichloro-5-phenylpyrimidine.

¹H NMR (CDCl₃, 400 MHz) 8.65 (s, 2H), 7.93 (s, 1H), 7.53-7.50 (m, 3H), 7.39-7.36
(m, 2H), 6.86 (s, 4H), 6.52 (s, 2H), 3.89 (s, 12H); ¹³C NMR (CDCl₃, 400 MHz)
163.54, 161.62, 161.37, 142.96, 142.55, 136.07, 133.47, 131.29, 129.96, 129.73,
129.43, 128.91, 126.91, 105.98, 99.79, 55.77; HRMS (ESI/APCI) m/z, 573.1350
(M + H⁺), calcd for C₃₂H₂₆N₂O₄Cl₂H⁺ 573.1342.



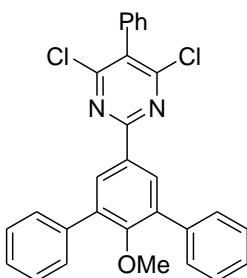
2-[3,5-bis(4-methylphenyl)phenyl]-4,6-dichloro-5-phenylpyrimidine.

^1H NMR (CDCl_3 , 400 MHz) 8.85 (s, 2H), 7.97 (s, 1H), 7.66 (d, $J=8.0$ Hz, 4H), 7.54-7.51 (m, 3H), 7.39-7.36 (m, 2H), 7.31 (d, $J=8.0$, 4H); ^{13}C NMR (CDCl_3 , 400 MHz) 163.84, 161.60, 142.48, 137.91, 137.79, 136.05, 133.51, 131.17, 129.82, 129.74, 129.53, 129.41, 128.90, 127.44, 126.16, 21.43.



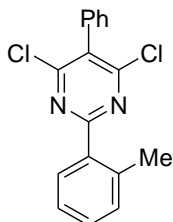
2-[3,5-bis(3,4-dimethoxyphenyl)phenyl]-4,6-dichloro-5-phenylpyrimidine:

HRMS (ESI/APCI) m/z , 573.1351 ($\text{M} + \text{H}^+$), calcd for $\text{C}_{32}\text{H}_{26}\text{N}_2\text{Cl}_2\text{O}_4\text{H}^+$ 573.1342.



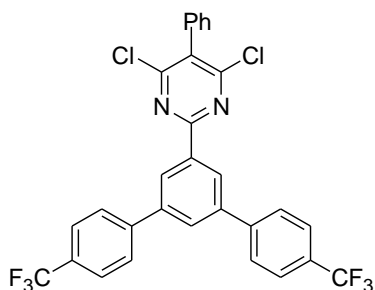
4,6-dichloro-2-(4-methoxy-3,5-diphenylphenyl)-5-phenylpyrimidine:

^1H NMR (CDCl_3 , 400 MHz) 8.50 (s, 2H), 7.71-7.68 (m, 4H), 7.51-7.39 (m, 11H), 3.28 (s, 3H); ^{13}C NMR (CDCl_3 , 400 MHz) 163.34, 161.56, 258.69, 138.45, 136.40, 133.51, 131.21, 130.86, 129.79, 129.63, 129.38, 128.89, 128.56, 127.72, 60.95.



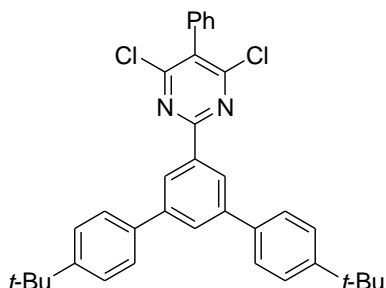
4,6-dichloro-2-(2-methylphenyl)-5-phenylpyrimidine:

^1H NMR (CDCl_3 , 400 MHz) 8.06 (d, $J=8.0$ Hz, 1H), 7.54-7.50 (m, 3H), 7.41-7.31 (m, 5H), 2.71 (s, 3H); ^{13}C NMR (CDCl_3 , 400 MHz) 166.11, 161.00, 138.75, 135.14, 133.36, 132.07, 131.31, 131.03, 130.53, 129.72, 129.44, 128.92, 126.38, 21.98.



2-(3,5-bis[4-(trifluoromethyl)phenyl]phenyl)-4,6-dichloro-5-phenylpyrimidine.

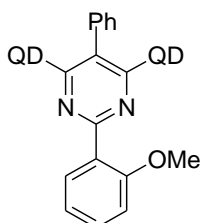
^1H NMR (CDCl_3 , 400 MHz) 8.72 (s, 2H), 7.96 (s, 1H), 7.85 (d, $J=8.4$ Hz, 4H), 7.75 (d, $J=8.4$ Hz, 4H), 7.54-7.50 (m, 3H), 7.37-7.35 (m, 2H); ^{13}C NMR (CDCl_3 , 400 MHz) 162.98, 161.82, 143.89, 141.48, 136.64, 133.21, 131.73, 130.44, 130.11, 129.84, 129.63, 129.56, 128.96, 127.94, 127.43, 126.17, 126.13, 125.77, 123.06.



2-[3,5-bis(4-tert-butylphenyl)phenyl]-4,6-dichloro-5-phenylpyrimidine:

This compound was prepared according to the representative procedure described above (white solid, 95% yield). Flash chromatography: 15% CH_2Cl_2 /Hexanes.

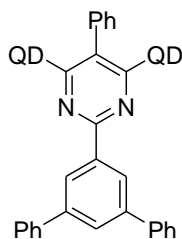
^1H NMR (CDCl_3 , 400 MHz) 8.68 (s, 2H), 8.00 (s, 1H), 7.71 (d, $J=8.0$ Hz, 4H), 7.55-7.51 (m, 7H), 7.40-7.37 (m, 2H), 4.41 (s, 18H); ^{13}C NMR (CDCl_3 , 400 MHz) 163.85, 161.60, 151.02, 142.43, 137.97, 136.04, 133.53, 131.15, 129.74, 129.61, 129.39, 128.90, 127.28, 126.32, 126.05, 34.86, 31.63; HRMS (ESI/APCI) m/z , 565.2172 ($\text{M} + \text{H}^+$), calcd for $\text{C}_{36}\text{H}_{34}\text{N}_2\text{Cl}_2\text{H}^+$ 565.2172.



2-(2-methoxyphenyl)-5-phenylpyrimidine-bis-(9-O-quinidine) ether (QD-13). This compound was prepared according to the representative procedure described above (white foam, 96% yield). Flash chromatography: 50% EtOAc/Hexanes.

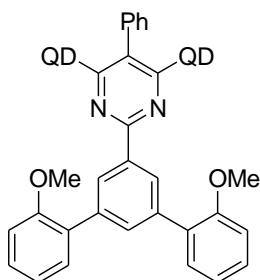
^1H NMR (CDCl_3 , 400 MHz) 8.75 (d, $J=4.0$ Hz, 2H), 8.02 (d, $J=8.8$ Hz, 2H), 7.57-7.47 (m, 5H), 7.38-7.35 (m, 6H), 7.23 (t, $J=8.0$ Hz, 1H), 6.97 (d, $J=6.0$, 2H), 6.73 (d, $J=8.0$ Hz, 2H), 6.61 (t, $J=7.2$, 1H), 5.47-5.40 (m, 2H), 4.87 (d, $J=17.2$ Hz, 2H), 4.76 (d, $J=8.4$ Hz, 2H), 3.62 (s, 6H), 3.20-3.16 (m, 2H), 3.08 (s, 3H), 2.75-2.60 (m, 6H), 2.13-2.00 (m, 4H), 1.86-1.82 (m, 2H), 1.64 (m, 2H), 1.45-1.26 (m, 6H); ^{13}C NMR (CDCl_3 , 400 MHz) 166.38, 162.10, 157.92, 147.76, 145.45, 144.87, 140.60,

131.93, 131.85, 131.34, 130.94, 130.80, 128.52, 127.88, 127.44, 127.38, 122.08, 119.90, 114.77, 111.30, 104.08, 102.17, 59.77, 55.62, 55.03, 49.90, 49.67, 40.65, 28.42, 26.52; HRMS (ESI/APCI) m/z, 907.4522 (M + H⁺), calcd for C₅₇H₅₈N₆O₅H⁺ 907.4541.



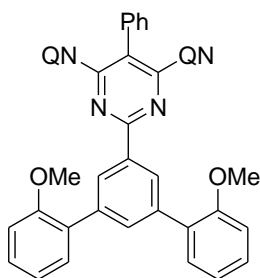
2-(3,5-diphenylphenyl)-5-phenylpyrimidine-bis-(9-O-quinidine)ether (QD-31). This compound was prepared according to the representative procedure described above (white foam, 92% yield). Flash chromatography: 50% EtOAc/Hexanes.

HRMS (ESI/APCI) m/z, 1029.5071 (M + H⁺), calcd for C₆₈H₆₄N₆O₄H⁺ 1029.5062.



2-[3,5-bis(2-methoxyphenyl)phenyl]-5-phenylpyrimidine-bis-(9-O-quinidine)ether:

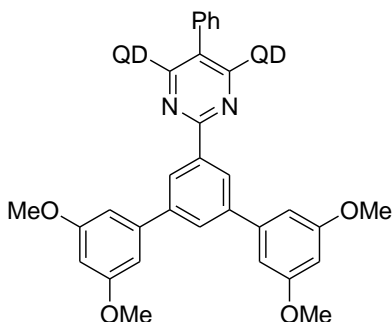
HRMS (ESI/APCI) m/z , 1089.5287 ($M + H^+$), calcd for $C_{70}H_{68}N_6O_6H^+$ 1089.5273.



2-[3,5-bis(2-methoxyphenyl)phenyl]-5-phenylpyrimidine-bis-(9-O-quinine)ether (QN-71).

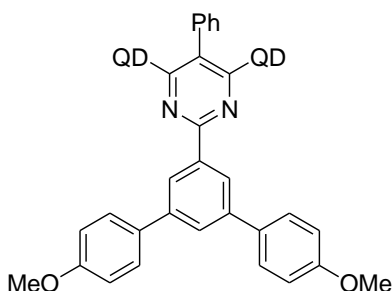
1H NMR ($CDCl_3$, 400 MHz) 8.67 (d, $J=4.0$ Hz, 2H), 7.95 (d, $J=8.8$ Hz, 2H), 7.80 (s, 2H), 7.62-7.55 (m, 5H), 7.48 (t, 1H), 7.38-7.30 (m, 4H), 7.27-7.21 (m, 4H), 7.02-6.93 (m, 8H), 5.70-5.65 (m, 2H), 4.92-4.86 (m, 4H), 3.62 (s, 6H), 3.46 (s, 6H), 3.23 (m, 2H), 3.09-2.94 (m, 6H), 2.55-2.50 (m, 4H), 2.15 (m, 2H), 1.67-1.58 (m, 4H), 1.27-1.16 (m, 4H).

^{13}C (CDCl_3 , 400 MHz) 166.57, 162.08, 157.97, 156.58, 147.53, 144.89, 144.60, 142.12, 138.25, 136.65, 133.76, 131.82, 131.41, 130.85, 130.76, 130.69, 128.83, 128.45, 127.97, 126.76, 122.42, 121.12, 114.46, 111.44, 104.69, 101.08, 59.51, 57.26, 55.65, 55.49, 43.11, 40.07, 29.70, 27.90, 27.51;



2-[3,5-bis(3,5-dimethoxyphenyl)phenyl]-5-phenylpyrimidine-bis-(9-O-quinidine)ether (QD-72).

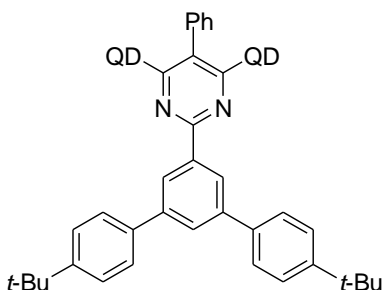
HRMS (ESI/APCI) m/z , 1149.5442 ($\text{M} + \text{H}^+$), calcd for $\text{C}_{72}\text{H}_{72}\text{N}_6\text{O}_8\text{H}^+$ 1149.5484.



2-[3,5-bis(4-methoxyphenyl)phenyl]-5-phenylpyrimidine-bis-(9-O-quinidine)ether (QD-74). This compound was prepared according to the

representative procedure described above (white foam, 98% yield). Flash chromatography: 40% EtOAc/Hexanes.

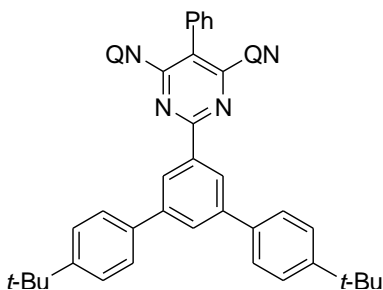
¹H NMR (CDCl₃, 400 MHz) 7.77 (d, J=4.4 Hz, 2H), 8.05 (d, J=9.2 Hz, 2H), 7.88 (s, 2H), 7.71-7.54 (m, 6H), 7.45-7.34 (m, 6H), 7.17-7.10 (m, 6H), 6.94-6.91 (d, J=8.0 Hz, 4H), 5.17 (m, 2H), 4.86 (d, J=16.0 Hz, 2H), 4.76 (d, 8.4 Hz, 2H), 3.90 (s, 6H), 3.56 (s, 6H), 3.18 (m, 2H), 2.80-2.77 (m, 6H), 2.66-2.60 (m, 2H), 2.10-2.03 (m, 2H), 1.90-1.85 (m, 2H), 1.61 (m, 2H), 1.41-1.21 (m, 8H); HRMS (ESI/APCI) m/z, 1089.5283 (M + H⁺), calcd for C₇₀H₆₈N₆O₆H⁺ 1089.5273.



2-[3,5-bis(4-tert-butylphenyl)phenyl]-5-phenylpyrimidine-bis-(9-O-quinidine)ether (QD-75). This compound was prepared according to the representative procedure described above (white foam, 97% yield). Flash chromatography: 30% EtOAc/Hexanes.

¹H NMR (CDCl₃, 400 MHz) 8.87 (d, J=4.0 Hz, 2H), 8.07 (d, J=9.6 Hz, 2H), 7.96 (s, 2H), 7.74-7.56 (m, 6H), 7.47-7.35 (m, 10H), 7.23-7.15 (m, 6H), 5.13 (m, 2H), 4.89-

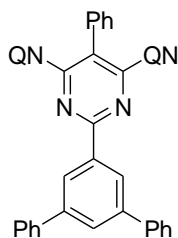
4.75 (m, 4H), 3.53 (s, 6H), 3.19 (m, 2H), 2.80-2.64 (m, 8H), 2.11-2.04 (m, 2H), 1.92-1.86 (m, 2H), 1.60 (m, 2H), 1.43 (s, 18H), 1.26-1.11 (m, 6H); ¹³C NMR (CDCl₃, 400 MHz) 166.62, 161.62, 158.19, 150.43, 147.69, 144.96, 144.81, 141.61, 140.45, 138.02, 137.66, 132.18, 131.52, 130.86, 129.02, 128.92, 128.73, 128.21, 126.78, 126.68, 126.04, 125.32, 122.64, 114.94, 104.92, 100.86, 59.43, 55.48, 50.21, 40.92, 34.82, 31.65, 28.78, 26.48; HRMS (ESI/APCI) m/z, 1141.6323 (M + H⁺), calcd for C₇₆H₈₀N₆O₄H⁺ 1141.6314.



2-[3,5-bis(4-tert-butylphenyl)phenyl]-5-phenylpyrimidine-bis-(9-O-quinine)ether (QD-75). This compound was prepared according to the representative procedure described above (white foam, 95% yield). Flash chromatography: 30% EtOAc/Hexanes.

¹H NMR (CDCl₃, 400 MHz) 8.78 (d, J=4.8 Hz, 2H), 8.08 (d, J=8.8 Hz, 2H), 7.95 (s, 2H), 7.70-7.60 (m, 4H), 7.51 (t, J=8.0 Hz, 1H), 7.43-7.40 (m, 9H), 7.34 (s, 2H), 7.15 (m, 4H), 7.01 (m, 2H), 7.70-5.61 (m, 2H), 4.92-4.85 (m, 4H), 3.60 (s, 6H), 3.25 (m,

2H), 3.09-3.00 (m, 4H), 2.60-2.55 (m, 4H), 2.17 (m, 2H), 1.64-1.60 (m, 4H), 1.43 (s, 18H), 1.23-1.05 (m, 6H); ^{13}C NMR (CDCl_3 , 400 MHz) 166.51, 161.77, 158.27, 150.49, 147.65, 144.98, 144.54, 142.11, 141.54, 137.89, 137.54, 132.21, 131.43, 130.82, 128.64, 128.50, 128.17, 126.64, 126.57, 126.04, 125.24, 122.70, 114.49, 105.12, 100.78, 59.49, 57.58, 55.62, 43.49, 40.11, 34.82, 31.65, 29.70, 27.96, 27.33; HRMS (ESI/APCI) m/z , 1141.6331 ($\text{M} + \text{H}^+$), calcd for $\text{C}_{76}\text{H}_{80}\text{N}_6\text{O}_4\text{H}^+$ 1141.6314.



2-(3,5-diphenylphenyl)-5-phenylpyrimidine-bis-(9-O-quinine)ether (QN-31).

^1H NMR (CDCl_3 , 400 MHz) 8.77 (d, $J=4.0$ Hz, 2H), 8.05 (d, $J=9.6$ Hz, 2H), 7.96 (s, 2H), 7.69-7.60 (m, 5H), 7.52 (m, 1H), 7.51-7.35 (m, 12H), 7.24 (m, 4H), 7.00 (s, 2H), 5.70-5.62 (m, 2H), 4.92-4.84 (m, 4H), 3.59 (s, 6H), 3.26 (m, 2H), 3.11-2.97 (m, 4H), 2.60-2.56 (m, 4H), 2.16 (m, 2H), 1.65-1.55 (m, 6H), 1.26-1.05 (m, 6H);

^{13}C NMR (CDCl_3 , 400 MHz) 166.59, 161.66, 158.21, 147.66, 144.99, 144.48, 142.08, 141.90, 140.87, 137.80, 132.18, 131.35, 130.82, 129.10, 128.91, 128.65, 128.22, 127.64, 127.06, 126.65, 125.68, 122.60, 114.51, 105.23, 100.95, 59.48, 57.52, 55.65, 43.43, 40.06, 27.94, 27.34;

HRMS (ESI/APCI) m/z , 1029.5050 ($\text{M} + \text{H}^+$), calcd for $\text{C}_{68}\text{H}_{64}\text{N}_6\text{O}_4\text{H}^+$ 1029.5062.

Copies of NMR Spectra

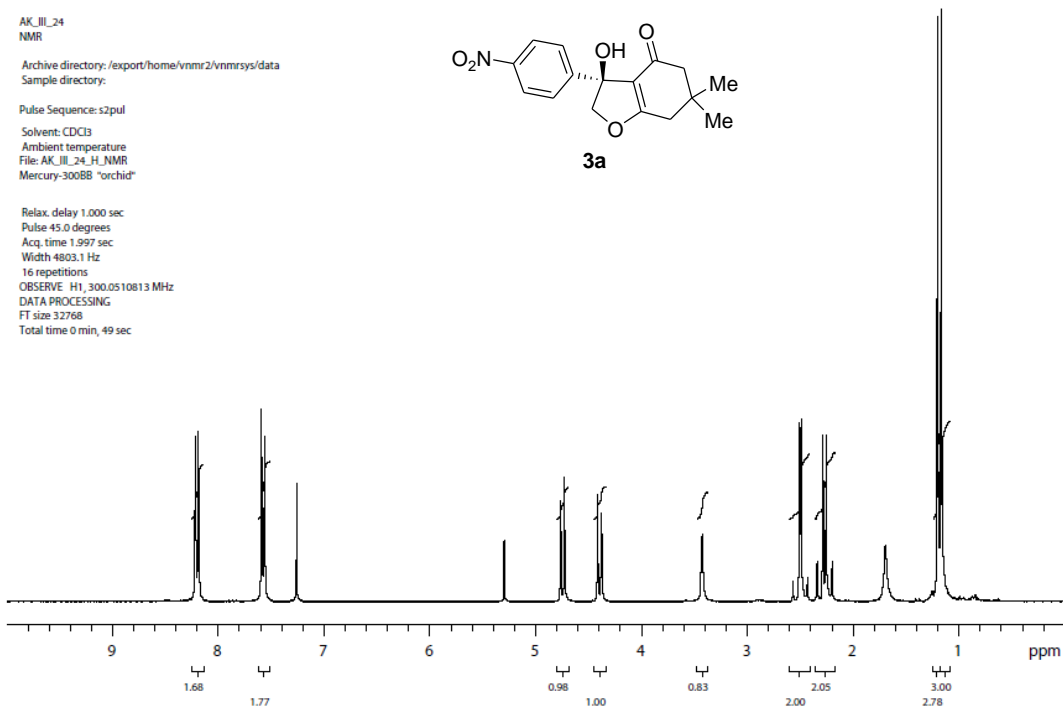
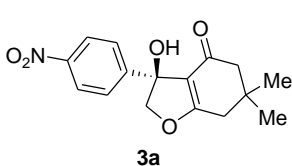
AK_ILI_24
NMR

Archive directory: /export/home/vnmr2/vnmrsys/data
Sample directory:

Pulse Sequence: s2pul

Solvent: CDCl₃
Ambient temperature
File: AK_ILI_24_H_NMR
Mercury-300BB "orchid"

Relax. delay 1.000 sec
Pulse 45.0 degrees
Acq. time 1.997 sec
Width 4803.1 Hz
16 repetitions
OBSERVE H1, 300.0510813 MHz
DATA PROCESSING
FT size 32768
Total time 0 min, 49 sec



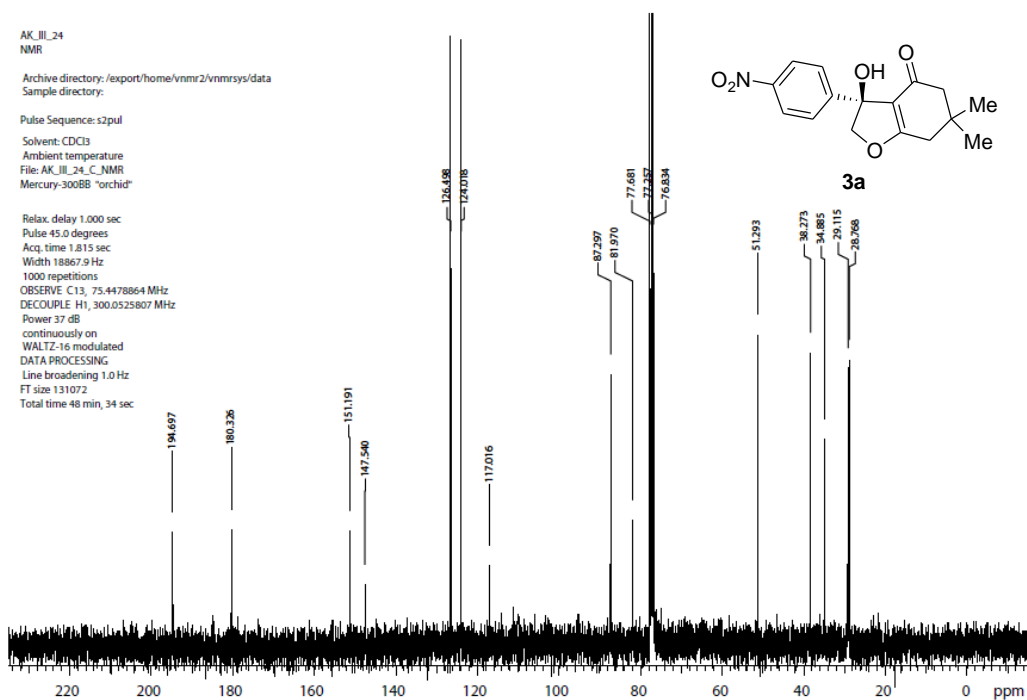
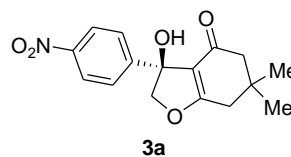
AK_ILI_24
NMR

Archive directory: /export/home/vnmr2/vnmrsys/data
Sample directory:

Pulse Sequence: s2pul

Solvent: CDCl₃
Ambient temperature
File: AK_ILI_24_C_NMR
Mercury-300BB "orchid"

Relax. delay 1.000 sec
Pulse 45.0 degrees
Acq. time 1.815 sec
Width 18867.9 Hz
1000 repetitions
OBSERVE C13, 75.4478864 MHz
DECUPLE H1, 300.0525807 MHz
Power 37 dB
continuously on
WALTZ-16 modulated
DATA PROCESSING
Line broadening 1.0 Hz
FT size 131072
Total time 48 min, 34 sec

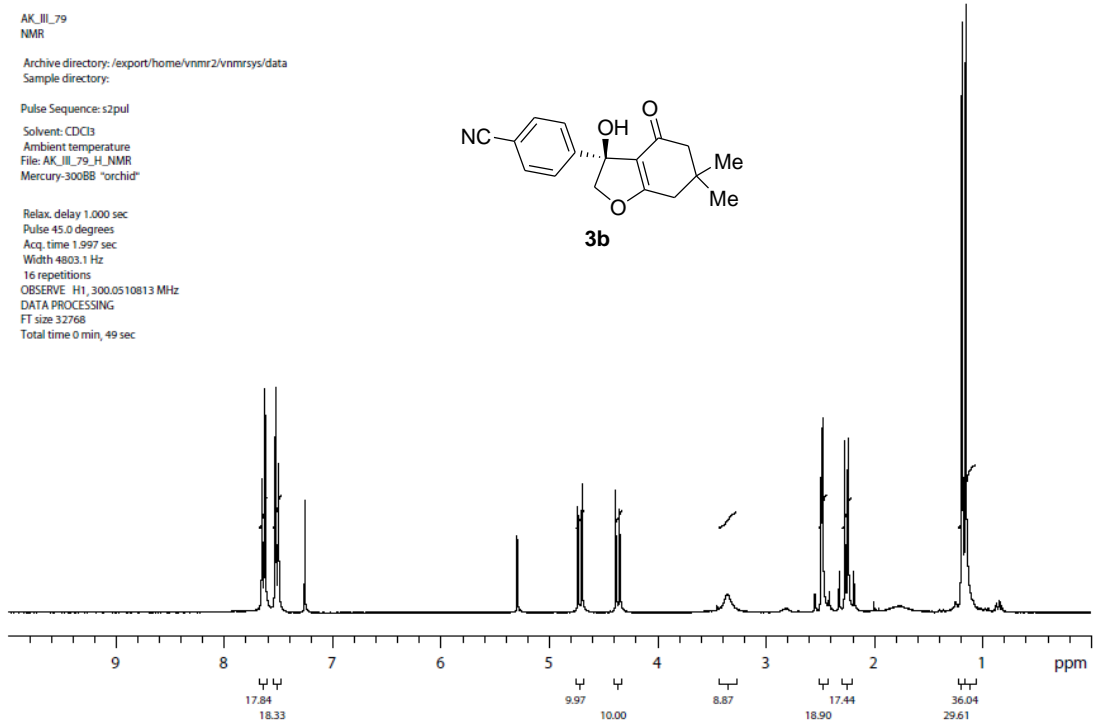
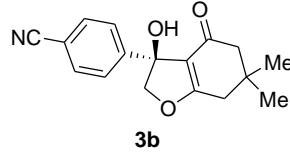


AK_IL_79
NMR

Archive directory: /export/home/vnmr2/vnmrSYS/data
Sample directory:

Pulse Sequence: s2pul
Solvent: CDCl3
Ambient temperature
File: AK_IL_79_H_NMR
Mercury-300BB "orchid"

Relax. delay 1.000 sec
Pulse 45.0 degrees
Acq. time 1.997 sec
Width 4803.1 Hz
16 repetitions
OBSERVE H1, 300.0510813 MHz
DATA PROCESSING
FT size 32768
Total time 0 min, 49 sec

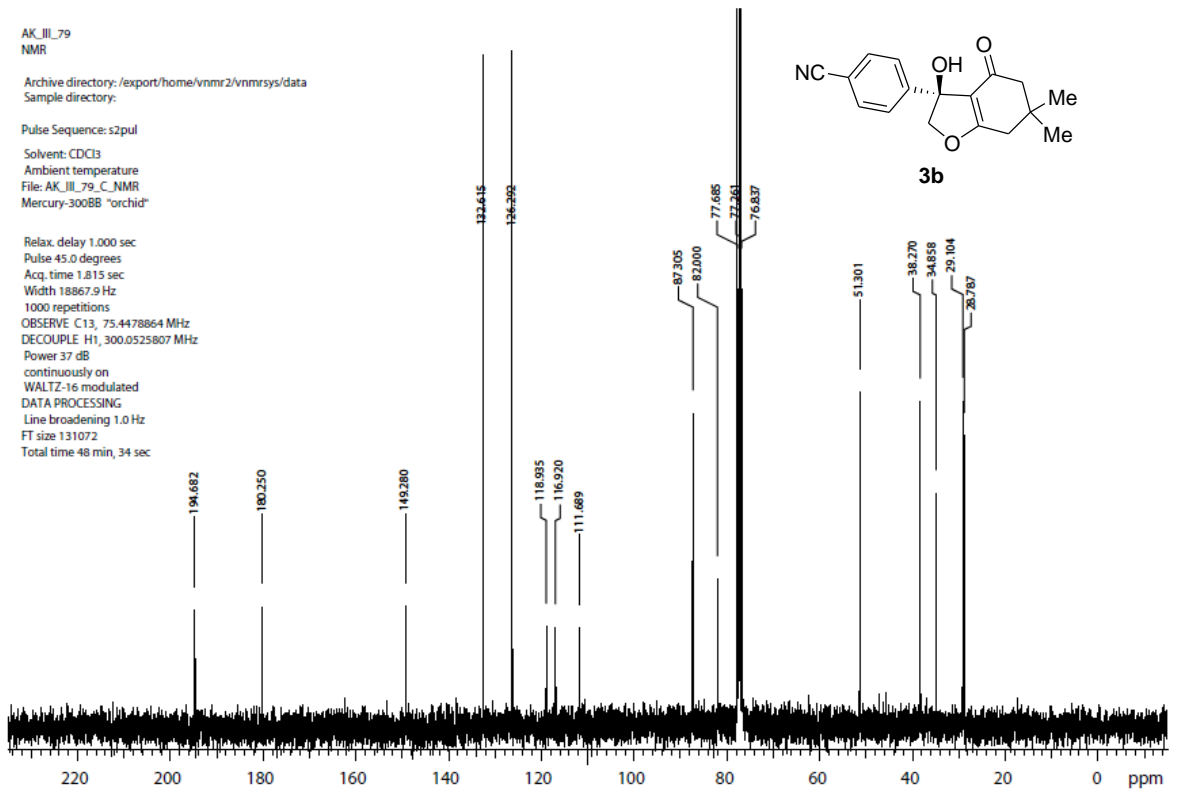
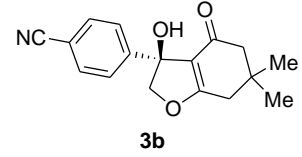


AK_IL_79
NMR

Archive directory: /export/home/vnmr2/vnmrSYS/data
Sample directory:

Pulse Sequence: s2pul
Solvent: CDCl3
Ambient temperature
File: AK_IL_79_C_NMR
Mercury-300BB "orchid"

Relax. delay 1.000 sec
Pulse 45.0 degrees
Acq. time 1.815 sec
Width 18867.9 Hz
1000 repetitions
OBSERVE C13, 75.4478864 MHz
DECOUPLE H1, 300.0525807 MHz
Power 37 dB
continuously on
WALTZ-16 modulated
DATA PROCESSING
Line broadening 1.0 Hz
FT size 131072
Total time 48 min, 34 sec

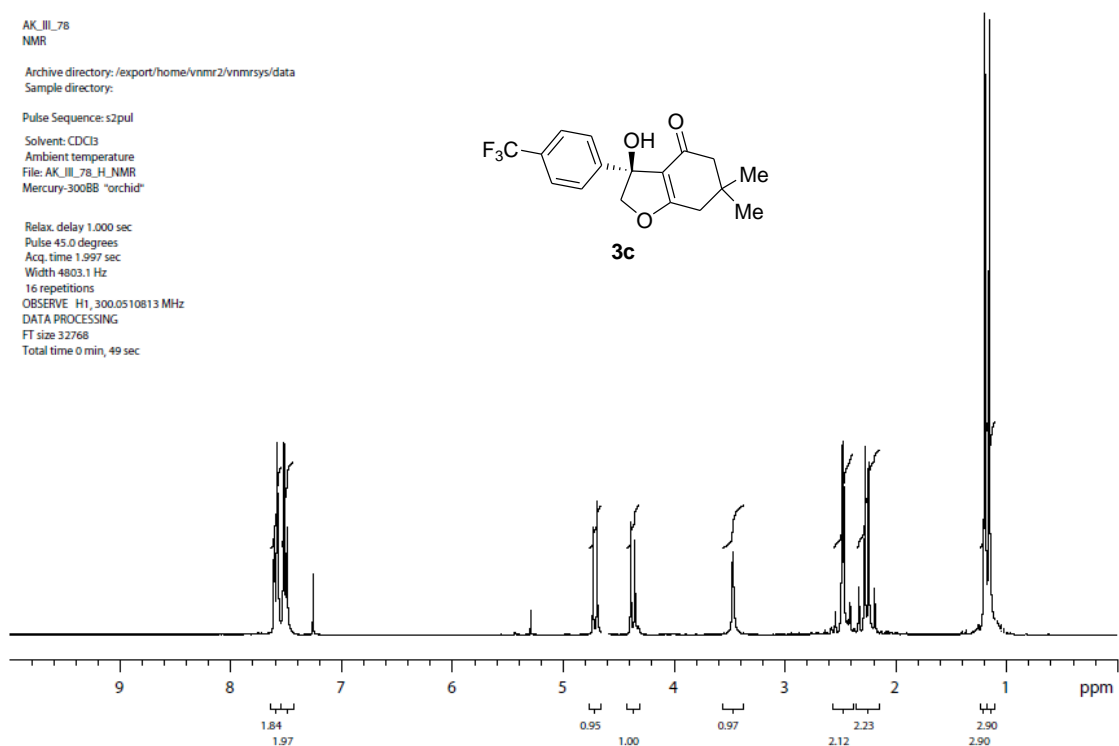
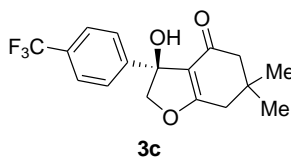


AK_JIL_78
NMR

Archive directory: /export/home/vnmr2/vnmrsys/data
Sample directory:

Pulse Sequence: s2pul
Solvent: CDCl3
Ambient temperature
File: AK_JIL_78_H_NMR
Mercury-300BB "orchid"

Relax. delay 1.000 sec
Pulse 45.0 degrees
Acq. time 1.997 sec
Width 4803.1 Hz
16 repetitions
OBSERVE H1, 300.0510813 MHz
DATA PROCESSING
FT size 32768
Total time 0 min, 49 sec

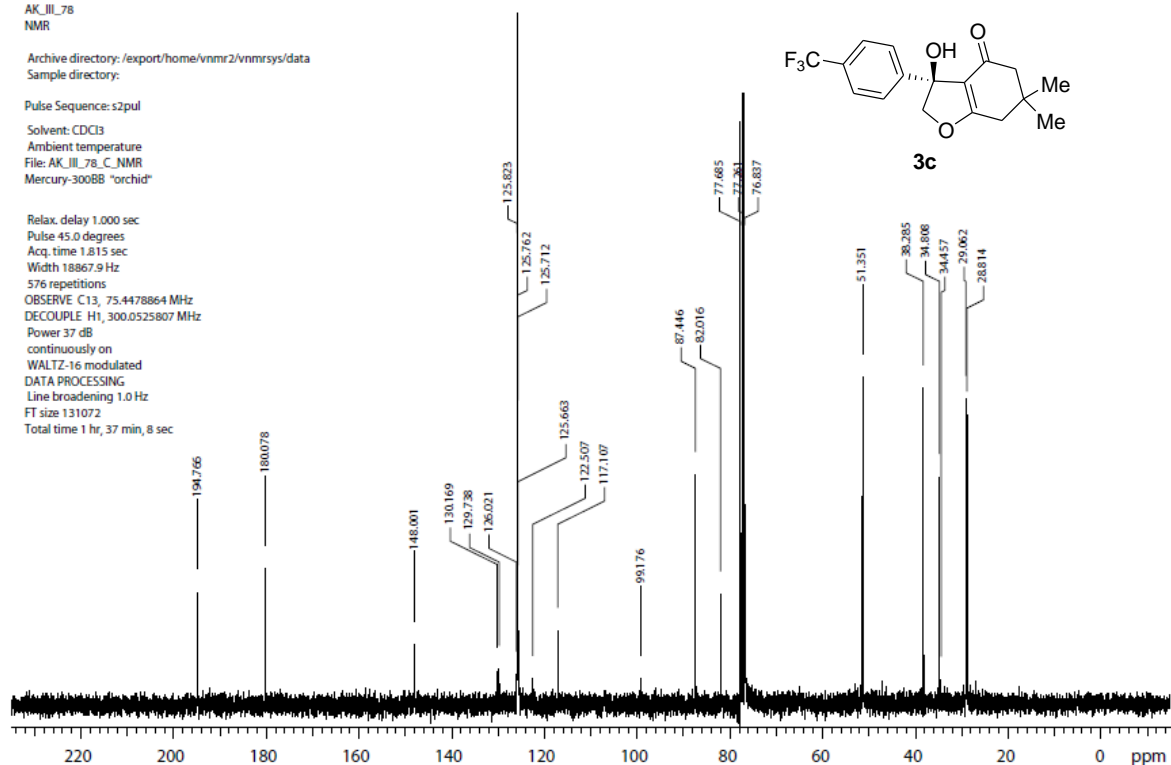
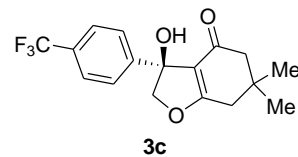


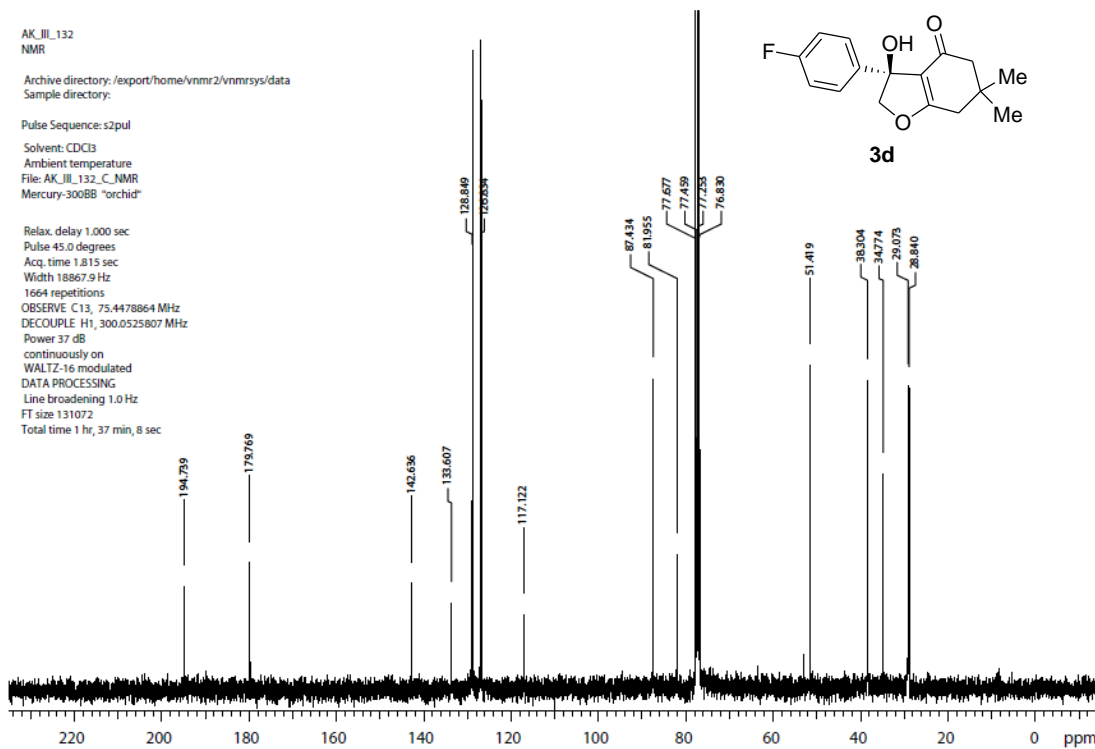
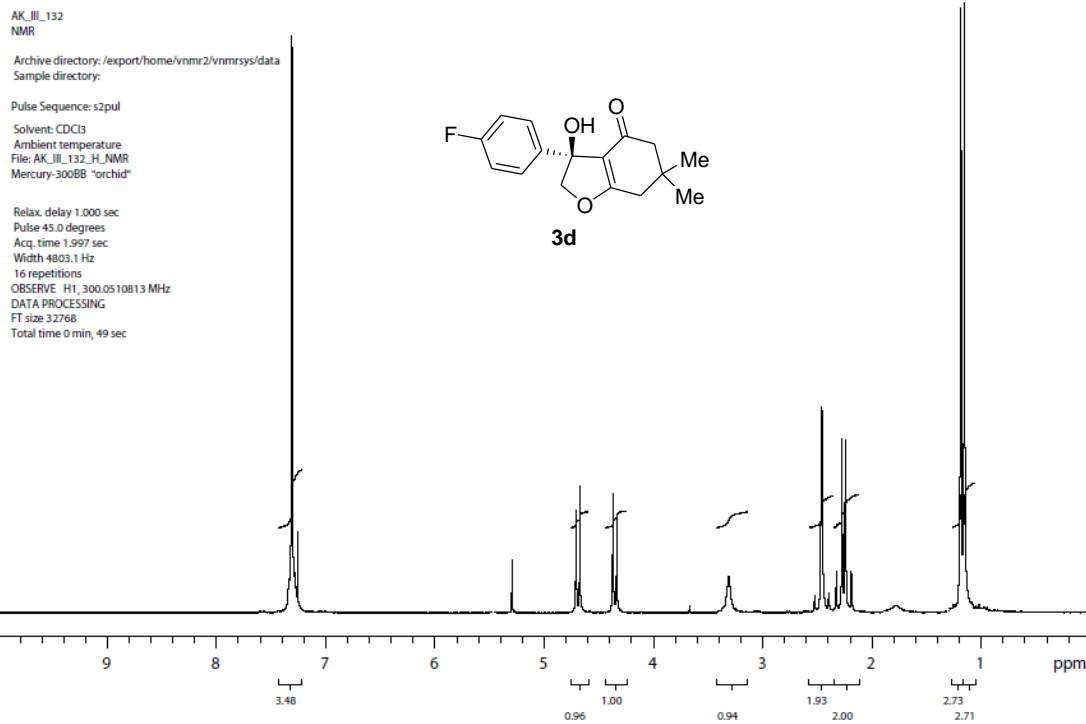
AK_JIL_78
NMR

Archive directory: /export/home/vnmr2/vnmrsys/data
Sample directory:

Pulse Sequence: s2pul
Solvent: CDCl3
Ambient temperature
File: AK_JIL_78_C_NMR
Mercury-300BB "orchid"

Relax. delay 1.000 sec
Pulse 45.0 degrees
Acq. time 1.815 sec
Width 18867.9 Hz
576 repetitions
OBSERVE C13, 75.4478864 MHz
DECOUPLE H1, 300.0525807 MHz
Power 37 dB
continuously on
WALTZ-16 modulated
DATA PROCESSING
Line broadening 1.0 Hz
FT size 131072
Total time 1 hr, 37 min, 8 sec





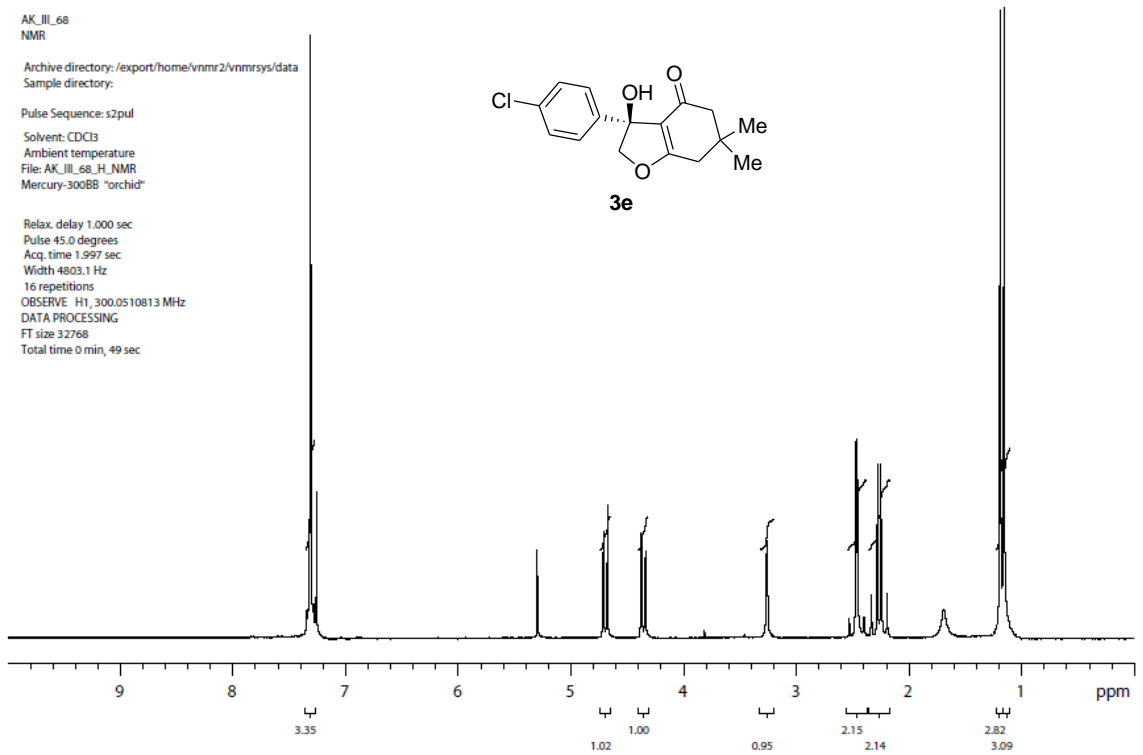
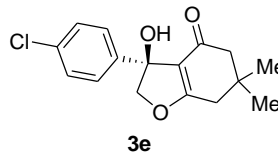
AK_III_68
NMR

Archive directory: /export/home/vnmr2/vnmrSYS/data
Sample directory:

Pulse Sequence: s2pul

Solvent: CDCl3
Ambient temperature
File: AK_III_68_H_NMR
Mercury-300BB "orchid"

Relax. delay 1.000 sec
Pulse 45.0 degrees
Acq. time 1.997 sec
Width 4803.1 Hz
16 repetitions
OBSERVE H1, 300.0510813 MHz
DATA PROCESSING
FT size 32768
Total time 0 min, 49 sec



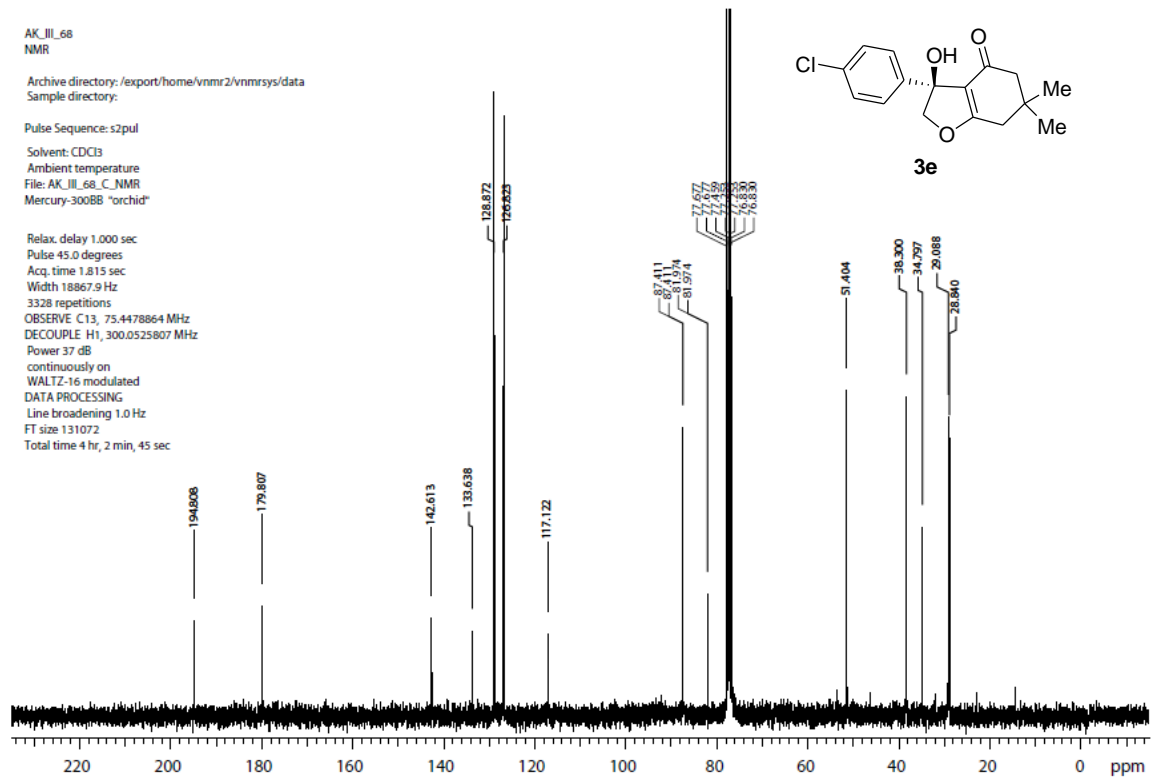
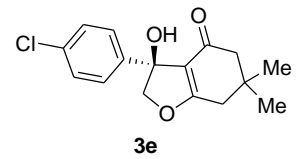
AK_III_68
NMR

Archive directory: /export/home/vnmr2/vnmrSYS/data
Sample directory:

Pulse Sequence: s2pul

Solvent: CDCl3
Ambient temperature
File: AK_III_68_C_NMR
Mercury-300BB "orchid"

Relax. delay 1.000 sec
Pulse 45.0 degrees
Acq. time 1.815 sec
Width 18867.9 Hz
3328 repetitions
OBSERVE C13, 75.4478864 MHz
DECOUPLE H1, 300.0525807 MHz
Power 37 dB
continuously on
WALTZ-16 modulated
DATA PROCESSING
Line broadening 1.0 Hz
FT size 131072
Total time 4 hr, 2 min, 45 sec



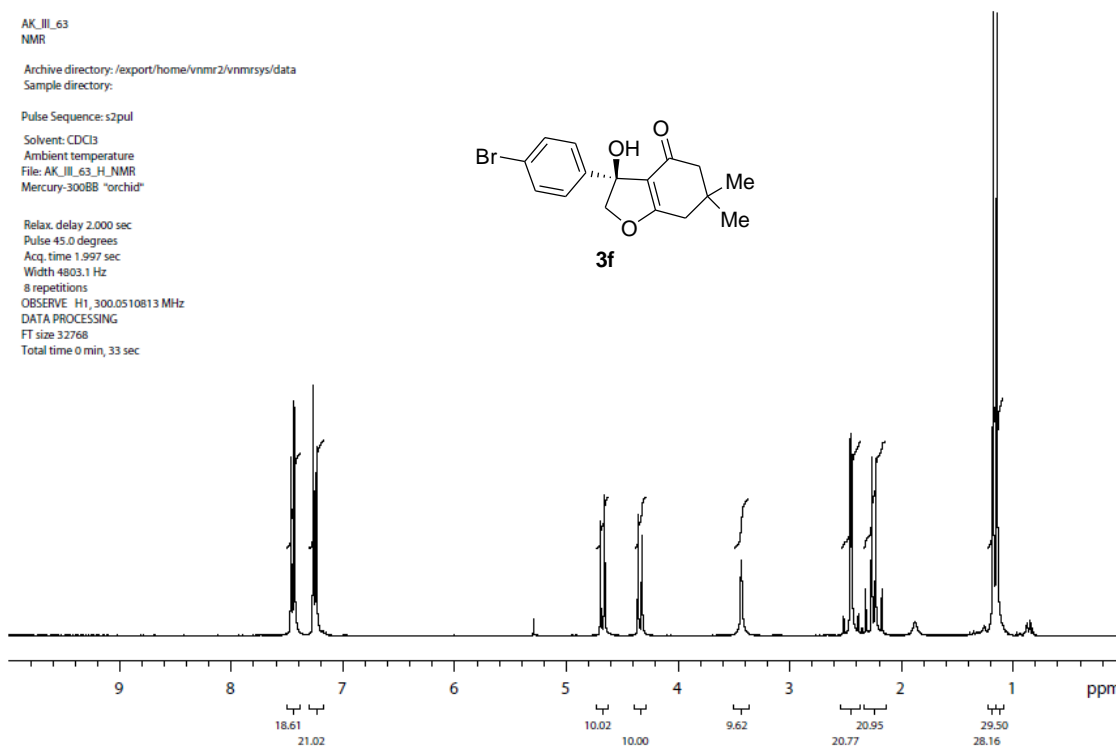
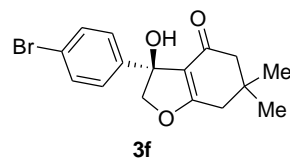
AK_III_63
NMR

Archive directory: /export/home/vnmr2/vnmrsys/data
Sample directory:

Pulse Sequence: s2pul

Solvent: CDCl3
Ambient temperature
File: AK_III_63_H_NMR
Mercury-300BB "orchid"

Relax. delay 2.000 sec
Pulse 45.0 degrees
Acq. time 1.997 sec
Width 4803.1 Hz
8 repetitions
OBSERVE H1, 300.0510813 MHz
DATA PROCESSING
FT size 32768
Total time 0 min, 33 sec



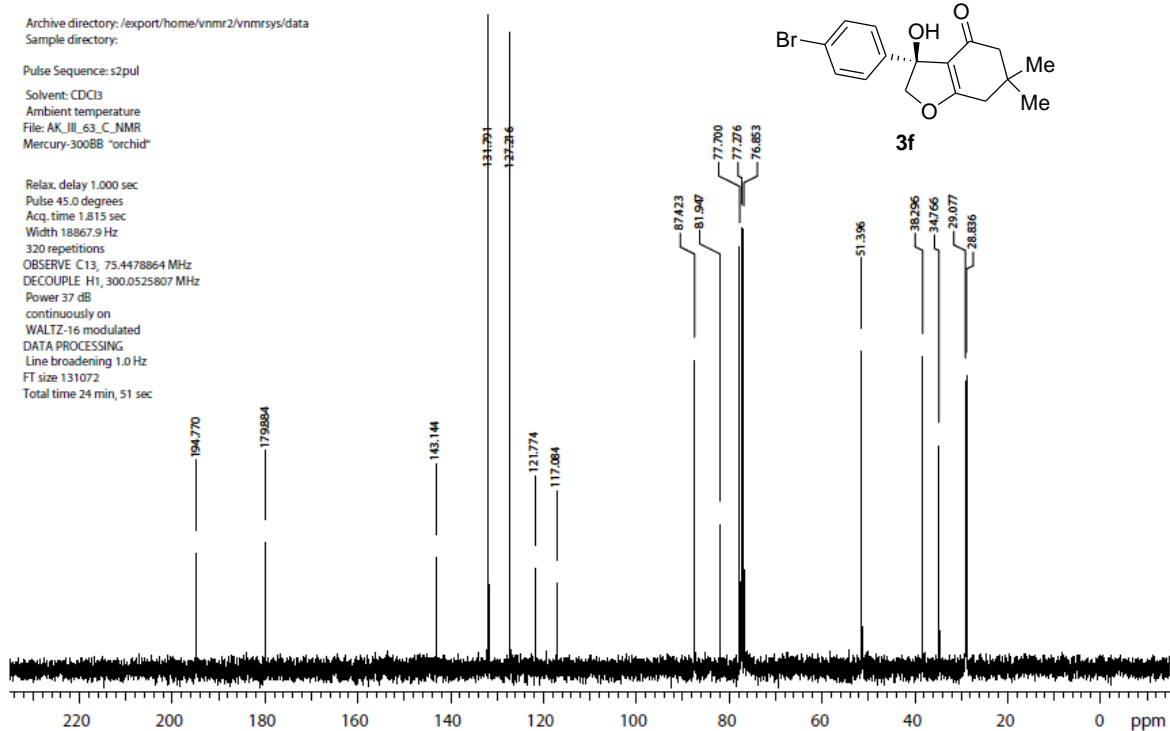
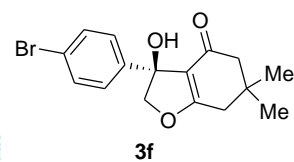
AK_III_63
NMR

Archive directory: /export/home/vnmr2/vnmrsys/data
Sample directory:

Pulse Sequence: s2pul

Solvent: CDCl3
Ambient temperature
File: AK_III_63_C_NMR
Mercury-300BB "orchid"

Relax. delay 1.000 sec
Pulse 45.0 degrees
Acq. time 1.815 sec
Width 18867.9 Hz
320 repetitions
OBSERVE C13, 75.4478864 MHz
DECOUPLE H1, 300.0525807 MHz
Power 37 dB
continuously on
WALTZ-16 modulated
DATA PROCESSING
Line broadening 1.0 Hz
FT size 131072
Total time 24 min, 51 sec

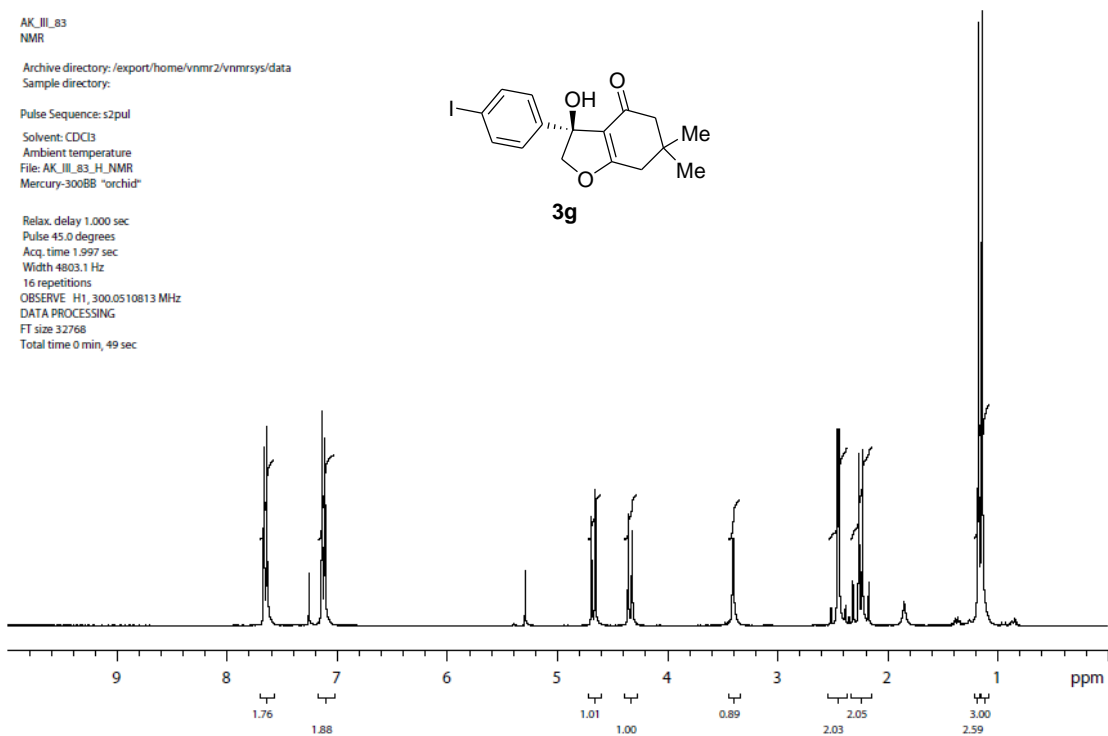
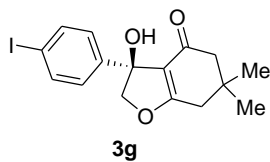


AK_JII_83
NMR

Archive directory: /export/home/vnmr2/vnmrsys/data
Sample directory:

Pulse Sequence: s2pul
Solvent: CDCl3
Ambient temperature
File: AK_JII_83_H_NMR
Mercury-300BB "orchid"

Relax, delay 1.000 sec
Pulse 45.0 degrees
Acq, time 1.997 sec
Width 4803.1 Hz
16 repetitions
OBSERVE H1, 300.0510813 MHz
DATA PROCESSING
FT size 32768
Total time 0 min, 49 sec

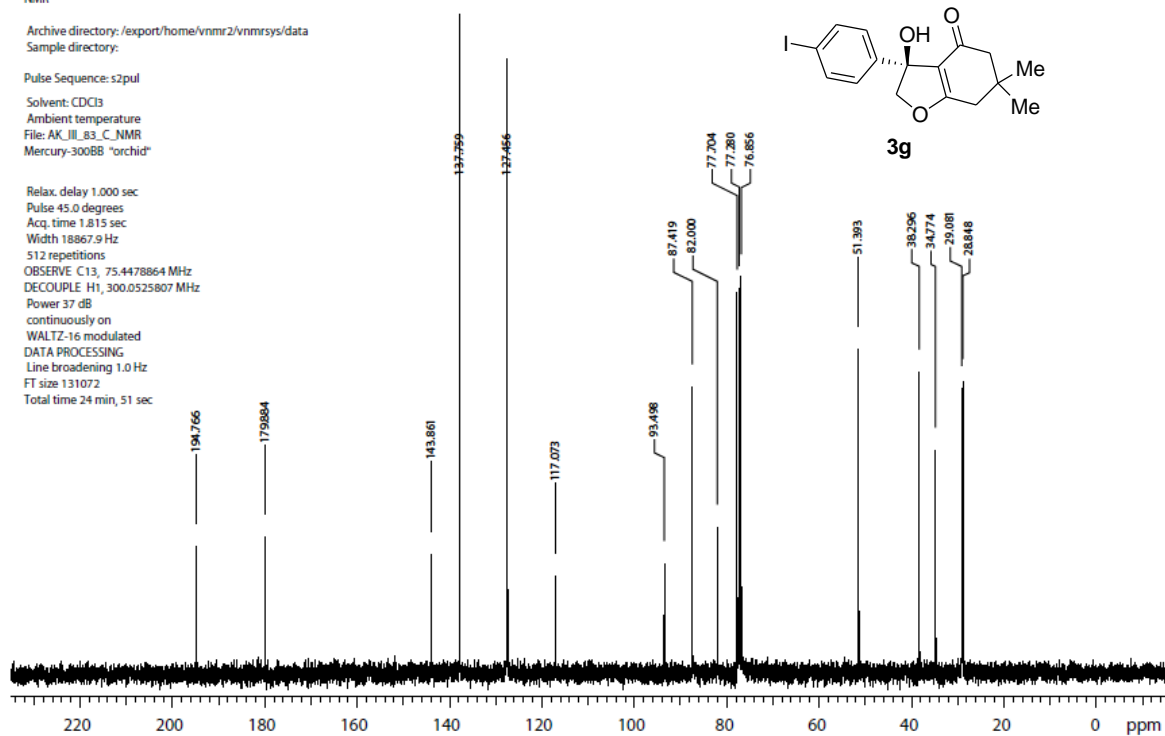
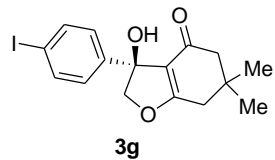


AK_JII_83
NMR

Archive directory: /export/home/vnmr2/vnmrsys/data
Sample directory:

Pulse Sequence: s2pul
Solvent: CDCl3
Ambient temperature
File: AK_JII_83_C_NMR
Mercury-300BB "orchid"

Relax, delay 1.000 sec
Pulse 45.0 degrees
Acq, time 1.815 sec
Width 18867.9 Hz
512 repetitions
OBSERVE C13, 75.4478864 MHz
DECOUPLE H1, 300.0525807 MHz
Power 37 dB
continuously on
WALTZ-16 modulated
DATA PROCESSING
Line broadening 1.0 Hz
FT size 131072
Total time 24 min, 51 sec

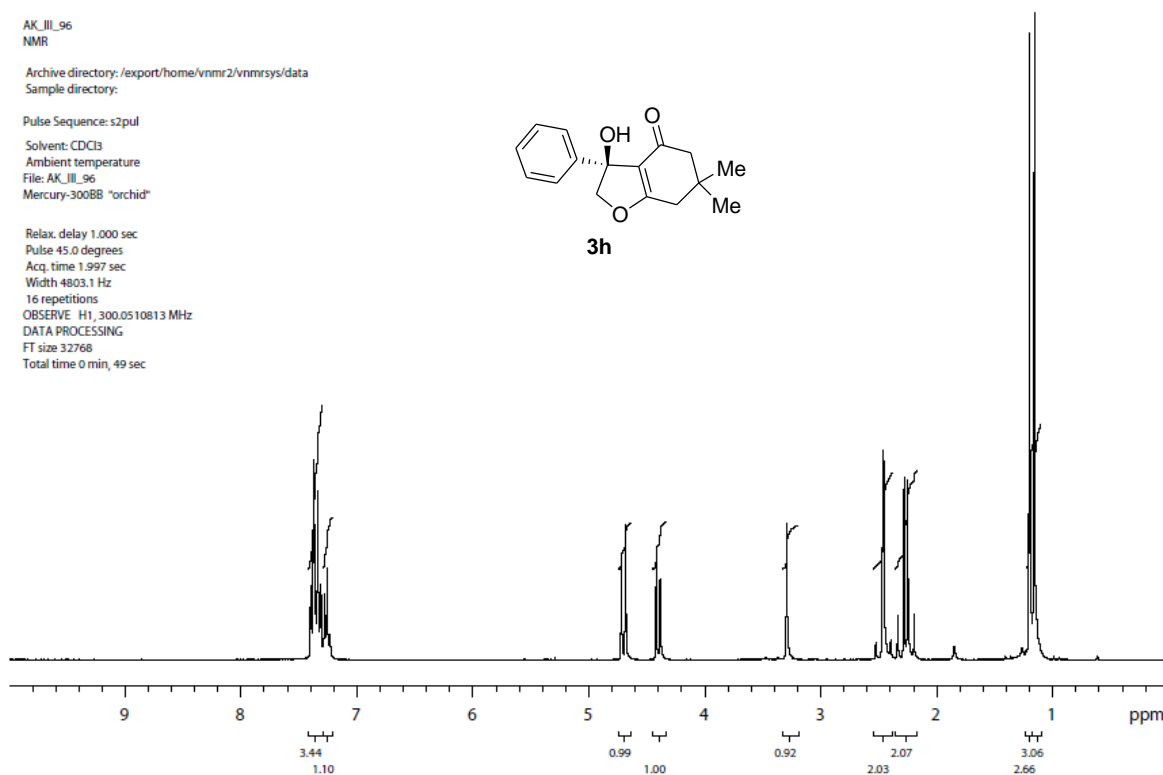
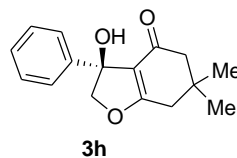


AK_III_96
NMR

Archive directory: /export/home/vnmr2/vnmrsys/data
Sample directory:

Pulse Sequence: s2pul
Solvent: CDCl3
Ambient temperature
File: AK_III_96
Mercury-300BB "orchid"

Relax. delay 1.000 sec
Pulse 45.0 degrees
Acq. time 1.997 sec
Width 4803.1 Hz
16 repetitions
OBSERVE H1, 300.0510813 MHz
DATA PROCESSING
FT size 32768
Total time 0 min, 49 sec

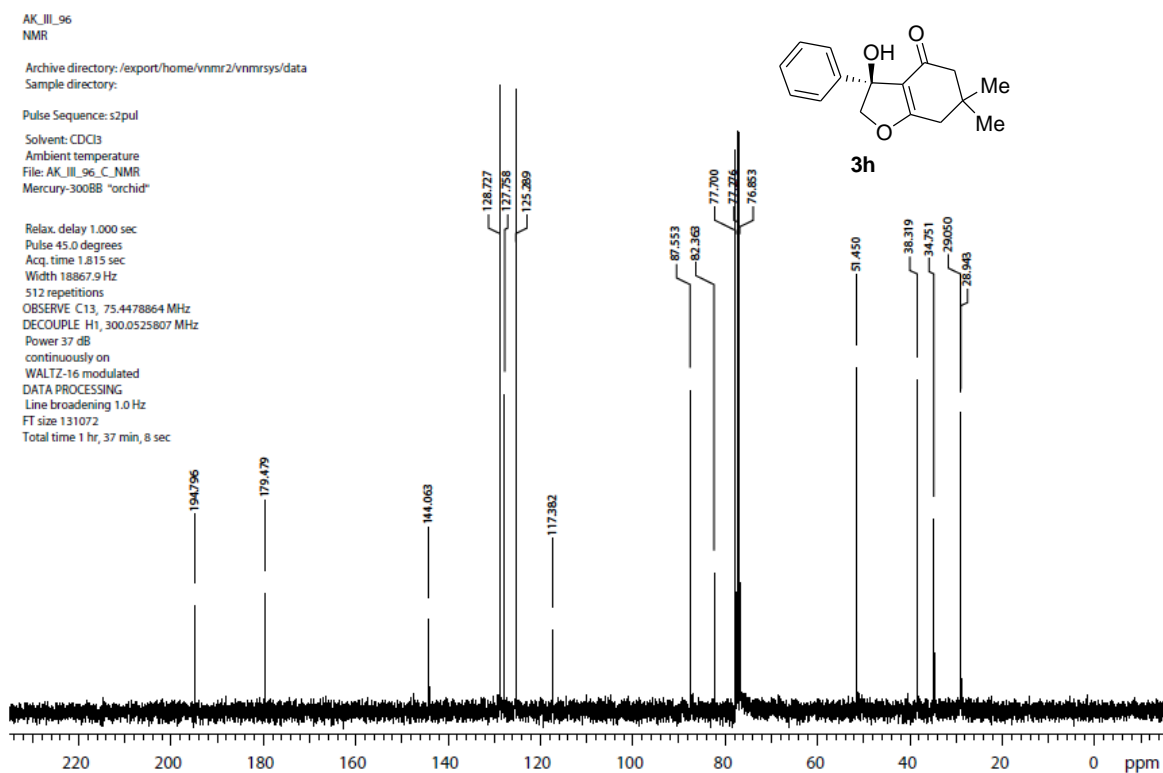
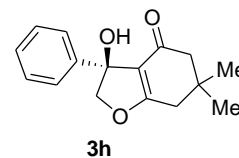


AK_III_96
NMR

Archive directory: /export/home/vnmr2/vnmrsys/data
Sample directory:

Pulse Sequence: s2pul
Solvent: CDCl3
Ambient temperature
File: AK_III_96_C_NMR
Mercury-300BB "orchid"

Relax. delay 1.000 sec
Pulse 45.0 degrees
Acq. time 1.815 sec
Width 18867.9 Hz
512 repetitions
OBSERVE C13, 75.4478864 MHz
DECOUPLE H1, 300.0525807 MHz
Power 37 dB
continuously on
WALTZ-16 modulated
DATA PROCESSING
Line broadening 1.0 Hz
FT size 131072
Total time 1 hr, 37 min, 8 sec



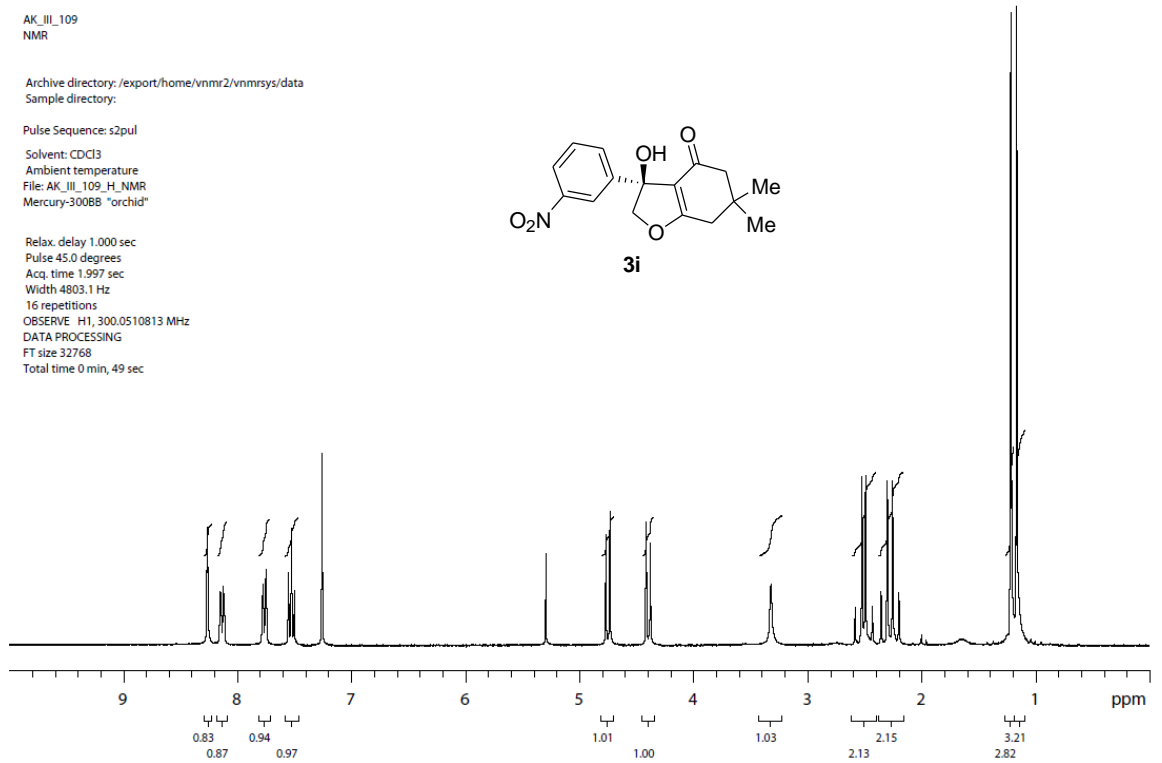
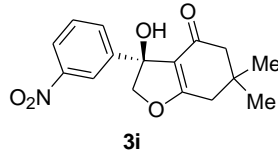
AK_III_109
NMR

Archive directory: /export/home/vnmr2/vnmrsys/data
Sample directory:

Pulse Sequence: s2pul

Solvent: CDCl3
Ambient temperature
File: AK_III_109_H_NMR
Mercury-300BB "orchid"

Relax. delay 1.000 sec
Pulse 45.0 degrees
Acq. time 1.997 sec
Width 4803.1 Hz
16 repetitions
OBSERVE H1, 300.0510813 MHz
DATA PROCESSING
FT size 32768
Total time 0 min, 49 sec



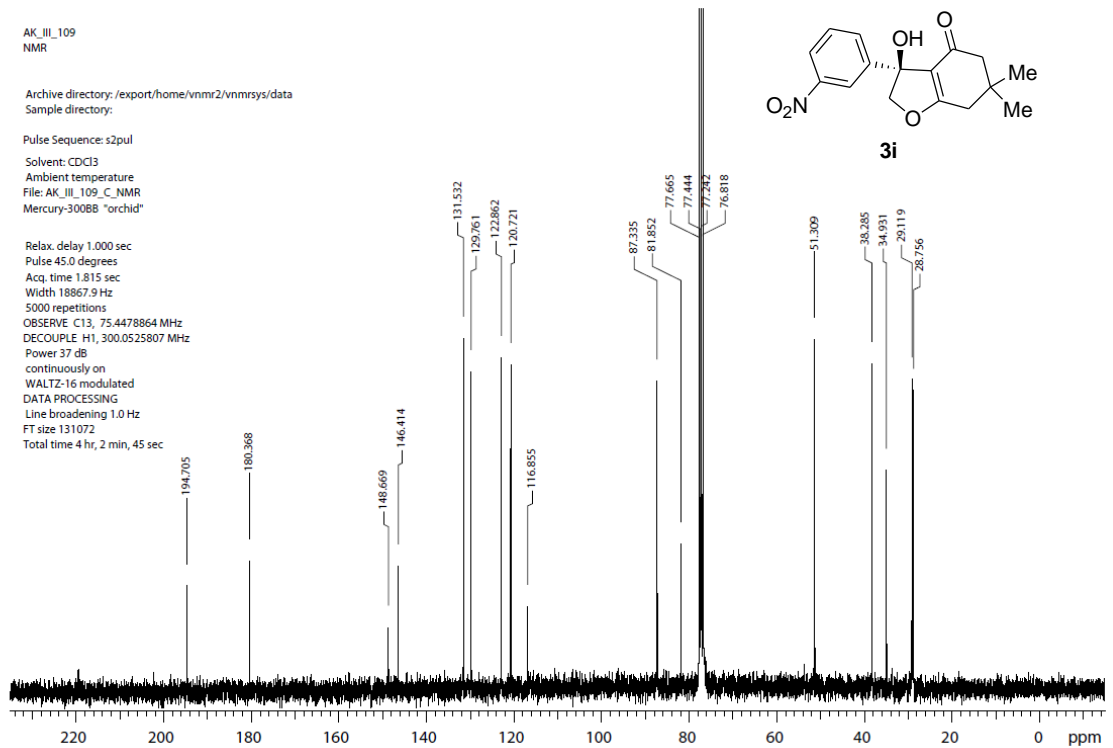
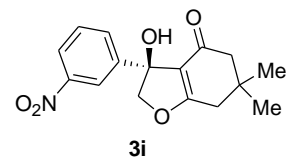
AK_III_109
NMR

Archive directory: /export/home/vnmr2/vnmrsys/data
Sample directory:

Pulse Sequence: s2pul

Solvent: CDCl3
Ambient temperature
File: AK_III_109_C_NMR
Mercury-300BB "orchid"

Relax. delay 1.000 sec
Pulse 45.0 degrees
Acq. time 1.815 sec
Width 18857.9 Hz
5000 repetitions
OBSERVE C13, 75.4478964 MHz
DECOUPLE H1, 300.0525807 MHz
Power 37 dB
continuously on
WALTZ-16 modulated
DATA PROCESSING
Line broadening 1.0 Hz
FT size 131072
Total time 4 hr, 2 min, 45 sec



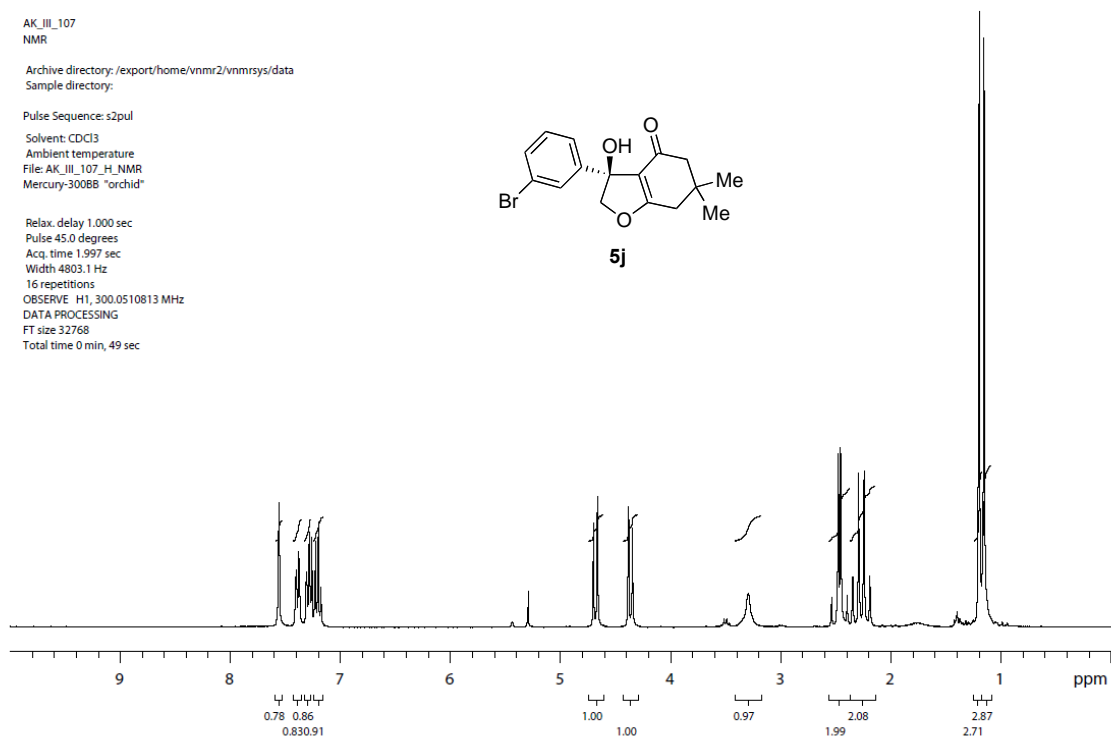
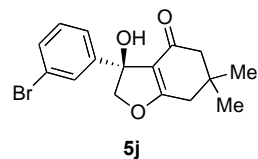
AK_III_107
NMR

Archive directory: /export/home/vnmr2/vnmrSYS/data
Sample directory:

Pulse Sequence: s2pul

Solvent: CDCl3
Ambient temperature
File: AK_III_107_H_NMR
Mercury-300BB "orchid"

Relax. delay 1.000 sec
Pulse 45.0 degrees
Acq. time 1.997 sec
Width 4803.1 Hz
16 repetitions
OBSERVE H1, 300.0510813 MHz
DATA PROCESSING
FT size 32768
Total time 0 min, 49 sec



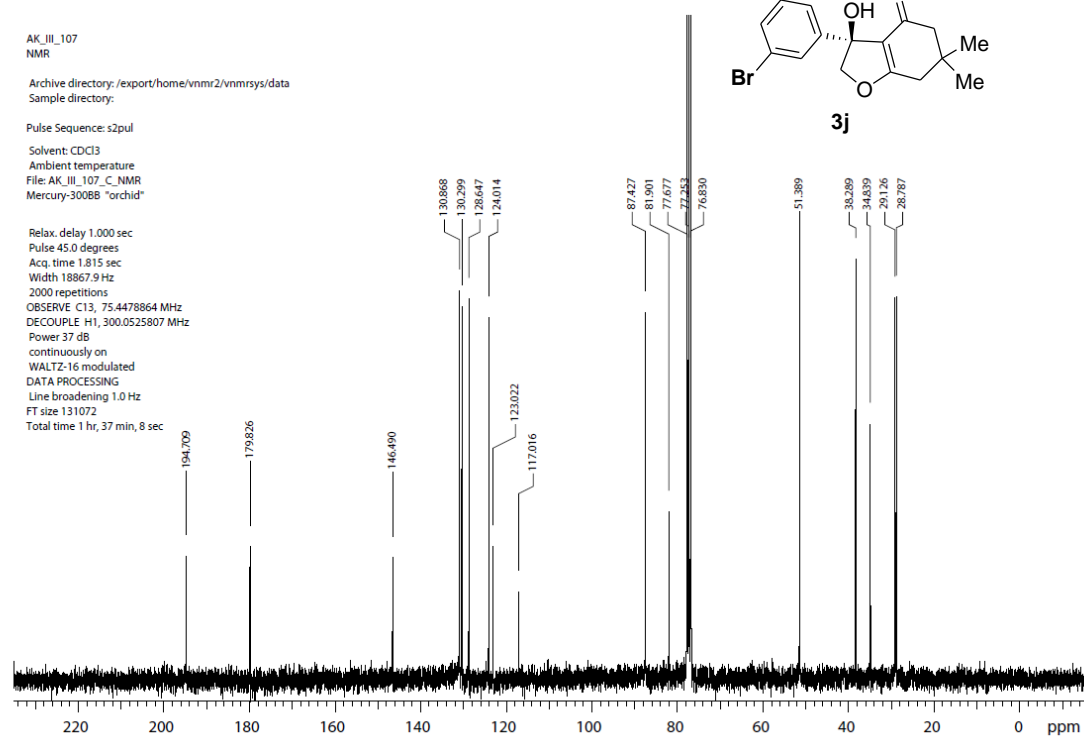
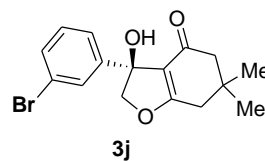
AK_III_107
NMR

Archive directory: /export/home/vnmr2/vnmrSYS/data
Sample directory:

Pulse Sequence: s2pul

Solvent: CDCl3
Ambient temperature
File: AK_III_107_C_NMR
Mercury-300BB "orchid"

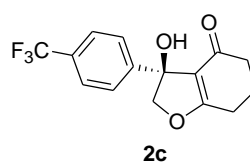
Relax. delay 1.000 sec
Pulse 45.0 degrees
Acq. time 1.815 sec
Width 18867.9 Hz
2000 repetitions
OBSERVE C13, 75.4478864 MHz
DECOUPLE H1, 300.0525807 MHz
Power 37 dB
continuously on
WALTZ-16 modulated
DATA PROCESSING
Line broadening 1.0 Hz
FT size 131072
Total time 1 hr, 37 min, 8 sec



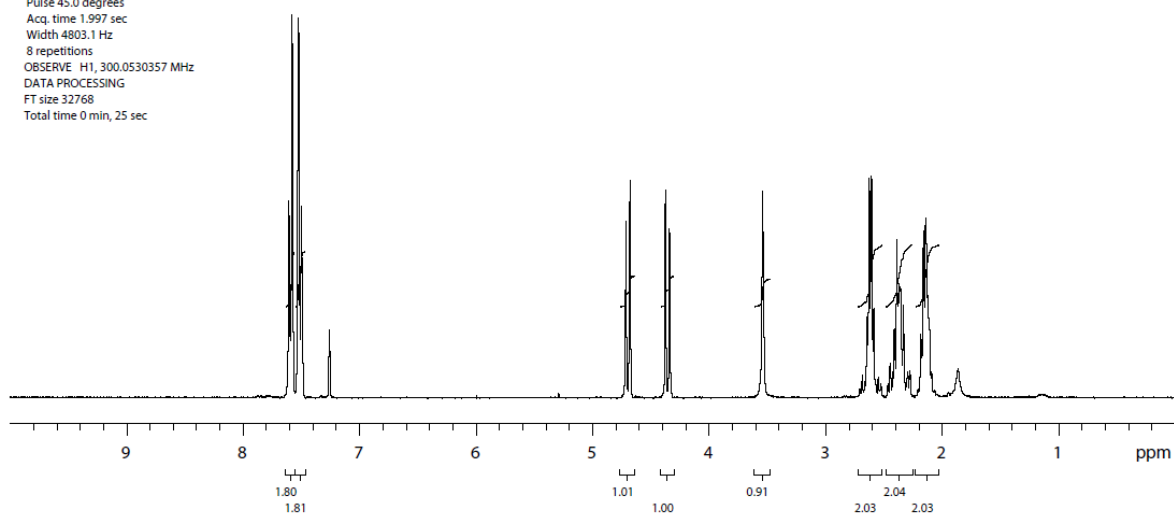
AK_II_21
1H NMR

Archive directory: /export/home/vnmr2/vnmrsys/data
Sample directory:

Pulse Sequence: s2pul
Solvent: CDCl3
Ambient temperature
File: AK_II_21_1H1NMR
Mercury-300BB "orchid"



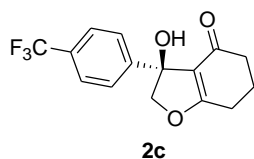
Relax. delay 1.000 sec
Pulse 45.0 degrees
Acq. time 1.997 sec
Width 4803.1 Hz
8 repetitions
OBSERVE H1, 300.0530357 MHz
DATA PROCESSING
FT size 32768
Total time 0 min, 25 sec



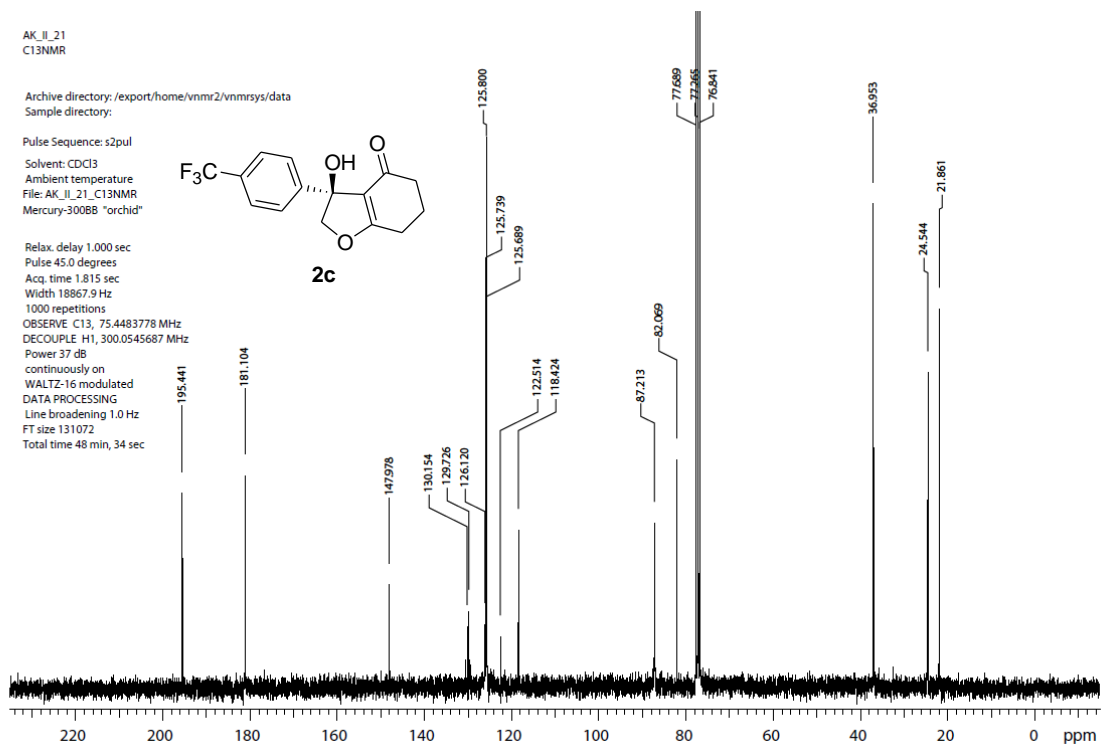
AK_II_21
13C NMR

Archive directory: /export/home/vnmr2/vnmrsys/data
Sample directory:

Pulse Sequence: s2pul
Solvent: CDCl3
Ambient temperature
File: AK_II_21_131NMR
Mercury-300BB "orchid"

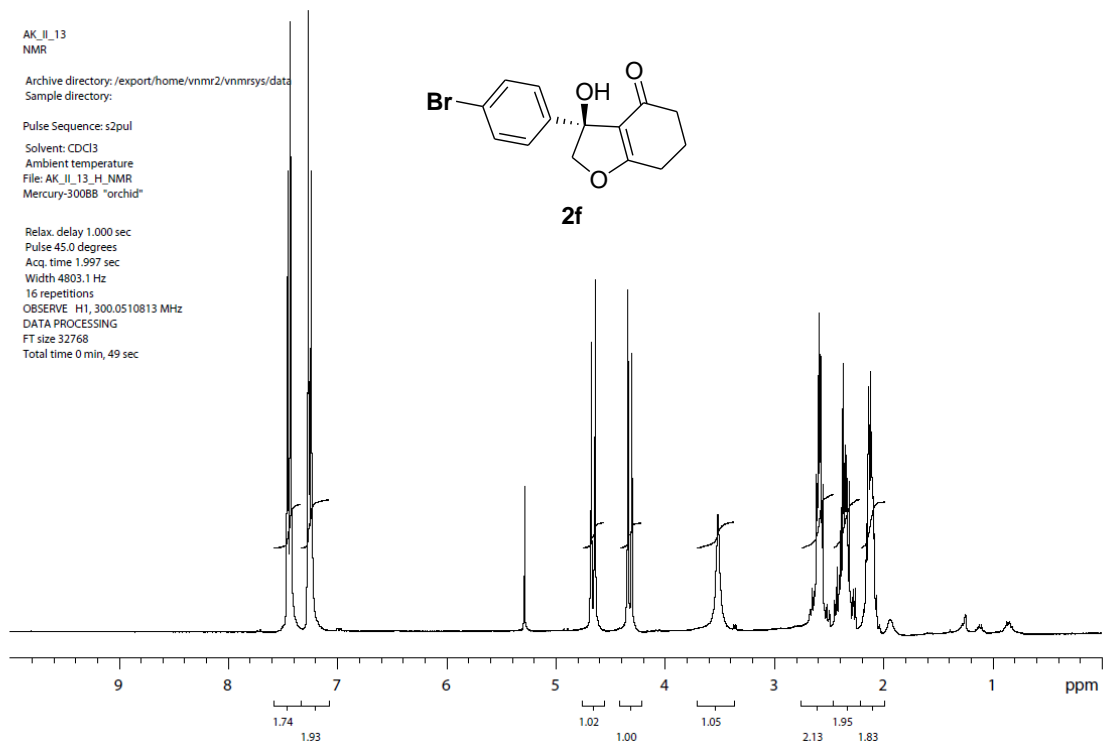
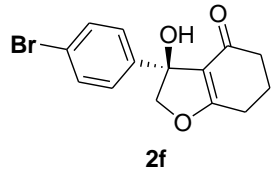


Relax. delay 1.000 sec
Pulse 45.0 degrees
Acq. time 1.815 sec
Width 18867.9 Hz
1000 repetitions
OBSERVE C13, 75.4483778 MHz
DECOUPLE H1, 300.0545687 MHz
Power 37 dB
continuously on
WALTZ-16 modulated
DATA PROCESSING
Line broadening 1.0 Hz
FT size 131072
Total time 48 min, 34 sec



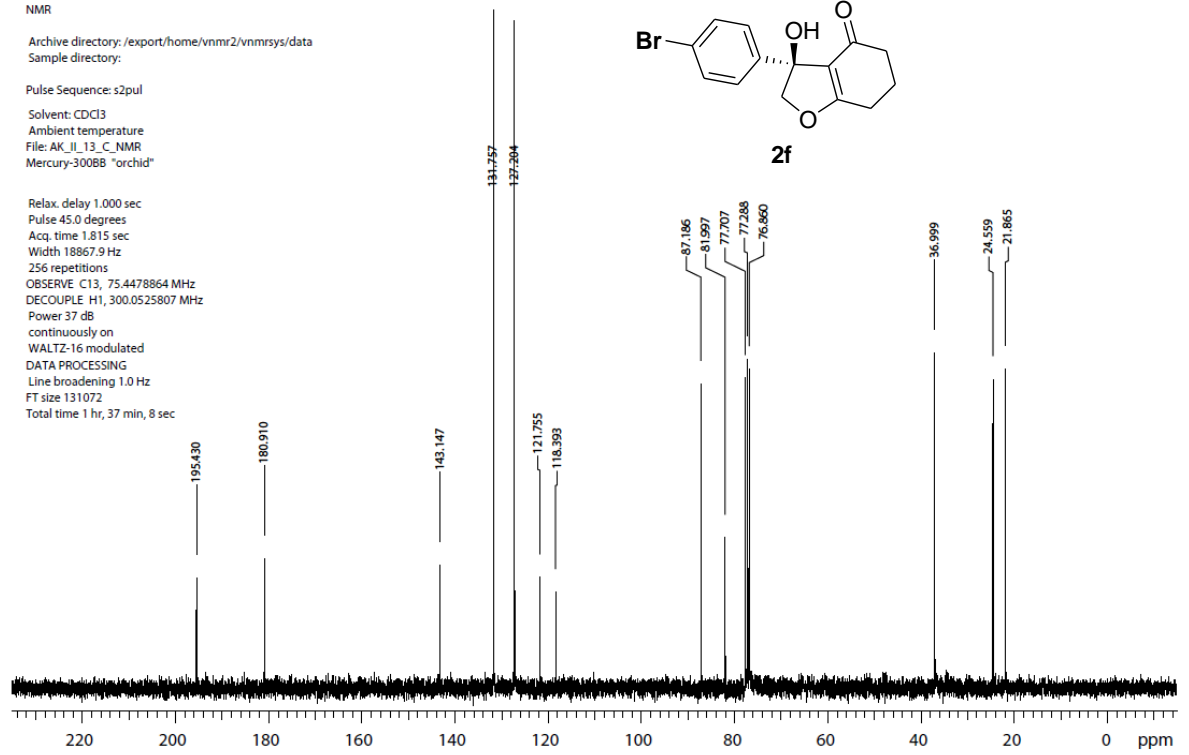
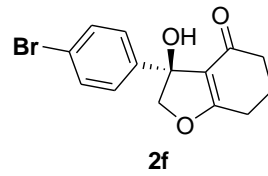
AK_IL_13
 NMR
 Archive directory: /export/home/vnmr2/vnmrsys/data
 Sample directory:
 Pulse Sequence: s2pul
 Solvent: CDCl3
 Ambient temperature
 File: AK_IL_13_H_NMR
 Mercury-300BB "orchid"

Relax. delay 1.000 sec
 Pulse 45.0 degrees
 Acq. time 1.997 sec
 Width 4803.1 Hz
 16 repetitions
 OBSERVE H1, 300.0510813 MHz
 DATA PROCESSING
 FT size 32768
 Total time 0 min, 49 sec

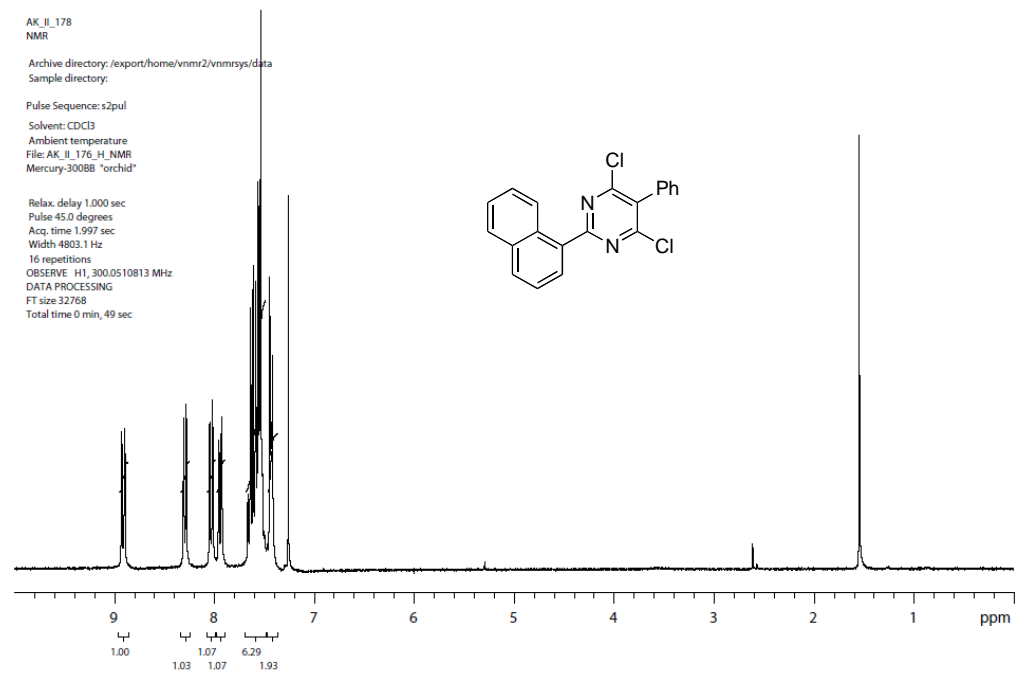
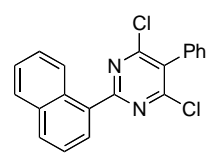


AK_IL_13
 NMR
 Archive directory: /export/home/vnmr2/vnmrsys/data
 Sample directory:
 Pulse Sequence: s2pul
 Solvent: CDCl3
 Ambient temperature
 File: AK_IL_13_C_NMR
 Mercury-300BB "orchid"

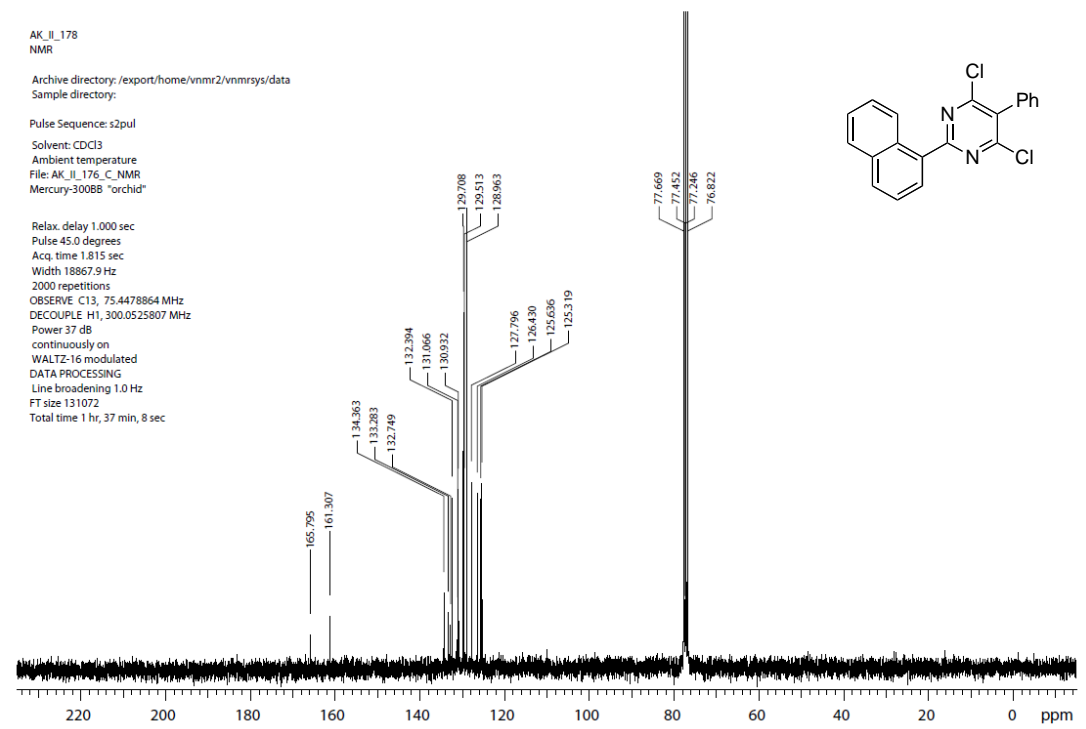
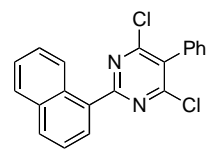
Relax. delay 1.000 sec
 Pulse 45.0 degrees
 Acq. time 1.815 sec
 Width 18867.9 Hz
 256 repetitions
 OBSERVE C13, 75.4478864 MHz
 DECOUPLE H1, 300.0525807 MHz
 Power 37 dB
 continuously on
 WALTZ-16 modulated
 DATA PROCESSING
 Line broadening 1.0 Hz
 FT size 131072
 Total time 1 hr, 37 min, 8 sec



AK_IL_178
 NMR
 Archive directory: /export/home/vnmr2/vnmrsys/data
 Sample directory:
 Pulse Sequence: s2pul
 Solvent: CDCl3
 Ambient temperature
 File: AK_IL_176_H_NMR
 Mercury-300BB "orchid"
 Relax: delay 1.000 sec
 Pulse 45.0 degrees
 Acq: time 1.997 sec
 Width 4803.1 Hz
 16 repetitions
 OBSERVE H1, 300.0510813 MHz
 DATA PROCESSING
 FT size 32768
 Total time 0 min, 49 sec



AK_IL_178
 NMR
 Archive directory: /export/home/vnmr2/vnmrsys/data
 Sample directory:
 Pulse Sequence: s2pul
 Solvent: CDCl3
 Ambient temperature
 File: AK_IL_176_C_NMR
 Mercury-300BB "orchid"
 Relax: delay 1.000 sec
 Pulse 45.0 degrees
 Acq: time 1.815 sec
 Width 18867.9 Hz
 2000 repetitions
 OBSERVE C13, 75.4478864 MHz
 DECOUPLE H1, 300.0525807 MHz
 Power 37 dB
 continuously on
 WALTZ-16 modulated
 DATA PROCESSING
 Line broadening 1.0 Hz
 FT size 131072
 Total time 1 hr, 37 min, 8 sec

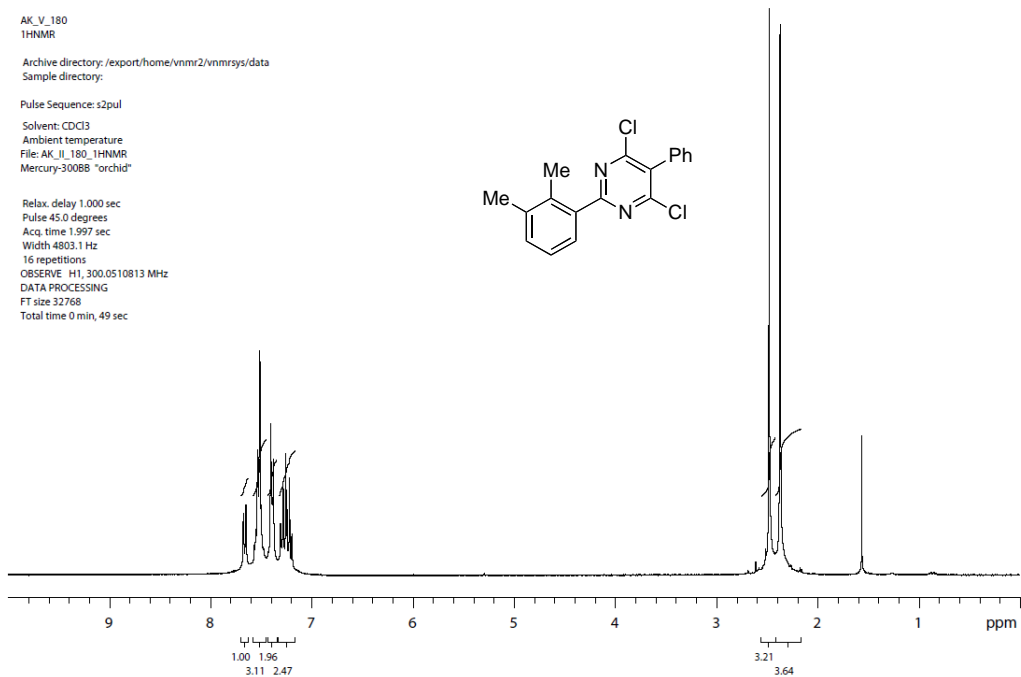
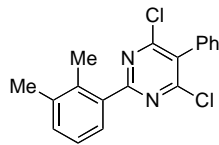


AK_V_180
1HNMR

Archive directory: /export/home/vnmr2/vnmrSYS/data
Sample directory:

Pulse Sequence: s2pul
Solvent: CDCl3
Ambient temperature
File: AK_V_180_1HNMR
Mercury-300BB "orchid"

Relax. delay 1.000 sec
Pulse 45.0 degrees
Acq. time 1.997 sec
Width 4803.1 Hz
16 repetitions
OBSERVE: H1, 300.0510813 MHz
DATA PROCESSING
FT size 32768
Total time 0 min, 49 sec

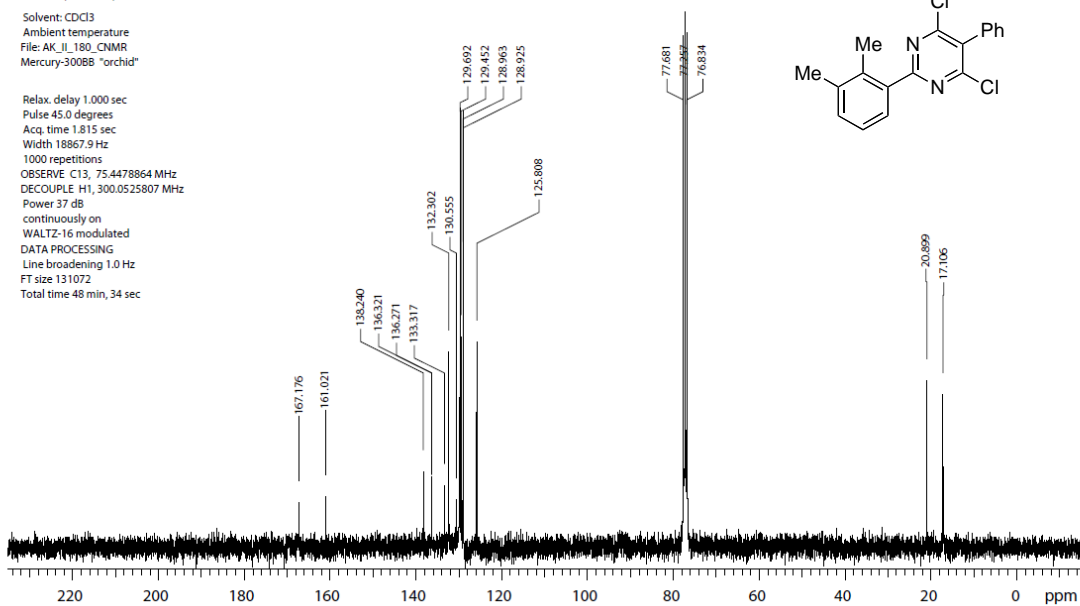
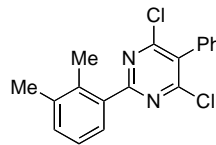


AK_V_180
13CNMR

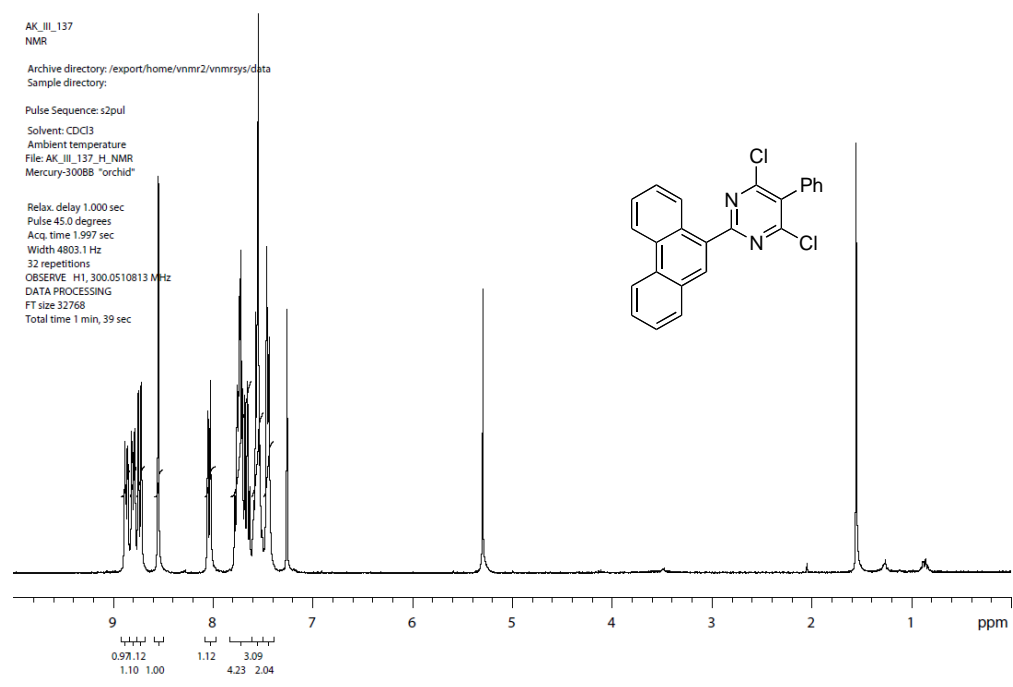
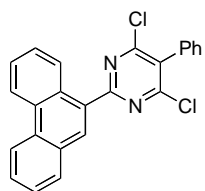
Archive directory: /export/home/vnmr2/vnmrSYS/data
Sample directory:

Pulse Sequence: s2pul
Solvent: CDCl3
Ambient temperature
File: AK_V_180_13CNMR
Mercury-300BB "orchid"

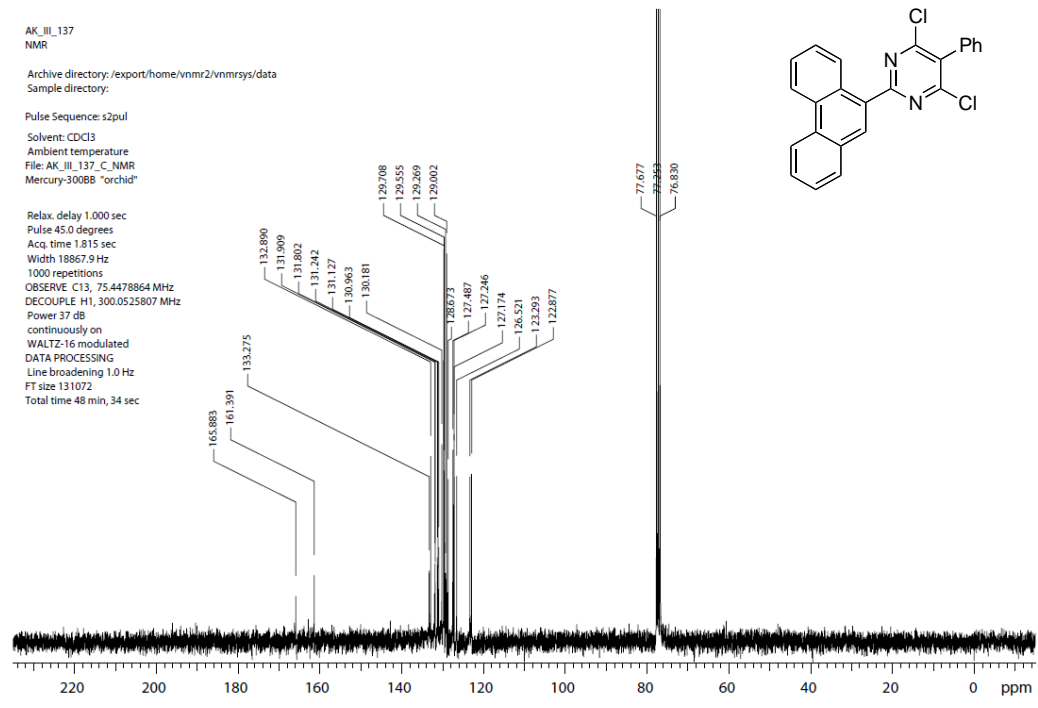
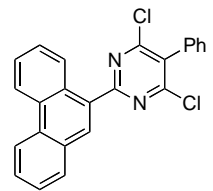
Relax. delay 1.000 sec
Pulse 45.0 degrees
Acq. time 1.815 sec
Width 18867.9 Hz
1000 repetitions
OBSERVE: C13, 75.4478864 MHz
DECOUPLE: H1, 300.0525807 MHz
Power 37 dB
continuously on
WALTZ-16 modulated
DATA PROCESSING
Line broadening 1.0 Hz
FT size 131072
Total time 48 min, 34 sec



AK_III_137
NMR
Archive directory: /export/home/vnmr2/vnmrSYS/data
Sample directory:
Pulse Sequence: s2pul
Solvent: CDCl3
Ambient temperature
File: AK_III_137_H_NMR
Mercury-300BB "orchid"
Relax. delay 1.000 sec
Pulse 45.0 degrees
Acq. time 1.997 sec
Width 4803.1 Hz
32 repetitions
OBSERVE H1, 300.0510813 MHz
DATA PROCESSING
FT size 32768
Total time 1 min, 39 sec



AK_III_137
NMR
Archive directory: /export/home/vnmr2/vnmrSYS/data
Sample directory:
Pulse Sequence: s2pul
Solvent: CDCl3
Ambient temperature
File: AK_III_137_C_NMR
Mercury-300BB "orchid"
Relax. delay 1.000 sec
Pulse 45.0 degrees
Acq. time 1.815 sec
Width 18867.9 Hz
1000 repetitions
OBSERVE C13, 75.4478864 MHz
DECOUPLE H1, 300.0525807 MHz
Power 37 dB
continuously on
WALTZ-16 modulated
DATA PROCESSING
Line broadening 1.0 Hz
FT size 131072
Total time 48 min, 34 sec

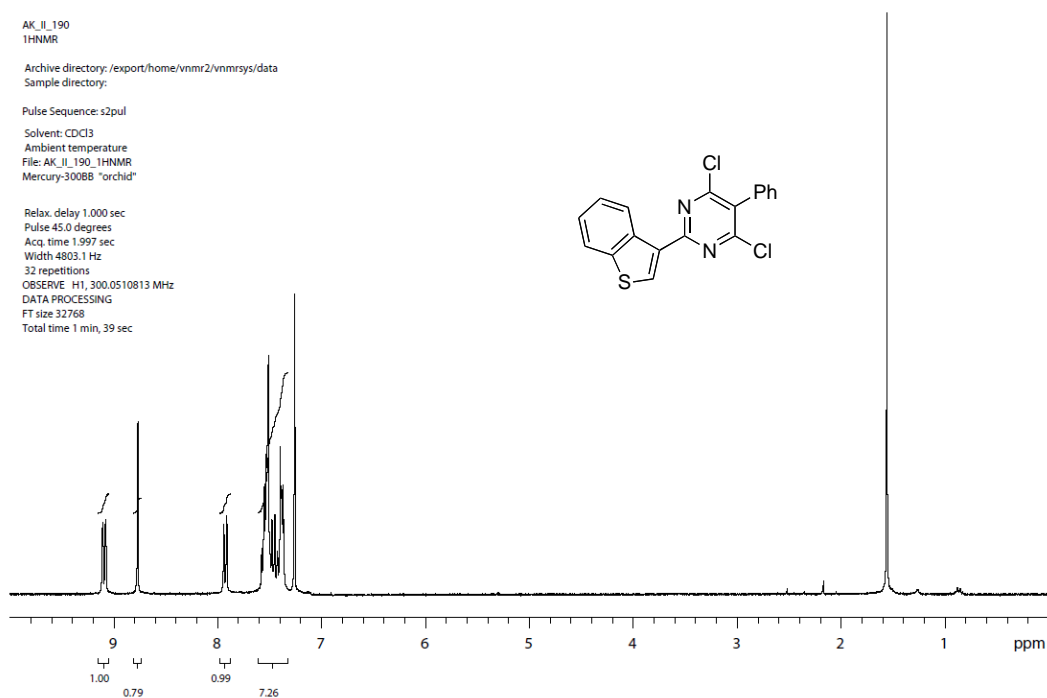
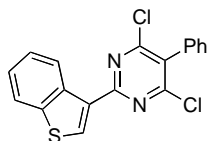


AK_IL_190
1H NMR

Archive directory: /export/home/vnmr2/vnmrSYS/data
Sample directory:

Pulse Sequence: s2pul
Solvent: CDCl3
Ambient temperature
File: AK_IL_190_1HNMR
Mercury-300BB "orchid"

Relax. delay 1.000 sec
Pulse 45.0 degrees
Acq. time 1.997 sec
Width 4803.1 Hz
32 repetitions
OBSERVE H1, 300.0510813 MHz
DATA PROCESSING
FT size 32768
Total time 1 min, 39 sec

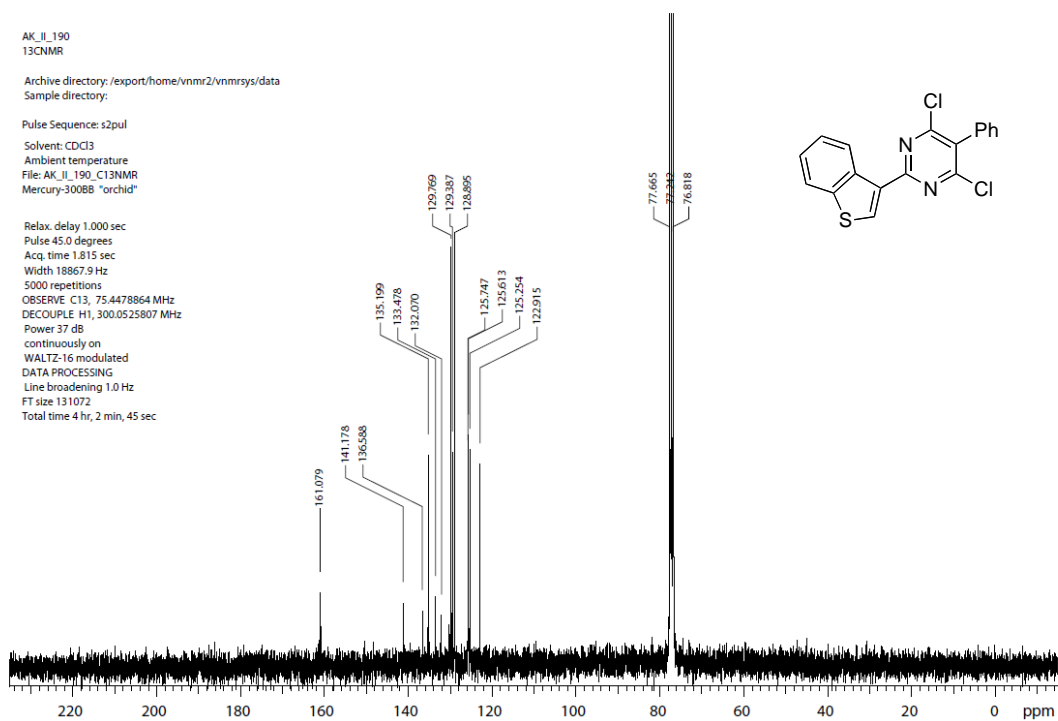
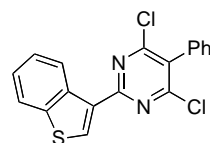


AK_IL_190
13C NMR

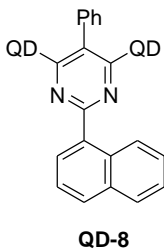
Archive directory: /export/home/vnmr2/vnmrSYS/data
Sample directory:

Pulse Sequence: s2pul
Solvent: CDCl3
Ambient temperature
File: AK_IL_190_C13NMR
Mercury-300BB "orchid"

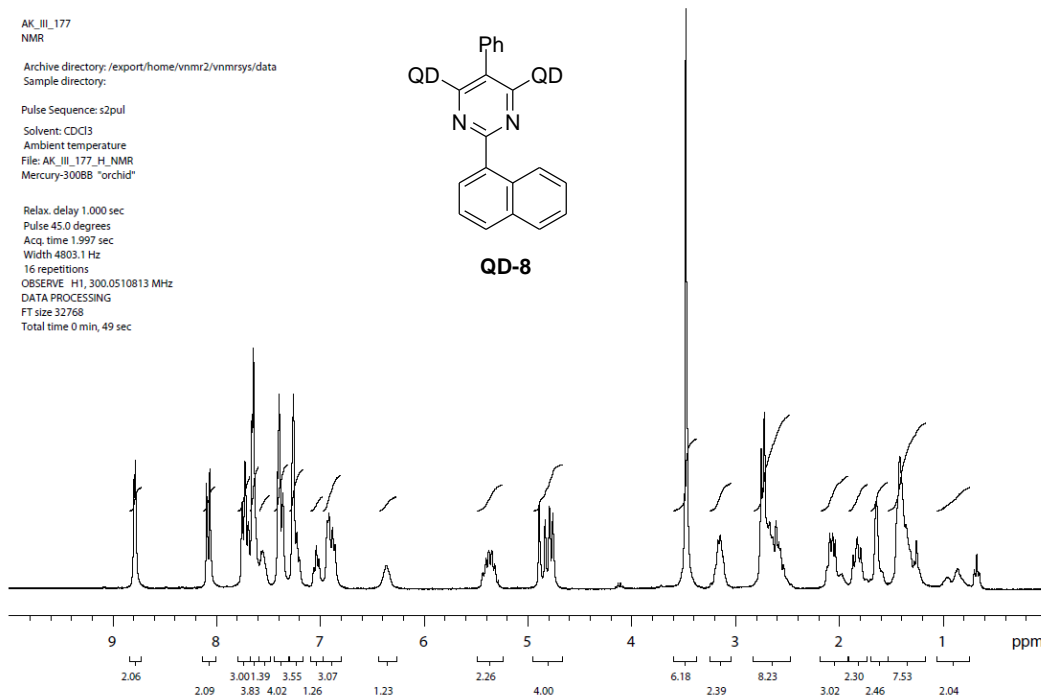
Relax. delay 1.000 sec
Pulse 45.0 degrees
Acq. time 1.815 sec
Width 18867.9 Hz
5000 repetitions
OBSERVE C13, 75.4478864 MHz
DECOUPLE H1, 300.0525807 MHz
Power 37 dB
continuously on
WALTZ-16 modulated
DATA PROCESSING
Line broadening 1.0 Hz
FT size 131072
Total time 4 hr, 2 min, 45 sec



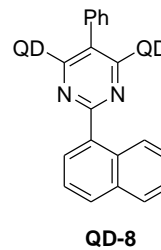
AK_III_177
 NMR
 Archive directory: /export/home/vnmr2/vnmrSYS/data
 Sample directory:
 Pulse Sequence: s2pul
 Solvent: CDCl3
 Ambient temperature
 File: AK_III_177_H_NMR
 Mercury-300BB "orchid"



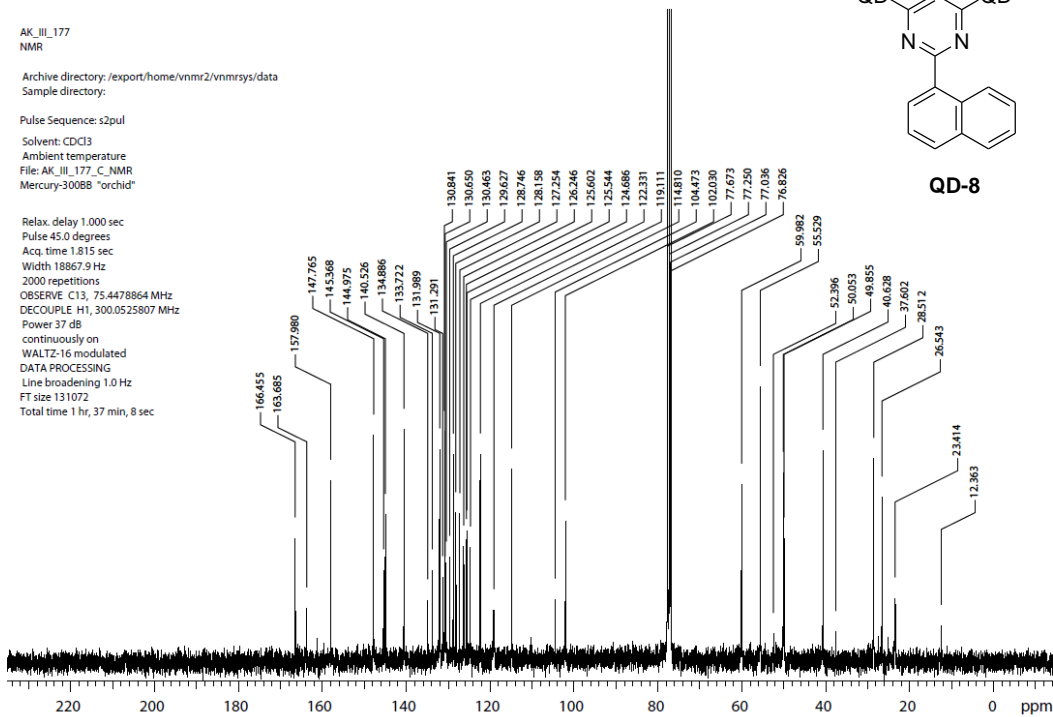
Relax. delay 1.000 sec
 Pulse 45.0 degrees
 Acq. time 1.997 sec
 Width 4803.1 Hz
 16 repetitions
 OBSERVE H1, 300.0510813 MHz
 DATA PROCESSING
 FT size 32768
 Total time 0 min, 49 sec



AK_III_177
 NMR
 Archive directory: /export/home/vnmr2/vnmrSYS/data
 Sample directory:
 Pulse Sequence: s2pul
 Solvent: CDCl3
 Ambient temperature
 File: AK_III_177_C_NMR
 Mercury-300BB "orchid"



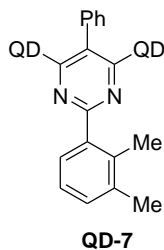
Relax. delay 1.000 sec
 Pulse 45.0 degrees
 Acq. time 1.815 sec
 Width 18867.9 Hz
 2000 repetitions
 OBSERVE C13, 75.4478864 MHz
 DECOUPLE H1, 300.0525807 MHz
 Power 37 dB
 continuously on
 WALTZ-16 modulated
 DATA PROCESSING
 Line broadening 1.0 Hz
 FT size 131072
 Total time 1 hr, 37 min, 8 sec



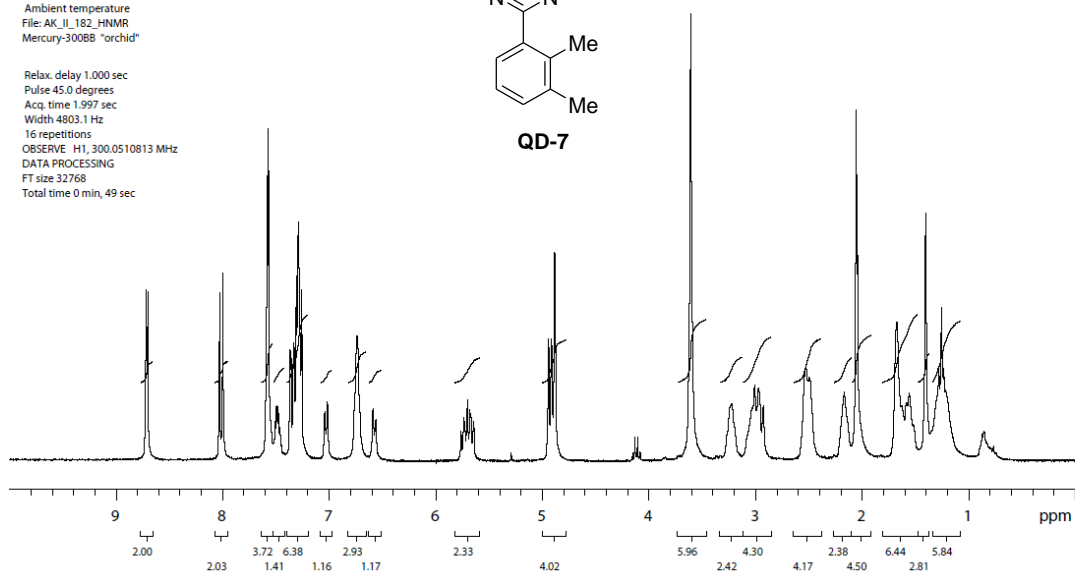
AK_IL_182
HNMR
Archive directory: /export/home/vnmr2/vnmrSYS/data
Sample directory:

Pulse Sequence: s2pul
Solvent: CDCl3
Ambient temperature
File: AK_IL_182_HNMR
Mercury-300BB "orchid"

Relax. delay 1.000 sec
Pulse 45.0 degrees
Acq. time 1.997 sec
Width 4803.1 Hz
16 repetitions
OBSERVE H1, 300.0510813 MHz
DATA PROCESSING
FT size 32768
Total time 0 min, 49 sec



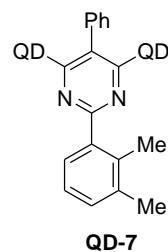
QD-7



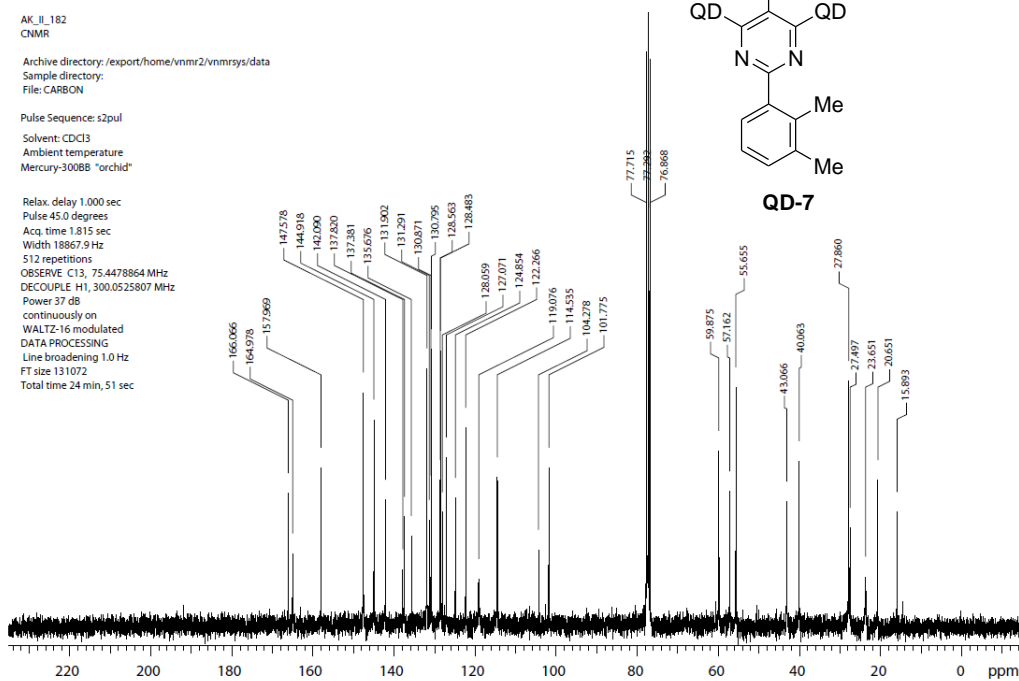
AK_IL_182
CNMR
Archive directory: /export/home/vnmr2/vnmrSYS/data
Sample directory:
File: CARBON

Pulse Sequence: s2pul
Solvent: CDCl3
Ambient temperature
Mercury-300BB "orchid"

Relax. delay 1.000 sec
Pulse 45.0 degrees
Acq. time 1.815 sec
Width 18867.9 Hz
512 repetitions
OBSERVE C13, 75.4478864 MHz
DECOUPLE H1, 300.0525807 MHz
Power 37 db
continuously on
WALTZ-16 modulated
DATA PROCESSING
Line broadening 1.0 Hz
FT size 131072
Total time 24 min, 51 sec



QD-7

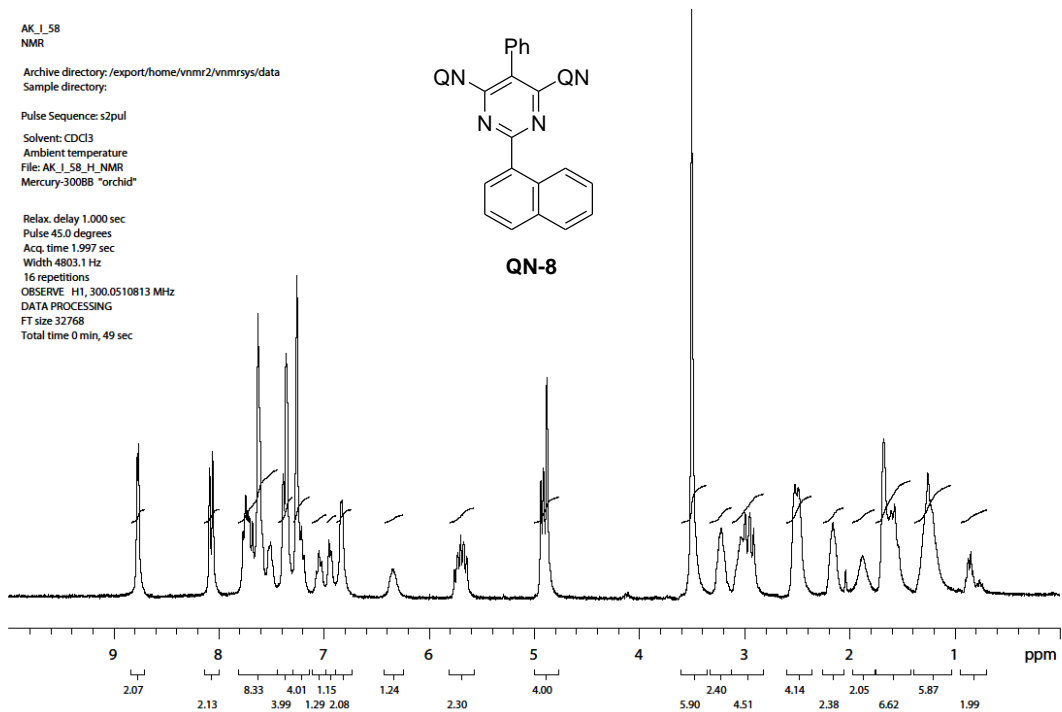
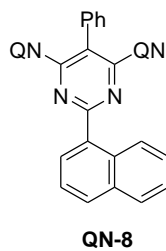


AK_I_58
NMR

Archive directory: /export/home/vnmr2/vnmrsys/data
Sample directory:

Pulse Sequence: s2pul
Solvent: CDCl3
Ambient temperature
File: AK_I_58_H_NMR
Mercury-300BB "orchid"

Relax. delay 1.000 sec
Pulse 45.0 degrees
Acq. time 1.997 sec
Width 4803.1 Hz
16 repetitions
OBSERVE H1, 300.0510813 MHz
DATA PROCESSING
FT size 32768
Total time 0 min, 49 sec

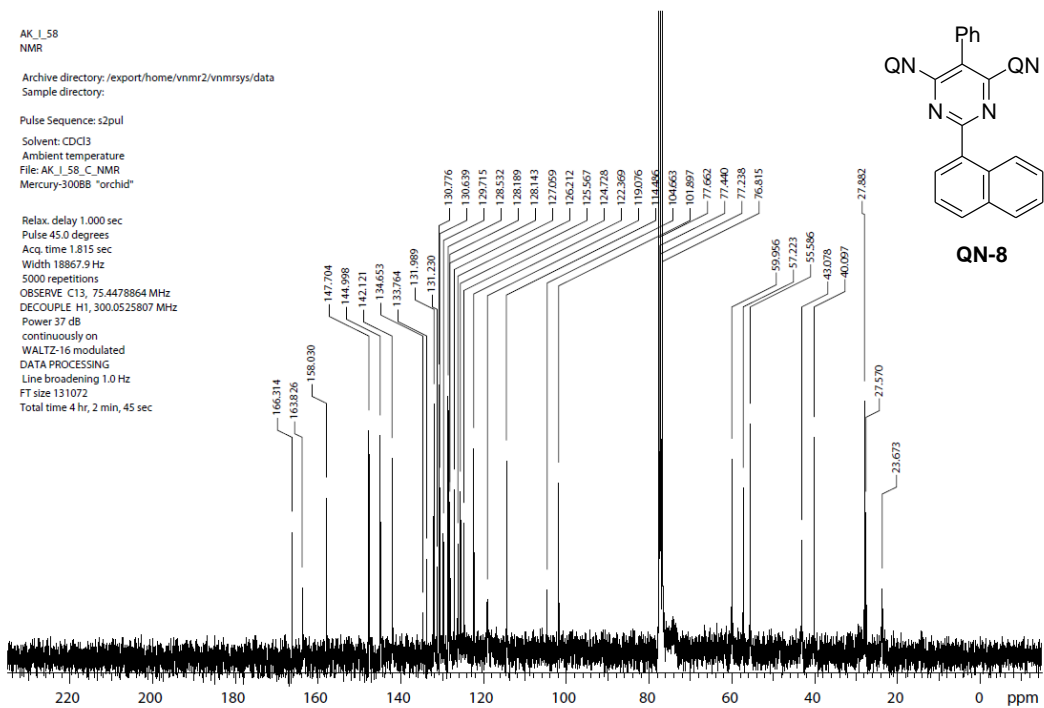
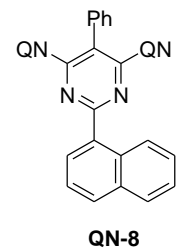


AK_I_58
NMR

Archive directory: /export/home/vnmr2/vnmrsys/data
Sample directory:

Pulse Sequence: s2pul
Solvent: CDCl3
Ambient temperature
File: AK_I_58_C_NMR
Mercury-300BB "orchid"

Relax. delay 1.000 sec
Pulse 45.0 degrees
Acq. time 1.815 sec
Width 18867.9 Hz
5000 repetitions
OBSERVE C13, 75.4478864 MHz
DECOUPLE H1, 300.0525807 MHz
Power 37 dB
continuously on
WALTZ-16 modulated
DATA PROCESSING
Line broadening 1.0 Hz
FT size 131072
Total time 4 hr, 2 min, 45 sec

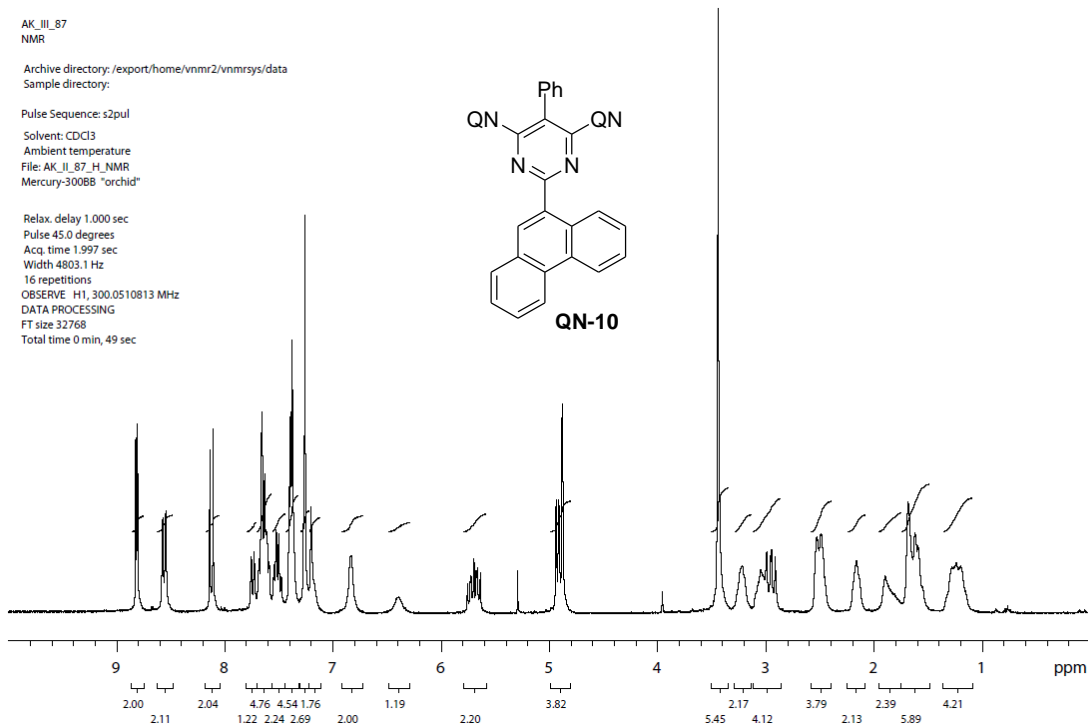
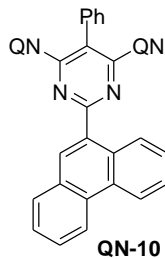


AK_IL_87
NMR

Archive directory: /export/home/vnmr2/vnmrsys/data
Sample directory:

Pulse Sequence: s2pul
Solvent: CDCl3
Ambient temperature
File: AK_IL_87_H_NMR
Mercury-30088 "orchid"

Relax. delay 1.000 sec
Pulse 45.0 degrees
Acq. time 1.997 sec
Width 4803.1 Hz
16 repetitions
OBSERVE H1, 300.0510813 MHz
DATA PROCESSING
FT size 32768
Total time 0 min, 49 sec

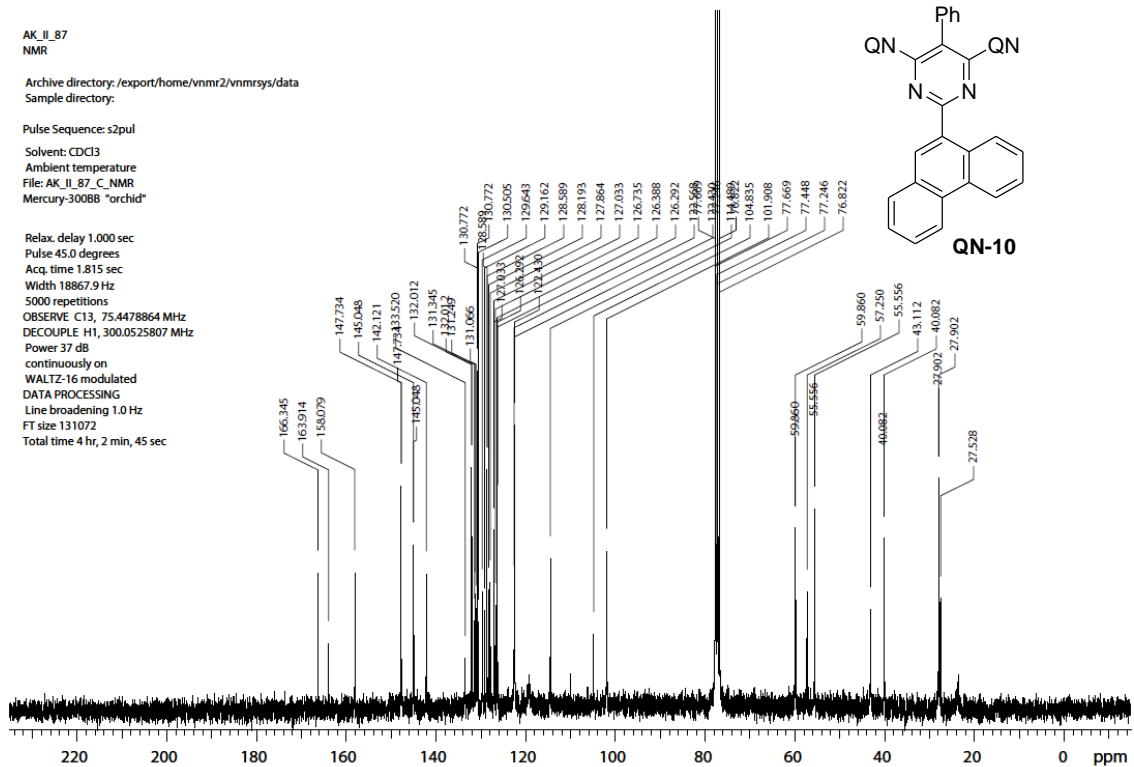
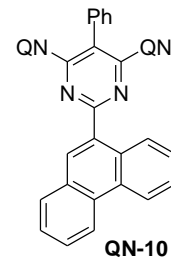


AK_IL_87
NMR

Archive directory: /export/home/vnmr2/vnmrsys/data
Sample directory:

Pulse Sequence: s2pul
Solvent: CDCl3
Ambient temperature
File: AK_IL_87_C_NMR
Mercury-30088 "orchid"

Relax. delay 1.000 sec
Pulse 45.0 degrees
Acq. time 1.815 sec
Width 18867.9 Hz
5000 repetitions
OBSERVE C13, 75.4478864 MHz
DECOUPLE H1, 300.0525807 MHz
Power 37 dB
continuously on
WALTZ-16 modulated
DATA PROCESSING
Line broadening 1.0 Hz
FT size 131072
Total time 4 hr, 2 min, 45 sec

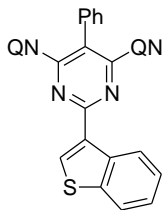


AK_IL_194
HNMR

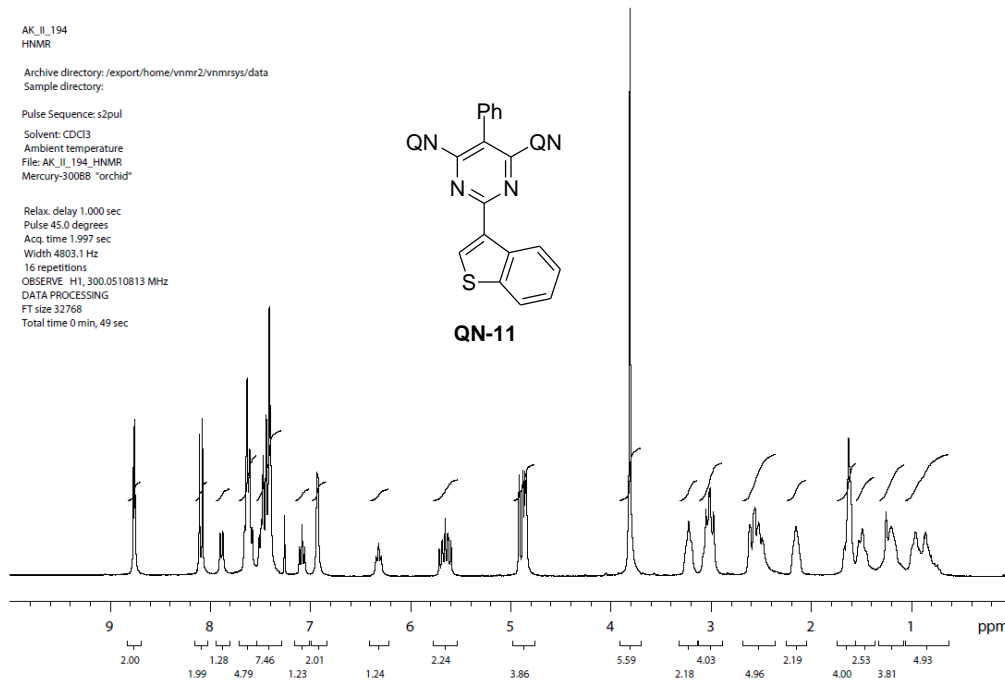
Archive directory: /export/home/vnmr2/vnmrsys/data
Sample directory:

Pulse Sequence: s2pul
Solvent: CDCl3
Ambient temperature
File: AK_IL_194_HNMR
Mercury-300BB "orchid"

Relax. delay 1.000 sec
Pulse 45.0 degrees
Acq. time 1.997 sec
Width 4803.1 Hz
16 repetitions
OBSERVE H1, 300.0510813 MHz
DATA PROCESSING
FT size 32768
Total time 0 min, 49 sec



QN-11

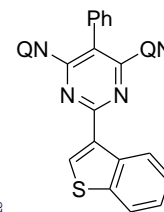


AK_IL_194
CNMR

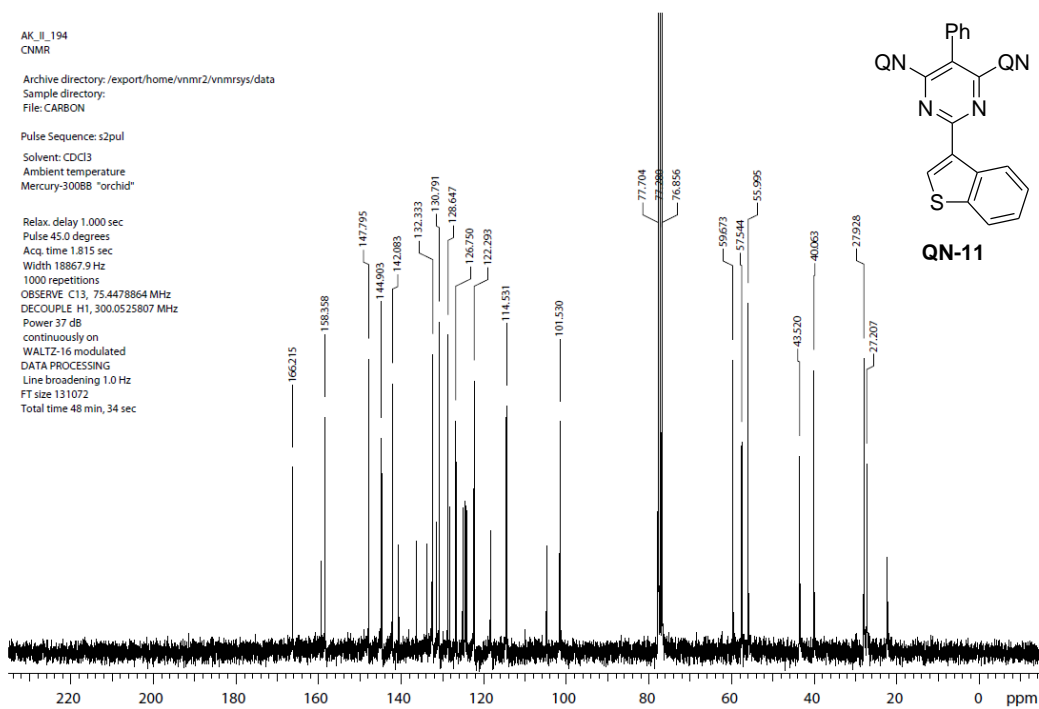
Archive directory: /export/home/vnmr2/vnmrsys/data
Sample directory:
File: CARBON

Pulse Sequence: s2pul
Solvent: CDCl3
Ambient temperature
Mercury-300BB "orchid"

Relax. delay 1.000 sec
Pulse 45.0 degrees
Acq. time 1.815 sec
Width 18867.9 Hz
1000 repetitions
OBSERVE C13, 75.4478864 MHz
DECOUPLE H1, 300.0525807 MHz
Power 37 dB
continuously on
WALTZ-16 modulated
DATA PROCESSING
Line broadening 1.0 Hz
FT size 131072
Total time 48 min, 34 sec

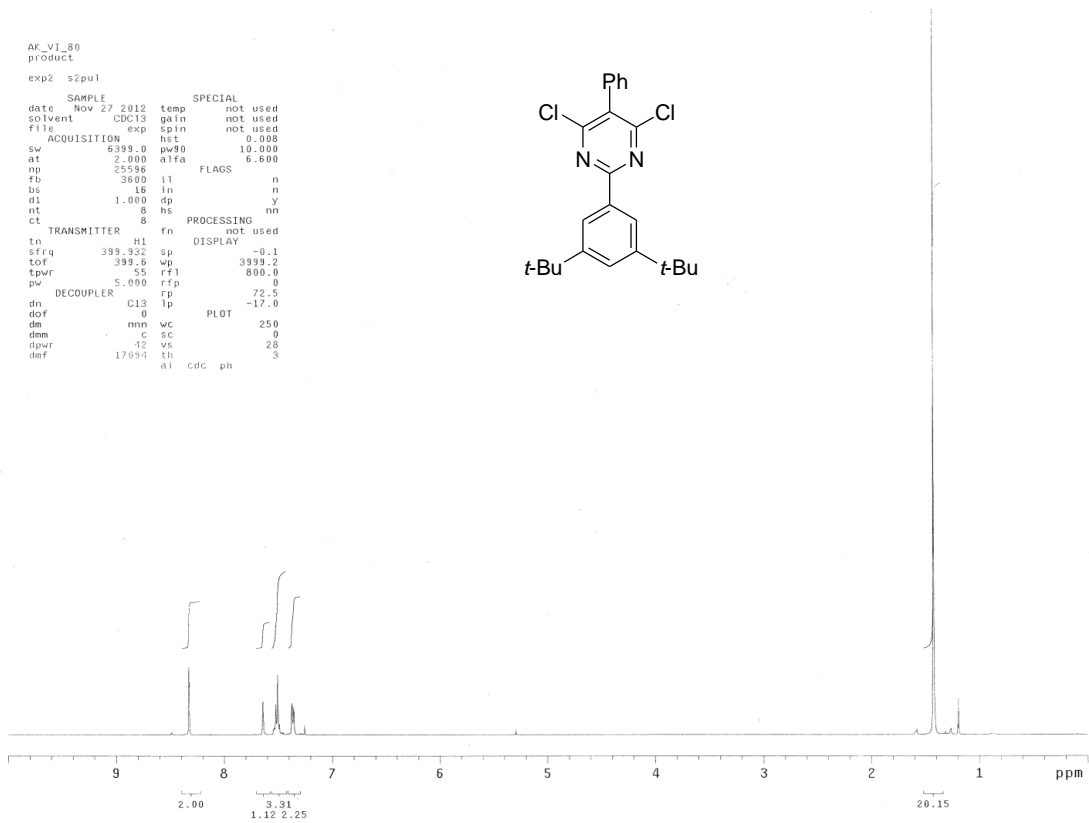
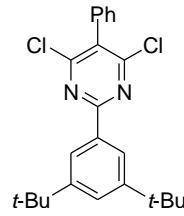


QN-11



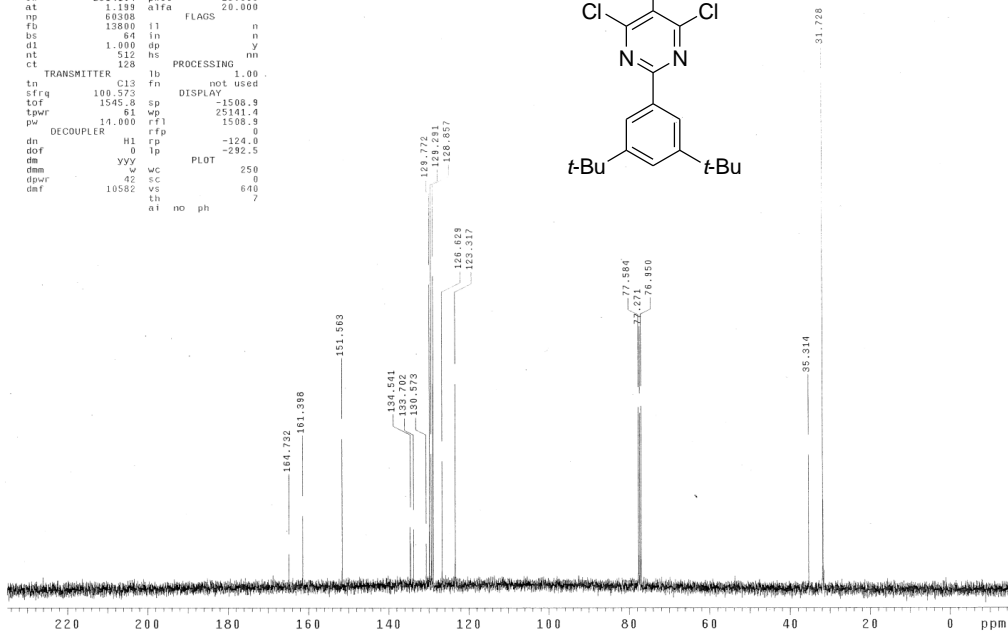
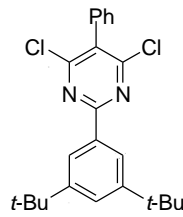
AK_VI_80
product
exp2 s2pu1

SAMPLE		SPECIAL	
date	Nov 27 2012	temp	not used
solvent	CDC13	gain	not used
file	exp	spin	not used
ACQUISITION		hst	0.008
sw	6399.0	pw90	10.000
at	2.000	afqa	6.600
np	25596	FLAGS	n
fb	3600	il	n
bs	18	in	n
d1	1.000	dp	y
nt	8	hs	nn
ct	8	PROCESSING	not used
tn	H1	fn	DISPLAY
sfrq	399.932	sp	-0.1
tof	399.6	wp	3999.2
tpwr	55	rfl	800.0
pw	5.000	rfp	0
DECOUPLER		rp	-72.5
dn	C13	lp	-17.0
dof	0	PLOT	250
dm	mm	wc	0
dmm	42	sc	0
dpwr	42	vs	28
def	17097	th	3
	al	cdc	ph



AK_VI_80
product
exp2 s2pu1

SAMPLE		SPECIAL	
date	Nov 27 2012	temp	not used
solvent	CDC13	gain	not used
file	exp	spin	not used
ACQUISITION		hst	0.008
sw	25141.4	pw90	28.000
at	1.199	afqa	20.000
np	60308	FLAGS	n
fb	13800	il	n
bs	64	in	n
d1	1.000	dp	y
nt	512	hs	nn
ct	128	PROCESSING	1.00
tn	C13	fn	DISPLAY
sfrq	100.573	sp	-1508.9
tof	1545.8	wp	25141.4
tpwr	61	rfl	1508.9
pw	14.000	rfp	0
dn	H1	lp	-124.0
dof	0	PLOT	-292.5
dm	yyy	wc	250
dmm	42	sc	0
dpwr	10502	vs	640
def		th	7
	al	no	ph



AK_IJ_24
NMR

Archive directory: /export/home/vnmr2/vnmrSYS/data
Sample directory:

Pulse Sequence: s2pul

Solvent: CDCl3

Ambient temperature

File: AK_IJ_23_H_NMR

Mercury-300BB "orchid"

Relax. delay 1.000 sec

Pulse 45.0 degrees

Acq. time 1.997 sec

Width 4803.1 Hz

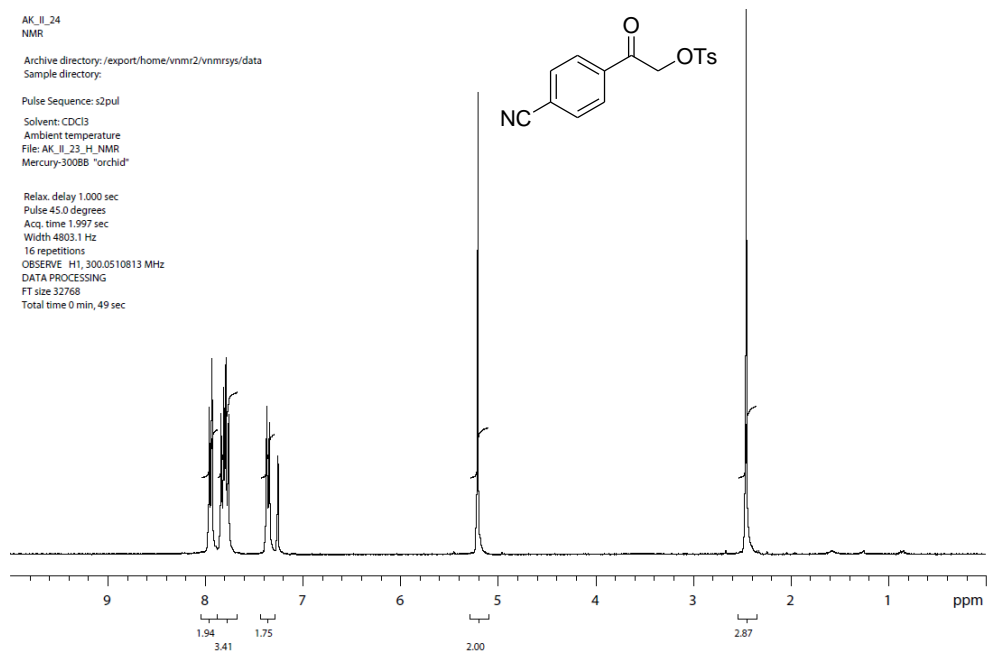
16 repetitions

OBSERVE H1, 300.0510813 MHz

DATA PROCESSING

FT size 32768

Total time 0 min, 49 sec



AK_IJ_24
NMR

Archive directory: /export/home/vnmr2/vnmrSYS/data
Sample directory:

Pulse Sequence: s2pul

Solvent: CDCl3

Ambient temperature

File: AK_IJ_23_C_NMR

Mercury-300BB "orchid"

Relax. delay 1.000 sec

Pulse 45.0 degrees

Acq. time 1.815 sec

Width 18867.9 Hz

1000 repetitions

OBSERVE C13, 75.4478864 MHz

DECOUPLE H1, 300.0525807 MHz

Power 37 dB

continuously on

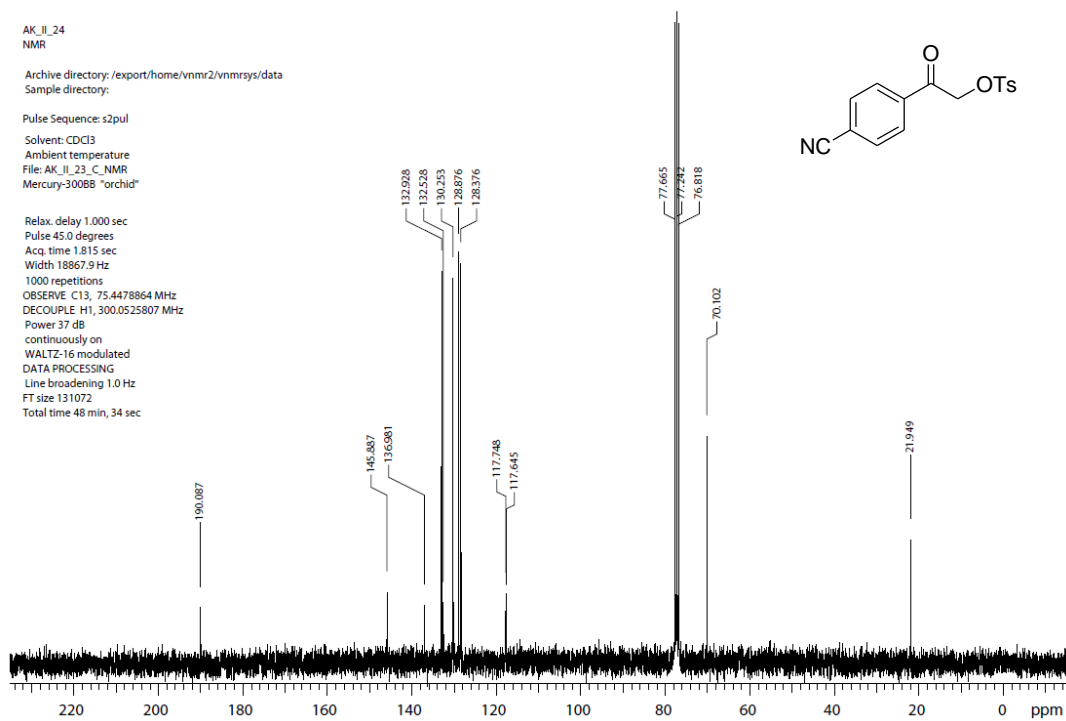
WALTZ-16 modulated

DATA PROCESSING

Line broadening 1.0 Hz

FT size 131072

Total time 48 min, 34 sec



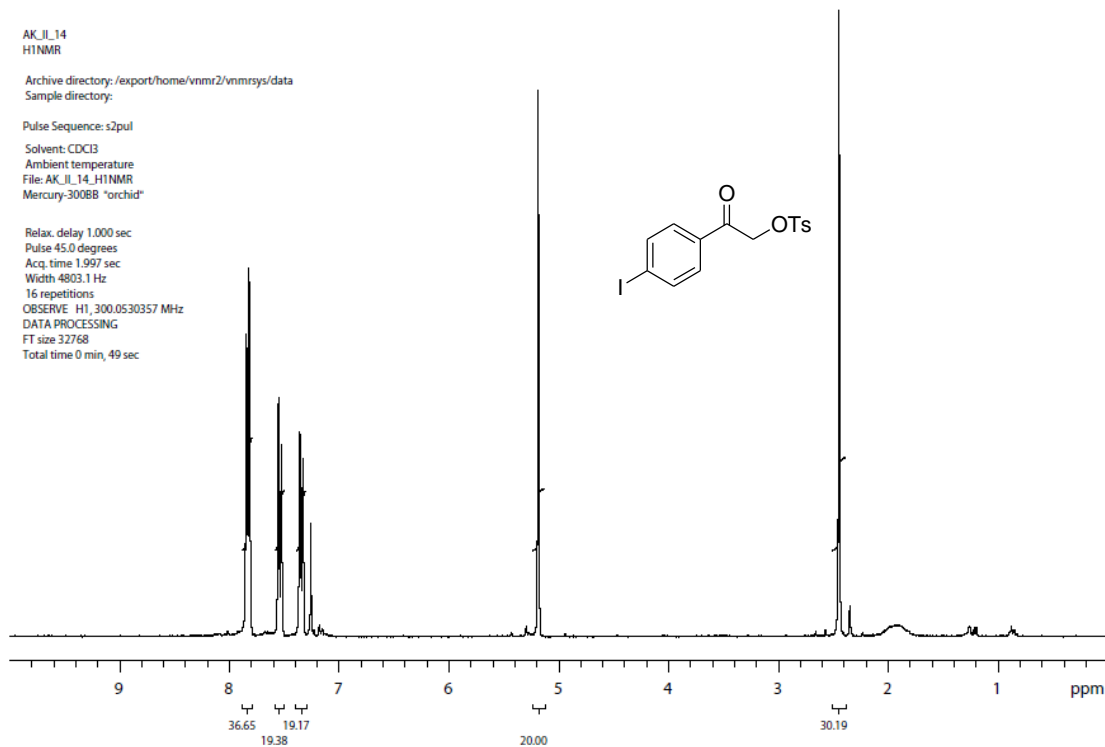
AK_IL_14
H1NMR

Archive directory: /export/home/vnmr2/vnmrsys/data
Sample directory:

Pulse Sequence: s2pul

Solvent: CDCl3
Ambient temperature
File: AK_IL_14_H1NMR
Mercury-300BB "orchid"

Relax, delay 1.000 sec
Pulse 45.0 degrees
Acq, time 1.997 sec
Width 4803.1 Hz
16 repetitions
OBSERVE H1, 300.0530357 MHz
DATA PROCESSING
FT size 32768
Total time 0 min, 49 sec



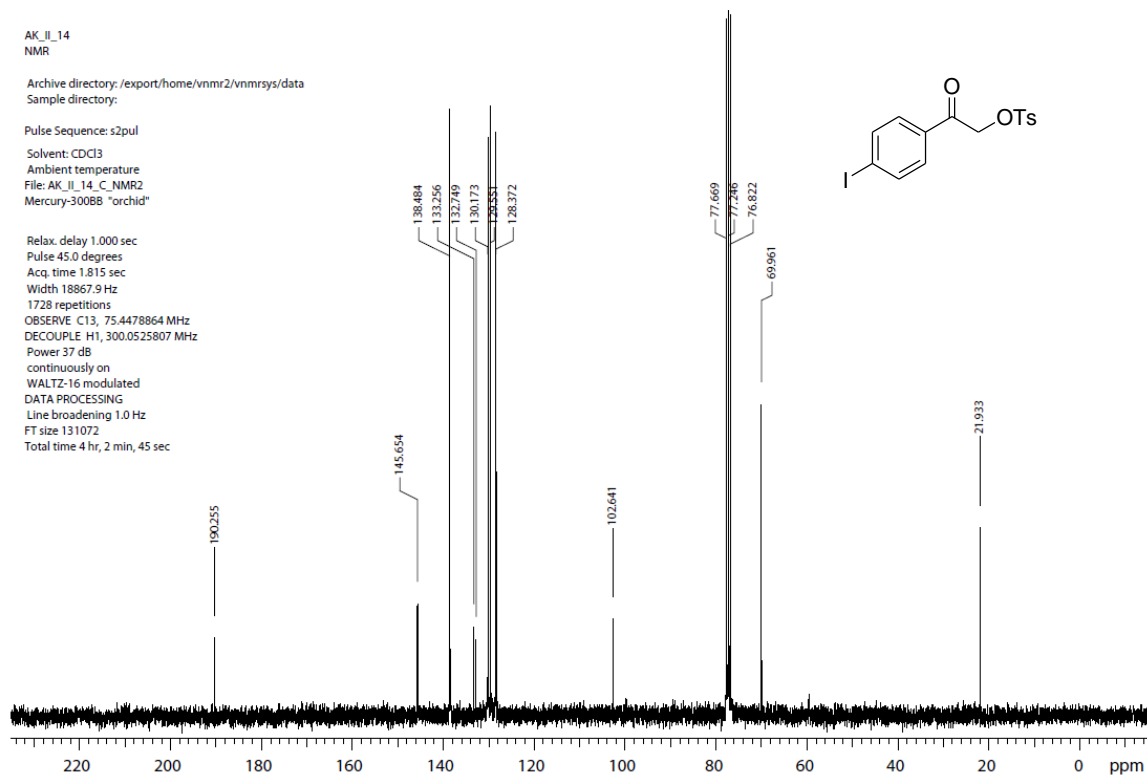
AK_IL_14
NMR

Archive directory: /export/home/vnmr2/vnmrsys/data
Sample directory:

Pulse Sequence: s2pul

Solvent: CDCl3
Ambient temperature
File: AK_IL_14_C_NMR2
Mercury-300BB "orchid"

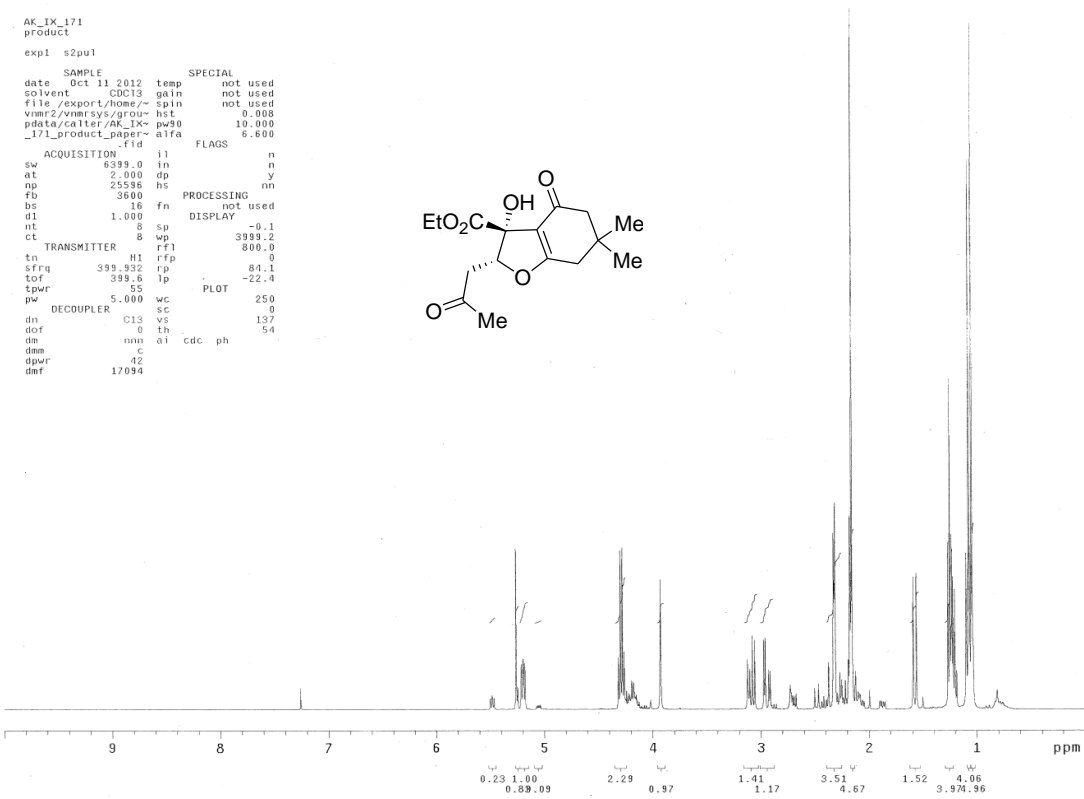
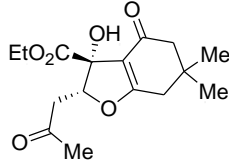
Relax, delay 1.000 sec
Pulse 45.0 degrees
Acq, time 1.815 sec
Width 18867.9 Hz
1728 repetitions
OBSERVE C13, 75.4478864 MHz
DECOUPLE H1, 300.0525807 MHz
Power 37 dB
continuously on
WALTZ-16 modulated
DATA PROCESSING
Line broadening 1.0 Hz
FT size 131072
Total time 4 hr, 2 min, 45 sec



AK_IX_171
product

expl s2pu1

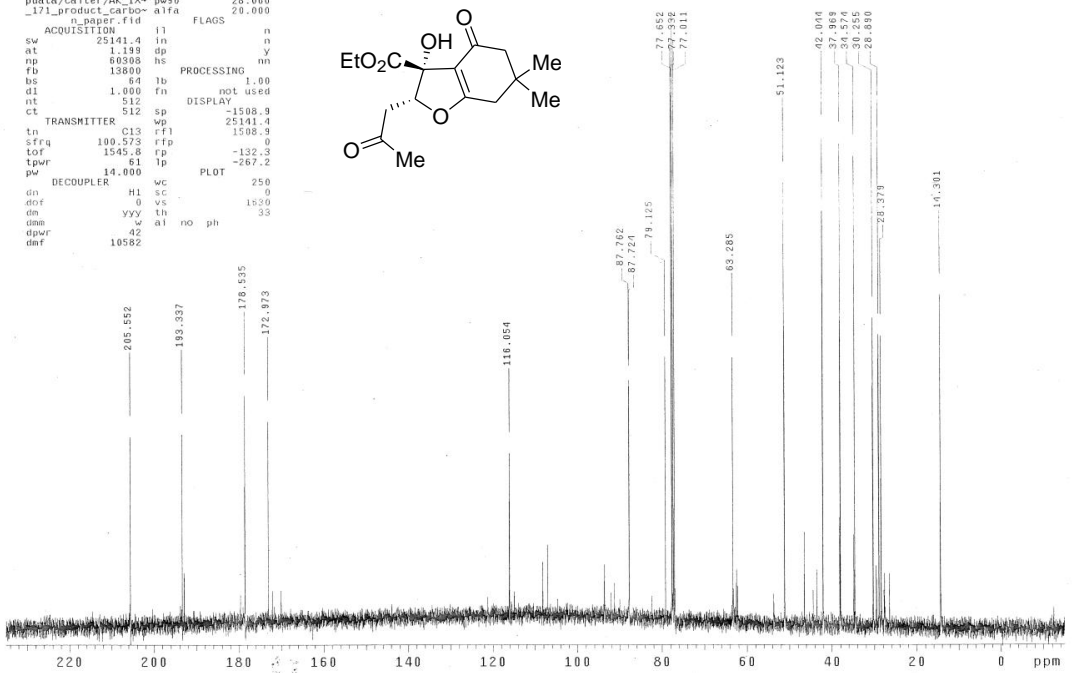
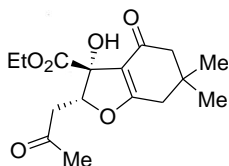
SAMPLE		SPECIAL	
date	Oct 11 2012	temp	not used
solvent	CDCl3	gain	not used
file	/export/home/~	spin	not used
vnmr2/vnmr.sys/grou	hst	hst	0.008
pdata/calter/ak_ix	pw90	pw90	10.000
_171_product_paper	alfa	alfa	6.600
ACQUISITION		flags	n
sw	6339.0	in	n
at	2.000	dp	y
np	25986	hs	nn
fb	3800	PROCESSING	nn
bs	18	fn	not used
d1	1.000	DISPLAY	-0.1
nt	8	sp	0
ct	8	wp	3999.2
TRANSMITTER		rfl	800.0
tn	H1	rfl	0
sfrq	399.932	rp	84.1
tof	399.6	lp	-22.4
tpwr	55	PLOT	
pw	5.000	wc	250
DECOUPLER		sc	0
dn	C13	vc	137
dof	0	th	54
dsm	mm	ai	cdc ph
dpwr	42		
dmf	17094		



AK_IX_171
product

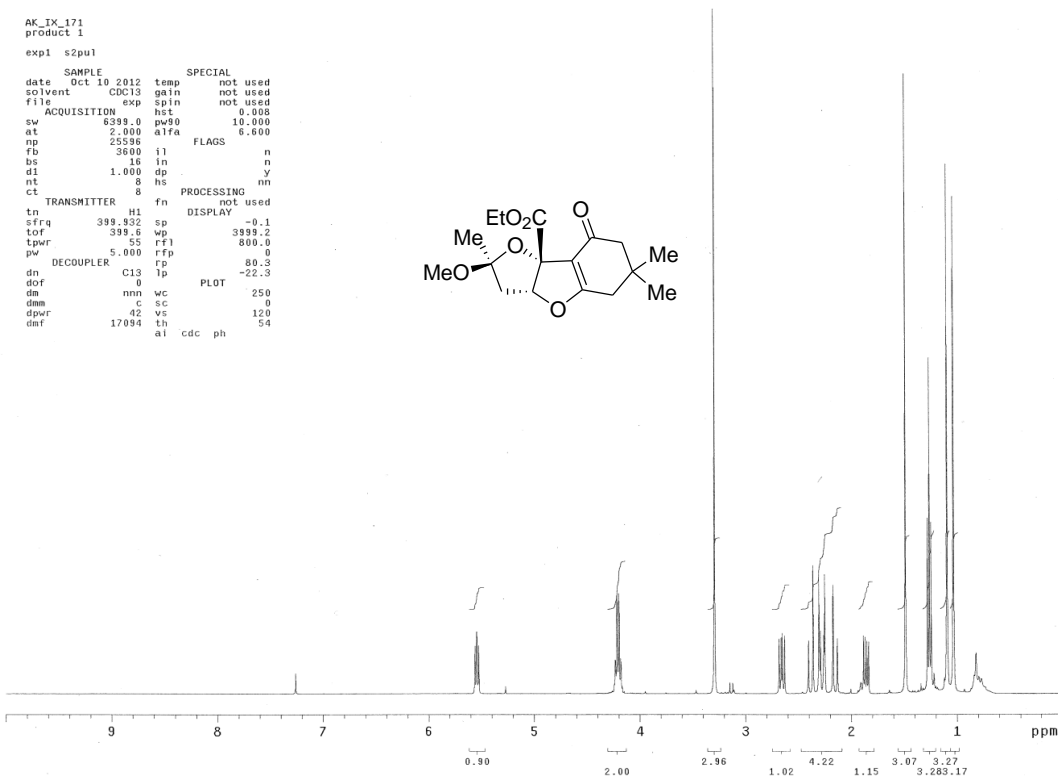
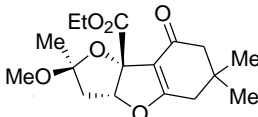
expl s2pu1

SAMPLE		SPECIAL	
date	Oct 11 2012	temp	not used
solvent	CDCl3	gain	not used
file	/export/home/~	spin	not used
vnmr2/vnmr.sys/grou	hst	hst	0.008
pdata/calter/ak_ix	pw90	pw90	28.000
_171_product_carbon	alfa	alfa	20.000
n_paper_fid	fid	flags	n
sw	25141.4	in	n
at	1.193	dp	y
np	60308	hs	nn
fb	13800	PROCESSING	nn
bs	84	tb	1.00
d1	1.000	fn	not used
nt	512	DISPLAY	not used
ct	512	sp	-1508.9
TRANSMITTER		wp	25141.4
tn	C13	rfl	1508.9
sfrq	100.573	rfl	0
tof	1545.8	rp	-132.8
tpwr	61	lp	-267.2
pw	14.000	PLOT	
DECOUPLER		wc	250
dn	H1	sc	0
dof	0	vs	1830
dsm	w	ai	no ph
dpwr	42		
dmf	10582		



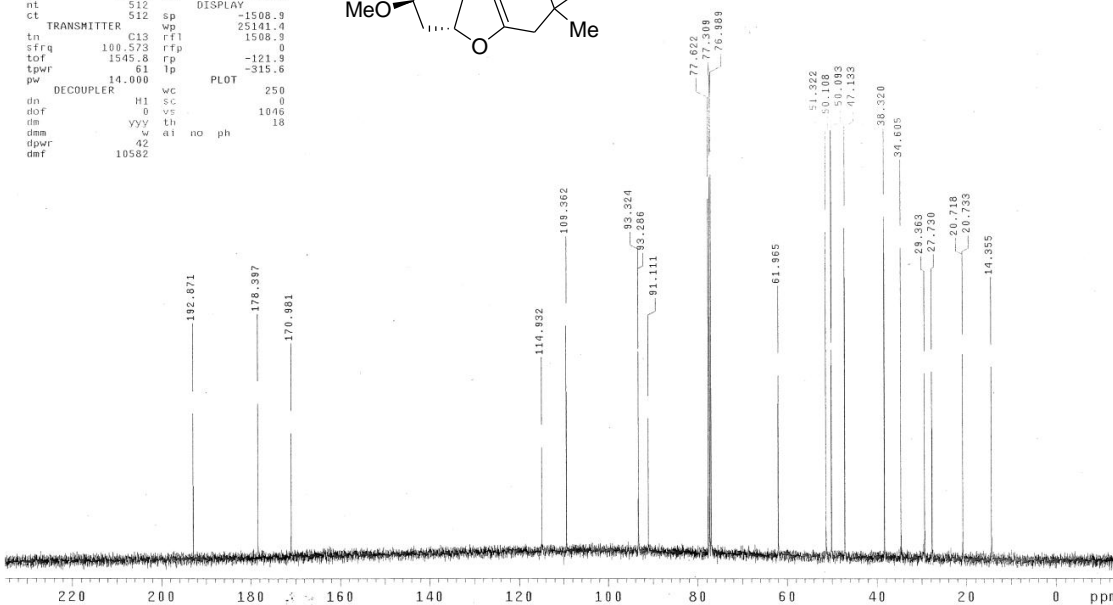
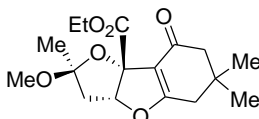
AK_IX_171
product 1
exp1 s2pul

SAMPLE		SPECIAL	
date	Oct 10 2012	temp	not used
solvent	CDCl3	gain	not used
file	exp	spin	not used
ACQUISITION		hst	0.008
sw	6399.0	pw90	10.000
at	2.000	alfa	8.800
np	25596	FLAGS	
fb	3600	il	n
bs	16	in	n
d1	1.000	dp	y
nt	8	hs	nm
ct	8	fn	not used
tn	H1	DISPLAY	-0.1
sfrq	399.932	sp	3999.2
tof	399.6	wp	800.0
tpwr	55	rfl	0
pw	5.000	rfp	80.3
DECOUPLER		lp	-22.3
dn	C13	lp	
dof	0	wc	250
dmm	nnn	sc	0
dpr	42	vs	120
dmf	17094	th	54
	ai	cdc	ph



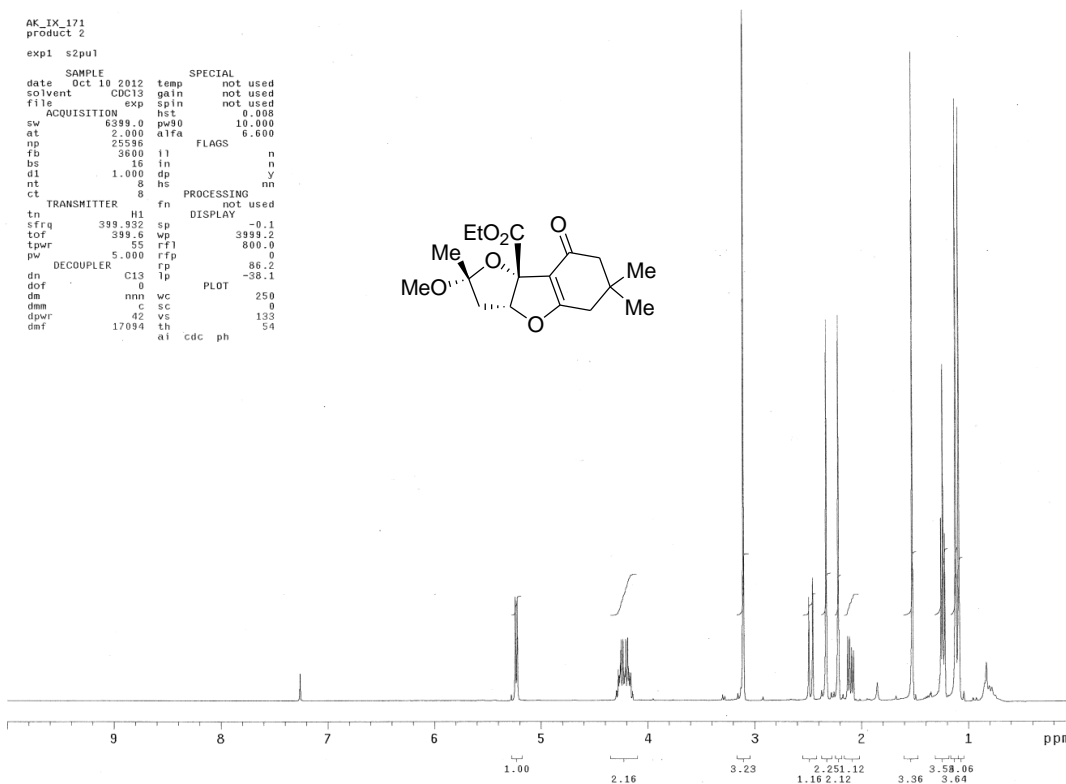
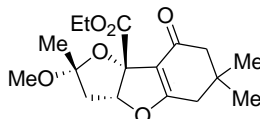
AK_IX_171
product 1
exp1 s2pul

SAMPLE		SPECIAL	
date	Oct 10 2012	temp	not used
solvent	CDCl3	gain	not used
file	export/home/~	spin	not used
vnmr2/vnmrsys/grou	-	hst	0.008
pdata/caliter/AK_IX	-	pw90	28.000
_171_product1_carb	-	alfa	20.000
on_fid		FLAGS	
ACQUISITION	il	n	
sw	25141.4	in	n
at	1.199	dp	y
np	60308	hs	nm
fb	13900		
bs	64	tb	1.00
d1	1.000	fn	not used
nt	512	DISPLAY	-1508.9
ct	512	sp	25141.4
tn	C13	rfl	1508.9
sfrq	100.573	rfp	0
tof	1545.8	rp	-121.9
tpwr	61	lp	-315.6
pw	14.000		
DECOUPLER		wc	250
dn	H1	sc	0
dof	0	vs	1046
dmm	yyy	th	18
dpr	42	ai	no
dmf	10582	ph	



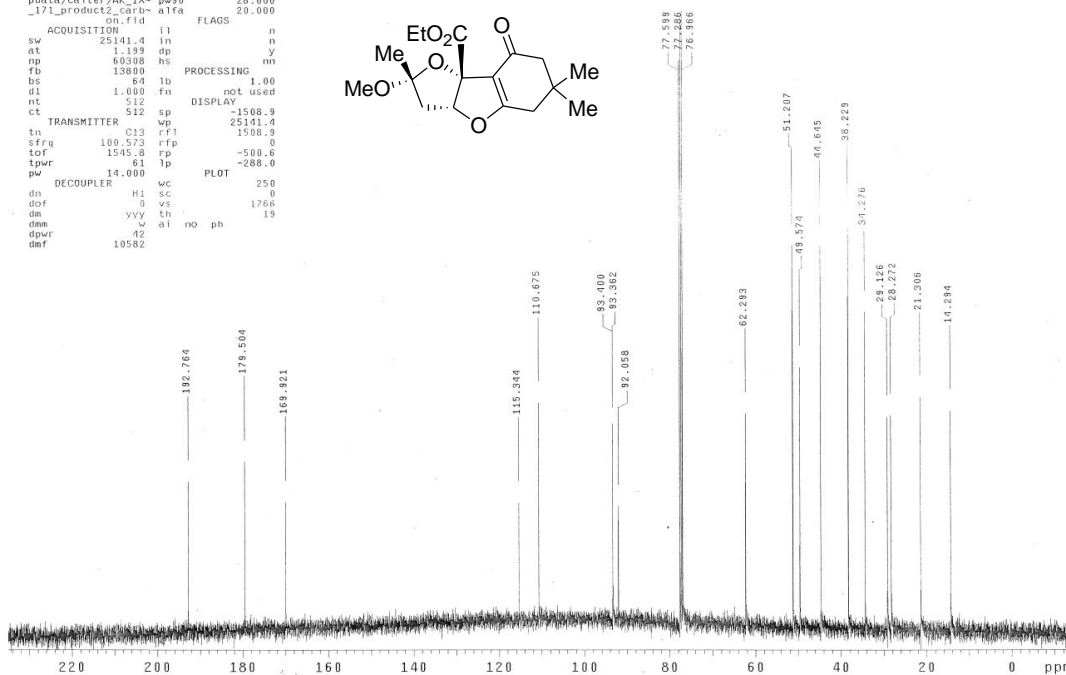
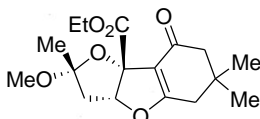
AK_IX_171
product 2
expl s2pul

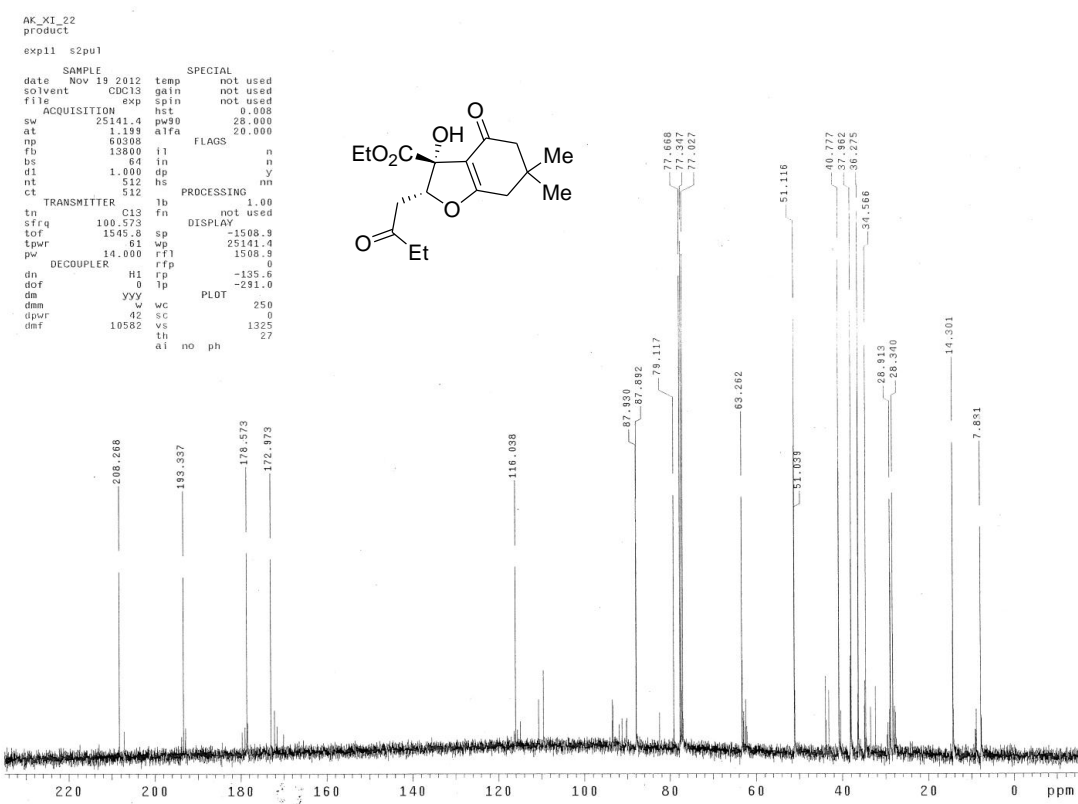
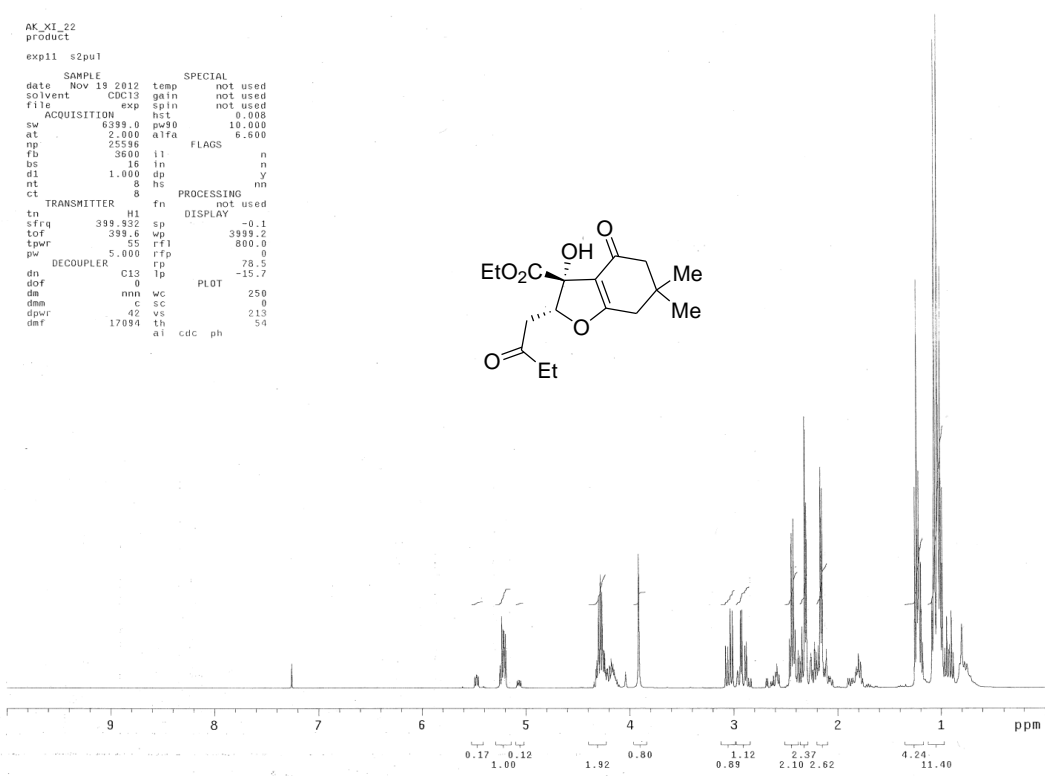
```
SAMPLE SPECIAL
date Oct 10 2012 temp not used
solvent CDCl3 gain not used
file /export/home/~ spin not used
vmer2/vmer3/grou hst 0.008
pddata/calter/AR_IX~ pw90 28.000
_171_product2_Carb~ alfa 20.000
ACQUISITION il
sw 25141.4 in n
at 1.139 dp y
np 60308 hs nn
fb 13300 sc
bs 64 lb 1.00
d1 1.000 fn not used
nt 512 sp DISPLAY -1508.9
ct 512 sp DISPLAY -1508.9
TRANSMITTER C13 rft 1508.9
tn 100.573 rfp 0
sfrq 1545.8 rp -500.0
tof 61 lp -288.0
tpwr 14.000 PLOT 250
DECOUPLER H1 sc 0
dof 0 vs 1766
dm yyy th 15
dms w al no ph
dpwr 42
dntf 10582
```



AK_IX_171
product 2
expl s2pul

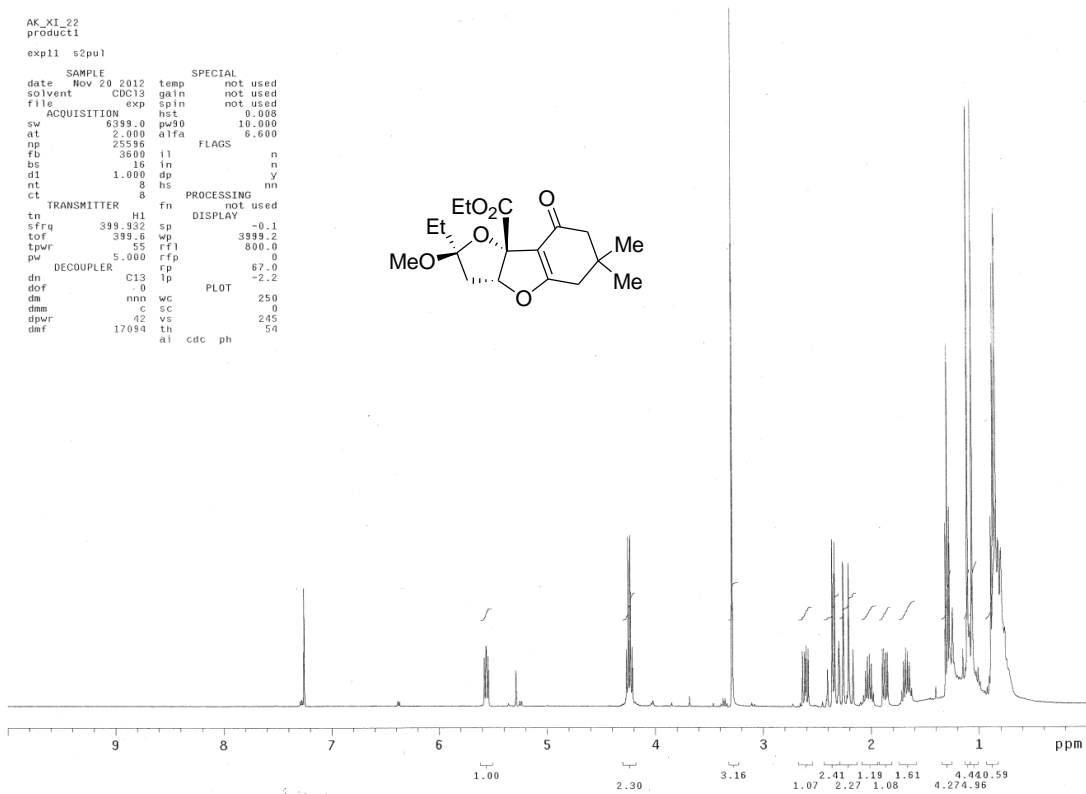
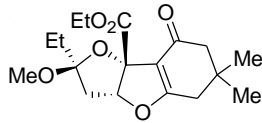
```
SAMPLE SPECIAL
date Oct 10 2012 temp not used
solvent CDCl3 gain not used
file /export/home/~ spin not used
vmer2/vmer3/grou hst 0.008
pddata/calter/AR_IX~ pw90 28.000
_171_product2_Carb~ alfa 20.000
ACQUISITION il
sw 25141.4 in n
at 1.139 dp y
np 60308 hs nn
fb 13300 sc
bs 64 lb 1.00
d1 1.000 fn not used
nt 512 sp DISPLAY -1508.9
ct 512 sp DISPLAY -1508.9
TRANSMITTER C13 rft 1508.9
tn 100.573 rfp 0
sfrq 1545.8 rp -500.0
tof 61 lp -288.0
tpwr 14.000 PLOT 250
DECOUPLER H1 sc 0
dof 0 vs 1766
dm yyy th 15
dms w al no ph
dpwr 42
dntf 10582
```





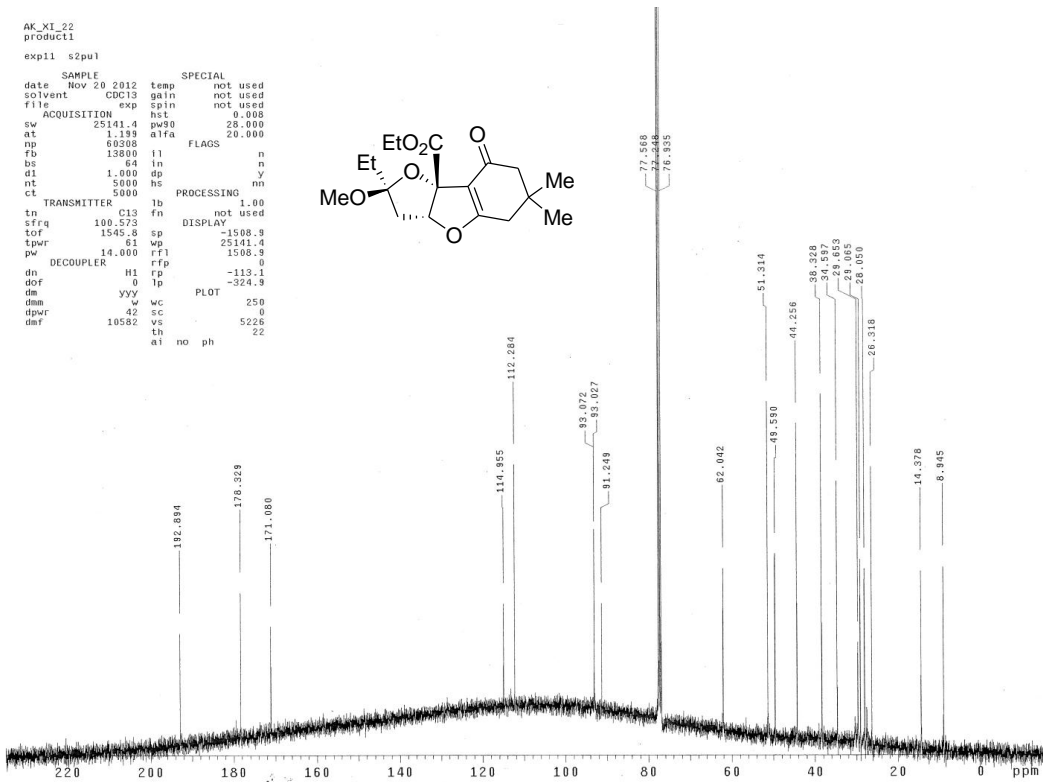
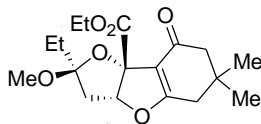
AK_XI_22
product1
exp11 s2pul

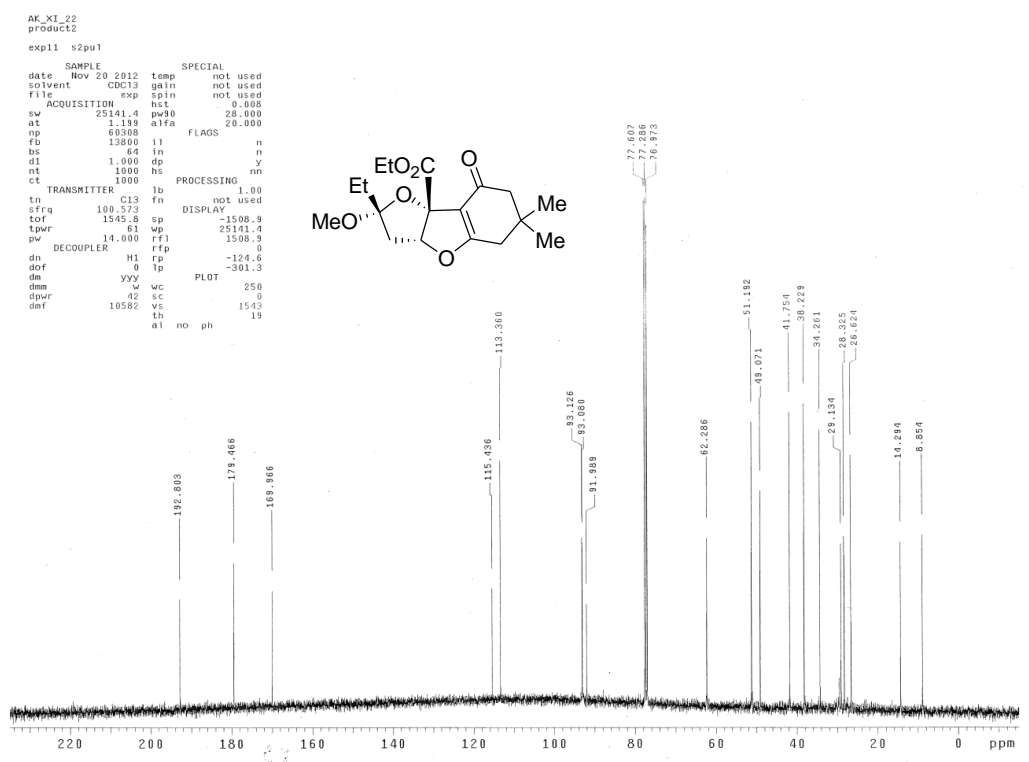
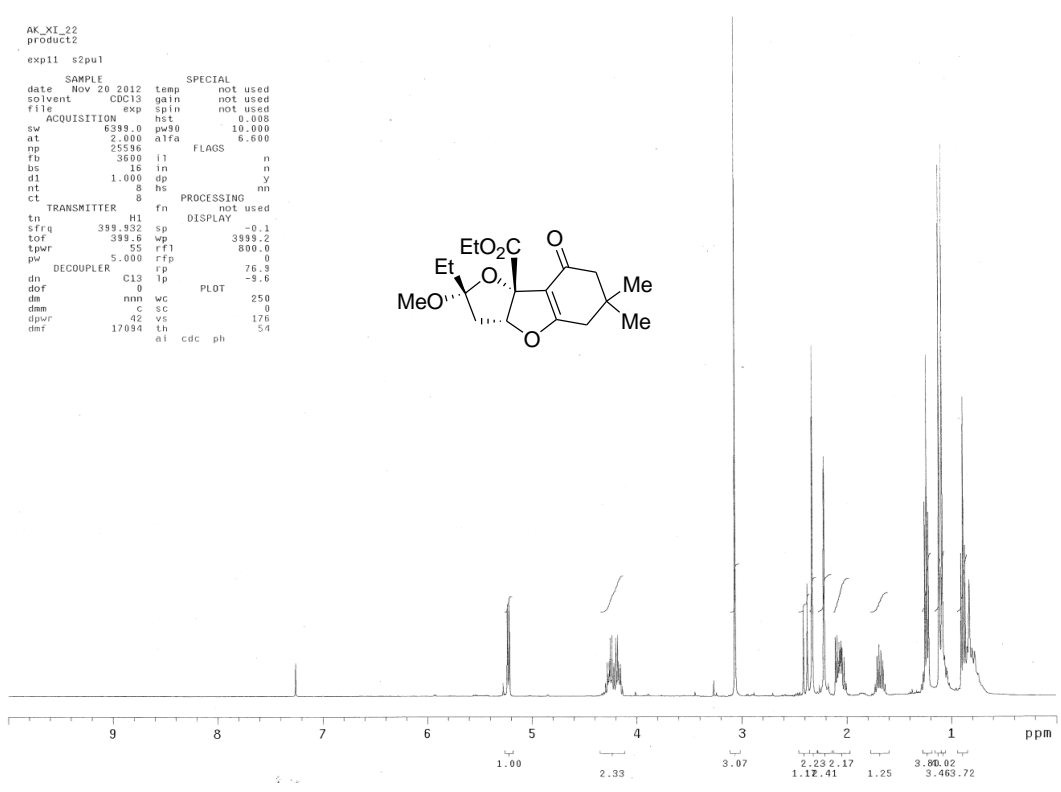
date	Nov 20 2012	temp	not used	SPECIAL
solvent	CDC13	gain	not used	
file	exp	spin	not used	
ACQUISITION	exp	hst	0.008	
sw	6399.0	pu90	10.000	
at	2.000	alfa	6.600	
np	25396	FLAGS		
fb	3600	il	n	
bs	16	in	n	
d1	1.000	dp	y	
nt	8	hs	nn	
ct	8	PROCESSING	nn	
TRANSMITTER	fn	not used		
tn	H1	DISPLAY		
effe	399.952	sp	-0.1	
tof	399.6	wp	3999.2	
tpwr	55	rfl	800.0	
pw	5.000	rfg	0	
DECOUPLER	C13	rp	67.0	
dn	0	lp	-2.2	
dof	0	PLOT		
dm	nnn	wc	250	
dmm	c	sc	0	
dpwr	42	vs	245	
dmf	17094	th	54	
	ai	cdc	ph	



AK_XI_22
product1
exp11 s2pul

date	Nov 20 2012	temp	not used	SPECIAL
solvent	CDC13	gain	not used	
file	exp	spin	not used	
ACQUISITION	exp	hst	0.008	
sw	25141.4	pu90	28.000	
at	1.193	alfa	20.000	
np	60308	FLAGS		
fb	13800	il	n	
bs	64	in	n	
d1	1.000	dp	y	
nt	5000	hs	nn	
ct	5000	PROCESSING	1.00	
TRANSMITTER	fb	not used		
tn	C13	fn	not used	
effe	100.573	sp	-1508.9	
tof	1545.8	wp	25141.4	
tpwr	61	rfl	1506.9	
pw	14.000	rfg	0	
DECOUPLER	H1	rp	-113.1	
dn	0	lp	-324.9	
dof	0	PLOT		
dm	yyy	wc	250	
dmm	w	sc	0	
dpwr	42	vs	5226	
dmf	10582	sh	22	
	ai	no	ph	

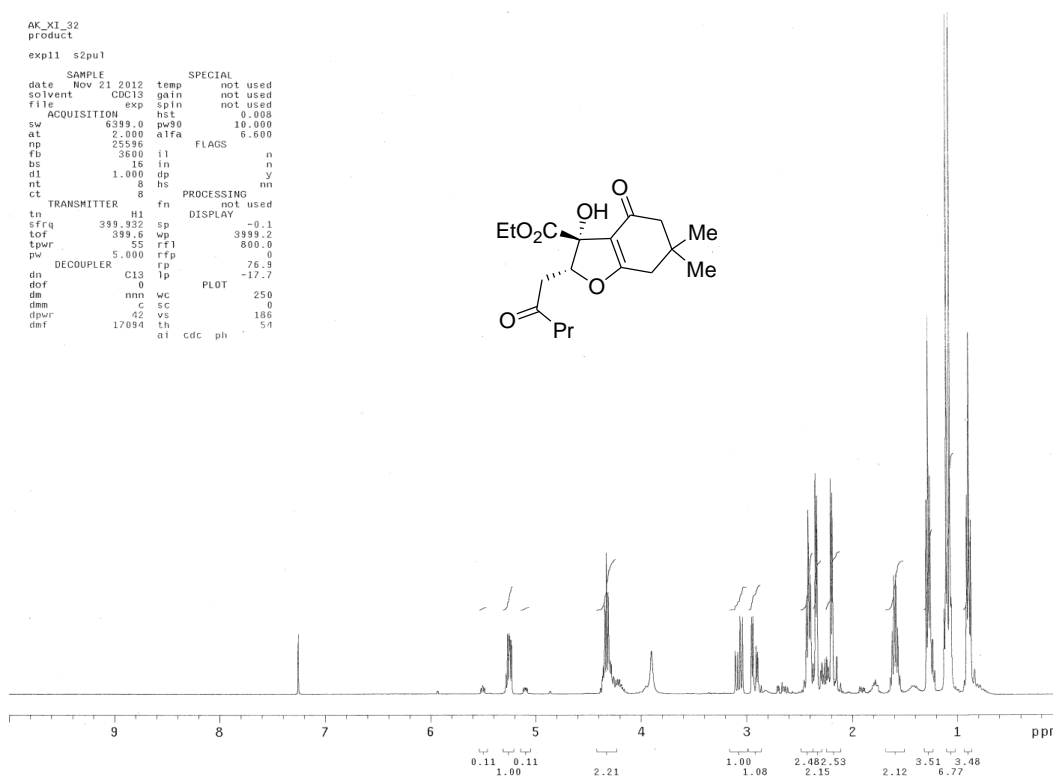
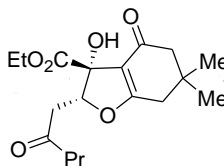




```

AK_XI_32
product
exp11 s2pu1
SAMPLE
date Nov 21 2012 temp not used
solvent CDCl3 gain not used
file exp spin not used
ACQUISITION hst 0.008
sw 6399.0 pw90 10.000
at 2.000 alfa 6.600
np 25596 FLAGS
fb 3600 il n
bs 16 in n
d1 1.000 dp y
nt 8 hs nn
ct 8
TRANSMITTER fn not used
tn H1 DISPLAY
sfrq 399.932 sp -0.1
tof 399.6 wp 3999.2
tpwr 55 rf1 800.0
pw 5.000 rfp 0
DECOUPLER rp 76.9
dn C13 lp -17.7
dof 0 PLOT
dm nnn wc 250
dmm c sc 0
dpwr 42 vs 186
dmf 17094 th ai cdc ph 54

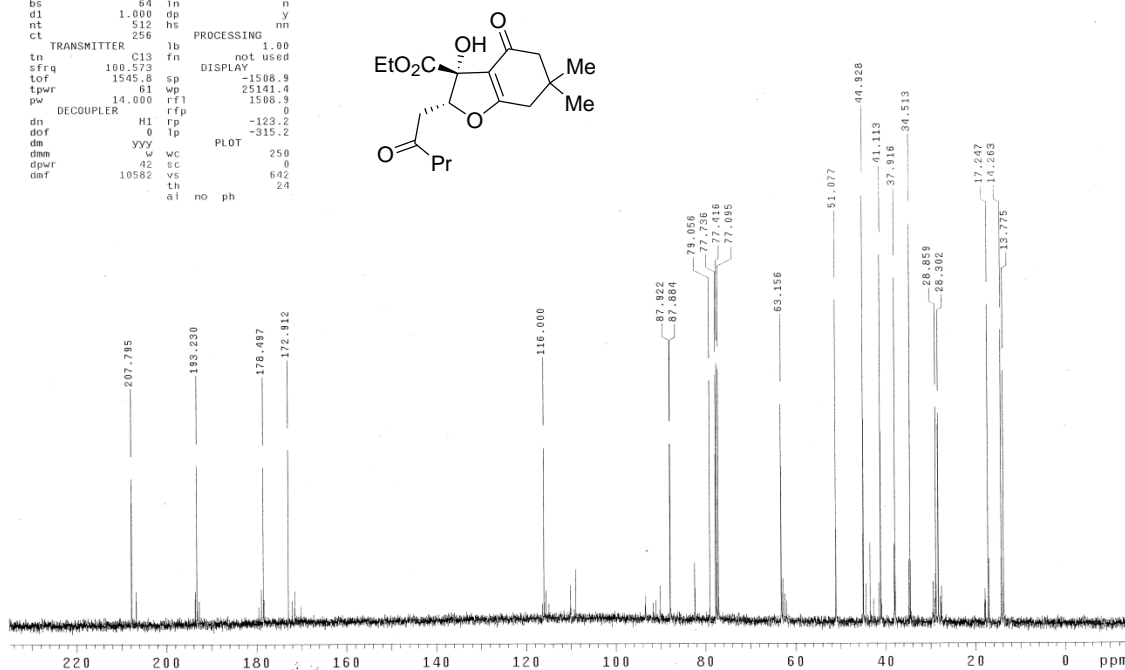
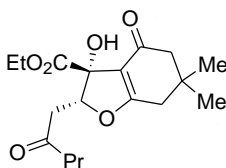
```



```

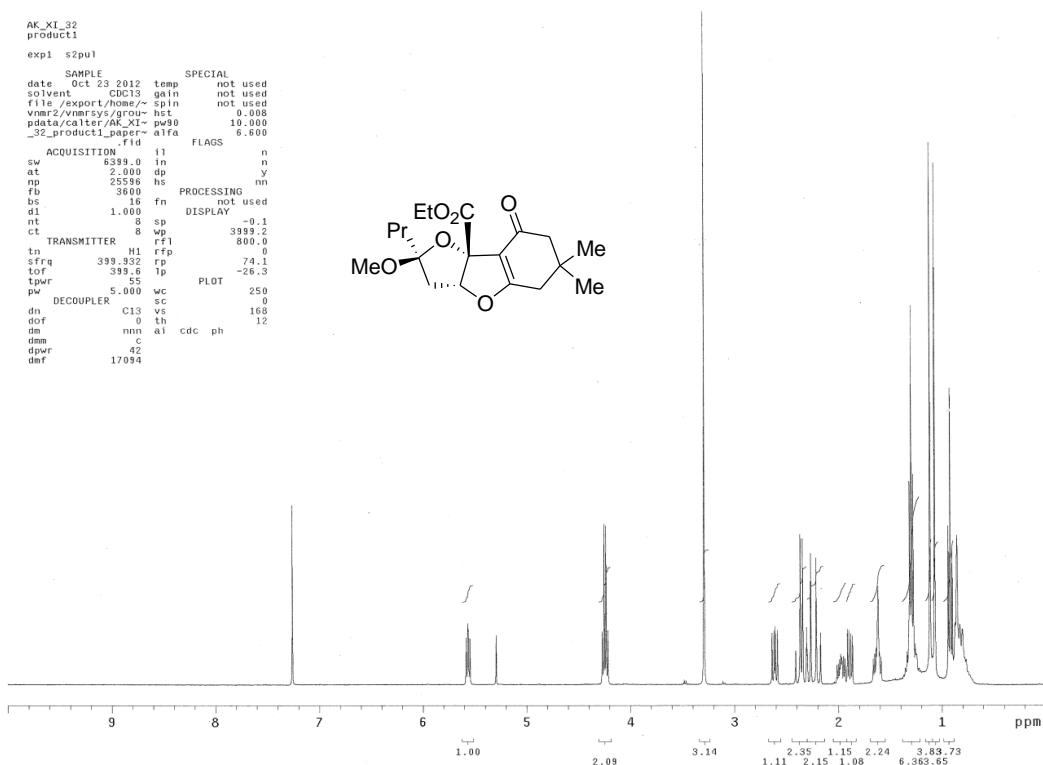
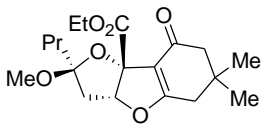
AK_XI_32
product
exp11 s2pu1
SAMPLE
date Nov 20 2012 temp not used
solvent CDCl3 gain not used
file exp spin not used
ACQUISITION hst 0.008
sw 25141.4 pw90 28.000
at 1.199 alfa 20.000
np 60308 FLAGS
fb 13800 il n
bs 64 in n
d1 1.000 dp y
nt 512 hs nn
ct 256
TRANSMITTER fb 1.00
tn C13 fn not used
sfrq 100.573 DISPLAY
tof 1545.8 sp -1508.9
tpwr 61 wp 25141.4
pw 14.000 rf1 1508.9
DECOUPLER rfp 0
dn H1 rp -123.2
dof 0 lp -315.2
dm yy wc 250
dmm 42 sc 0
dpwr 10582 vs 642
dmf ai no ph 24

```



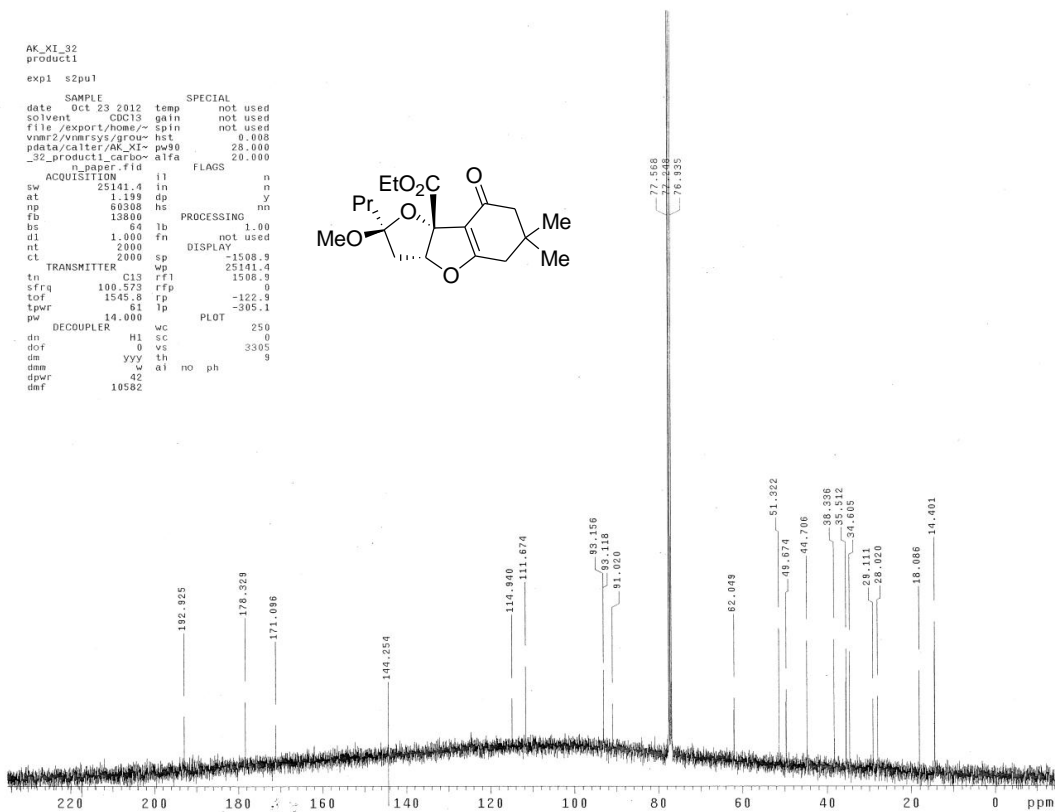
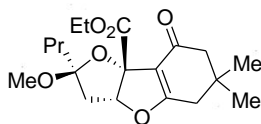
AK_XI_32
product1
exp1 s2pu1

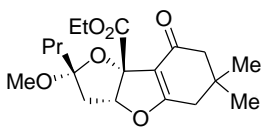
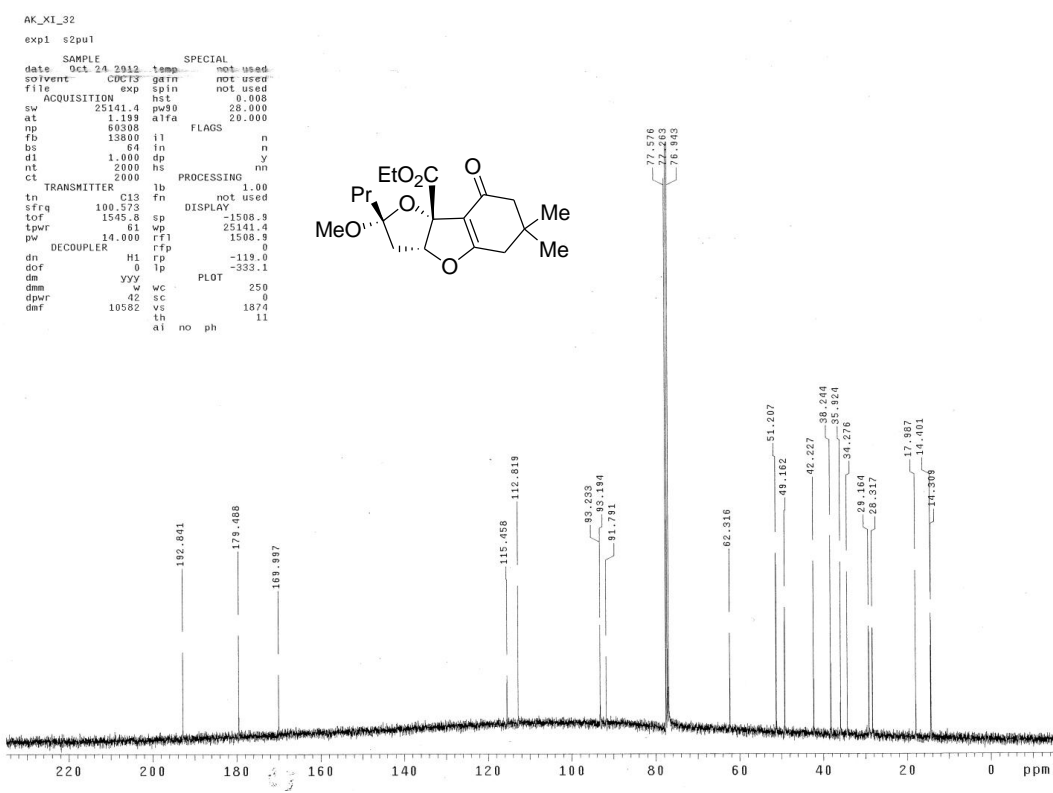
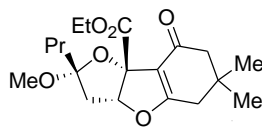
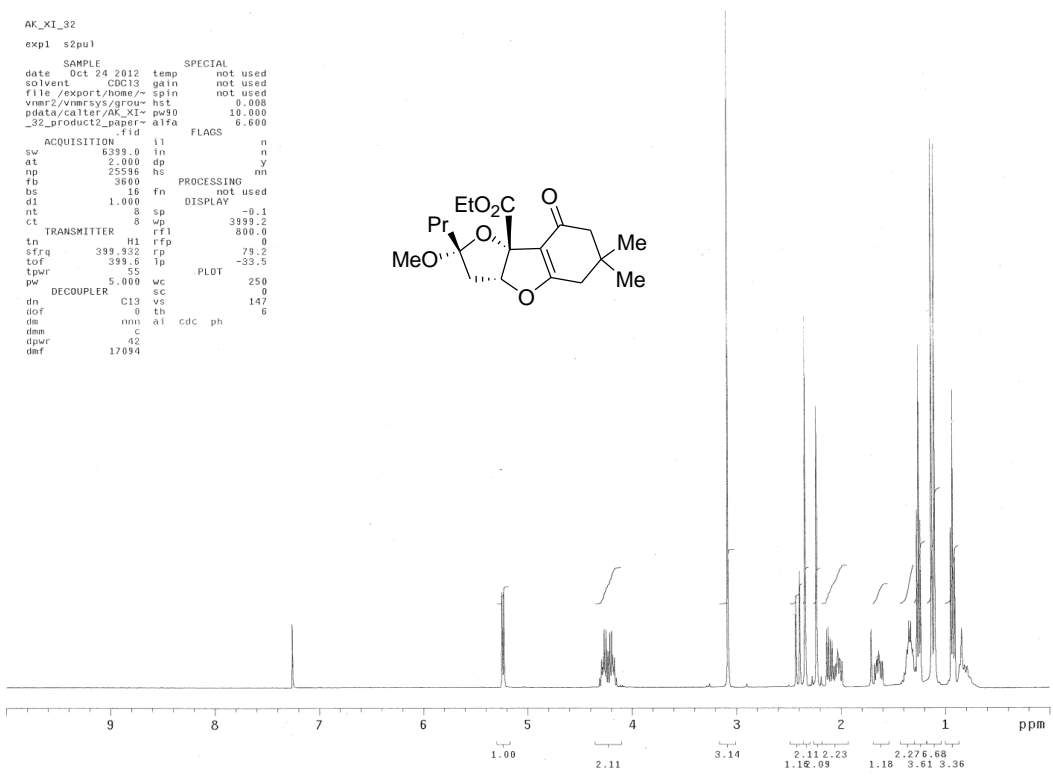
SAMPLE		SPECIAL	
date	Oct 23 2012	temp	not used
solvent	CDCl3	gain	not used
file	/export/home/~	spin	not used
vnmr2/vnmrsys/grou	hst	hst	0.008
pdata/caliter/AK_XI	pw90	pw90	10.000
_32_product1_paper	alfa	alfa	6.600
ACQUISITION		FLAGS	
sw	6389.0	in	n
at	2.000	dp	y
np	25596	hs	nn
fb	3000	PROCESSING	
bs	16	fn	not used
dl	1.000	DISPLAY	
nt	9	sp	-0.1
ct	8	wp	3999.2
TRANSMITTER		rf1	800.0
tn	H1	rfp	0
sfrq	399.932	fp	74.1
tofr	399.9	lp	-26.3
tpwr	55	PLOT	
pw	5.000	wc	250
DECOUPLER		sc	0
dn	C13	vs	168
dofr	0	th	12
dm	nnn	al	cdc ph
dma	42		
dpr	17094		



AK_XI_32
product1
exp1 s2pu1

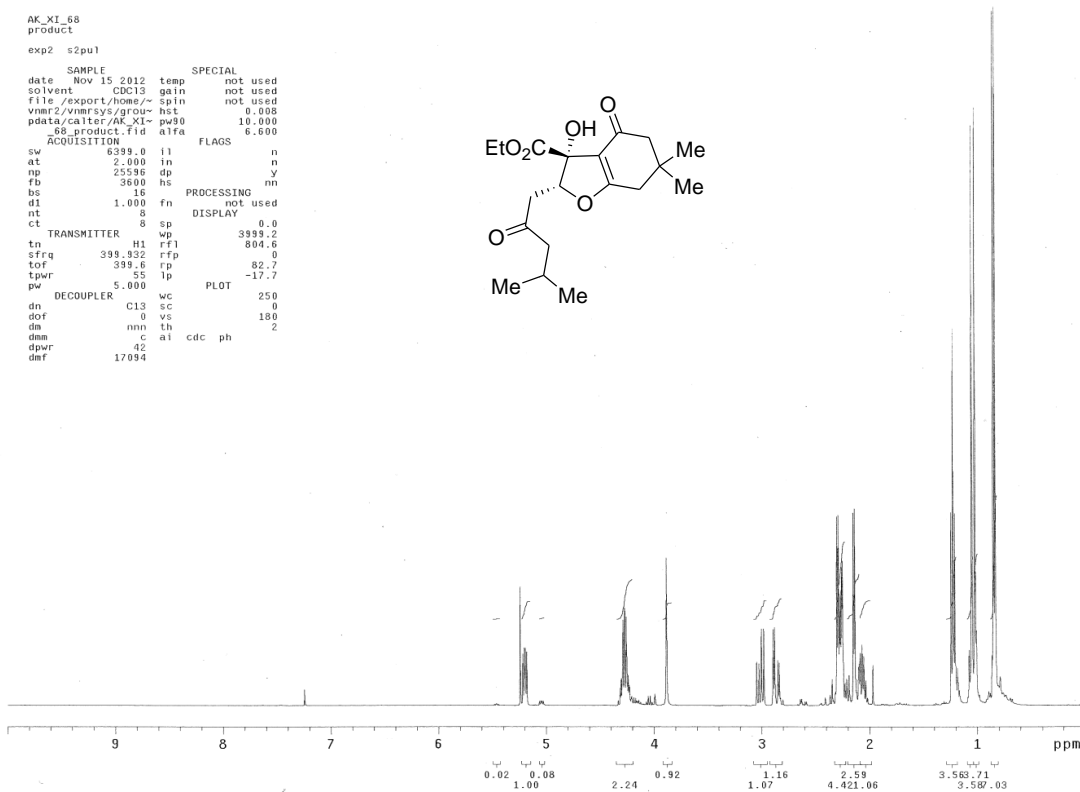
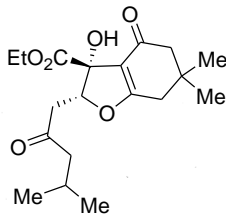
SAMPLE		SPECIAL	
date	Oct 23 2012	temp	not used
solvent	CDCl3	gain	not used
file	/export/home/~	spin	not used
vnmr2/vnmrsys/grou	hst	hst	0.008
pdata/caliter/AK_XI	pw90	pw90	20.000
_32_product1_carbo	alfa	alfa	20.000
n_paper_f1d			
ACQUISITION		FLAGS	
sw	25141.4	in	n
at	1.199	dp	y
np	96308	hs	nn
fb	13800	PROCESSING	
bs	64	lb	1.00
dl	1.000	fn	not used
nt	2000	DISPLAY	
ct	2000	sp	-1508.9
TRANSMITTER		wp	25141.4
tn	C13	rf1	1508.9
sfrq	100.625	rfp	0
tofr	1545.8	fp	-122.9
tpwr	61	lp	-305.1
pw	14.000	PLOT	
DECOUPLER		wc	250
dn	H1	sc	0
dofr	0	vs	3305
dm	yyy	th	9
dma	w	al	no ph
dpr	42		
dmf	10582		





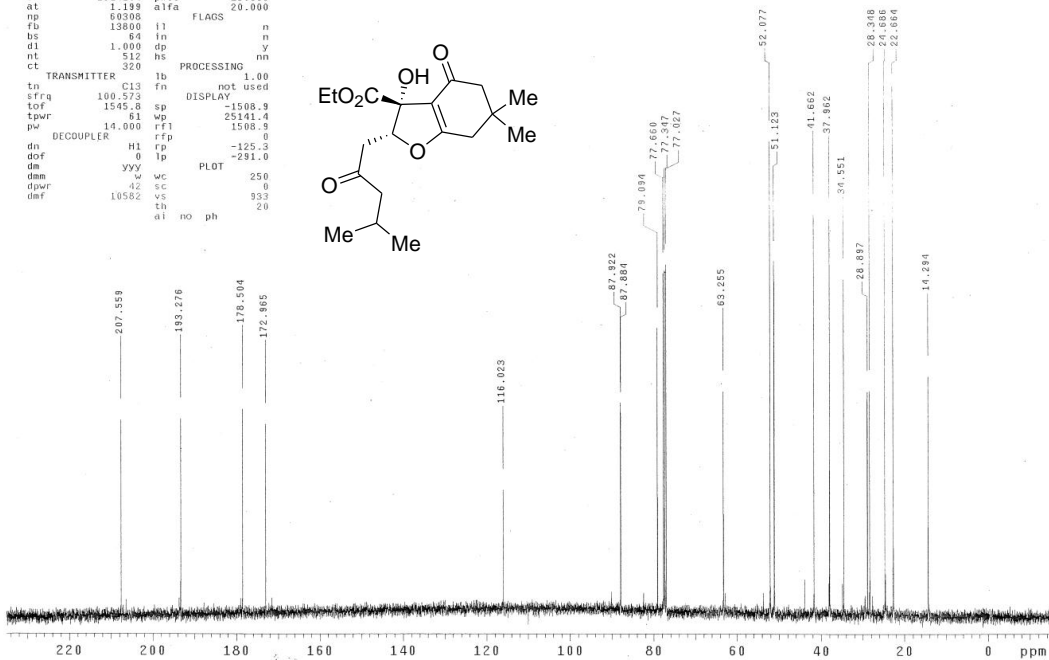
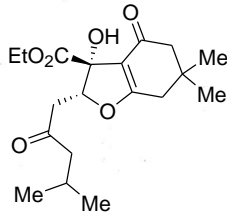
AK_XI_68
product
exp2 s2pu1

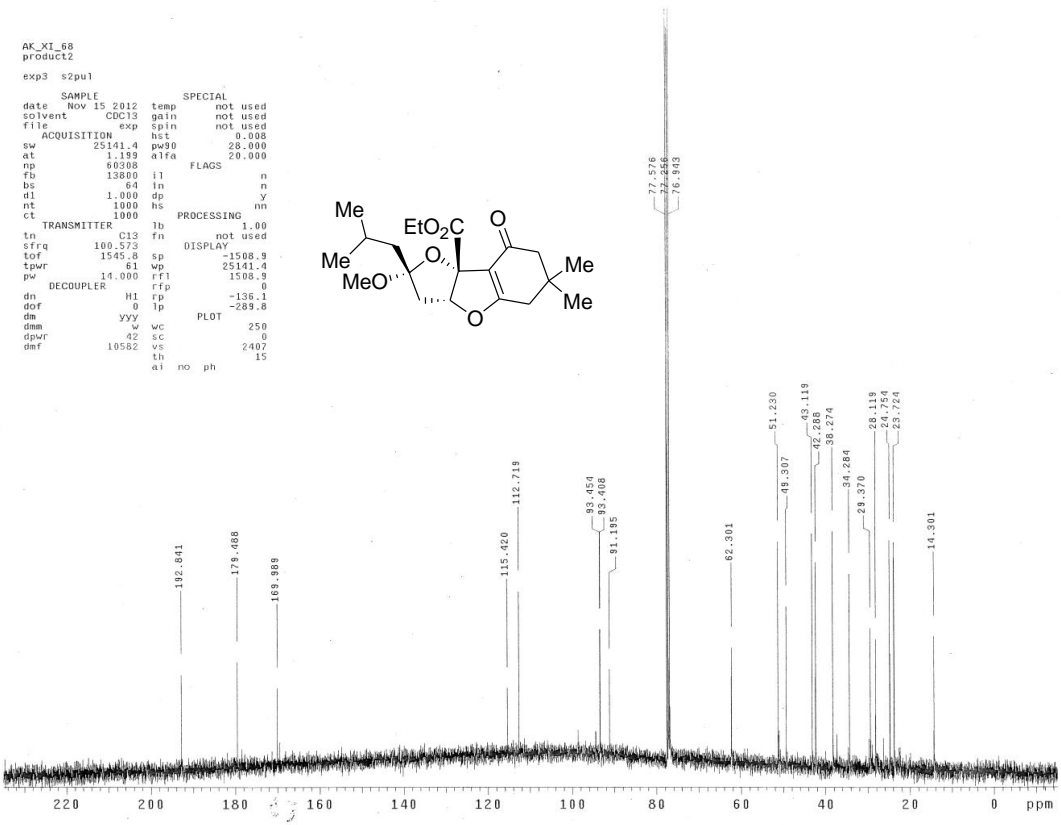
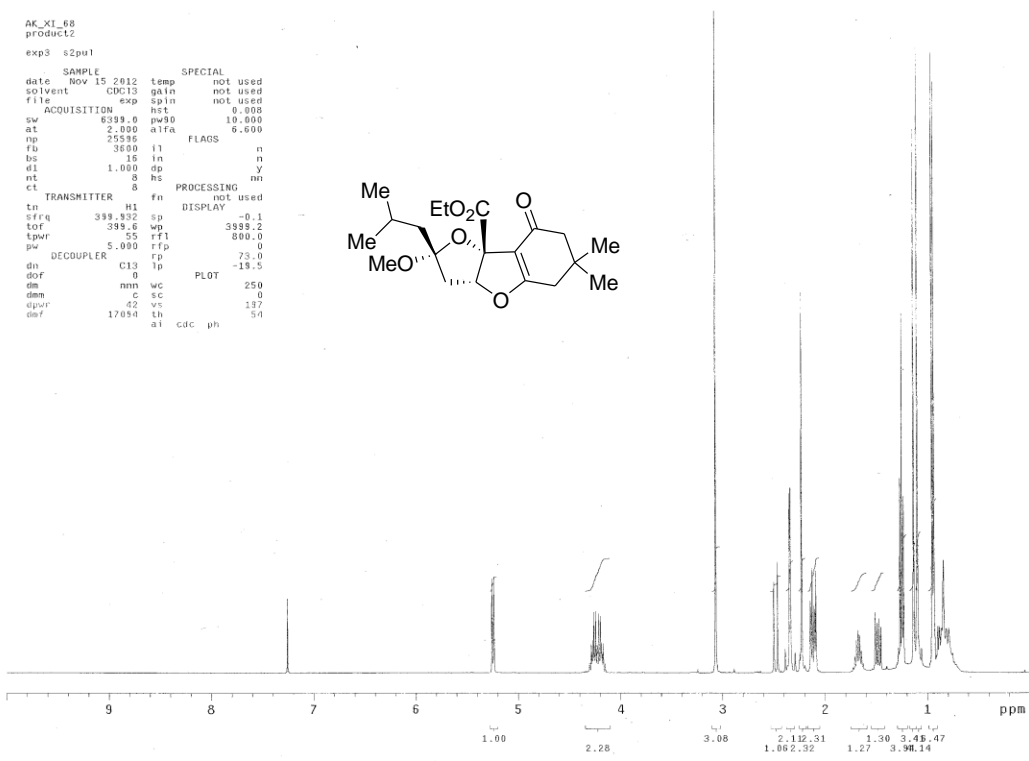
```
SAMPLE SPECIAL
date Nov 15 2012 temp not used
solvent CDCl3 gain not used
file /export/home/~ spin not used
vnmr2/vnmrsys/grou~ hst 0.008
pdata/caliter/AK_XI~ pw90 10.000
68 product. F1u a1ra 6.600
ACQUISITION FLAGS
sw 6399.0 f1 n
at 2.000 in n
np 25596 dp n
fb 3600 hs y
bs 16 PROCESSING nn
d1 1.000 fn not used
nt 8 DISPLAY
ct 8 sp 0.0
TRANSMITTER H1 rf1 399.2
tn 399.932 rfp 804.6
sfrq 399.6 rp 0
tor 55 lp 82.7
tpwr 5.000 PLOT -17.7
pw DECOUPLER wc 250
dn C13 sc 0
dof 0 vs 180
dm nnn lh 2
dam c a1 cdc ph
dpwr 42
def 17094
```



AK_XI_68
product
exp3 s2pu1

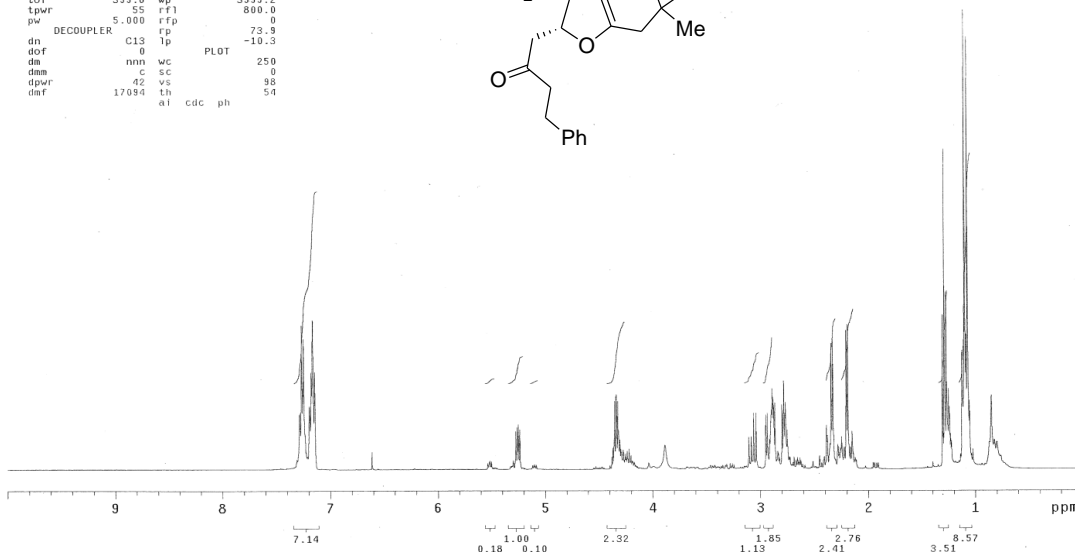
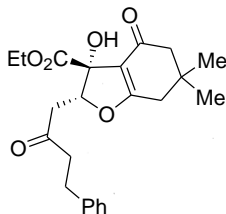
```
SAMPLE SPECIAL
date Nov 15 2012 temp not used
solvent CDCl3 gain not used
file /export/home/~ spin not used
ACQUISITION exp pw90 28.000
at 1.189 f1a 20.000
np 60308 FLAGS
fb 13800 f1 n
bs 84 in n
d1 1.000 dp y
nt 512 hs nn
ct 320 PROCESSING
TRANSMITTER C13 fb 1.00
tn 100.573 fn DISPLAY
sfrq 1545.8 sp -1508.9
tpwr 81 wp 25141.4
pw 14.000 rfp 1508.9
DECOUPLER H1 rf1 -125.3
dn 0 lp -291.0
dm yyy PLOT
dam wc 250
dpwr 42 sc 933
def 10562 vs th 20
al no ph
```





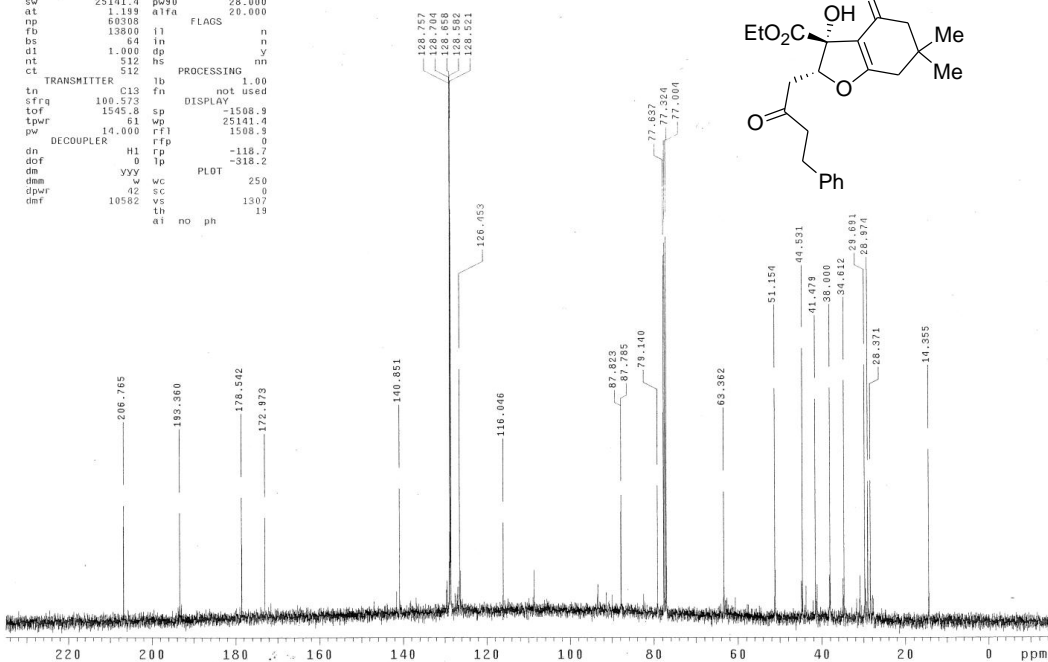
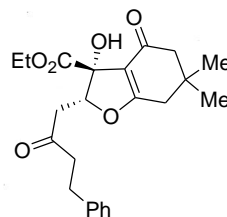
AK_X_201
product
exp11 s2pu1

SAMPLE		SPECIAL	
date	Nov 21 2012	temp	not used
solvent	CDCl3	gain	not used
file		spin	not used
ACQUISITION		hst	0.008
sw	6399.0	pw90	10.000
at	2.000	atfa	6.600
np	25336	FLAGS	
fb	3600	il	n
bs	16	in	n
d1	1.000	dp	y
nt	8	hs	nn
ct	8	PROCESSING	
TRANSMITTER		fn	not used
tn	H1	DISPLAY	
sfrq	399.332	sp	-0.1
tof	399.6	wp	3999.2
tpwr	55	rf1	800.0
pw	5.000	rfp	0
DECOUPLER		rp	73.9
dn	C13	lp	-10.3
dof	0	PLOT	
dm	nnn	wc	250
dmm	C	sc	0
dpwr	42	vs	88
dmf	17094	th	54
	ai	cdc	ph



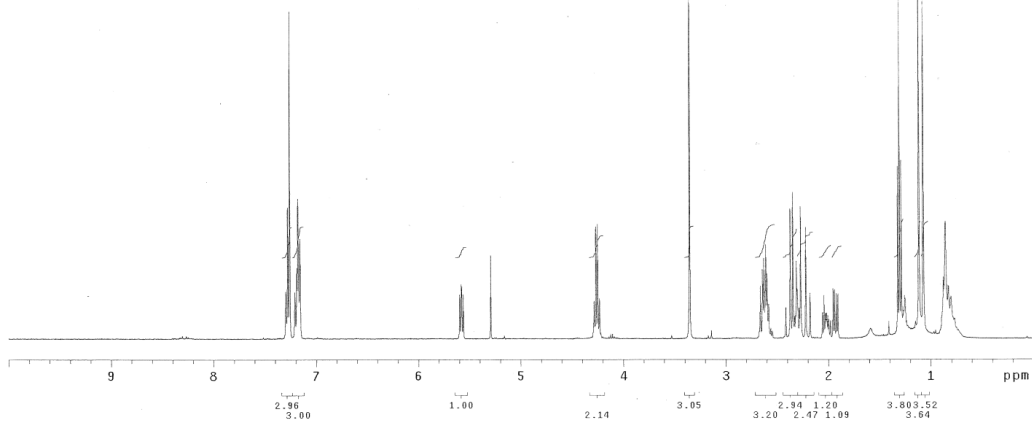
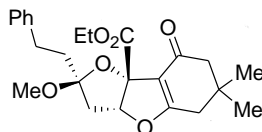
AK_X_201
product
exp11 s2pu1

SAMPLE		SPECIAL	
date	Nov 21 2012	temp	not used
solvent	CDCl3	gain	not used
file		spin	not used
ACQUISITION		hst	0.008
sw	25141.4	pw90	28.000
at	1.189	atfa	20.000
np	60308	FLAGS	
fb	13800	il	n
bs	64	in	n
d1	1.000	dp	y
nt	512	hs	nn
ct	512	PROCESSING	
TRANSMITTER		fb	not used
tn	C13	fn	1.00
sfrq	100.573	DISPLAY	
tof	1545.8	sp	-1508.9
tpwr	61	wp	25141.4
pw	14.000	rf1	1508.9
DECOUPLER		rfp	0
dn	H1	rp	-118.7
dof	0	lp	-318.2
dm	yyy	PLOT	
dmm	w	wc	250
dpwr	42	sc	0
dmf	10582	vs	1307
	th	no	19
	ai	no	ph



AK_XI_16
product1
exp1 s2pu1

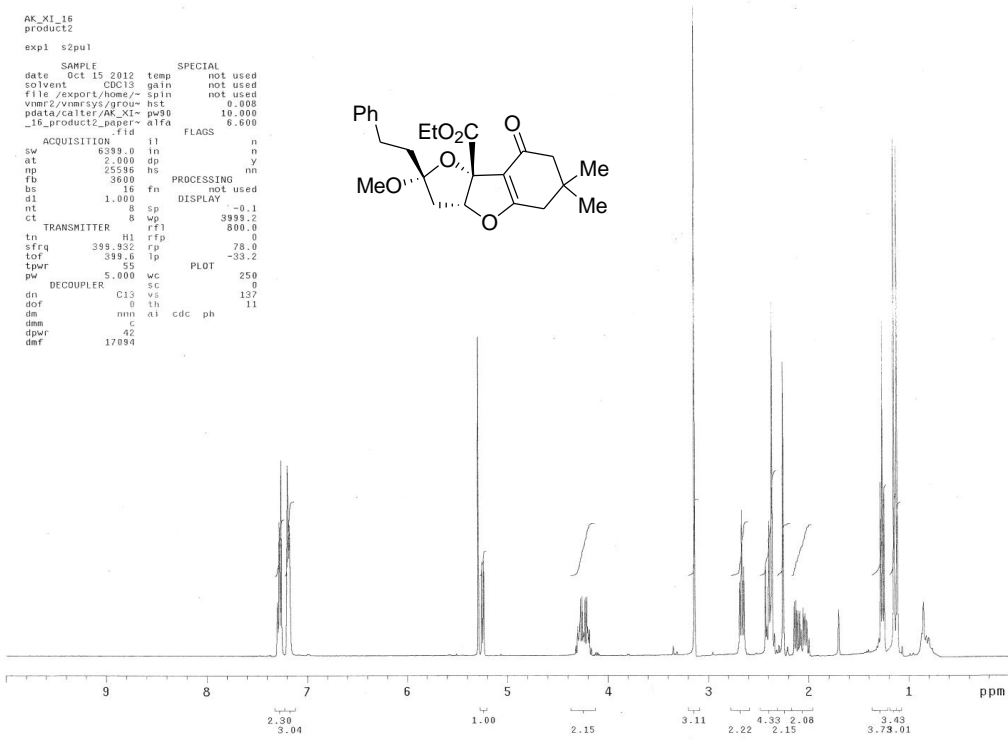
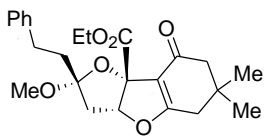
SAMPLE		SPECIAL	
date	Nov 18 2012	temp	not used
solvent	CDCl3	gain	not used
file	exp	spin	not used
ACQUISITION		hst	0.008
sw	6399.0	pw90	10.000
at	2.000	atfa	6.600
rp	25396	FLAGS	
fb	3600	il	n
bs	16	in	n
d1	1.000	dp	y
nt	8	hs	nn
ct	8	PROCESSING	
TRANSMITTER		fn	not used
tn	h1	DISPLAY	
sfrq	399.332	sp	-0.1
tof	399.6	wp	3999.2
tpwr	55	rfl	800.0
pw	5.000	rfp	0
DECOUPLER		rp	72.9
dn	C13	lp	-17.4
dof	0	PLOT	
dm	nmn	wc	250
dmm	c	sc	0
dpwr	42	vs	247
daf	17094	th	54
	ai	cdc	ph



AK_XI_16
product2
expl s2pul

date	Oct 15 2012	temp	not used
solvent	CDCl3	gain	not used
file	/export/home/	spin	not used
nmr2/vmr/sy/grou	hst	0.008	
pdata/cater/	AK_XI-	pu90	10.000
-is_product_	paper-	alfa	0.000

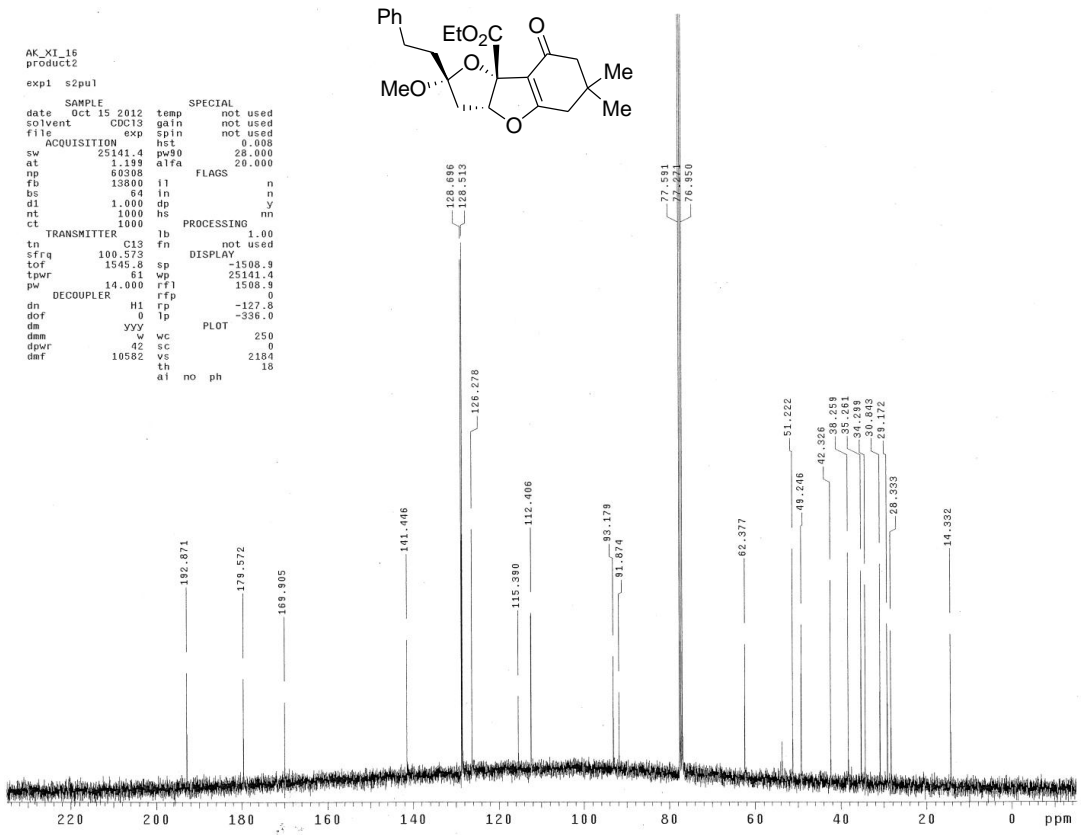
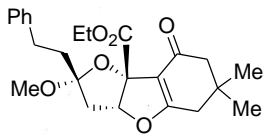
ACQUISITION	.fid	FLAGS	n
sw	6399.0	in	n
at	2.000	dp	nm
np	25336	hs	not used
fb	3600	fn	not used
bs	16	DISPLAY	-0.1
d1	1.000	sp	3999.2
nt	8	rf1	800.0
ct	8	rf2	0
tn	TRANSMITTER	H1	rfp
sfrq	399.932	rp	78.0
tof	399.6	lp	-33.2
tpwr	55	PLOT	250
pw	5.000	wc	0
DECOUPLER	SC	vs	137
dn	C13	lh	11
dof	0	cdc	ph
dm	nm	oi	
dma	c		
dpwr	42		
dmf	17094		



AK_XI_16
product2
expl s2pul

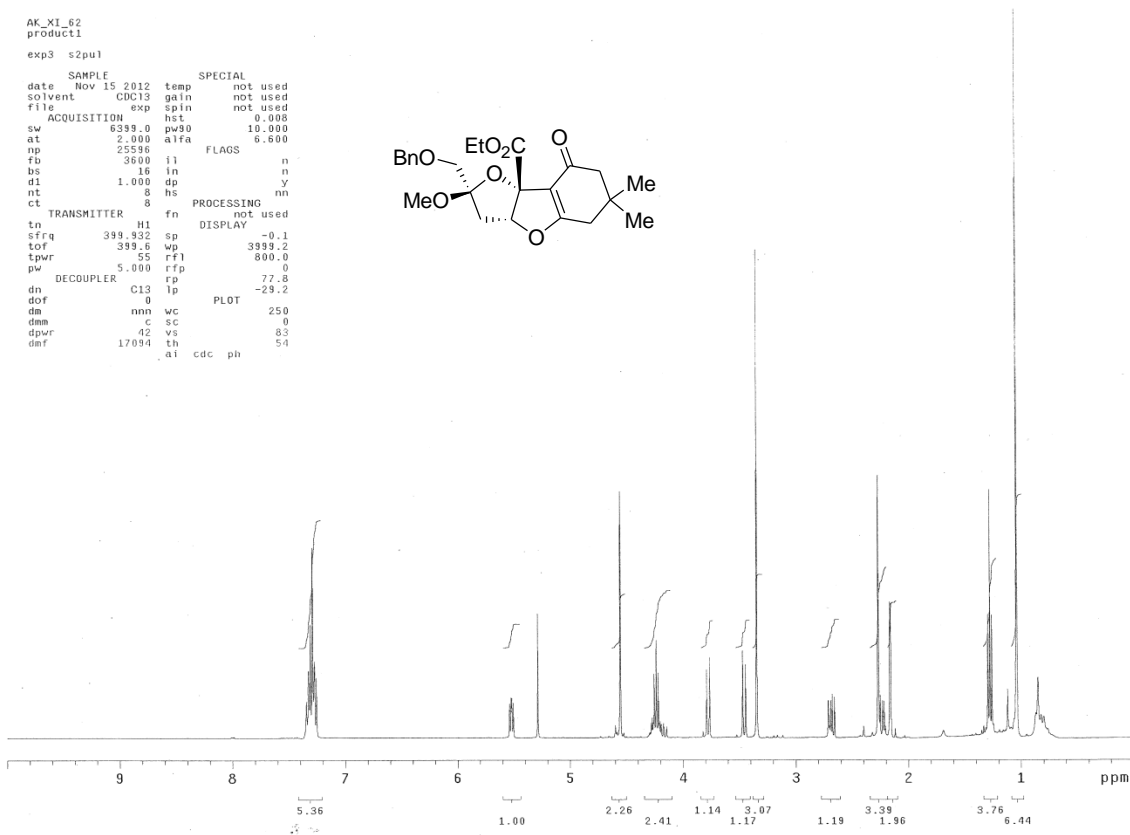
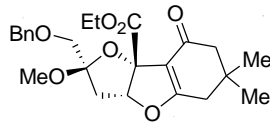
date	Oct 15 2012	temp	not used
solvent	CDCl3	gain	not used
file	/export/home/	spin	not used
nmr2/vmr/sy/grou	hst	0.008	
pdata/cater/	AK_XI-	pu90	20.000
-is_product_	paper-	alfa	0.000

ACQUISITION	25141.4	alpha	20.000
sw	1.199	FLAGS	n
at	60308	in	n
np	13900	dp	y
fb	64	hs	nm
d1	1.000	fn	not used
nt	1000	DISPLAY	1.00
ct	1000	sp	-1508.9
tn	TRANSMITTER	C13	rfp
sfrq	100.572	rp	25141.4
tof	1545.8	lp	1508.9
tpwr	61	rf2	0
pw	14.000	wc	-127.8
DECOUPLER	H1	vs	-336.0
dn	0	lh	250
dof	0	cdc	0
dm	yyy	oi	2184
dma	w	th	18
dpwr	42	no	ph
dmf	10582		



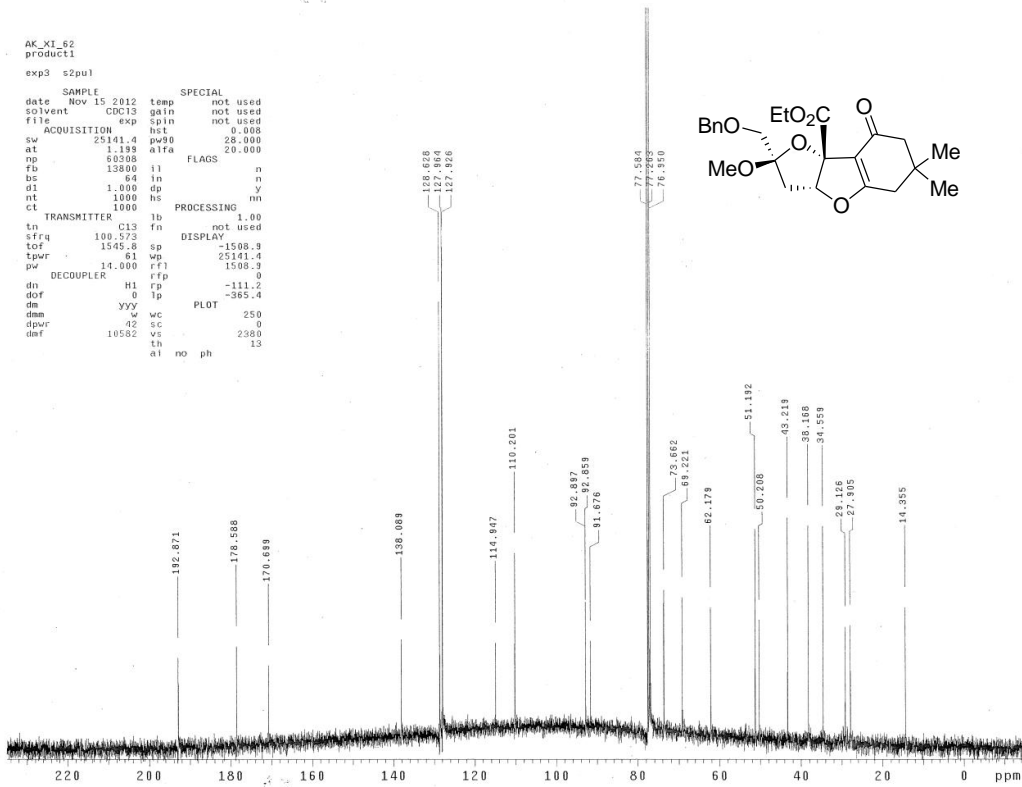
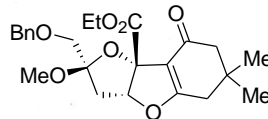
AK_XI_62
product1
exp3 s2pu1

SAMPLE		SPECIAL	
date	Nov 15 2012	temp	not used
solvent	CDCl3	gain	not used
file	exp	spin	not used
ACQUISITION		exp	hst
sw	6339.0	pw90	10.000
at	2.000	alfa	6.600
np	2536	FLAGS	
fb	3600	il	n
bs	18	in	n
d1	1.000	dp	y
nt	8	hs	nn
ct	8		
TRANSMITTER		fn	not used
tn	H1	DISPLAY	
sfrq	399.932	sp	-0.1
tof	399.8	wp	399.2
tpwr	55	rfl	800.0
pw	5.000	rpf	0
DECOUPLER		rp	77.8
dn	C13	lp	-29.2
dof	0	PLOT	250
dm	mm	wc	0
dmm	c	sc	0
dpwr	42	vs	83
daf	17034	th	54
	ai	cdc	ph



AK_XI_62
product1
exp3 s2pu1

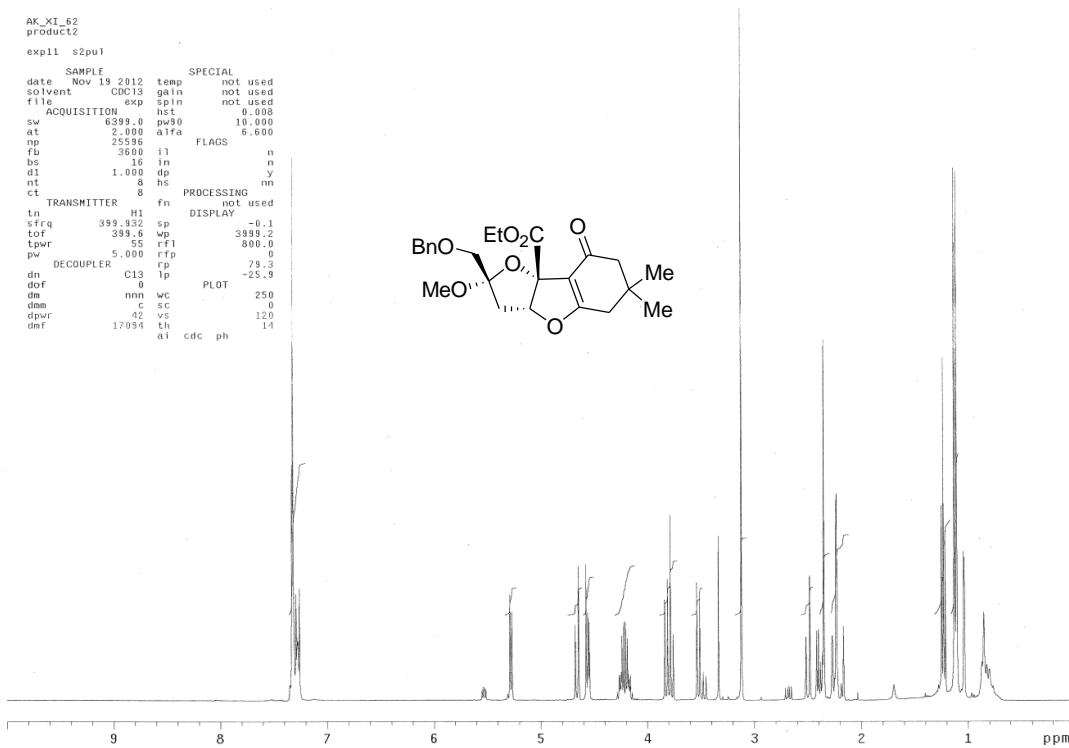
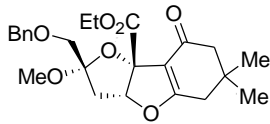
SAMPLE		SPECIAL	
date	Nov 15 2012	temp	not used
solvent	CDCl3	gain	not used
file	exp	spin	not used
ACQUISITION		exp	hst
sw	25141.4	pw90	8.000
at	1.199	alfa	20.000
np	60308	FLAGS	
fb	13800	il	n
bs	64	in	n
d1	1.000	dp	y
nt	1000	hs	nn
ct	1000		
TRANSMITTER		lb	not used
tn	C13	fn	1.00
sfrq	100.573	DISPLAY	
tof	1545.8	sp	-1508.9
tpwr	61	wp	2511.4
pw	14.000	rfl	1508.9
DECOUPLER		rpf	0
dn	H1	rp	-111.2
dof	0	lp	-365.4
dm	yyy	wc	250
dmm		sc	0
dpwr	42	vs	2360
daf	10582	th	13
	ai	no	ph



AK_XI_62
product2

exp11 s2pu1

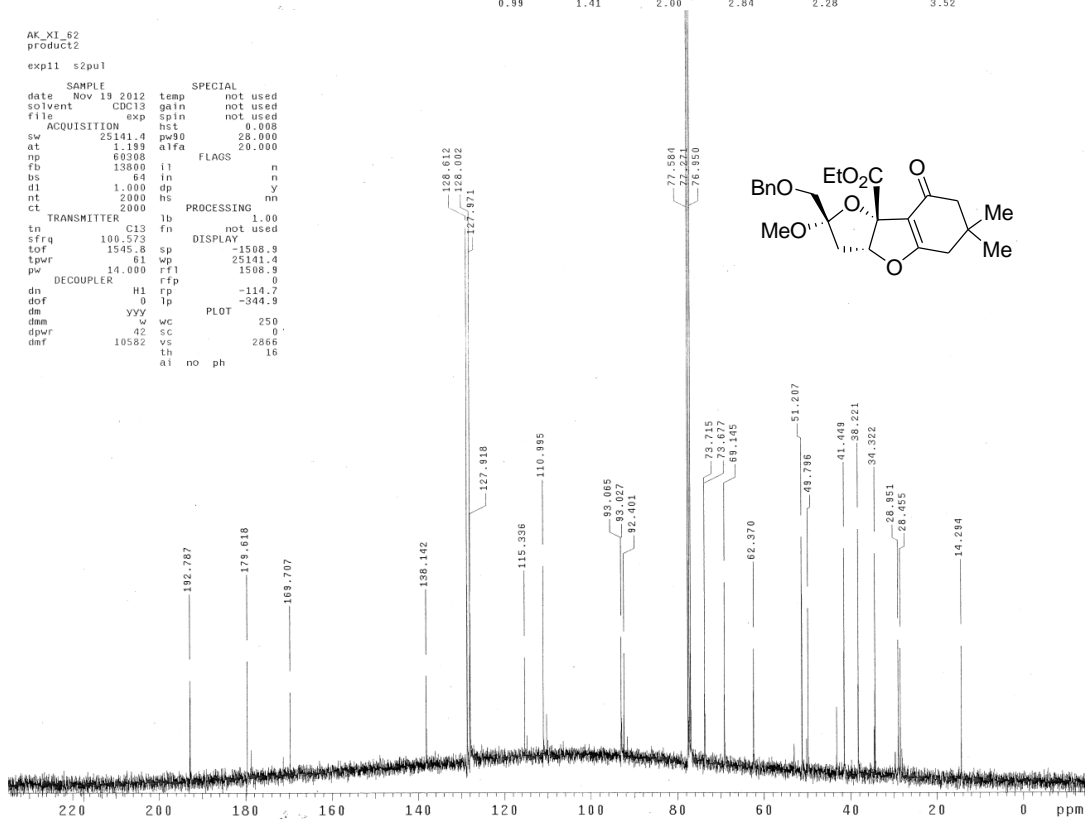
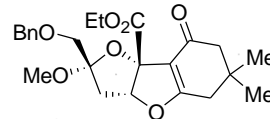
SAMPLE		SPECIAL	
date	Nov 19 2012	temp	not used
solvent	CDCl3	gain	not used
file	exp	spin	not used
ACQUISITION		hst	0.008
sw	6399.0	pw90	10.000
at	2.000	alpha	6.600
np	25596	ifl	FLAGS
fb	3600	il	n
bs	16	in	n
d1	1.000	dp	y
nt	8	hs	n
ct	8	hs	n
TRANSMITTER		PROCESSING	
tn	H1	fn	not used
sfrq	399.932	sp	DISPLAY
tof	399.6	wp	-0.1
tpwr	55	rf1	3999.2
pw	5.000	rft	800.0
DECOUPLER		rfp	0
dn	C13	lp	-79.3
dof	0	lp	-25.9
dm	nm	wc	PLOT
dma	c	sc	250
dpwr	42	vs	0
dmf	17934	th	120
		ai	cdc ph
			14



AK_XI_62
product2

exp11 s2pu1

SAMPLE		SPECIAL	
date	Nov 19 2012	temp	not used
solvent	CDCl3	gain	not used
file	exp	spin	not used
ACQUISITION		hst	0.008
sw	25141.4	pw90	28.000
at	1.199	alpha	20.000
np	60268	ifl	FLAGS
fb	13800	il	n
bs	64	in	n
d1	1.000	dp	y
nt	2000	hs	n
ct	2000	hs	n
TRANSMITTER		PROCESSING	
tn	C13	fn	not used
sfrq	100.573	sp	DISPLAY
tof	1545.8	wp	-1508.9
tpwr	61	rf1	25141.4
pw	14.000	rft	1508.9
DECOUPLER		rfp	0
dn	H1	lp	-114.7
dof	0	lp	-344.9
dm	yyy	wc	PLOT
dma	w	sc	250
dpwr	42	vs	0
dmf	10582	th	2866
		ai	no ph
			16



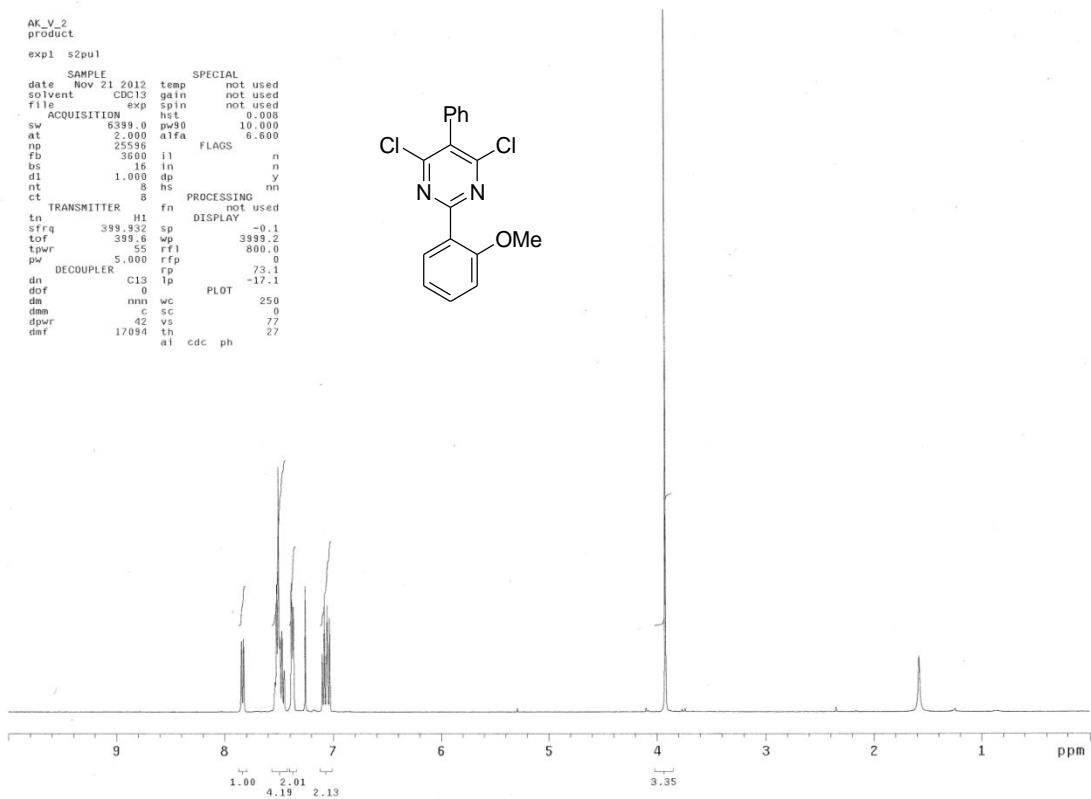
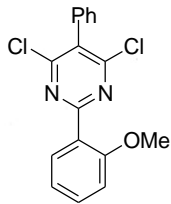
```

AK_V_2
product
exp1 s2pu1

SAMPLE
date Nov 21 2012 temp not used
solvent CDCl3 gain not used
file exp sp1n not used
ACQUISITION
sw 6399.0 pw90 10.000
at 2.000 a1fa 6.600
np 25536 FLAGS
fb 3600 il n
bs 16 in n
d1 1.000 dp y
nt 8 hs nn
ct

TRANSMITTER 8 fn not used
tn H1 DISPLAY
sfrq 399.332 sp -0.1
tof 399.8 wp 3999.2
tpwr 55 rfl 800.0
pw 5.000 rfp 0
DECOUPLER rp 73.1
dn C13 lp -17.1
dof 0 PLOT
dm nnu wc 250
dmm c sc 0
dpr 42 vs 77
def 17094 th 27
ai cdc ph

```



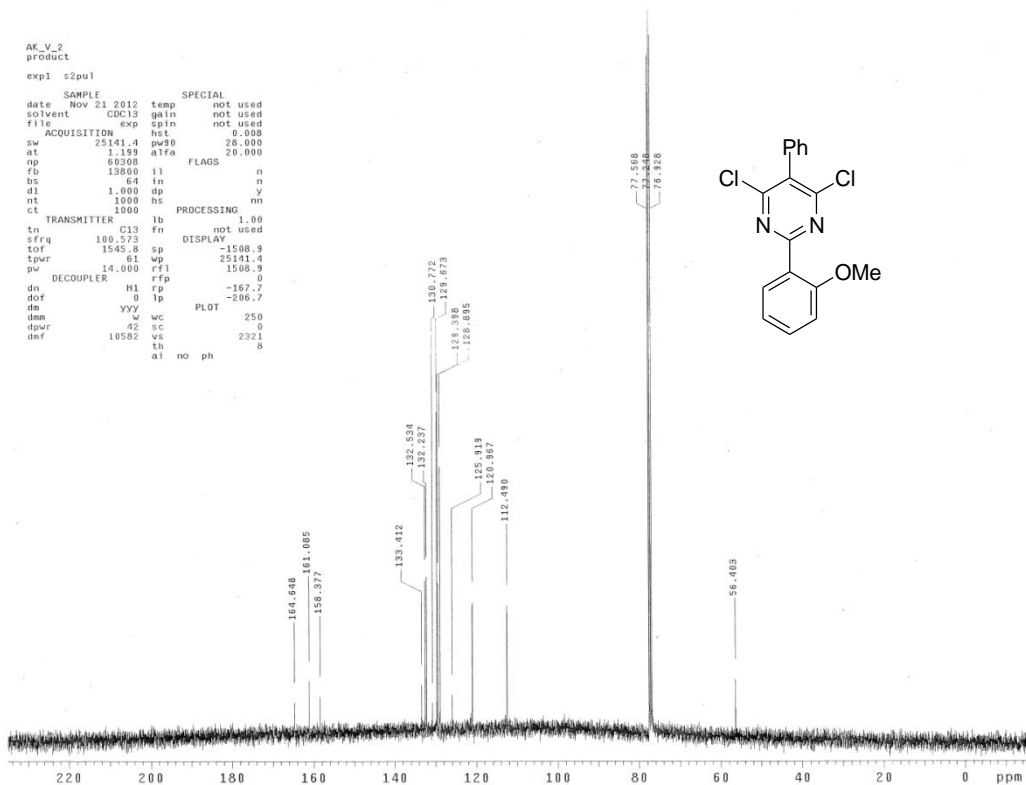
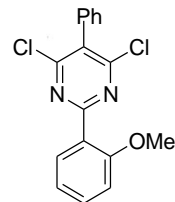
```

AK_V_2
product
exp1 c2pu1

SAMPLE
date Nov 21 2012 temp not used
solvent CDCl3 gain not used
file exp sp1n not used
ACQUISITION
sw 2541.4 pw90 26.000
at 1.199 a1fa 20.000
np 60300 FLAGS
fb 4300 il n
bs 64 in n
d1 1.000 dp y
nt 1000 hs nn
ct

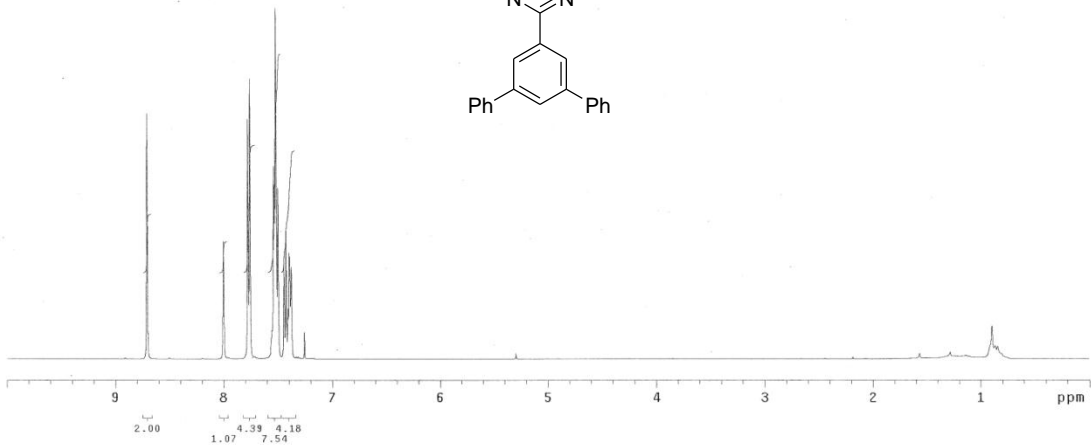
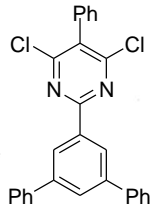
TRANSMITTER 1000 lb PROCESSING 1.00
tn C13 fn not used
sfrq 100.573 DISPLAY
tof 1545.8 sp -1508.9
tpwr 61 wp 25141.4
pw 14.000 rfl 1508.9
DECOUPLER H1 rfp 0
dn 0 lp -167.7
dof 0 PLOT
dm yyy wc 250
dmm 42 sc 2321
dpr 10582 vs th 8
def ai no ph

```



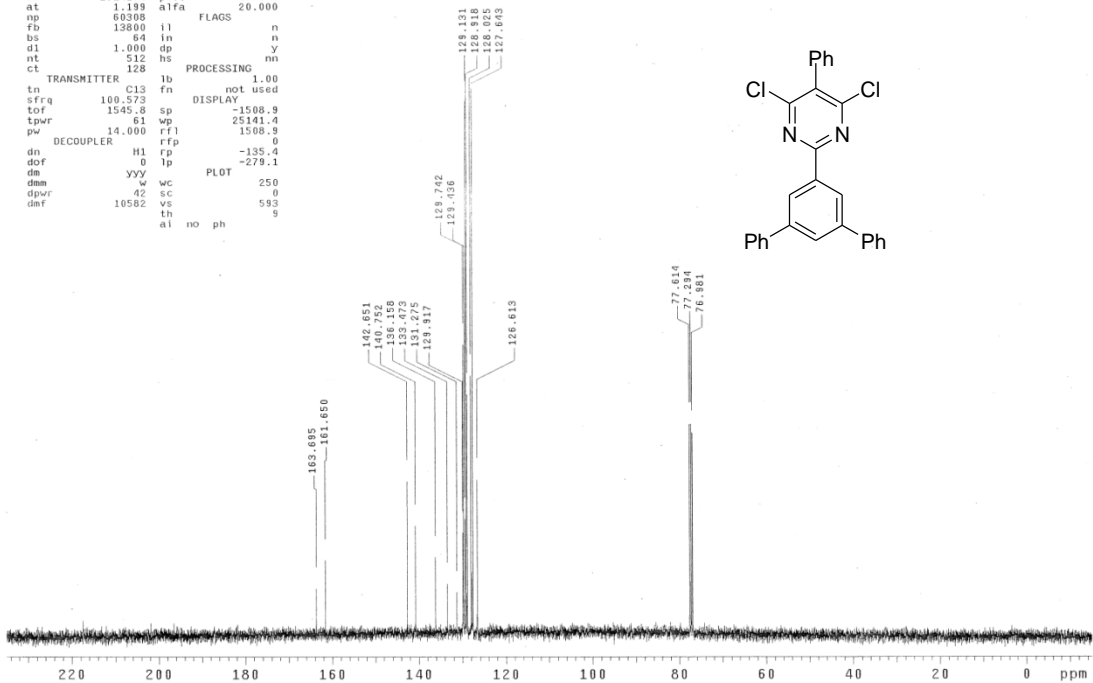
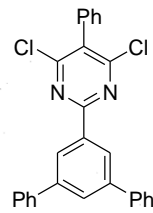
AK_IV_164
product
exp11 s2pu1

```
SAMPLE          SPECIAL
date Nov 19 2012 temp not used
solvent CDC13   gain not used
file          exp spin not used
ACQUISITION    hst  0.008
sw            6399.0 pw90 10.000
at            2.000 atfa 6.600
np            25596
fb            3600    FLAGS
bs            16    in  n
d1            1.000 dp  y
nt            8     hs  nn
ct            8
TRANSMITTER    fn  not used
tn            N1    DISPLAY
sfrq          399.932 sp  -0.1
tof           399.8  wp  3999.2
tpwr          55    rfl  800.0
pw            5.000 rfp  0
DECOUPLER     C13  lp  -27.9
dn            0     PLOT
dm            nmn  wc  250
dam           c   sc  0
dpwr          42   vs  87
dof           17094 ai  cdc ph 16
```



AK_IV_164
product
exp11 s2pu1

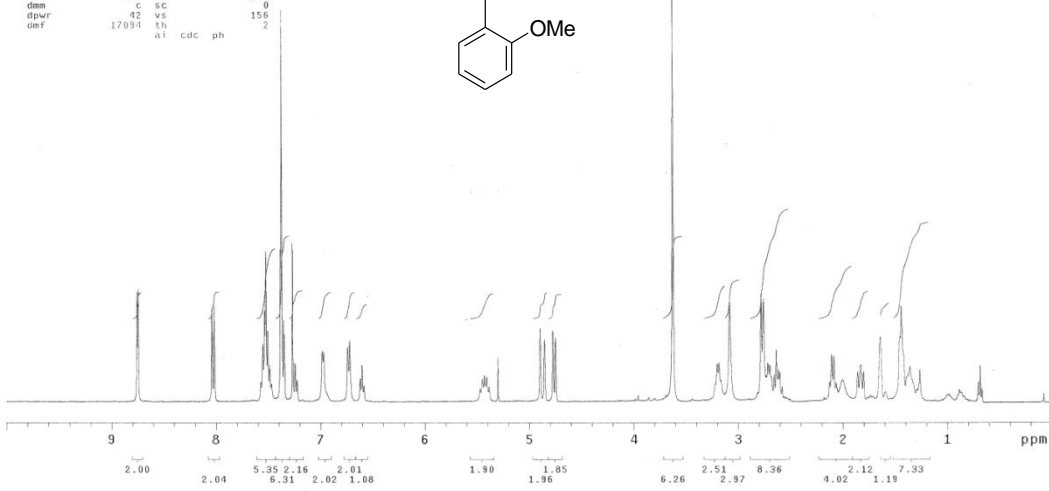
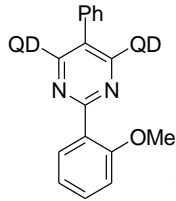
```
SAMPLE          SPECIAL
date Nov 19 2012 temp not used
solvent CDC13   gain not used
file          exp spin not used
ACQUISITION    hst  0.008
sw            25141.4 pw90 28.000
at            1.199 atfa 20.000
np            60308
fb            13800    FLAGS
bs            64    in  n
d1            1.000 dp  y
nt            512   hs  nn
ct            128
TRANSMITTER    fb  not used
tn            C13  DISPLAY
sfrq          100.573 sp  -1508.9
tof           1545.8 wp  25101.4
tpwr           61    rfl  1508.9
pw            14.000 rfp  0
DECOUPLER     H1  rp  -135.4
dn            0     PLOT
dm            yyy  wc  250
dam           v   sc  0
dpwr          10582 th  vs  593
dof           ai  no ph  9
```



AK_V_8

exp2 s2pu1

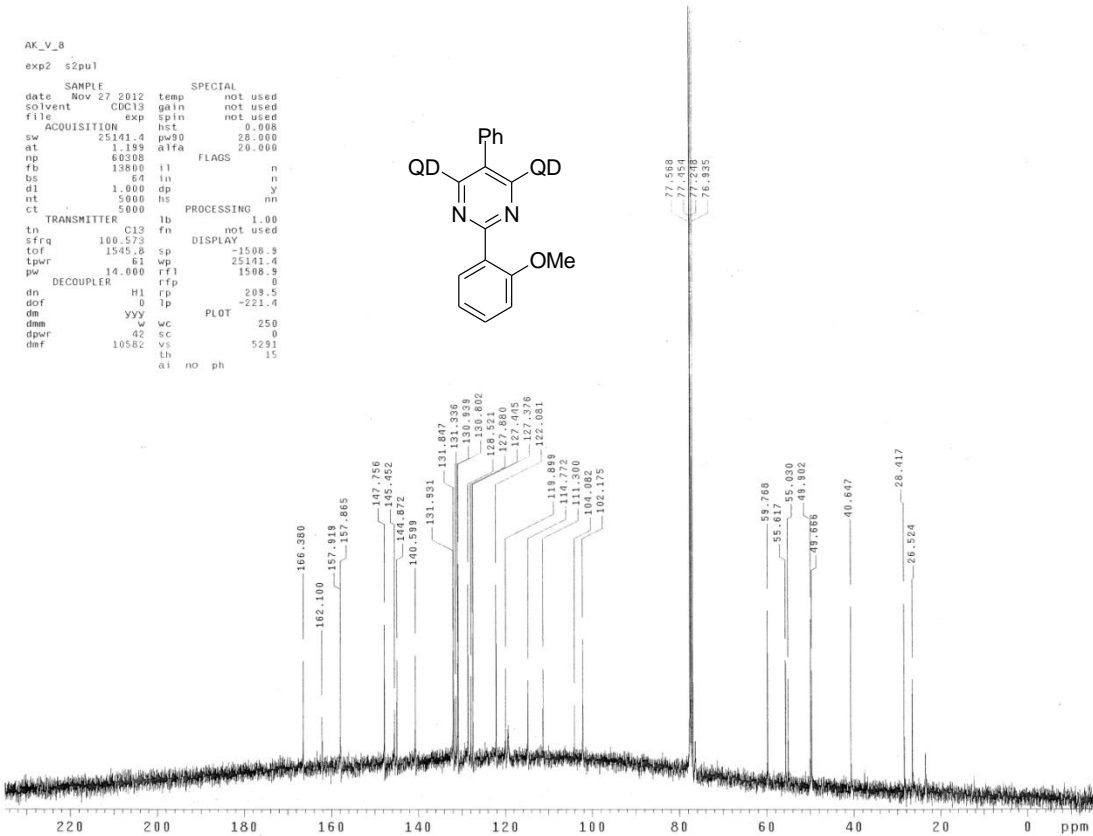
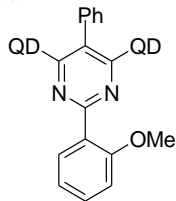
```
SAMPLE SPECIAL
date Nov 27 2012 temp not used
solvent CDCl3 gain not used
file exp spin not used
ACQUISITION hst 0.008
sw 6399.0 pw90 10.000
at 2.000 a1fa 6.600
np 25598
fb 3600 f1 n
bs 15 ln n
d1 1.000 dp y
nt 8 hs nn
ct 8
TRANSMITTER fn PROCESSING
tn H1 fn not used
sfrq 399.932 sp DISPLAY -0.1
tof 399.6 wp 3995.2
tpwr 55 rft1 2914.2
pw 5.000 rfp 2119.6
DECOUPLER C13 rp 80.9
dn 0 lp -29.9
dot 0 PLOT
dm nm wc 250
dmm c sc 0
dpwr 42 vs 156
daf 17091 th 2
ai cdc ph 2
```



AK_V_8

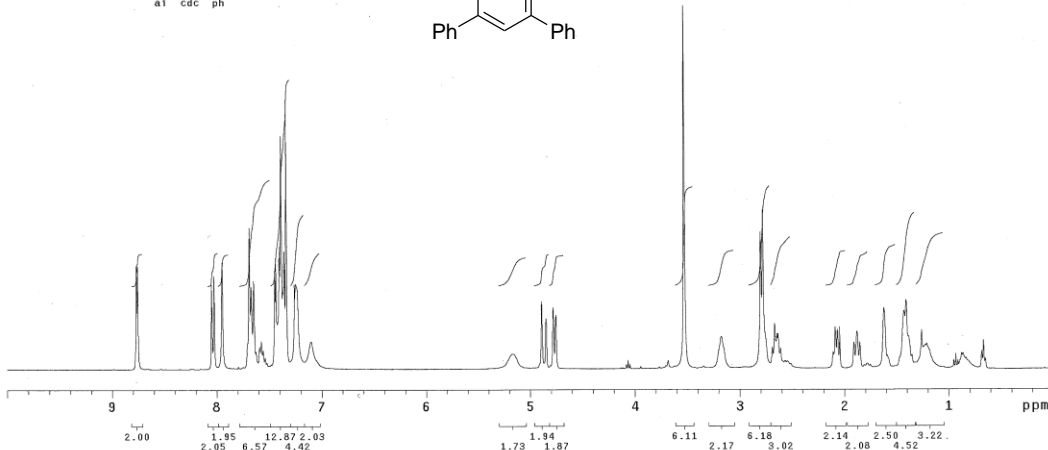
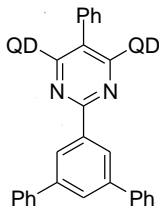
exp2 s2pu1

```
SAMPLE SPECIAL
date Nov 27 2012 temp not used
solvent CDCl3 gain not used
file exp spin not used
ACQUISITION hst 0.008
sw 25141.4 pw90 20.000
at 1.189 a1fa 20.000
np 13800
fb 3600 f1 n
bs 64 ln n
d1 1.000 dp y
nt 5000 hs nn
ct 5000
TRANSMITTER lb PROCESSING
tn C13 fn not used
sfrq 100.573 sp DISPLAY -1508.9
tof 1545.0 wp 25141.4
tpwr 61 rft1 1508.9
pw 14.000 rfp 0
DECOUPLER H1 rp 209.5
dn 0 lp -221.4
dot 0 PLOT
dm yyy wc 250
dmm 42 sc 0
dpwr 10582 vs 5291
daf th 15
ai no ph
```



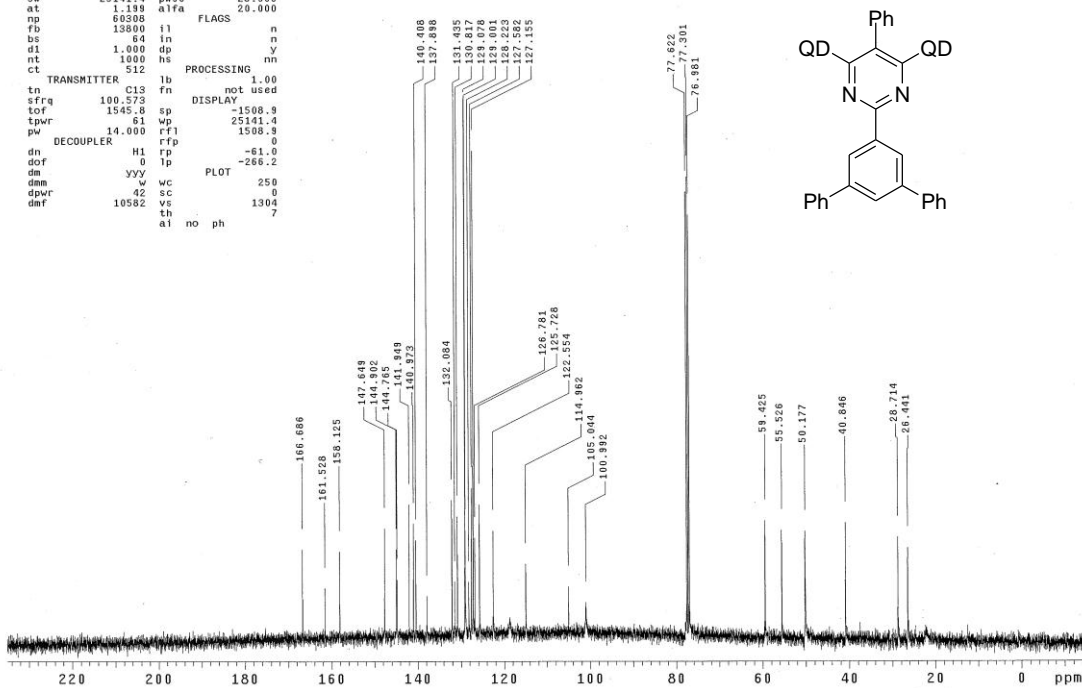
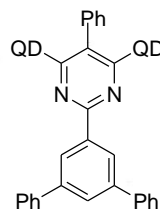
AK_IV_167
 exp1 s2pu1

date	Feb 28 2013	temp	not used
solvent	CDCl3	gain	not used
file	exp	spin	not used
ACQUISITION	hst	0.008	
sw	6399.0	pw90	10.000
at	2.000	alpha	6.000
np	25596	alpha	6.000
fb	3600	fl	n
bs	16	in	n
d1	1.000	dp	y
nt	8	hs	nn
ct	8	hs	nn
TRANSMITTER	H1	fn	not used
tn	399.932	sp	-0.1
sfrq	399.6	wp	3999.2
tof	55	rfl	800.0
tpwr	5.000	rfp	0
pw	5.000	rfp	164.7
DECOUPLER	C13	lp	-26.0
dn	0	lp	250
dof	0	mm	0
dm	mm	wc	0
dmm	c	sc	0
dpwr	42	vs	126
dmf	9500	th	54
		ai	cdc ph



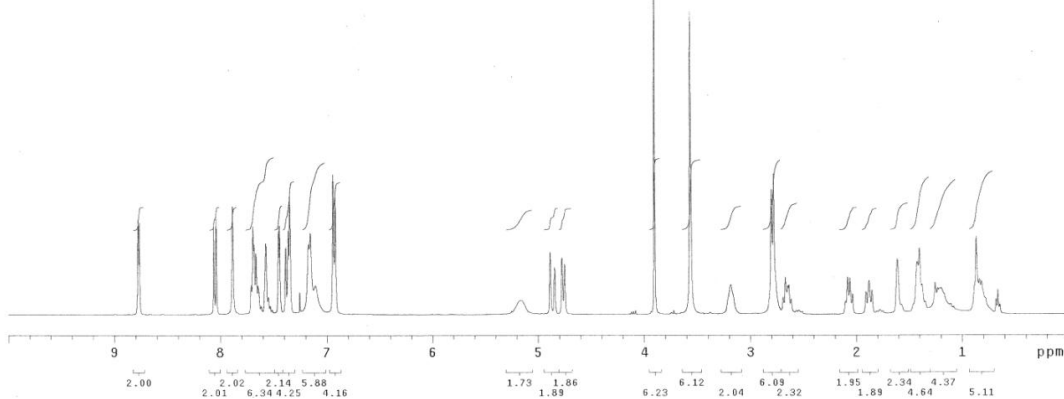
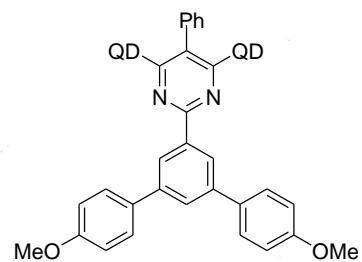
AK_IV_167
 exp1 s2pu1

date	Feb 28 2013	temp	not used
solvent	CDCl3	gain	not used
file	exp	spin	not used
ACQUISITION	hst	0.008	
sw	25141.4	pw90	20.000
at	1.199	alpha	20.000
np	60308	alpha	20.000
fb	18800	fl	n
bs	64	in	n
d1	1.000	dp	y
nt	1000	hs	nn
ct	512	hs	nn
TRANSMITTER	H1	fn	not used
tn	100.573	sp	-1508.9
sfrq	100.573	wp	25141.4
tof	1945.8	rfl	1508.9
tpwr	61	rfl	1508.9
pw	14.000	rfp	0
DECOUPLER	H1	lp	-61.0
dn	0	lp	-266.2
dof	0	mm	250
dm	yy	wc	0
dmm	w	sc	0
dpwr	42	vs	1304
dmf	10582	th	7
		ai	no ph



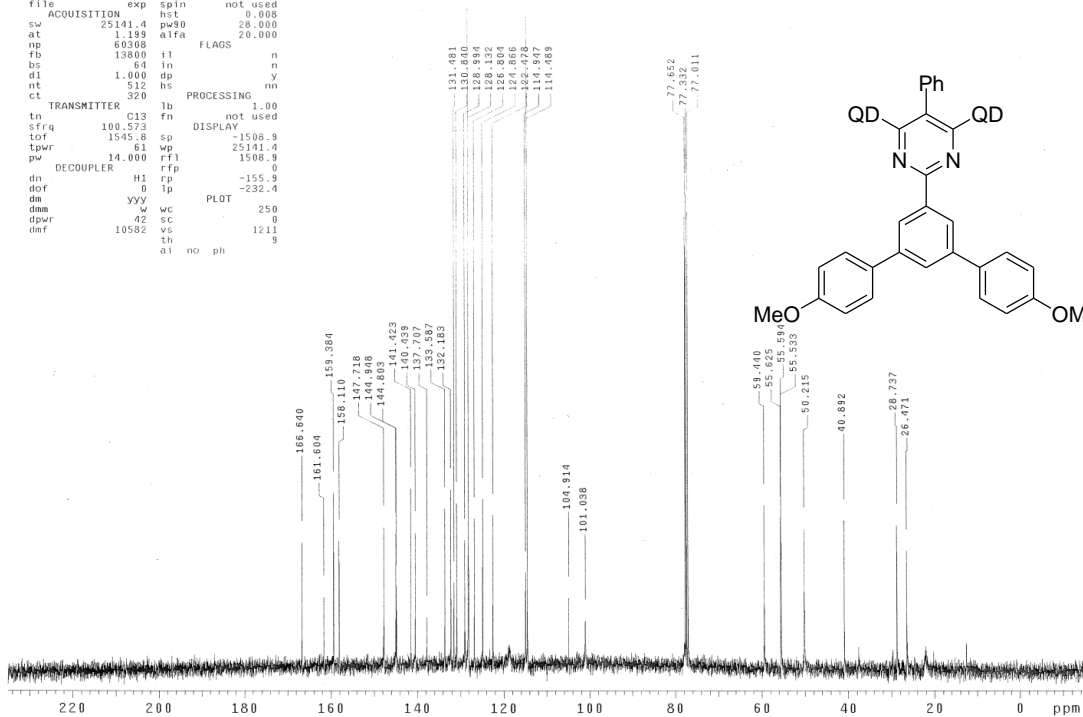
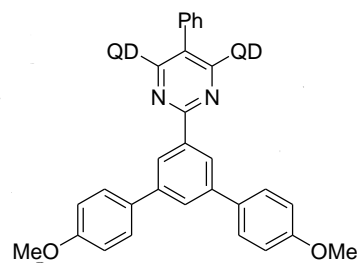
AK_X_103
exp2 s2pu1

SAMPLE		SPECIAL	
date	Nov 27 2012	temp	not used
solvent	CDCl3	gain	not used
file	exp	spin	not used
ACQUISITION	exp	hst	0.008
sw	6399.0	pw90	10.000
at	2.000	alFa	6.600
np	25598	FLAGS	
fb	3600	il	n
bs	15	in	n
d1	1.000	dp	y
nt	8	hs	nn
ct		PROCESSING	nn
TRSMITTER	H1	fn	not used
tn		DISPLAY	-0.1
sfrq	399.932	sp	
tof	399.6	wp	3999.2
tpwr	55	rfl	800.0
pw	5.000	rfa	0
DECOUPLER	C13	rp	76.7
dn	0	lp	-17.2
dof	0	PLOT	
dm	nm	wc	250
dmm	5	sc	0
dpar	42	vs	159
daf	17094	lu	54
		al	cdc ph



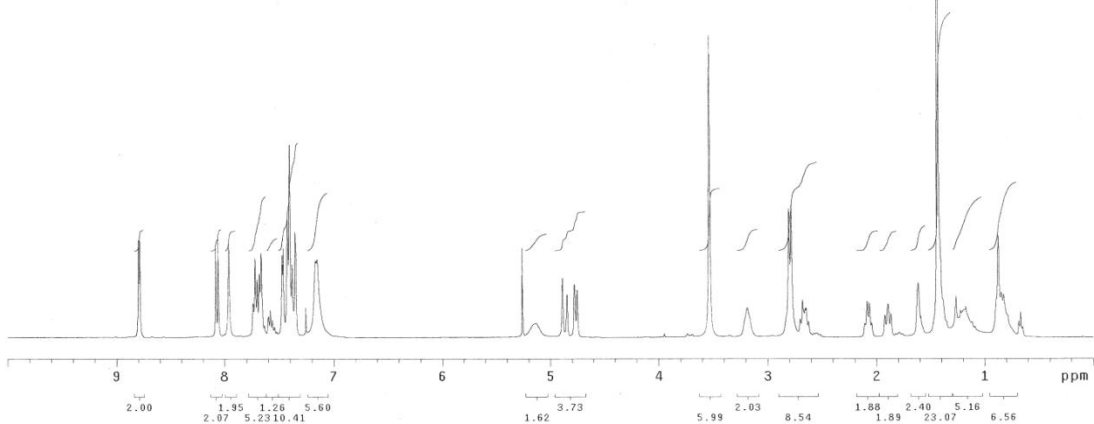
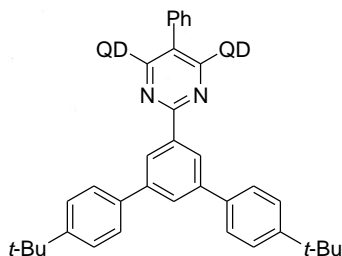
AK_X_103
exp2 s2pu1

SAMPLE		SPECIAL	
date	Nov 27 2012	temp	not used
solvent	CDCl3	gain	not used
file	exp	spin	not used
ACQUISITION	exp	hst	0.008
sw	25141.4	pw90	26.000
at	1.199	alFa	20.000
np	60308	FLAGS	
fb	19800	il	n
bs	64	in	n
d1	1.000	dp	y
nt	512	hs	nn
ct		PROCESSING	1.00
TRSMITTER	C13	fn	not used
tn		DISPLAY	
sfrq	100.573	sp	-1508.9
tof	1545.8	wp	25141.4
tpwr	61	rfl	1508.9
pw	14.000	rfa	0
DECOUPLER	H1	rp	-155.9
dn	0	lp	-232.4
dof	0	PLOT	
dm	YYY	wc	250
dmm	42	sc	0
dpar	10582	vs	1211
daf		th	9
		al	no ph



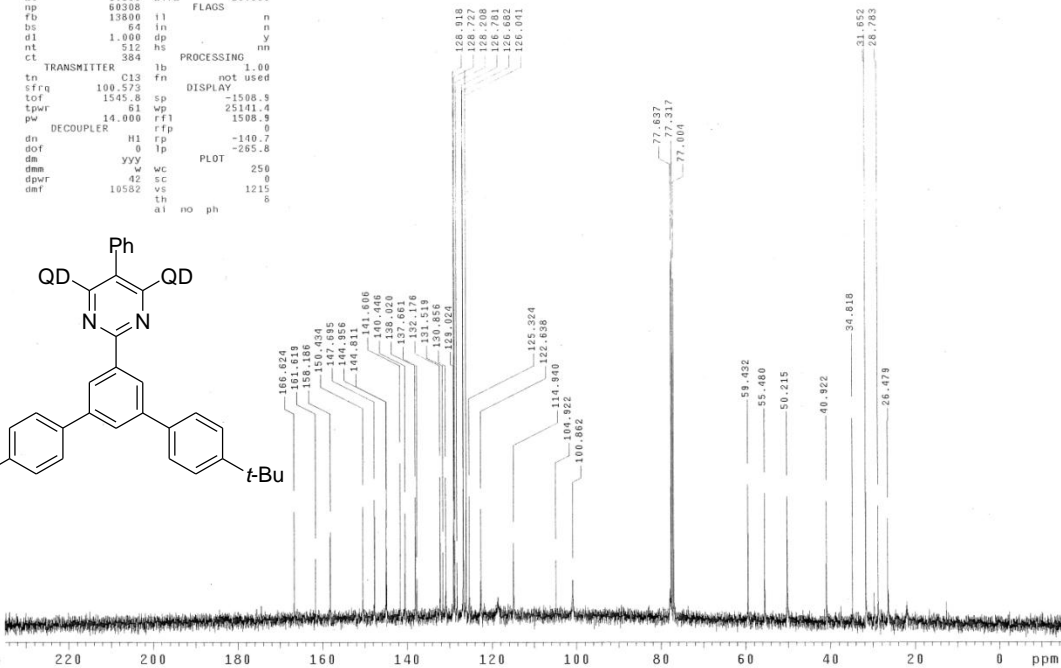
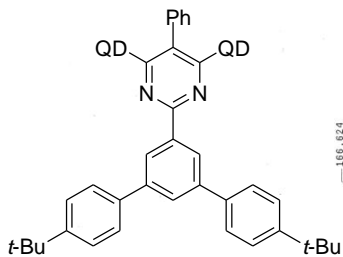
AK_X_175
exp2 s2pu1

```
SAMPLE          SPECIAL
date Nov 27 2012 temp not used
solvent CDCl3   gain  not used
file            exp  spin not used
ACQUISITION    hst   0.008
sw 6399.0      pu90  10.000
at 2.000       alfa  6.600
np 25596
fb 3600        il    n
bs 16          in    n
d1 1.000       dp    y
nt 8           hs    nn
ct 8
TRANSMITTER     fn    not used
tn H1          DISPLAY -0.1
sfrq 399.932   sp
tof 399.6      wp    3999.2
lpwr 55        rffl  800.0
pw 5.000       rfp    0
DECOUPLER      rp    75.8
dn C13        lp    -14.6
dot 0
dm nnn        wc    PLOT 250
dmm c         sc    0
dpar 42       vs    183
dnt 17089    lh    14
ai cdc ph
```



AK_X_175
exp2 s2pu1

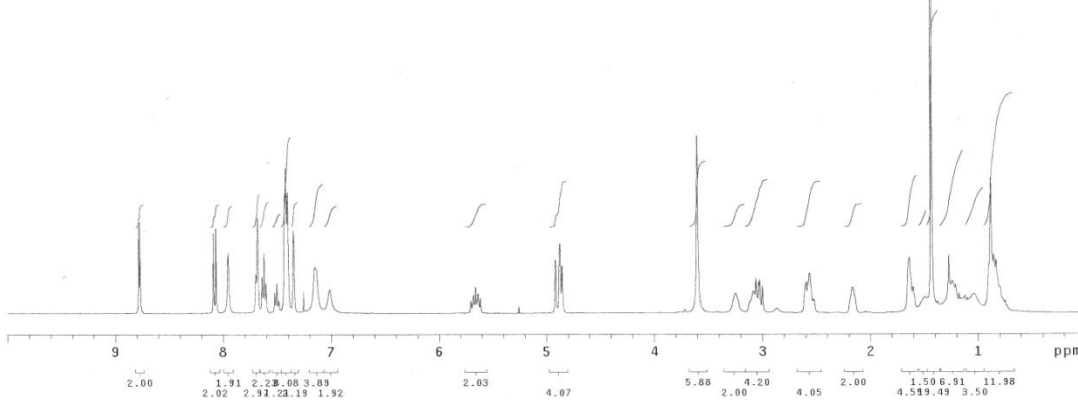
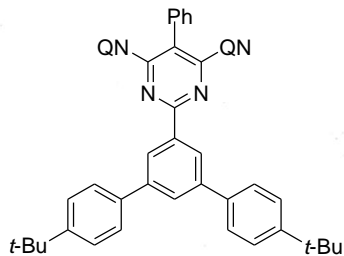
```
SAMPLE          SPECIAL
date Nov 27 2012 temp not used
solvent CDCl3   gain  not used
file            exp  spin not used
ACQUISITION    hst   0.008
sw 25141.4     pu90  28.000
at 1.189       alfa  20.000
np 60308
fb 13800       il    n
bs 84          in    n
d1 1.000       dp    y
nt 512         hs    nn
ct 384
TRANSMITTER     fb    not used
tn C13         DISPLAY 1.00
sfrq 100.573   sp
tof 1545.8     wp    -1508.3
lpwr 81        rffl  25141.4
pw 14.000     rfp    1508.3
DECOUPLER      H1    0
dn H1         lp    -140.7
dot 0         vs    -265.8
dm yyy        wc    PLOT 250
dmm w         sc    0
dpar 42       vs    1212
dnt 10592    th    8
ai no ph
```



AK_X_207

exp2 s2pu1

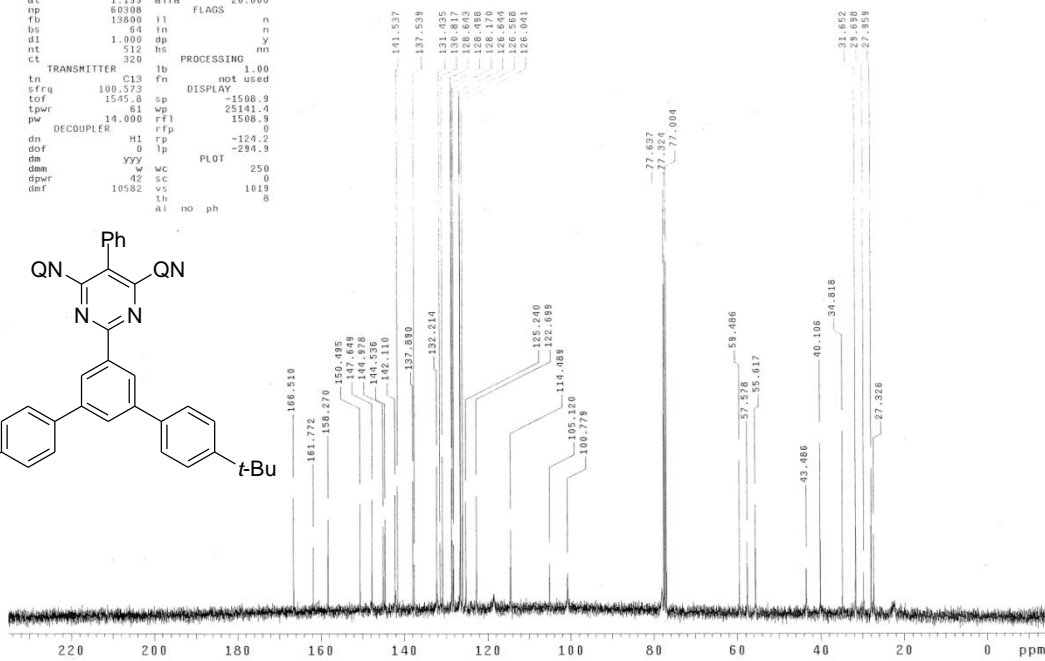
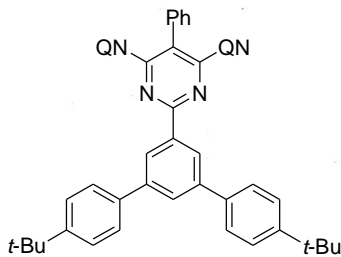
SAMPLE		SPECIAL	
date	Nov 27 2012	temp	not used
solvent	CDCl3	gain	not used
file		spin	not used
ACQUISITION		SPECIAL	
sw	6399.0	pw90	10.000
at	2.000	alfa	6.000
np	25596	FLAGS	
fb	3600	il	n
bs	16	in	n
d1	1.000	dp	y
nt	8	hs	nn
ct	8		
TRANSMITTER		PROCESSING	
tn	h1	fn	not used
sfreq	399.932	sp	DISPLAY
tof	399.6	wp	-0.1
tpwr	5.000	rfp	3999.2
pw	5.000	rfp	800.0
DECOUPLER		PLOT	
dn	C13	rp	74.3
dof	0	lp	-14.8
dm	nnn	wc	250
dpr	42	vs	116
dmf	17094	th	14
	al	cdc	ph



AK_X_207

exp2 s2pu1

SAMPLE		SPECIAL	
date	Nov 27 2012	temp	not used
solvent	CDCl3	gain	not used
file		spin	not used
ACQUISITION		SPECIAL	
sw	25141.4	pw90	0.008
at	1.199	alfa	20.000
np	60308	FLAGS	
fb	13909	il	n
bs	64	in	n
d1	1.000	dp	y
nt	512	hs	nn
ct	320		
TRANSMITTER		PROCESSING	
tn	C13	fn	not used
sfreq	100.623	sp	DISPLAY
tof	1545.8	wp	-1508.9
tpwr	61	wp	25141.4
pw	14.000	rfp	1508.9
DECOUPLER		PLOT	
dn	H1	rp	-124.2
dof	0	lp	-294.3
dm	yyy	wc	250
dpr	42	vs	1019
dmf	10582	th	8
	al	no	ph



References

1. Koser, G. F.; Relenyi, A. G.; Kalos, A. N.; Rebrovic, L.; Wettach, R. H., One-Step Alpha-Tosyloxylation of Ketones with [Hydroxy(Tosyloxy)Iodo]Benzene. *J Org Chem* **1982**, *47* (12), 2487-2489.
2. Ueno, M.; Nabana, T.; Togo, H., Novel oxidative alpha-tosyloxylation of alcohols with iodosylbenzene and p-toluenesulfonic acid and its synthetic use for direct preparation of heteroaromatics. *J Org Chem* **2003**, *68* (16), 6424-6426.
3. Liebeskind, L. S.; Srogl, J., Heteroaromatic thioether-boronic acid cross-coupling under neutral reaction conditions. *Org Lett* **2002**, *4* (6), 979-981.
4. Lu, L. G.; Chen, Q. Y.; Zhu, X. Z.; Chen, C. F., A new convenient synthesis of alkoxyanthracenes from alkoxy-9,10-anthraquinones. *Synthesis-Stuttgart* **2003**, (16), 2464-2466.
5. Liu, Q.; Perreault, S.; Rovis, T., Catalytic Asymmetric Intermolecular Stetter Reaction of Glyoxamides with Alkylidenemalonates. *J Am Chem Soc* **2008**, *130* (43), 14066-+.